Theory of mechanisms and machines

VL. A. ZINOVIEV

THEORY OF MECHANISMS AND MACHINES

THE HIGHER SCHOOL PUBLISHING HOUSE
Moscow

Translated from the Russian by A. GLADSTEIN

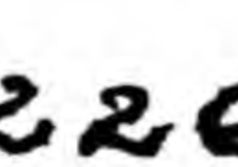

Printed in the Union of Soviet Socialist Republics

CONTENTS

The author of this book, Vladimir Andreyevich ZINOVIEV, Doctor of Technical Sciences, spent over fifty years of his life in industry and teaching. Vl. A. Zinoviev took an active part in the planning of large plants and shops. He also designed new types of standard equipment which is being applied in industry.

Since 1932 Vl. A. Zinoviev had been head of the department of machine elements in the Mendeleyev Chemico-Technological Institute in Moscow.

Vl. A. Zinoviev is also the author of a text-book on machine elements for students in the nonmechanical faculties of technical institutes, and of several text-books on method.

AUTHOR'S NOTE

The theory of mechanisms and machines is the first branch of technical science, a study of which is essential for successful activity in the sphere of mechanical engineering, and is the basis of the education of specialists in this field.

In the Soviet Union special attention is given to machine building which is one of the principal branches of industry. The other important branches of industry can develop successfully only by proper development of machine building. Without machines it is impossible to attain any significant increase in productivity, mechanization and automation of the process of production.

The theory of mechanisms and machines first became an independent science in the Soviet Union and has made outstanding progress. Based on the works of the distinguished Russian scientists, Chebyshev and Zhukovsky, it was further developed in the works of contemporary scientists and has far outstripped the scientific schools of other countries. In order to produce new types of machines, to develop machine-tool construction, textile manufacturing, food production, printing and publishing, and other branches of industry, as well as instrument-making, Soviet scientists had first to develop the methods of analysis, synthesis and the design of compound mechanisms and machines.

The main fields of the science of mechanisms and machines. the structure and classification of mechanisms, kinematic analysis of mechanisms, the combined static and inertia-force analysis of mechanisms and elementary knowledge about the dynamics of mechanisms and machines, are presented in this book in simple form.

Vl. A. Zinoviev

INTRODUCTION

The various devices, which man creates for different purposes, may be classified into two large groups. The first group includes those devices the elements of which cannot move relative to each other, not taking into account the insignificant motion arising at deformation under the action of forces; the second group consists of devices the elements of which move relative to each other while the device is performing its functions. The first group includes structures for various purposes, i. e. buildings, bridges, reservoirs for fluids or gases, etc.

The theory of mechanisms and machines deals only with devices which belong to the second group. Of the many devices in this group we shall mention some basic types which are widely employed and are of the utmost value in modern engineering:

1) engines which are designed to transform different forms of energy into mechanical energy (steam engines, steam and water turbines, internal-combustion engines, electric motors, etc.);

2) electric generators which convert mechanical energy into electrical energy;

3) machine-tools which perform various operations; for example machines for processing metals and wood, agricultural machinery, spinning frames and looms, sewing machines, mechanical mixers for chemical apparatus, centrifuges, etc.;

4) transporting mechanisms which serve to transfer solids, fluids and gaseous materials;

5) instruments for various purposes — clocks, computers, etc.

The work of a machine is performed directly by its working member. For instance, the working member of a machine for working metal or wood, is the tool which cuts the material, in a sewing machine it is the needle, in a hoist — the hook onto which the load is suspended, etc.

In its performance a machine has to utilize the forces which impart motion to it. Therefore, one of the indispensable members of any machine is the member which absorbs the work performed by external forces.

In a piston engine (steam engine or internal-combustion engine) this member is the piston, in a lathe — the pulley, in a bicycle — the pedal, etc.

Problems concerning the shapes and sizes of operating members and of those members which absorb the work of external forces, concerning the most expedient forms of motion and the forces that

act upon such members are dealt with in special branches of courses on power engineering and technology, but not in the theory of mechanisms and machines.

The theory of mechanisms and machines deals with problems connected with the design and study of devices which consist of moving elements and which connect the members, that absorb the work of external forces, with the operating members.

In solving the problems of work transmission and motion it is not essential to know the design shapes and sizes of all machine elements, it is sufficient to deal only with the kinematic diagrams (skeleton of the machine). The methods of drawing up kinematic diagrams and their study are presented in the handbook *Theory of Mechanisms and Machines.*

After a study of the kinematic diagrams, the shapes and sizes of all machine elements are chosen preliminarily, then a dynamic investigation is performed in order to determine the data which are necessary to verify the preliminary calculation. The method of dynamic investigation of machines is also expounded in the theory of mechanisms and machines.

Thus, along with the subjects included in courses on power engineering and technology, by whose methods are determined the shapes and sizes of working members and of those members which absorb the work of external forces, the theory of mechanisms and machines based on the data of theoretical mechanics, stands in line with the scientific subjects which expound the methods for determining the design shapes and sizes of machine elements.

Chapter I

STRUCTURAL ANALYSIS OF PLANE MECHANISMS

1. KINEMATIC PAIR

Motion, which is one of the features of a machine, distinguishes it from a structure that remains stationary while fulfilling its functions.

An instrument which is guided by the hand of a human being, for instance a needle, axe, hammer, screwdriver, is also in a state of motion while fulfilling its functions. The machine differs from instruments, able to perform varied movements, in that the movements of its elements are determined: a needle guided by the seamstress or a hammer in the hand of a blacksmith can perform various movements, but a sewing machine needle or a steam hammer perform only determined movements.

Any given body can be made to move in a determined way only by limiting its motion with other bodies. For example, a cylindrical bar which is not limited by anything may perform various movements, but when the same bar is placed in a hollow cylinder, as shown in Fig. 1, then bar *1* is able to revolve relative to hollow cylinder *2* only about the common axis $x—x$ of both cylinders and move in the direction which coincides with their common axis $x—x$. Should the same cylindrical bar, placed in a hollow cylinder, be provided with shoulders (Fig. 2) which are resting against the end surfaces of the hollow cylinder, then bar *1* relative to hollow cylinder *2* will be able to revoive only about the common axis $x—x$ of both cylinders. If instead of the cylindrical bar a prismatic bar will be

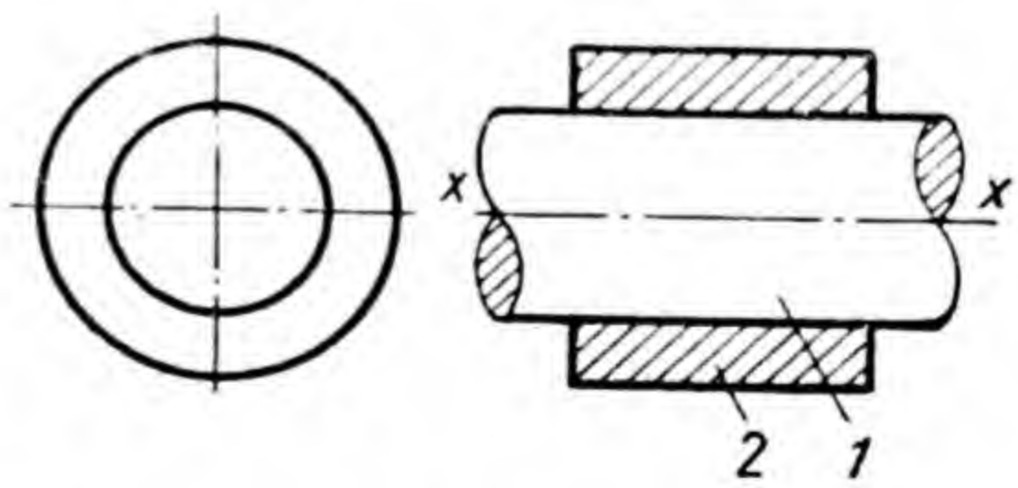

Fig. 1

placed in a hollow prism (Fig. 3), then bar *1* will be able to move relative to hollow prism *2* only in the rectilinear direction along the axis *x*—*x*.

Since the determined motion of any given body can be attained only by limiting its motion by other bodies, it is necessary in the study of the movement of any given machine element to examine it alongside another element which limits its movability to a greater or lesser extent. In those cases where the motion of the machine element under examination is being limited by two or more parts, we shall be able to acquire a complete understanding of the possible movement of the element under examination by considering the limitations being imposed on this element

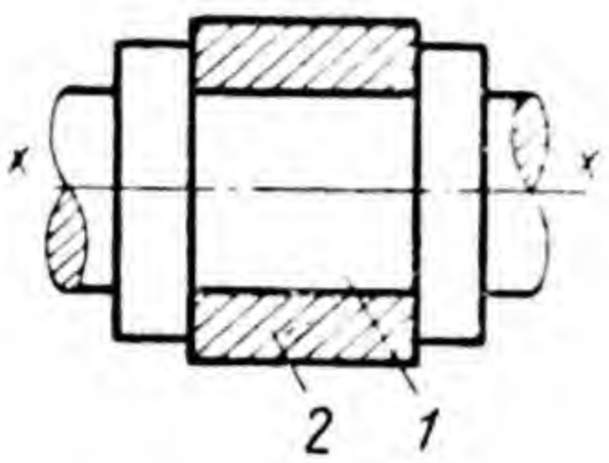

Fig. 2

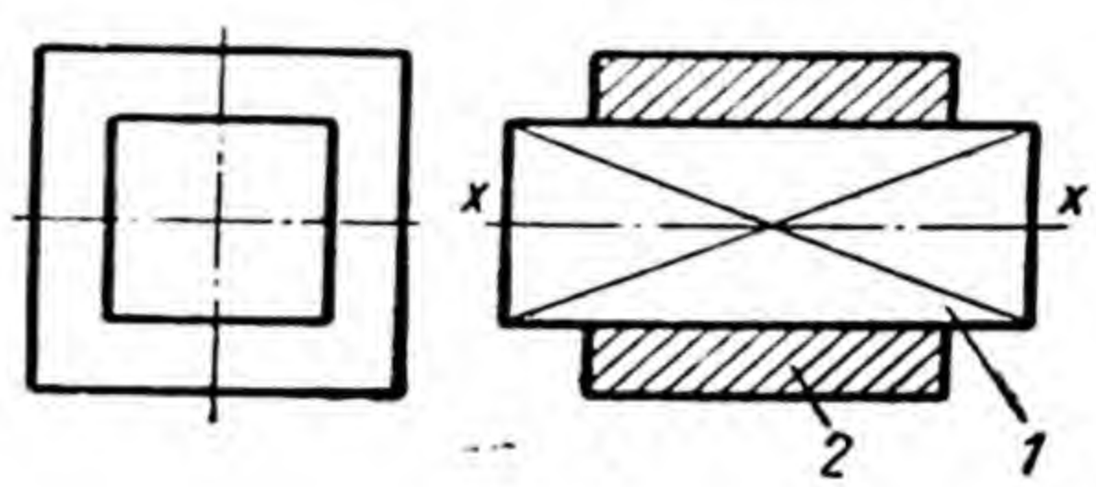

Fig. 3

by all the other machine elements with which it is in contact. In other words, by studying a machine from the kinematic point of view we can acquire a complete understanding of possible movements of all of its elements by examining not every element separately, but by paying attention to the pairs of such elements which mutually limit the movement of each other — to the kinematic pairs.

A k i n e m a t i c p a i r is a movable joint of two solid bodies which are in contact.

Bodies which form a pair are called l i n k s.

From this definition of a kinematic pair follows that a kinematic pair cannot be constituted by bodies which are not in contact, or by bodies which, although in contact, cannot move relative to each other.

The degree, to which the motion of one link of a kinematic pair relative to another is limited, may depend only on the geometric forms of contact points of links, known as e l e m e n t s o f a k i n e m a t i c p a i r: neither the material from which the link is manufactured, nor the shape of that part of it which does not come into contact

with the other link can limit the motion of the other link, and that is why they are not examined in the theory of mechanisms and machines.

2. CLASSIFICATION OF KINEMATIC PAIRS

Kinematic pairs may be classified according to various features. We shall confine ourselves only to classification according to the nature of contact of the links. According to this characteristic pairs should be classified into lower and higher.

A lower pair is a pair whose links contact along the surface, a higher pair is a pair whose links have line or point contact.

The pairs shown in Figs. 1, 2 and 3 can serve as examples of lower pairs. An example of a higher pair, the links of which contact along straight line, is a cylinder on a plane; in circumference — a ball in a hollow cylinder, whose diameter equals that of the ball, at point — a ball on a plane.

Lower pairs are much superior to higher pairs: in lower pairs, given similar forces of reaction in the pairs, and similar coefficients of friction, other conditions being equal, the links in the contact points wear more slowly than in higher pairs; however, higher pairs make possible the performance of motions which are difficult to accomplish by the application of lower pairs only.

If all the points of one link of a lower pair can move only rectilinearly relative to another link as, for example, in the kinematic pair shown in Fig. 3, such a pair is called a sliding pair. If all the points of both links of a lower pair can only revolve about the geometric axis of the contact surface of the links as, for example, in the pair shown in Fig. 2, such a kinematic pair is called a turning pair.

3. DIAGRAMMATIC REPRESENTATIONS OF KINEMATIC PAIRS

Figs. 4-12 show the conventional way of depicting different types of kinematic pairs in kinematic diagrams.

Fig. 4 shows a turning pair with links which can freely displace within the limits of a plane. The circle, which connects links *1* and *2*, only indicates diagrammatically the extent to which one link relative to the other can rotate

about the geometric axis of the pair. In a most simple design shape a turning pair can be imagined in the form of a cylindrical pin with a bushing turning on it. The designs of links may vary greatly.

Fig. 4

Fig. 5

Fig. 6

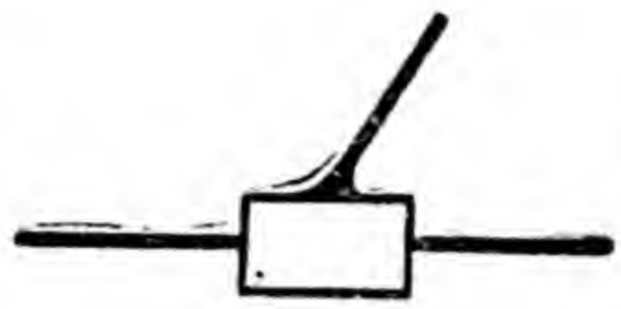

Fig. 7

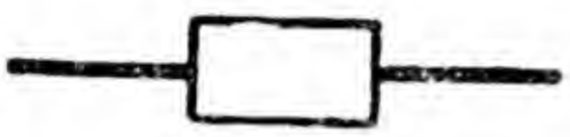

Fig. 8

Fig. 9

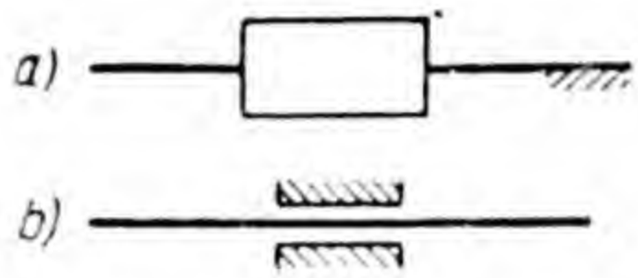

Fig. 10

The fixed position of links in pairs of all types is indicated in the diagrams by dotted lines. Figs. 5 and 6 give a diagrammatic representation of a turning pair with one fixed link.

Figs. 7 and 8 give a diagrammatic representation of a sliding pair with free links, and in Figs. 9 and 10, *a* and *b* — with one fixed link.

Fig. 11

Fig. 12

Figs. 11 and 12 give a diagrammatic representation of a higher pair with free links and with one fixed link. The curvilinear profiles show diagrammatically the contact of links along a line (perpendicular to the drawing plane) or at a point.

In using diagrammatic representations of kinematic pairs it should always be borne in mind that in no way do they reflect the forms of design.

4. KINEMATIC CHAIN

A system of links joined in kinematic pairs is called a k i n e m a t i c c h a i n.

Kinematic chains are classified, according to the nature of the motion performed by the points of links, into plane

and space chains. Chains whose links move in parallel planes are called plane chains. Chains in which the points of the links move either along space curves, or along plane curves which lie in nonparallel planes are called space chains.

Kinematic chains may be closed or unclosed. A kinematic chain is called closed when each of its links is connected in kinematic pairs with adjacent links. If a chain has links which constitute only one kinematic pair, it is called an unclosed or open chain.

5. KINEMATIC DIAGRAMS

A kinematic study of any mechanism (engine mechanism, machine-tool, etc.), which is in the design stage or in operation, is performed by its kinematic diagram. In the course of a kinematic study it is necessary to determine the paths, velocities and accelerations of the points of moving elements. A kinematic diagram should depict only what is essential for its specific purpose, and therefore all elements of a device under investigation should be represented on the diagram as links of kinematic pairs.

We shall now explain by example how to proceed from a design scheme of a mechanism to its kinematic diagram.

Fig. 13, *a* shows a design scheme whereas Fig. 13, *b* — a kinematic diagram of an internal-combustion engine. This engine is designed for the transformation of chemical energy from fuel (oil, kerosene, benzine, fuel gas, etc.) into mechanical energy. During engine operation, piston *3* (Fig. 13, *a*) performs reciprocating motion in cylinder *2*.

The design scheme does not show many engine elements, which do not affect the kinematics of the mechanism.

Pin *4* enclosed by element *5* which is called a connecting rod is secured in piston *3*. With its other end the connecting rod encloses pin *6*, which is secured in element *7* which is called a crank. The crank is firmly connected with shaft *8* which rotates in fixed bearings. In the design representation shaft *8*, crank *7* and pin *6* are always made as one piece and called a crankshaft. They are shown separately in Fig. 13, *a* only for the purpose of clarifying the subsequent discussion.

The cylinder is the fixed part of the engine which is in contact with the cover and piston. The cover is firmly

connected with the cylinder, and therefore they do not form a kinematic pair; for technological reasons it has to be manufactured separately from the cylinder. The piston can move relative to the cylinder, and therefore the piston and the cylinder are links of a kinematic pair — a lower pair, because the links contact along the surface. This is a sliding pair since the piston cannot rotate in the cylinder; pin *4* connected with the piston would then also rotate and together with the pin the connecting rod would rotate with all the other engine parts, including the frame and the cylinder.

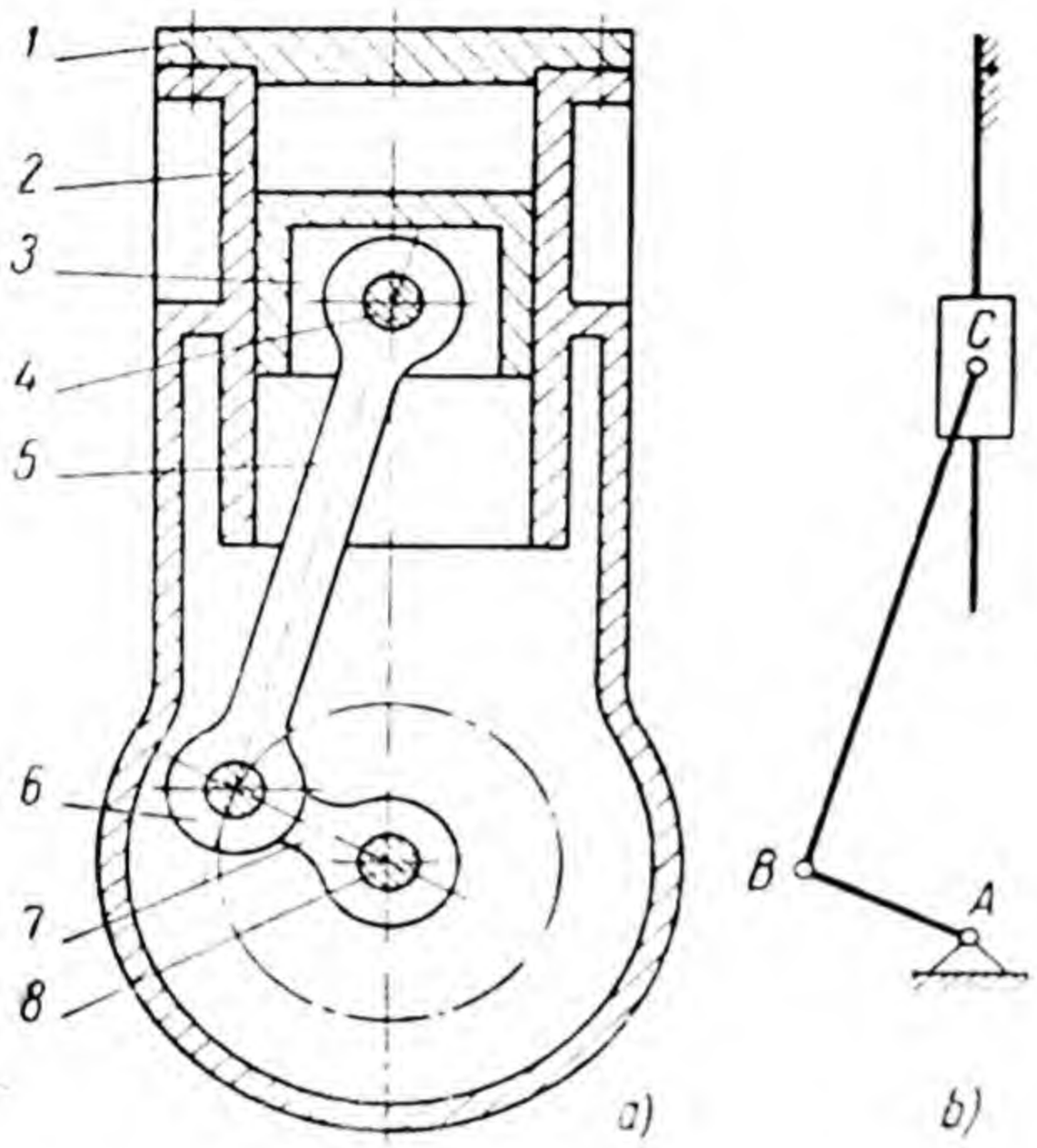

Fig. 13

Piston *3* is the moving link of this sliding pair, cylinder *2* — the fixed link guiding the motion of the moving link. In the kinematic diagram the cylinder is represented by a shaded line, which stands for the fixed position of the link, the piston is shaped as a slider, which is the conventional way of showing the moving link of a sliding pair.

Shaft *8* is firmly connected with element *7* and therefore does not form a kinematic pair, but forms together with it one moving link. Shaft *8* rotates in a fixed cylindrical bearing which is not shown in Fig. 13, *a*, and forms together with this bearing turning pair *A*.

For practical purposes the shaft is mounted not in one, but in two or more bearings, and in such cases all bearings belong to one fixed link.

In the design scheme the geometric axis of shaft *8*, which is perpendicular to the drawing plane, crosses at right angles the extension of the common geometric axis of the cylinder and piston. Therefore, in the kinematic diagram the centre of turning pair *A* must be located on the extension of the straight line, which represents a fixed link of the sliding pair.

Element *7* and element *5* are also joined in a turning pair. This pair is indicated by the letter *B* in the kinematic diagram. In the design scheme the distance between the geometric axes of elements *6* and *8* is definite and invariable; the centres of the circles, which depict pairs *A* and *B* in the kinematic diagram, must be located at the same distance to the chosen scale for the kinematic diagram. Thus, the engine crankshaft in the kinematic diagram is represented by link *AB*.

Element *5* (the connecting rod) in the design scheme is joined in turning pairs with piston *3* and element *7*. In the kinematic diagram the connecting rod is depicted by link *BC*. The distance between the centres of turning pairs *B* and *C* to the chosen scale for the kinematic diagram must be equal to the distance between the axes of the same pairs in the design scheme.

The kinematic diagram of the engine as represented in Fig. 13, *b* is a closed kinematic chain with one fixed link, three moving links, one sliding pair and three turning pairs.

6. DEGREES OF FREEDOM OF A PLANE KINEMATIC CHAIN

The position of link AB (Fig. 14) within the plane limits is defined by three parameters: by two coordinates of a given point of this link and the angle of inclination of the link to any of the coordinate axes. The free link on the plane, changing these three parameters, utilizes three degrees of freedom; whether these three degrees of freedom are utilized at once during compound motion or in turn in any sequence is immaterial for obtaining the final result.

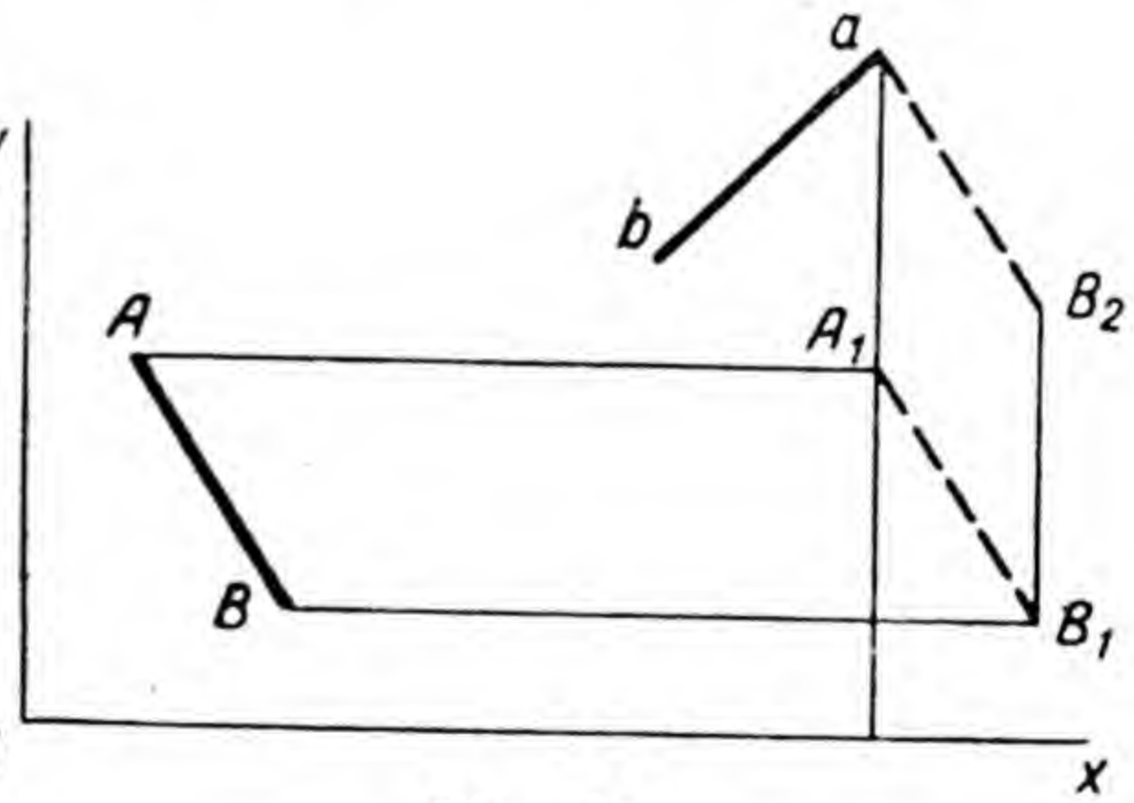

Fig. 14

By utilizing three degrees of freedom in turn at motion in a parallel plane the link can move from position *AB* into another given position *ab* in the following manner:

1) to displace parallel to itself in a direction parallel

to axis x as far as the coincidence of point A with the perpendicular drawn from point a to axis x; as a result of this displacement the link will assume the position A_1B_1;

2) to displace from position A_1B_1 also parallel to itself in a direction, parallel to axis y, as far as the coincidence of points A_1 and a; as a result of such displacement the link will assume the position aB_2;

3) to rotate about point a as far as the coincidence of points B_2 and b.

Two links which are not connected with each other have at motion in a parallel plane six degrees of freedom, allowing displacement of these links from any given position into any other given position. Two links which are joined in a kinematic pair at motion in a parallel plane, that is without changing their relative position, can utilize only the three degrees of freedom which are at the disposal of one link. But, since they are connected in a kinematic pair, the links do not lose the freedom of relative displacement: links of a turning pair can utilize one more degree of freedom for turning one link about the pair centre, and links of a sliding pair — for the sliding of one link on another. In contrast to links of lower pairs, links of higher pairs at their relative displacement can utilize two degrees of freedom — one for the sliding and the other for the rolling of one link on the other.

Hence, a lower pair takes away from two links two degrees of freedom or, as it is customary to say, imposes two connections; a higher pair imposes one connection.

When it becomes part of a machine, the kinematic chain must be firmly coupled through one of its links with the machine frame. With one fixed link, called a frame, the structural formula of a plane kinematic chain is:

$$3n - 2p - k = W, \qquad (1)$$

where n is the number of moving links or the total number of links less the one, which becomes a frame;
p — the number of lower pairs;
k — the number of higher pairs;
W — the number of degrees of freedom or the number of free parameters.

The number of degrees of freedom of a kinematic chain relative to the fixed link as distinct from the number of degrees of freedom of a chain without a fixed link is termed the degree of movability of a kinematic chain. Hereafter we shall examine only kinematic chains with fixed links.

In deriving formula (1) it was assumed that each link introduces three degrees of freedom into the kinematic chain, and each of the lower pairs takes away two degrees of freedom. But we can imagine a chain without higher pairs all links of which are deprived of the possibility to turn, that is to change their angular parameters. This type of chain is a chain which contains only sliding pairs.

A link of such a chain introduces to the latter not three but two degrees of freedom, whereas a lower kinematic pair (in this case always a sliding one) imposes one connection and not two.

Therefore, in determining the number of degrees of freedom of a kinematic chain which contains only sliding pairs, it is necessary to proceed from the formula

$$W = 2n - p, \tag{2}$$

where W is the number of degrees of freedom;

n — the number of moving links;

p — the number of sliding pairs.

Kinematic chains which contain only sliding pairs are seldom of practical application.

The motion of a kinematic chain is characterized by the number of degrees of movability which is equal to the number of free parameters. When the number of degrees of movability is zero, all links can occupy only definite positions, from which they cannot be moved owing to the absence of free parameters, viz., because it is impossible to make any of the links move. At W degrees of movability a certain reciprocal disposition of all links is attained after such movements of one or more of its links, at which all W of the free parameters were utilized. When one part of the links, which move by given laws and utilize all free parameters, is in motion, the movement of the other links is thereby determined.

In the study of chains those links whose laws of motion are assumed as given are called d r i v i n g, the other links are called d r i v e n. Driving links should not be confused with links which are driven by external forces. To

distinguish such links from driving ones we shall call them motive links. A driving link may or may not be a motive link.

To illustrate the above we shall discuss some examples.

Fig. 15 shows the diagram of a three-link chain with fixed link (frame) AC and three turning pairs A, B, C. When $n=2$, $p=3$ and $k=0$, the number of degrees of movability according to formula (1) is

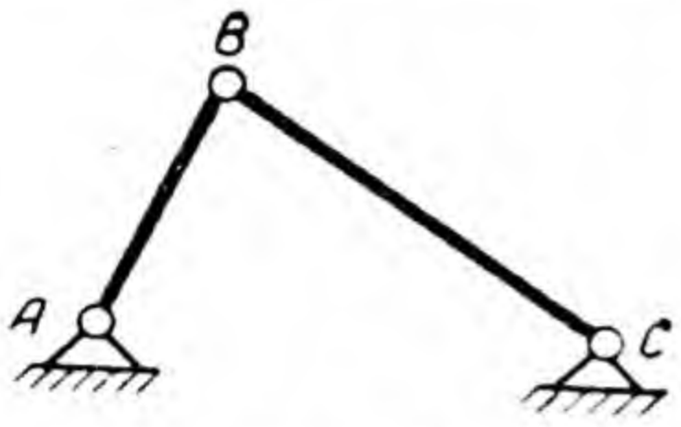

Fig. 15

$$3\times2-2\times3-0=0.$$

Consequently, there are no free parameters, and clearly, therefore, the chain is fixed.

By changing turning pair B in the kinematic chain (Fig. 15) to a higher one we obtain a chain as shown in Fig. 16. The higher pair permits the links to change their relative position, and therefore by retaining the contact in pair B it is possible for one of the links to turn through a certain angle. But when the turned link has been set in a certain position the other link cannot turn: its turning in one direction will be prevented by the first link, while turning in the opposite direction and coming out of contact with the first link would lead to the disappearance of the higher pair and the conversion of the kinematic chain from closed into unclosed. Hence, the number of degrees of movability of the chain is unity, which is substantiated as well by formula (1):

$$3\times2-2\times2-1=1.$$

Fig. 17 shows a chain with three moving links and four turning pairs. According to formula (1) we obtain

$$3\times3-2\times4-0=1.$$

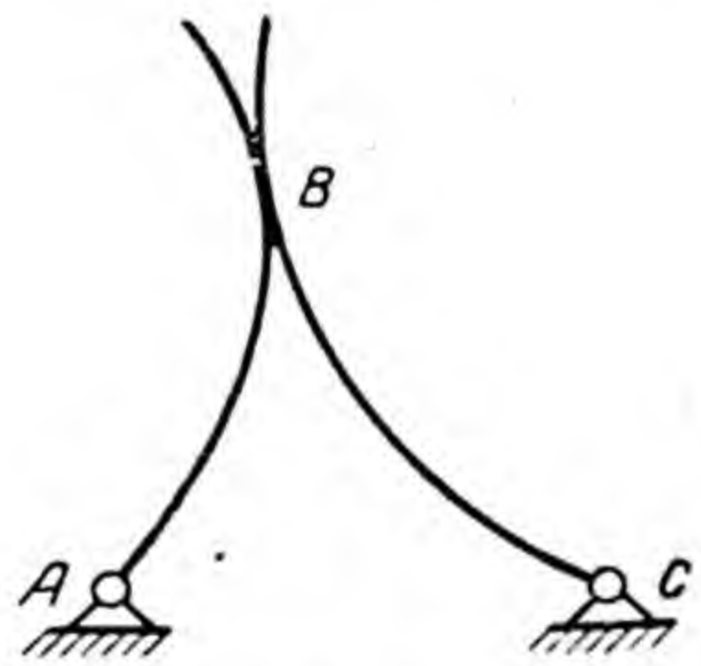

Fig. 16

As a result of turning link AB through a certain angle all links are set in a definite position, since the motion of any of the other links without a repeated change of the position of point B has become impossible. A similar result is also obtained when link CD utilizes one free parameter. It follows from this that link BC can freely change the position of only one

of its extreme points, whereas the position of the second point depends entirely on the position of the first.

Hence, the result obtained above by formula (1) is correct.

Fig. 18 shows a chain with four moving links and five turning pairs. By formula (1) we obtain

$$3\times4-2\times5-0=2.$$

When link AB turns one degree of movability is utilized and the length of imaginary side BE of tetragon $BCDE$ is determined. When points B and E are stationary the links of chain $BCDE$ have one degree of movability, as has already been determined from an examination of the chain, shown in Fig. 17. A similar result is obtained if link DE is

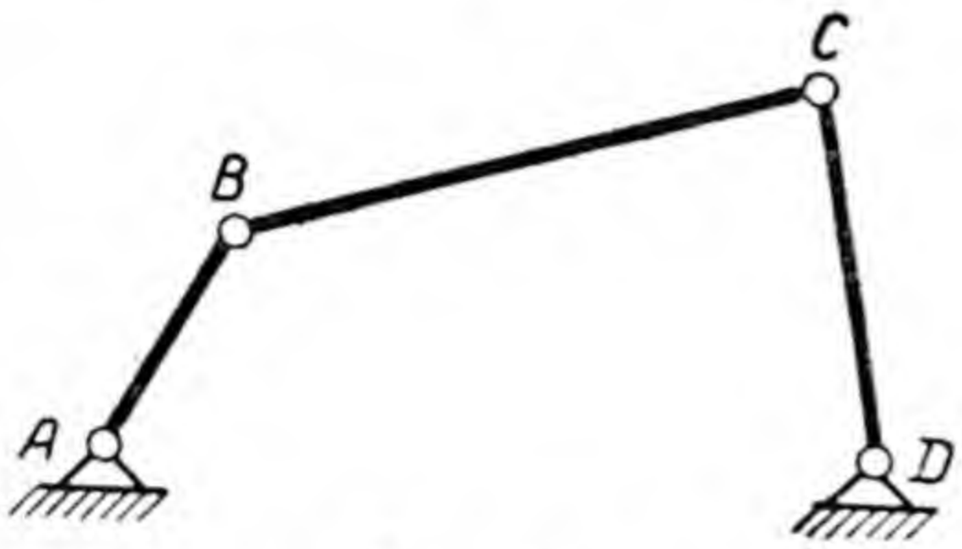

Fig. 17

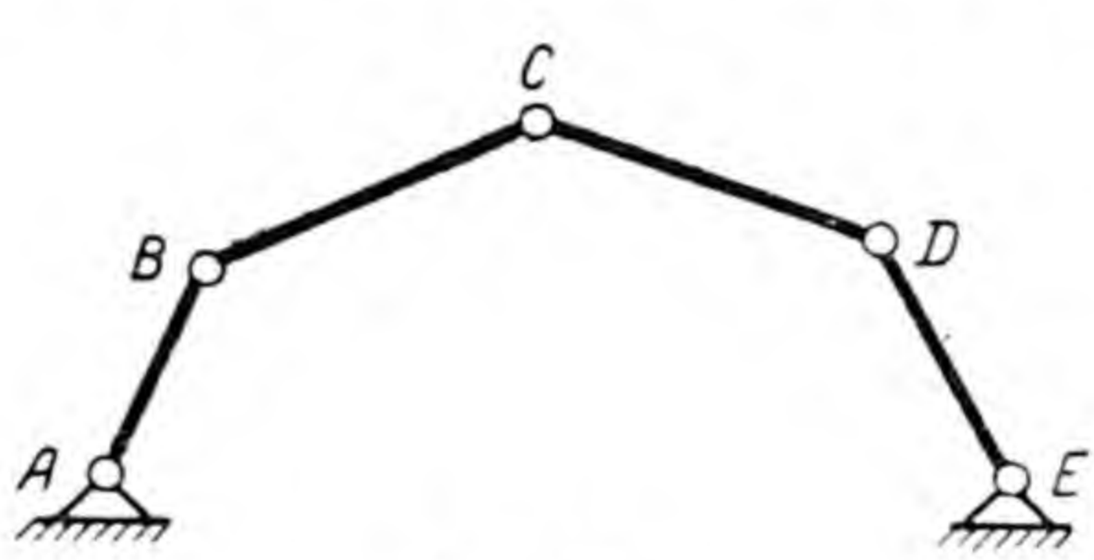

Fig. 18

turned instead of link AB. Hence, the chain shown in Fig. 18 has two degrees of movability, which substantiates the result obtained according to formula (1).

In this chain each of the links AB and DE can utilize only one free parameter, while each of links BC and CD, passing into a different position, utilizes two free parameters. For instance, in changing the position of point B link BC utilizes one free parameter, because point B, moving along the circumference of radius AB, can freely change only one coordinate; when point B is set in the new position, point C, moving along the circumference of radius BC, may also freely change only one coordinate.

Therefore, all links of the chain in Fig. 18 will move in a definite way either by two driving links AB and DE or by one driving link BC and CD.

Thus, having determined the number of degrees of movability of a plane kinematic chain, we can solve the problem of the number of driving links in various ways, depending on the number of degrees of movability at the

disposal of the links which are chosen as driving ones. In practice it is those links which have one degree of movability that are chosen as driving links. The number of degrees of movability of a plane kinematic chain may therefore be considered as equal to its possible number of driving links. It must, moreover, be noted that one of the links of the kinematic chain is converted into a frame and the others move according to definite laws.

Formula (1) makes it possible, even in the case of a complex chain, to solve rapidly the problem of the number of driving links which is required for a definite motion of all driven links.

7. MECHANISM AND MACHINE

A system of mutually connected links designed to perform a required motion is called a mechanism.

A machine is a mechanism or a group of mechanisms designed for performing useful work in the process of production, transformation of energy or transportation.

As already stated, links are coupled in kinematic pairs. A simple type of mechanism may be composed of a system of two links coupled in a kinematic pair — one moving link which can perform the required motion, and one fixed link, called a frame. A complex mechanism with one fixed link has a number of moving links, which are coupled in kinematic pairs, and thus represents a closed kinematic chain. All the links of such a chain can be made to move when one or a number of the links called driving links move according to given laws. The required number of driving links for a definite motion and the number of all the driven links can be defined by formula (1), which is a structural formula of a plane mechanism and is known as Chebyshev's formula. This formula was first developed by Academician P. L. Chebyshev in 1869 for mechanisms with turning pairs only, and subsequently it was extended to include mechanisms employing higher pairs as well as lower pairs of both types.

In the majority of cases we come across mechanisms with only one driving link; in future only such mechanisms will be discussed. For such mechanisms Chebyshev's formula reads as follows:

$$3n-2p-k=1. \qquad (3)$$

Since in deriving formula (1) only plane kinematic chains were considered, formula (1) and the resultant formula (3) do not cover space kinematic chains.

8. CLASSIFICATION OF MECHANISMS

Since the end of the 18th century scientists have proposed various systems for the classification of mechanisms, but none of them has had any considerable influence on the development of the science of mechanisms. Classification systems for mechanisms were proposed on the basis of the transformation of motion (for instance, from rectilinear into curvilinear, from continuous into periodic), on the basis of the conversion of velocities, on the basis of the types of connections between links of mechanisms, etc. All these classifications allowed the possibility of including in a single category mechanisms which differ in structure and therefore cannot be examined together.

In 1916 L. V. Assur, professor of the St. Petersburg Polytechnical Institute, proposed a system of classification which had great influence on the development of the science of mechanisms. This classification provided for mechanisms which incorporate only lower pairs, but subsequently in the works of Soviet scientists Assur's classification was extended to include mechanisms with higher pairs.

The relation between the number of moving links and the number of pairs in mechanisms, which have no higher pairs, in accordance with formula (3) is expressed by the equation

$$3n=2p+1. \tag{4}$$

This equation is satisfied by the following values which are components of its variables, while n and p are whole numbers:

$$\left.\begin{aligned} n&=2t+1;\\ p&=3t+1, \end{aligned}\right\} \tag{5}$$

where $t\geqslant 0$ and t is a whole number.

By giving the independent variable t gradual increasing values, starting with zero, we shall obtain the number of moving links and lower pairs suitable for the mechanism.

Where $t=0$ we have $n=p=1$ and, consequently, we obtain the diagrams of frequently encountered mechanisms which are shown in Figs. 19 and 20. Such mechanisms with one moving link and one pair, in which the moving link is coupled with the fixed link, are named according to Assur's classification mechanisms of class I order 1.

Fig. 19

Where $t=1$ we obtain $n=3$, $p=4$. A mechanism with this number of links and pairs can be obtained by connecting a group consisting of two links which are a part of three kinematic pairs, to a mechanism of class I order 1. Such a group is called a group of class I order 2 or a two-arm group. In such a group two links are connected in one kinematic pair, and on the ends of the links are positioned the elements of kinematic pairs in which the links are coupled with two different links of a certain mechanism. By introducing a two-arm group to the mechanism, i. e. by increasing the number of moving links of the mechanism by two and the number of lower pairs by three, the number of degrees of movability, in conformity with formula (1), does not undergo any change. Depending on the number of turning and sliding pairs included in the group, and their respective location, the groups can be of various types. Two different types of lower pairs may be located in the middle between the links and on the link ends in $2^3=8$ different combinations, as indicated below, where the letters T and S stand for turning and sliding pairs:

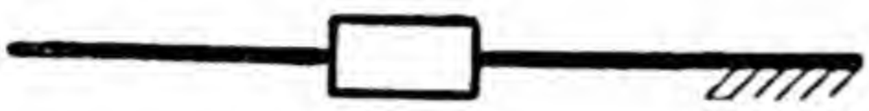

Fig. 20

Combination Nos.:

1	2	3	4	5	6	7	8
TTT	TTS	TST	TSS	STT	STS	SST	SSS

From the eight possible combinations Nos. 5 and 7 should be deleted, since in reverse order combination No. 5 repeats combination No. 2, and No. 7 repeats No. 4. Combination No. 8 is not suitable for the creation of a mechanism with one degree of movability by being joined with the basic mechanism of class I order 1 because it includes sliding pairs only, and for kinematic chains

which have only sliding pairs formula (2) will apply, not formula (1). From formula (2) we arrive at the number of degrees of movability of a group, which has sliding pairs only (combination No. 8), $W=1$. The introduction of such a group into the mechanism would lead to an increase in

Fig. 21

the number of degrees of movability of the mechanism by unity.

Thus only five types of two-arm groups are suitable for the creation of mechanisms with three moving links and four lower pairs. By joining five different two-arm groups to the basic mechanisms of class I order 1 we can obtain a number of different mechanisms with three moving links and four lower pairs. Figs. 17 and 21 show diagrams of such two mechanisms which are widely applied in modern engineering.

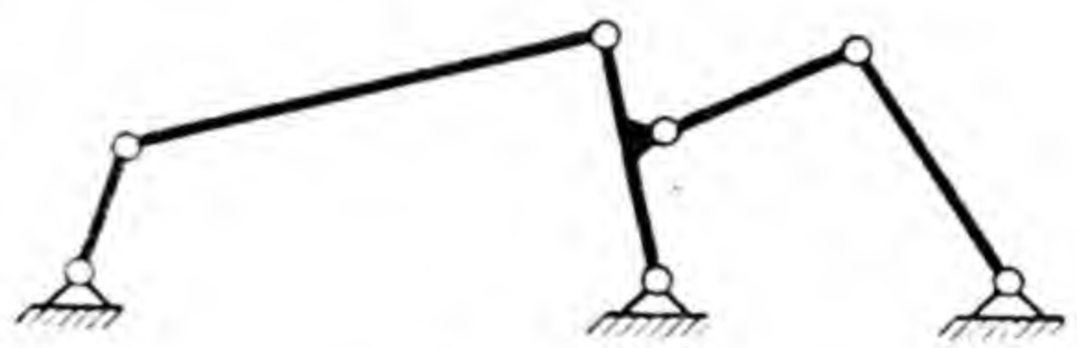

Fig. 22

Where $t=2$ we get $n=5$, $p=7$. Various mechanisms, each having these numbers of links and pairs, may be easily obtained by joining separate two-arm groups with different mechanisms of three moving links and four pairs.

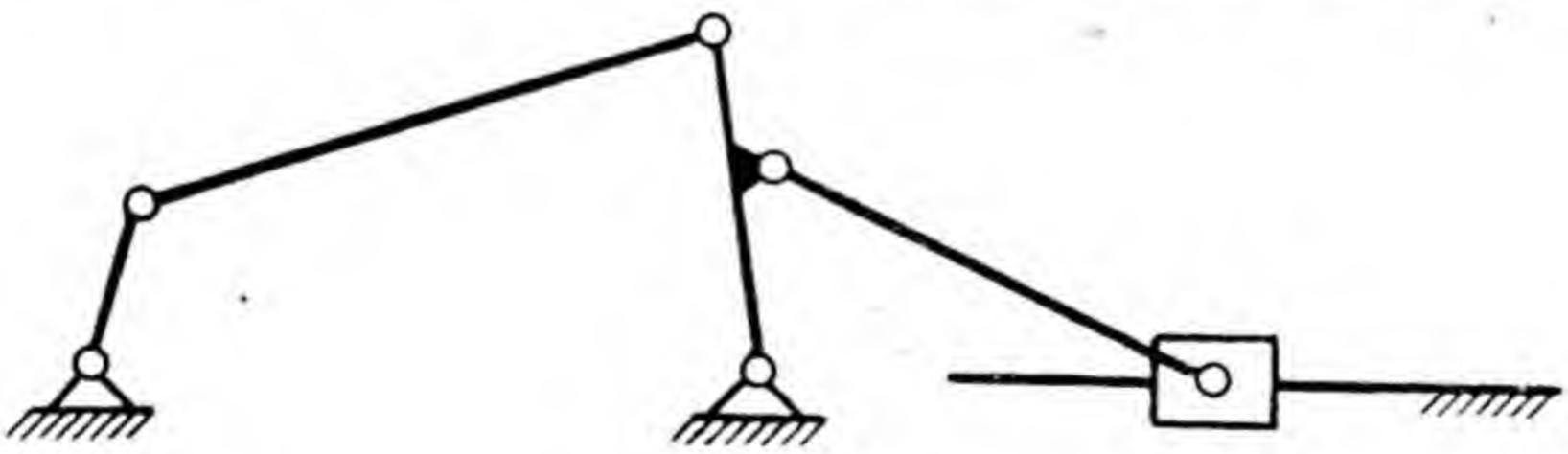

Fig. 23

Figs. 22 and 23 show two examples of the large number of such mechanisms possible.

With every increase of t by unity we shall get more and more complex mechanisms. Each successive mechanism of

increased complexity will result from the previous one by joining it with two different links of one group of class I order 2. All mechanisms obtained from the basic mechanism of class I order 1 by the successive joining of groups of class I order 2 are mechanisms of class I order 2, according to Assur's classification.

Mechanisms of class I order 2 are widespread in engineering, and by joining groups of order 2 with the basic mechanism we can obtain mechanisms with a large number of links and kinematic pairs. In order to proceed from the basic mechanism to the next in complexity, i. e., to a mechanism with $n=3$ and $p=4$, it was necessary to attach two links with three pairs to the basic mechanism; two links with three pairs are conceivable in only one form, that is in the form of a two-arm group, and therefore a mechanism with $n=3$ and $p=4$ can be created by one method only. But as soon as we proceed to the mechanism next in complexity, a mechanism with $n=5$ and $p=7$, we can raise the question: is it not possible to achieve it by means other than the attaching a two-arm group twice?

Another method for the creation of a mechanism with five links and seven pairs may be simply to connect such a group to the basic mechanism consisting of four links and six pairs, which could not be divided into two two-arm groups. This requirement is satisfied by a three-arm group, as shown in Fig. 24. A mechanism which consists of the basic mechanism and one such group will have a structure that differs from the structure of a mechanism of class I order 2, consisting of five moving links and seven pairs.

A three-arm group is called a group of class I order 3, and all mechanisms containing one or more such groups, regardless of whether or not they contain groups of class I order 2, are called mechanisms of class I order 3.

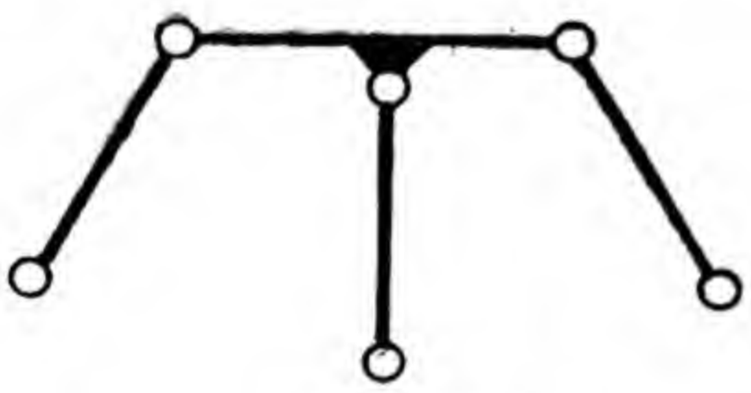

Fig. 24

A group of class I order 3, in the same way as a group of class I order 2, may be of various types, depending on the number of turning and sliding pairs it contains and their respective location. One of many possible mechanisms of class I order 3 with five moving links and seven pairs is shown in Fig. 25 (with the extreme left link as the driving one).

In a similar way we can obtain groups and mechanisms of higher orders, and by further complex combinations higher classes as well. We shall not discuss such mechanisms, since the majority of mechanisms employed in modern engineering should be treated according to Assur's classification as mechanisms of class I orders 1 and 2.

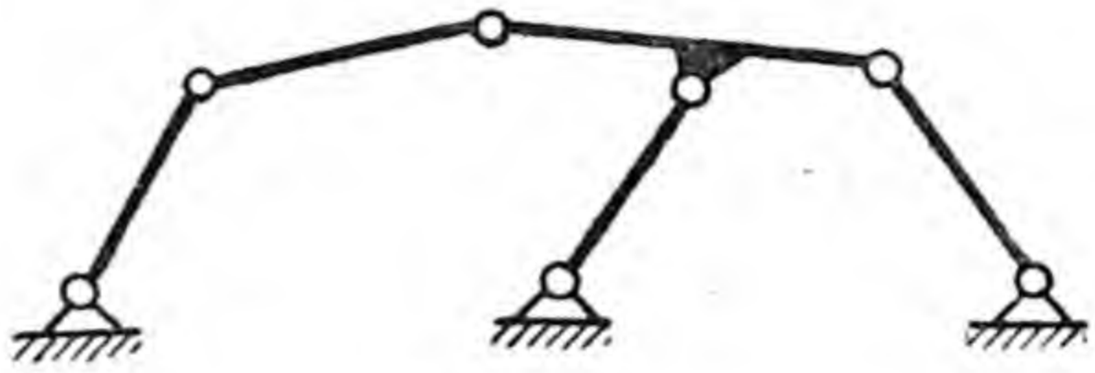

Fig. 25

Hence any mechanism, independent of its complexity and structure, can be created by Assur's classification through the successive joining of groups of different classes and orders to the basic mechanism of class I order 1. Therefore a kinematic and dynamic analysis of any mechanism, regardless of its complexity and structural design, may be reduced to the successive separation from it of the attached groups, starting with the last one attached, and to the analysis of the separate groups.

9. REPLACEMENT OF HIGHER PAIRS BY LOWER PAIRS

For purposes of determining the class and order of a mechanism with higher pairs, lower pairs should be substituted for the higher pairs.

Let us imagine a three-link mechanism with one higher pair (Fig. 26), the curvilinear profiles of whose links are circles. During the motion of links the point of contact of profiles will always be on line BC, which connects the centres of the circles. With a given motion of one link the motion of the other will proceed as if there were no higher pair, and instead there were link BC with turning pairs B and C. By replacing the higher pair with one link with two turning pairs, we shall obtain instead of a three-link mechanism, as shown in Fig. 26, the already familiar mechanism of class I order 2 which is shown in Fig. 17.

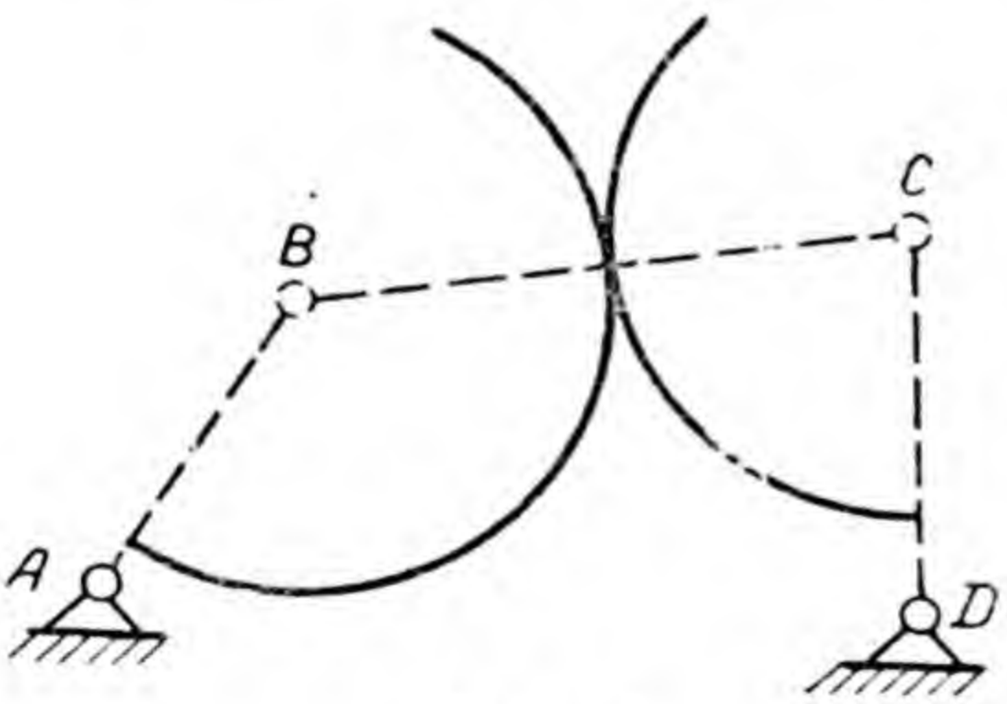

Fig. 26

The centres of the circles in Fig. 26 are curvature centres of the profiles of the higher pair links. The method of replacing a higher pair remains unchanged also in cases when the profiles are curves other than circles. The velocities and accelerations remain unchanged, if joints *B* and *C* are placed in the curvature centres. The point of contact of the profiles in this case will always be on the line connecting the curvature centres, and therefore the

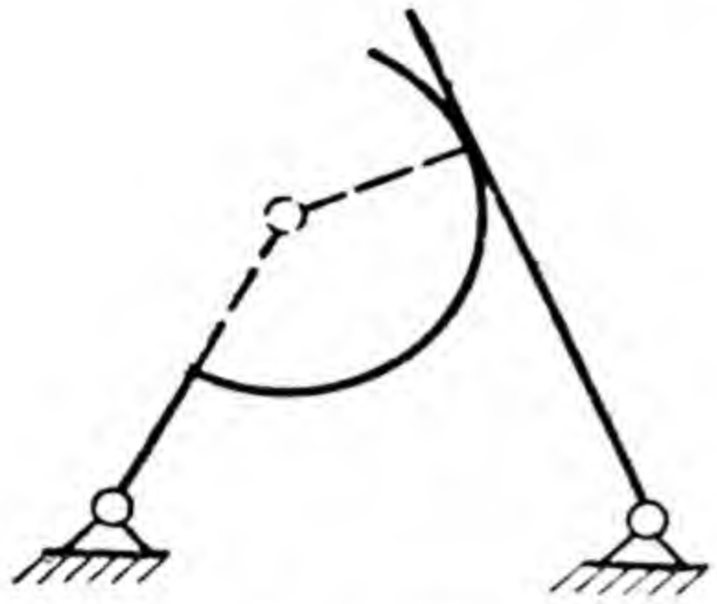

Fig. 27

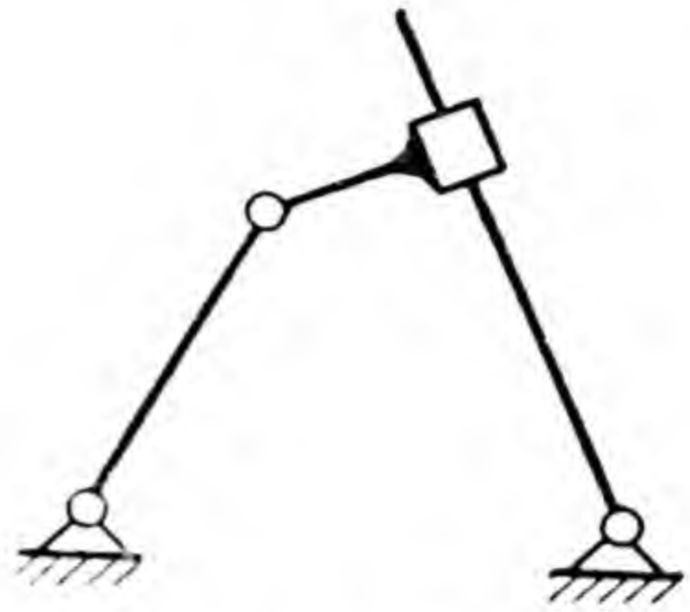

Fig. 28

replacement of a higher pair by one link with two turning pairs is also possible. Where the curvilinear profiles of higher pair links are curves other than circular arcs, the radii of profile curvatures at points of contact will vary at different positions of the links, but for determining the class and order of a mechanism this will be of no importance.

If the profile of one of the links of a higher pair is rectilinear (Fig. 27), the curvature radius of such a profile at the point of contact will be infinite. In this case one turning pair is located in the curvature centre of the curvilinear profile, and the other becomes a sliding pair (Fig. 28). In this case we also get a mechanism of class I order 2.

10. MOST WIDESPREAD TYPES OF MECHANISMS

In modern engineering the most widespread types of plane mechanisms with lower pairs are mechanisms of class I orders 1 and 2.

A mechanism of class I order 1, which is a moving link connected with a frame in a turning pair, has been applied since ancient times (for example, the wheel on an axle), it is widely used at present, and will undoubtedly be used in engineering in the future. A further example of a mecha-

nism with such a diagram is an electric motor, whose moving link is a rotor firmly coupled to the shaft which rotates freely in bearings of a fixed body. Such a mechanism is also shown diagrammatically in Fig. 29, which is a centrifugal pump, whose moving link is shaft *1* with secured blades *2*, by means of which the fluid is sucked into the pump during shaft rotation and is forced out from the pump into delivery pipeline *3* (the suction pipeline is not shown in Fig. 29; it is located perpendicular to the drawing plane which could be shown in another projection only). Such a mechanism is also a water or steam turbine; in each of these turbines the moving link is again a shaft with blades which absorb the power of the water or steam delivered to the turbine.

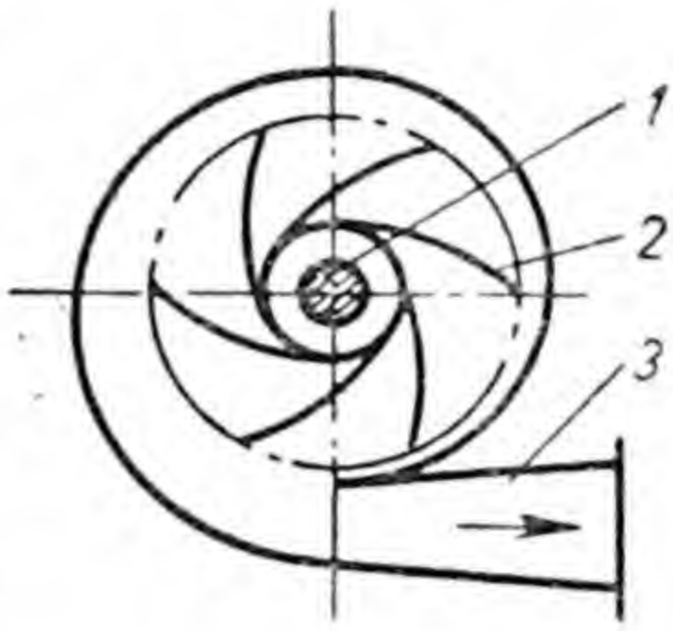

Fig. 29

A mechanism of class I order 1, which is a moving link connected with a frame in a kinematic pair, is a steam hammer, as shown diagrammatically in Fig. 30; its frame is steam cylinder *1* and hammer guides *2*, and the moving link is piston *3* with rod *4* which connects the piston with hammer *5*. When steam is admitted into the lower part of the cylinder, the pressure of steam moves the piston upwards and the hammer with it; when steam is discharged (through a hole which is not shown in Fig. 30) the hammer, entraining the piston, drops by its own weight on the processed part *6* which is located on the anvil. Another similar mechanism is the steam piston pump that is diagrammatically shown in Fig. 31. The steam and water cylinders *1* and *3* serve as its frame, and pistons *2* and *4*, which are connected to each other, are the moving link. When steam is admitted into the left-hand part of steam cylinder *1*, piston *2* forces out the exhaust steam of the previous stroke

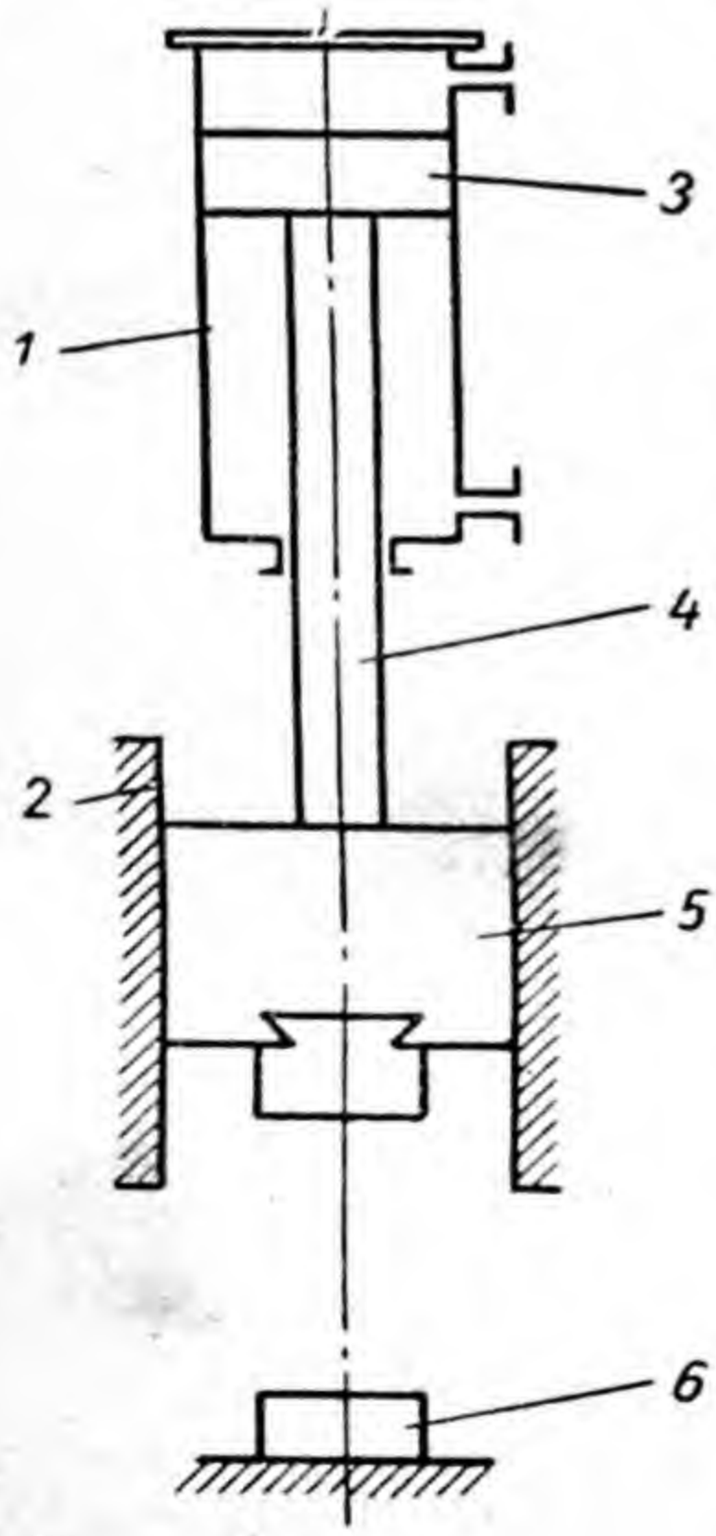

Fig. 30

through the right-hand part of the cylinder. At the same time from the right-hand part of the water cylinder the fluid is forced out into the delivery pipeline, and is sucked into the left-hand part from the suction pipeline. When steam is admitted into the right-hand part of cylinder *1* the right-

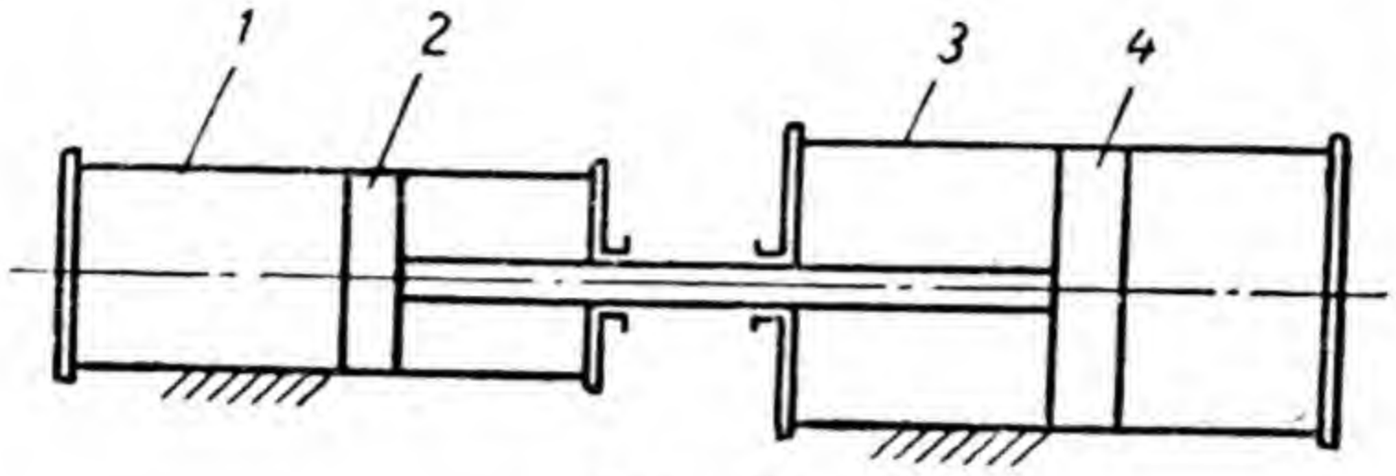

Fig. 31

hand part of the water cylinder performs the action of suction and the left-hand part that of expulsion. Fig. 31 shows neither the steam and fluid pipelines, nor the automatically closing holes by means of which the cylinders connect with the pipelines.

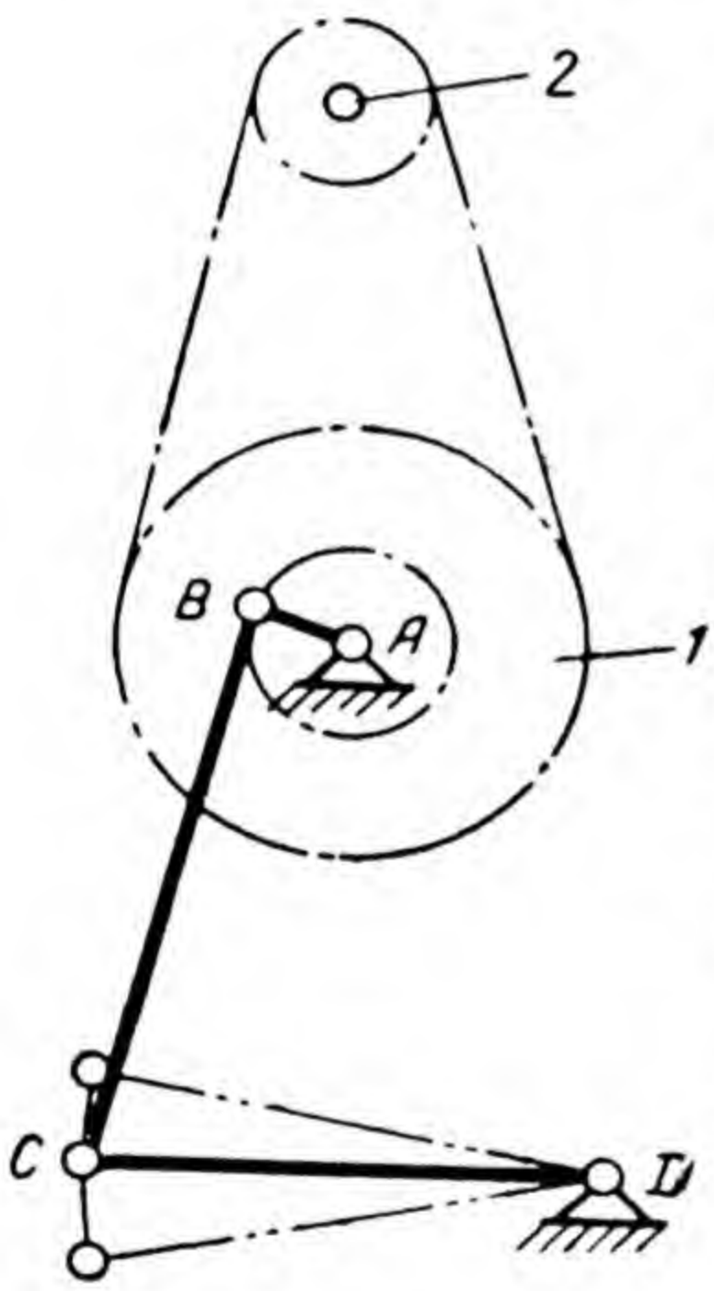

Fig. 32

Mechanisms of class I order 1 are widely employed not only in modern engineering, but also in everyday life in a number of simple hand-driven devices. The mechanism of class I order 1 is furthermore a basic component in the construction of all mechanisms of higher classes and orders.

Of all possible types of mechanisms of class I order 2 the two most common are: the four-bar mechanism (see Fig. 17) and the slider crank mechanism (see Fig. 21).

Depending on the relative dimensions of all links each of the links *AB* and *CD* of a four-bar mechanism can either perform a full revolution about the axis of a turning pair or turn only a part of a full revolution. In the first case the link is called a crank, and in the second, a rocker arm. Link *BC* is called a connecting rod. In engineering we come across various types of four-bar mechanisms, depending on the relative length of the links; they may be with one crank or two cranks, or with two

rocker arms. The motive link in the majority of cases is one of the turning links, whereas the link that performs the useful work is either the other turning link or a connecting rod.

Fig. 32 shows the diagram of a mechanism with a moving rocker arm which is used in various types of foot-driven machines: lathes, sewing machines, etc. In such mechanisms, under the action of the operator's foot, rocker arm *CD* performs rocking motion, deviating from the central position by small angles. Heavy element *1* is rigidly fastened to shaft *A* in order to enable the rocker arm to move upwards by inertia. Rotary motion can be transmitted through this element to another shaft, shaft *2*, which has a working member fixed to it with the help of a cord or by other means.

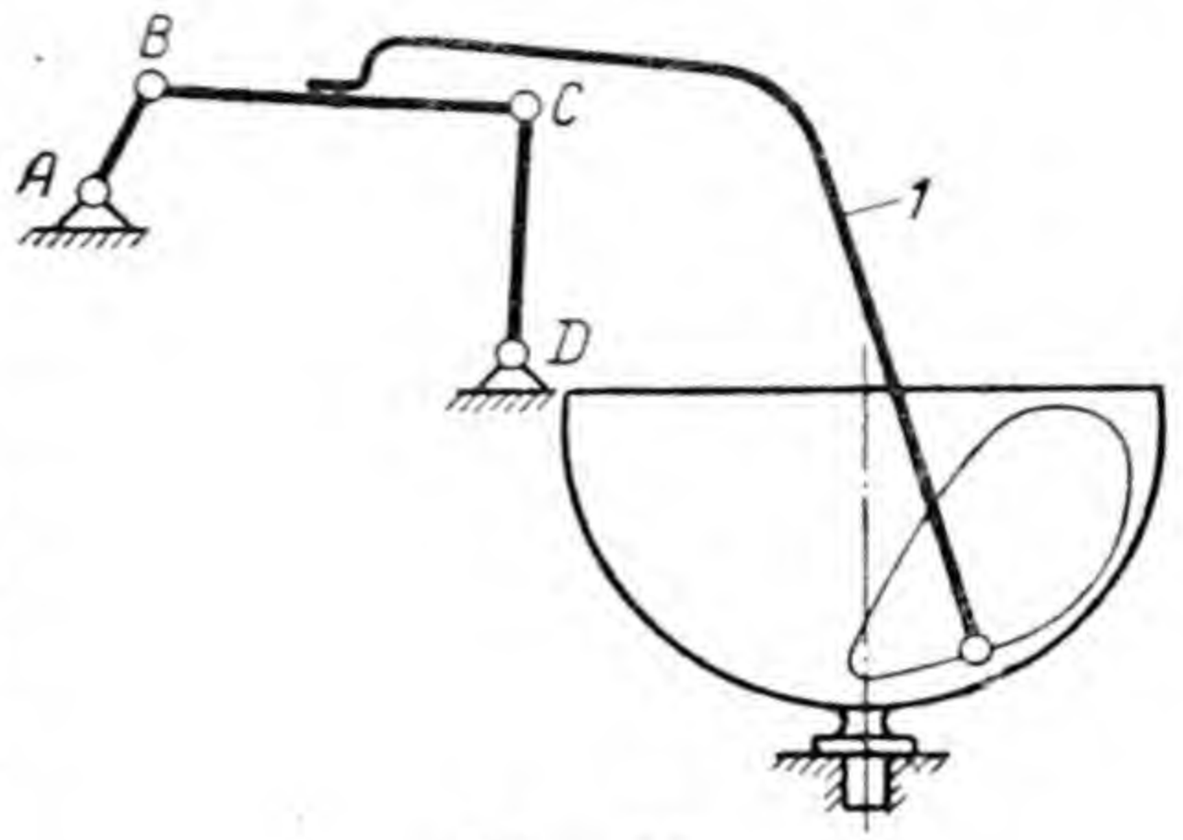

Fig. 33

Fig. 33 shows the diagram of a dough-making machine with a four-bar mechanism which has a crank as its driver link, and the link, which is connected with the operating member, is a connecting rod. During rotation of the crank, element *1*, rigidly coupled with connecting rod *BC*, describes a closed curve with its end inside the vessel containing the ingredients to be mixed which is turned by another one, not shown in the mechanism diagram.

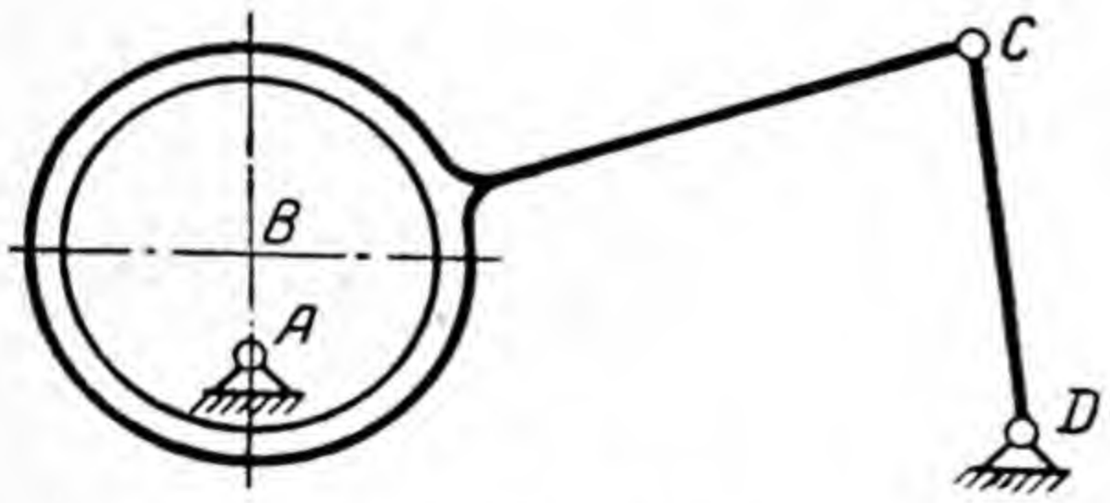

Fig. 34

A four-bar mechanism with one crank is often designed in the form of an eccentric mechanism as shown in Fig. 34. In this mechanism crank *AB* is designed as a cylindrical disk which rotates about axis *A* at a distance *AB* from geometric axis *B* of the cylindrical surface of the disk. The disk is enveloped by connecting rod *BC*, axis *B* is the axis of the turning pair which joins the connecting rod

with the crank, while the cylindrical surface of the disk is the contact surface of the links of this pair.

A four-bar mechanism with two cranks is often used as a mechanism with equal opposite links (Fig. 35). Such a mechanism is called p a r a l l e l or a p a r a l l e l o g r a m. The mechanism in Fig. 36 is called a n t i p a r a l l e l or an a n t i p a r a l l e l o g r a m.

Mechanisms with two cranks of unequal length are only rarely employed.

The slider crank mechanism (see Figs. 13, *b* and 21) is in most cases so designed that the fixed axis of turning pair *A* is located on the extension of the moving link guide of the sliding pair, called a s l i d e r.

The slider crank mechanism, which makes possible the transformation of rotary motion into translatory motion and vice versa, is the most widely applied four-link mecha-

Fig. 35

Fig. 36

nism in modern engineering. This type of mechanism is used as a basis in all piston engines (steam engines, stationary, automobile and aviation internal-combustion engines, and others), piston pumps and compressors, and is widely used in mechanical devices which serve other purposes.

In the piston engine the motive link is the slider which in the design scheme of Fig. 13, *a* is the piston, which is guided by the cylinder wall. The cylindrical surface of the piston is always designed so that the piston can slide freely along the cylindrical wall, while not allowing the escape of any gas or steam which is under pressure at one side of the piston. With a motive crank and a driven slider the slider crank mechanism is used in piston pumps and compressors: during one piston stroke fluid (in a pump) or gas (in a compressor) is sucked in; during its back stroke expulsion into the delivery pipeline takes place. In pumps and compressors the pistons often work with both

end surfaces: suction takes place at one piston end, and at the same time delivery takes place from the other end. In order to accomplish this, the turning pair is not connected directly with the piston, but with special element *1* (Fig. 37), which is rigidly fastened together with the

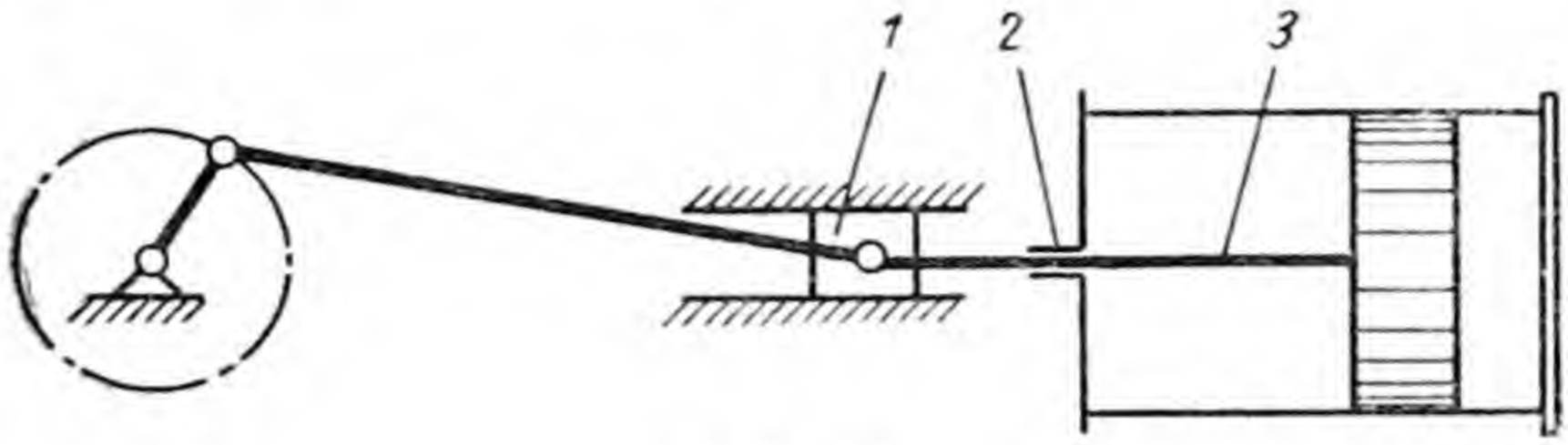

Fig. 37

piston through rod *3* that passes through sealing arrangement *2* (called "gland") in the cover. The slider crank mechanism of a double action steam engine is designed in a similar manner.

Among the mechanisms with higher pairs the g e a r d r i v e has found wide application; it consists of two engaged toothed wheels (Fig. 38, *a*). During rotation of the driving wheel the tooth of this wheel, pressing on the tooth of the driven wheel, turns the driven wheel until both teeth are disengaged. Rotation of the wheels proceeds continuously, because before one pair of teeth comes out of contact another pair of teeth is already coming into contact. This type of mechanism is a three-link mechanism with two turning pairs and one higher pair. A kinematic diagram of the toothed mechanism is shown in Fig. 38, *b*.

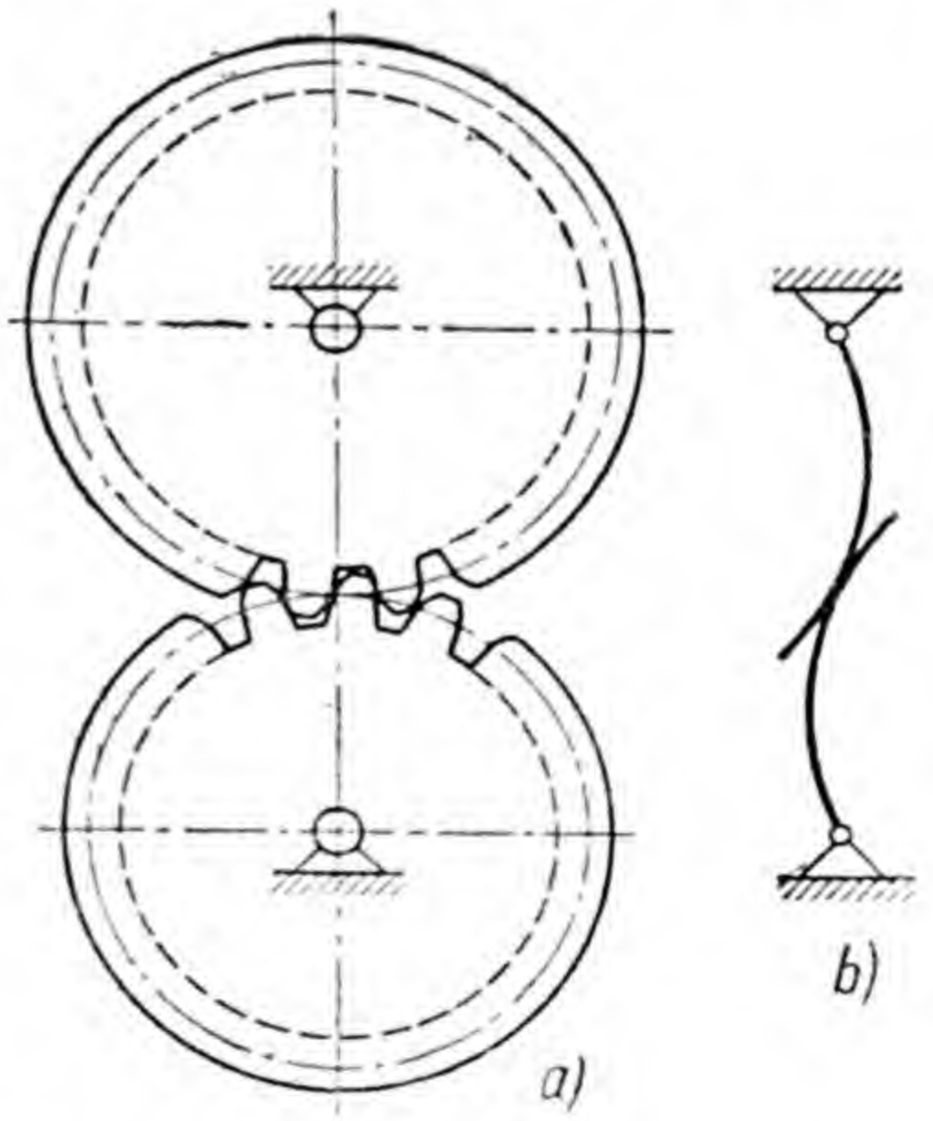

Fig. 38

In engines and other mechanical devices c a m m e c h a n i s m s are widely employed. A cam mechanism, whose diagram is shown in Fig. 39, consists of cam *1* and follower *2*. The cam is connected with a frame in a turning pair, and the follower is connected in a sliding pair. The cam and the follower are connected in a higher pair. In the

design arrangement constant contact of the follower with the cam is usually ensured by a spring. In order to diminish wear on friction surfaces the follower end, which thrusts against the cam, is usually given the form of a free turning cylindrical roller on the axis. The follower can serve many purposes. For example, in piston engines the follower actuates the valves which open and close the holes for the admission of steam or mixtures of fuel and air into the cylinder, and for discharging exhaust steam or combustion products. The great advantage of the mechanism, shown in Fig. 39, is that with quite a simple design it allows the easy transformation of rotary motion into reciprocating motion.

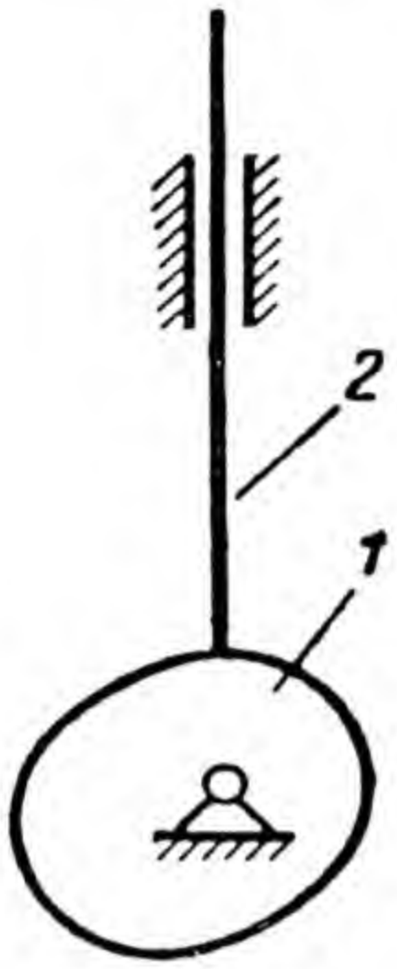

Fig. 39


Fig. 40

Fig. 40 shows the diagram of a cam mechanism in which the follower is replaced by a lever that is connected with the frame in a turning pair. In this mechanism too it is necessary to ensure constant contact of the higher pair links.

Chapter II

KINEMATIC ANALYSIS OF PLANE MECHANISMS

11. INTRODUCTORY

During the motion of the driving link every point of the driven links moves along a closed curve with definite velocities and accelerations in different positions of the mechanism. The velocities and accelerations of individual points of a mechanism are determined by the kinematic analysis, and in some cases (see, for example, the mechanism in Fig. 33) the paths of points are also found.

Determination of the velocities and accelerations is carried out at a number (12-24) of positions of the driving link; as a result of this it becomes possible to plot by points the curves which show the relations of velocities and accelerations to the positions of the driving link. The velocities and accelerations for other positions of the driving link, which have not been analysed, can also be determined by the plotted curves.

In order to be able to determine graphically the velocity and acceleration of any point of the mechanism at any given position of the driving link, it is necessary at that position to plot as well the positions of all the driven links.

12. DETERMINATION OF MECHANISM POSITIONS

As we know, any mechanism of class I order 2 which includes no higher pairs, regardless of its complexity, can be created by connecting two-arm groups in succession to the basic mechanism of class I order 1. For any given position of the driving link the positions of the links of all two-arm groups, starting with the first one connected, may be easily plotted with the help of dividers and a ruler. We shall explain this by example.

Fig. 41, *a* shows the diagram of an eight-link mechanism of class I order 2, which consists of the basic

mechanism of class I order 1, and three two-arm groups BCD, $B_1C_1D_1$ and B_2C_2x. At a new position of the driving link AB (Fig. 41, b) the positions of the other links are determined as follows.

1. The new position of point C is determined by the point of intersection of the circles of radii BC and CD which are drawn from the points B and D. The new position of point C is determined by that point of intersection of these circles to which point C can approach at continuous motion of link AB from the initial position.

2. The new position of point B_1 is determined by its invariable distance from points C and D respectively.

3. The new position of point C_1 is determined by the point of intersection of the circles of radii B_1C_1 and C_1D_1.

4. The new position of point B_2 is determined by its invariable distance from points C_1 and D_1 respectively.

5. The new position of point C_2 is determined by the point of intersection of the sliding pair rectilinear directrix with the circle of radius B_2C_2.

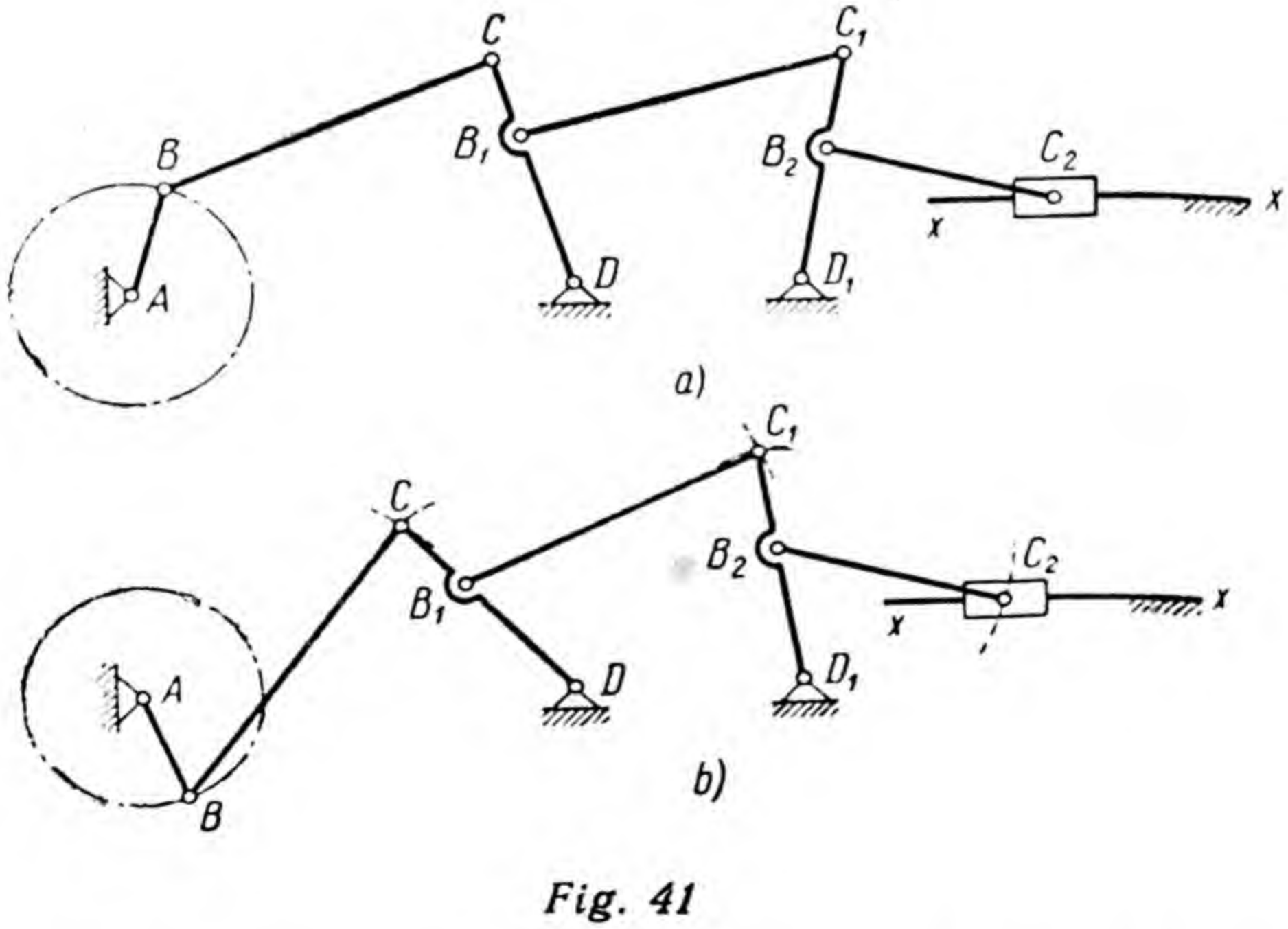

Fig. 41

In order to determine the positions of links of a higher pair, after changing the position of one of them, more complex constructions are required, since the relative disposition of these links depends on the shape of their

profiles. For instance, on turning link *1* of the higher pair, shown in Fig. 42, about the axis of turning pair *A* through a certain angle, and on drawing the profile of this link in turned position, it is necessary to determine the point of contact of the profiles and in accordance with the position of the point of contact to determine the turning angle of driven link *2* about the axis of turning pair *B*.

The position of higher pair links can be determined by using patterns of links. Plotting is simplified if the profiles are given in mathematical curves, and is altogether simple if the profiles or their portions are circles or straight lines.

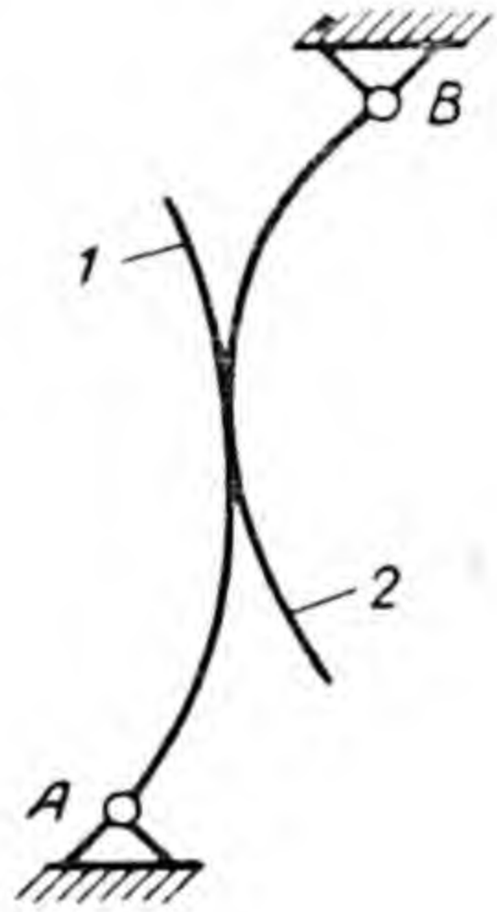

Fig. 42

13. VELOCITY DIAGRAM

The velocities of individual points of a mechanism at various positions can be determined by plotting velocity diagrams for corresponding positions. This method of determining velocities is as follows.

Let us assume that we know the magnitude and direction of the absolute velocities of points *B* and *D* of a rigid body that performs motion in a parallel plane (Fig. 43, *a*), and we have to determine the magnitude and direction of the absolute velocity of point *M* of this body.

Let us agree: 1) to denote absolute velocities by a small v, marking in the index with a capital letter the point whose velocity is designated: for instance v_B — the absolute velocity of point *B*; 2) to denote relative velocities also by small v with a two-letter index, the first of these to indicate the point whose velocity is designated, and the second, the point relative to which the velocity is examined: for example, v_{BD} — the velocity of point *B* relative to point *D*, v_{DB} — the velocity of point *D* relative to *B*; 3) a dash over letter v indicates that the velocity is examined as a vector, i. e. not only in magnitude but also in direction.

By joining points *B* and *D* with a straight line we get a diagram of the body in the form of a segment of line *BD*. Since the geometrical form of a body is of no significance for the kinematic analysis, and the position of a rigid body, regardless of its shape, is adequately determined by the

position of the line segment on it, we shall consider below the diagram (Fig. 43, *b*) *BD* of the body with point *M*, which is located at similar distances *BM* and *DM* from points *B* and *D* as in Fig. 43, *a*. By describing in Fig. 43, *b* the body as the diagram *BD*, we shall consider point *M*, which lies outside line *BD*, as the point which belongs to body *BD*, i. e. being rigidly connected with it.

To the chosen scale we lay off from arbitrary point *p* (Fig. 43, *c*) vectors $\overline{pb}$ and $\overline{pd}$ of absolute velocities $\bar{v}_B$ and $\bar{v}_D$. By joining points *b* and *d* with a straight line we get a velocity diagram of body *BD* in the form of triangle

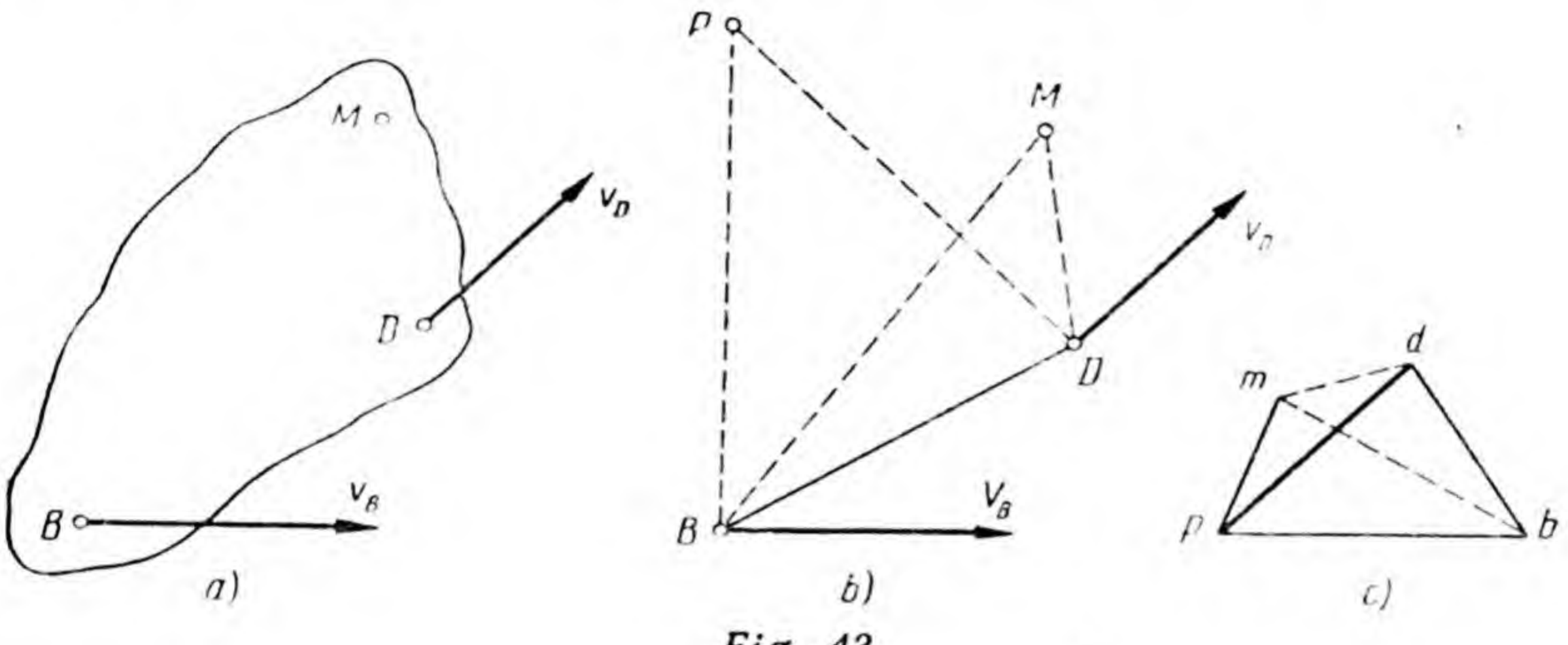

Fig. 43

pbd. The arrows which show the directions of absolute velocities at the termini of vectors $\overline{pb}$ and $\overline{pd}$ are unnecessary, since the directions of the vectors of absolute velocities which emerge from point *p* are quite clear without the arrows.

Point *p* is called the pole of the velocity diagram. Vector $\overline{db}$ (in the direction from *d* to *b*) is vector $\bar{v}_{BD}$; vector $\overline{bd}$ (in the direction from *b* to *d*) is vector $\bar{v}_{DB}$.

Since point *B* relative to *D* (i. e. with point *D* being arbitrarily fixed) and point *D* relative to *B* can move only along the circles of radii *BD*, velocities $\bar{v}_{BD}$ and $\bar{v}_{DB}$ can be directed only perpendicular to *BD*. Therefore side *bd* of triangle *pbd* is perpendicular to *BD*.

Capital letters *B* and *D* indicate in the body diagram the positions of points whose absolute velocities are given; the termini of vectors of absolute and relative velocities

of these points are marked in the velocity diagram by corresponding small letters b and d. Pole p of the diagram is the initial point of the vectors of absolute velocities of all the points of body BD. The point of body BD whose absolute velocity is zero is the instantaneous centre of rotation of body BD. In the velocity diagram the point which represents the absolute velocity of the instantaneous centre of rotation coincides with pole p.

Velocities $\bar{v}_B$ and $\bar{v}_D$ are directed perpendicular to the radii of rotation of points B and D about the instantaneous centre, therefore instantaneous centre of rotation P is located at the point of intersection of the perpendiculars to the vectors of velocities $\bar{v}_B$ and $\bar{v}_D$ which are drawn from points B and D. Triangle PBD is similar to triangle pbd and is similarly located. The similarity of the triangles results from the corresponding perpendicularity of the sides (for instance, side PD is perpendicular to side pd). The similarity of location is due to the fact that in passing the vertices of the angles of both triangles in the same direction, the vertices designated by the same letters are passed in similar succession (for example, in clockwise direction vertices $PDBP$ and $pdbp$ are passed in succession).

We shall proceed now to determine velocity v_M. In order to determine this velocity it is necessary to find on the velocity diagram point m, i. e. the vector terminus of the absolute velocity of point M.

Point M moves together with point B and, therefore, with velocity $\bar{v}_B$ of this point and, in addition, moves relative to this point with velocity $\bar{v}_{MB}$. Therefore, absolute velocity $\bar{v}_M$ is the geometric sum of velocities $\bar{v}_B$ and $\bar{v}_{MB}$, which is expressed by the following vector equation:

$$\bar{v}_M = \bar{v}_B + \bar{v}_{MB}.$$

The right-hand side of this equation signifies that in order to obtain the vector of velocity $\bar{v}_M$, which is the geometric sum of $\bar{v}_B$ and $\bar{v}_{MB}$, it is necessary to draw the vector of velocity $\bar{v}_B$, to add to the terminus of this vector the vector of velocity $\bar{v}_{MB}$ and then join the origin of the first vector with the terminus of the second one.

The vector of velocity $\bar{v}_B$ is already drawn — this is vector $\overrightarrow{pb}$ of the velocity diagram. It remains only to draw

onto the terminus of this vector, i. e. to point b, the vector of velocity $\bar{v}_{MB}$. Point M relative to point B can only rotate; hence, the vector of velocity $\bar{v}_{MB}$ from point b must be directed perpendicular to line BM. In order to obtain point m on the diagram it is necessary to determine the length of vector $\overline{bm}$, but this requires knowledge of the magnitude of velocity $\bar{v}_{MB}$, which is so far unknown. Therefore, from point b we do not draw vector $\overline{bm}$, but only the line of action of this vector. It therefore appears that one equation is insufficient for determining the velocity of point M.

In order to determine $\bar{v}_M$ we can also write a second vector equation:

$$\bar{v}_M = \bar{v}_D + \bar{v}_{MD}.$$

Considering that the vector of velocity $\bar{v}_D$, i. e. vector $\overline{pd}$, is already drawn and that velocity $\bar{v}_{MD}$ can be directed only perpendicular to MD, we draw from point d line of action $\bar{v}_{MD}$ perpendicular to MD. Point m, where the termini of the vectors of absolute and relative velocities of point M converge, must lie on both lines of action and is therefore located at the point of their intersection. By joining point m with pole p we get vector $\overline{pm}$ of absolute velocity $\bar{v}_M$.

In order to find point m on the velocity diagram we have joined on the diagram point M with points B and D, thus obtaining triangle BMD, and have drawn on the vector $\overline{bd}$ of relative velocities triangle bmd, which is similar to triangle BMD and also similarly located. In determining the absolute and relative velocities of any point of body BD it is necessary to proceed likewise. Triangle bmd on the velocity diagram is obtained in those cases when point M on the diagram lies outside line BD. If point M is located on segment BD or its extension, then on the velocity diagram point m will lie on segment bd or its extension. In this case as well segments bm and dm will be proportional to segments BM and DM.

If velocity $\bar{v}_M$ were specified and it were necessary to find on the diagram of the body point M, which in the position of the body, as shown in Fig. 43, moves with such velocity, it would be necessary to draw vector $\overline{pm}$ on the

diagram, to draw the triangle *bmd* and then plot on the diagram triangle *BDM*, which is similar to triangle *bmd* and similarly located.

The scale of the velocity diagram is found on drawing the first vector:

$$\mu_v = \frac{v_B}{pb},$$

where μ_v is the scale of the velocity diagram in m/sec × mm;

v_B — the magnitude of absolute velocity of point B in m/sec;

pb — the length of the vector of absolute velocity of point B in mm.

In order to determine the magnitude of the velocity of any point by the velocity diagram it is necessary to multiply the length of the vector of this velocity by the diagram scale.

The angular velocity ω of rotation of body BD may be obtained by dividing the absolute velocity of any point of the body by its distance to the instantaneous centre of rotation; for example:

$$\omega = \frac{v_B}{PB},$$

where v_B — in m/sec and PB — in m.

In order to get PB in m it is necessary to measure PB in mm on the diagram and multiply by diagram scale μ_l m/mm.

If point P lies beyond the drawing, then on the basis of the similarity of triangles PBD and pbd it is possible to substitute $k \times pb$ for PB, where k is the relation of the lengths of similar sides which equals $k = \frac{BD}{bd}$. In this way we get (by expressing pb in mm and multiplying v_B by 10^3 mm/m)

$$\omega = 10^3 \times v_B / k \times pb = \frac{10^3}{k} \mu_v.$$

In the above plotting of the velocity diagram we had four data at our disposal: the magnitudes and the directions of both velocities $\bar{v}_B$ and $\bar{v}_D$. The velocity diagram can be plotted also from any three of these data. For

example, if velocity $\bar{v}_D$ were known only in direction, then from pole p instead of vector $\overline{pd}$ we could have drawn only a line of action of this vector; the position of point d would have been determined in this case as a result of drawing line of action $\bar{v}_{DB}$, of the second geometric component of vector equation

$$\bar{v}_D = \bar{v}_B + \bar{v}_{DB}.$$

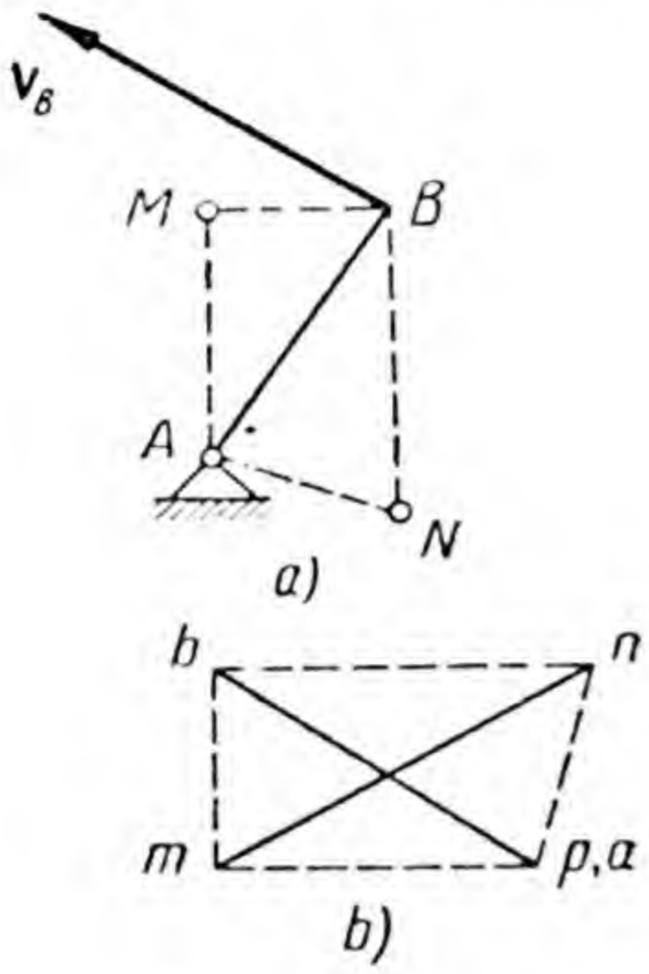

Fig. 44

Example 1. For a mechanism of class I order 1, in the position as shown in Fig. 44, *a*, plot the velocity diagram and using the diagram, determine $\bar{v}_{MN}$, considering points M and N as belonging to link AB. The velocity of point B is given by vector $\bar{v}_B$.

From pole p we draw $\overline{pb}$, vector $\bar{v}_B$ (Fig. 44, *b*). Since point A is fixed, point a, the terminus of vector $\overline{pa}$ of velocity v_A, will coincide with pole p. Line $\overline{pb}$ is the velocity diagram.

In order to determine $\bar{v}_M$ we plot on line pb triangle pmb, which is similar to triangle AMB and is similarly located; $\overline{pm}$ is vector $\bar{v}_M$. Similarly we obtain on the diagram pn, i. e. vector $\bar{v}_N$. By joining points m and n with a straight line we get nm, i. e. vector $\bar{v}_{MN}$.

Exmaple 2. Links BC and CD are connected at point C into a turning pair (Fig. 45, *a*).

The velocities of points B and D are given by vectors $\bar{v}_B$ and $\bar{v}_D$. Determine $\bar{v}_C$.

Point C, belonging to link BC, moves together with point B and consequently with velocity $\bar{v}_B$; it also moves about point B with velocity $\bar{v}_{CB}$.

Belonging to link CD, point

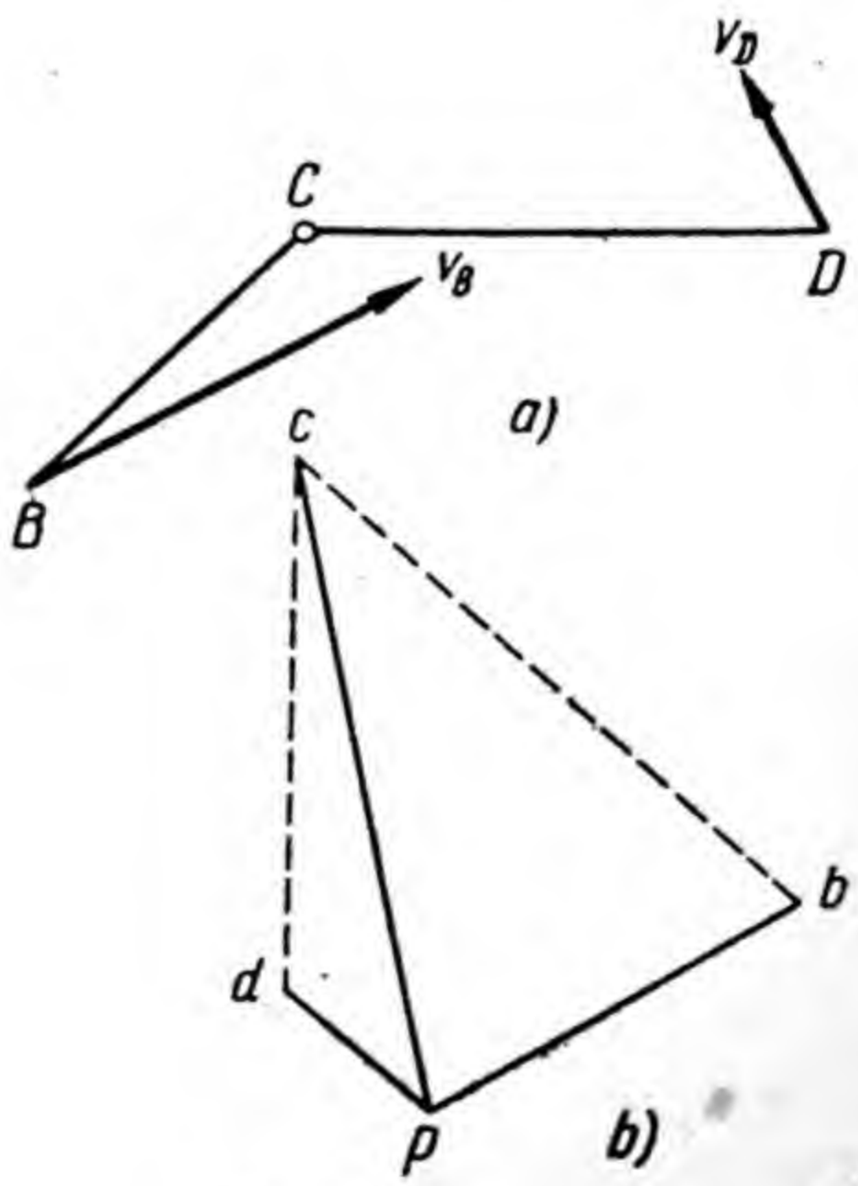

Fig. 45

C moves with point D and consequently with velocity $\bar{v}_D$, it also moves about point D with velocity $\bar{v}_{CD}$.

In both cases velocity $\bar{v}_C$ is obtained in the form of a geometric sum of two components. Therefore, for determining $\bar{v}_C$ we have at our disposal two vector equations:

$$\bar{v}_C = \bar{v}_B + \bar{v}_{CB};$$

$$\bar{v}_C = \bar{v}_D + \bar{v}_{CD}.$$

In accordance with the first of these equations we first have to draw vector $\overline{pb}$ of velocity $\bar{v}_B$ on the velocity diagram (Fig. 45, b), and then draw the vector of velocity $\bar{v}_{CB}$ to point b. Velocity $\bar{v}_{CB}$ can be directed only perpendicular to BC, since point C relative to point B can move only along the circumference of radius BC. Since the magnitude of $\bar{v}_{CB}$ is unknown we only draw from point b the line of action $\bar{v}_{CB}$ perpendicular to BC.

In accordance with the second equation and bearing in mind the considerations already stated we draw $\overline{pd}$, vector v_D, and from point d the line of action $\bar{v}_{CD}$ perpendicular to CD.

Since point c of the velocity diagram must lie on both lines of action, by joining their point of intersection with the pole we get $\overline{pc}$, vector $\bar{v}_C$.

Example 3. Fig. 46, a shows the diagram of a four-link mechanism with three turning pairs and one sliding pair. Driving link *1* and slider *2* together form a sliding pair; link *3*, connected with the crosshead, forms turning pair B. The angular velocity of link *1* is directed clockwise, its magnitude is known. Determine $\bar{v}_B$.

We mark on link *1* point B_x, which is located under point B, i. e. located at distance AB_x from point A, which equals AB.

In order to determine $\bar{v}_B$ we can write two vector equations:

$$\bar{v}_B = \bar{v}_{B_x} + \bar{v}_{BB_x};$$

$$\bar{v}_B = \bar{v}_C + \bar{v}_{BC}.$$

In accordance with the first equation we have to draw

$\overline{pb}_x$, i. e. vector $\bar{v}_{B_x}$, and to the terminus of this vector draw vector $\overline{b_x b}$ of velocity $\bar{v}_{BB_x}$.

The length of vector $pb_x = \frac{v_{B_x}}{\mu_v} = \frac{l_{AB_x} \times \omega}{\mu_v}$, where l_{AB_x} is the length of AB_x, ω is the angular velocity of link *1*, and μ_v is the scale of the velocity diagram.

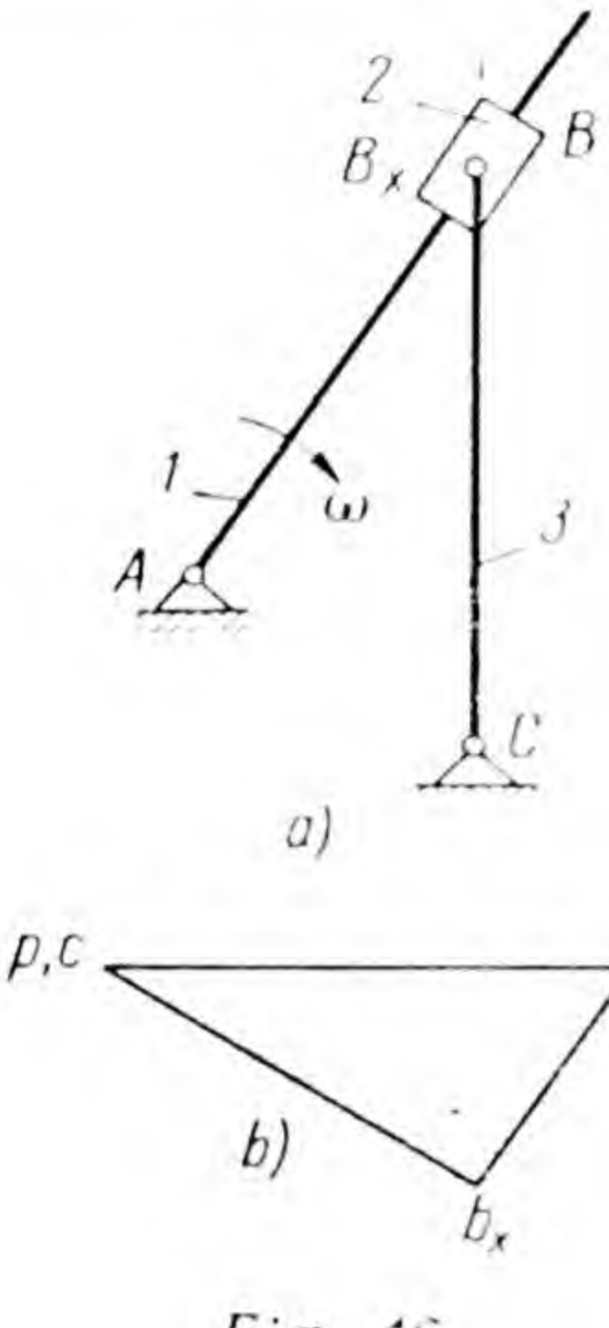

Fig. 46

The length of vector $b_x b$ cannot yet be determined because the magnitude of velocity $\bar{v}_{BB_x}$ is unknown. Since point B relative to point B_x can displace only along link *1*, by drawing vector $\overline{pb}_x$ perpendicular to link *1* we draw from point b_x the line of action $\bar{v}_{BB_x}$ parallel to link *1* (Fig. 46, *b*).

In accordance with the second equation we place point c in the pole since $v_C = 0$, and from point c, we draw the line of action $\bar{v}_{BC}$ perpendicular to BC, since point B relative to point C can displace only along the circle of radius BC. The magnitude and direction $\overline{pb}$, i. e. of vector $\bar{v}_B$ is determined by point b of intersection of the lines of action.

Example 4. At the instant corresponding to the position in Fig. 47, *a* of links *1* and *2* of the three-link mechanism with a higher pair, point R of link *1* and point S of link *2* are in contact. Angular velocity ω of rotation of driving link *1* is known. Determine $\bar{v}_{RS}$.

For the solution of this problem we have at our disposal the following data:

1) the magnitude and direction of velocity $\bar{v}_R$: magnitude $v_R = l_{AR}\omega$, where l_{AR} is the length AR, direction — to the right perpendicular to AR;

2) the direction of velocity v_S: to the right perpendicular to BS; magnitude $\bar{v}_S$ is unknown, since the angular velocity of rotation of the driven link is unknown;

3) the line of action of velocity $\bar{v}_{SR}$: tangentially to the profiles of the links at the point of contact. Point S relative

to point R can move only tangentially to the profiles at the point of contact, since otherwise point S would either cut into the profile of the driving link or would move away from it.

In accordance with vector equation

$$\bar{v}_S = \bar{v}_R + \bar{v}_{SR},$$

we draw vector $\overline{pr}$ of velocity $\bar{v}_R$, which equals $pr = v_R/\mu_v$, where μ_v is the scale of the velocity diagram, and from point r we draw the line of action v_{SR}. Since only the direction of velocity $\bar{v}_S$ is known we draw from pole p the line of action of this velocity (Fig. 47, b).

The position of point s on the velocity diagram is determined by the point of intersection of lines of action $\bar{v}_{SR}$ and $\bar{v}_S$. Vector $\overline{sr}$ is vector $\bar{v}_{RS}$.

Example 5. Plot the velocity diagram and determine the velocities $\bar{v}_{CB}$ and $\bar{v}_{CD}$ in the position of the four-bar mechanism which is shown in Fig. 122, a in accordance with the data given on p. 133 (numerical example).

Example 6. Plot the velocity diagram and determine velocity v_{CB} in the position of the slider crank mechanism which is shown in Fig. 123, a in accordance with the data given on p. 141 (numerical example).

Example 7. Plot the velocity diagram and determine velocities $\bar{v}_{CB}$, $\bar{v}_{ED}$, $\bar{v}_{EF}$ and the angular velocity of rotation of link EF in the position of the six-link mechanism which is shown in Fig. 124, a in accordance with the data given on p. 148 (numerical example).

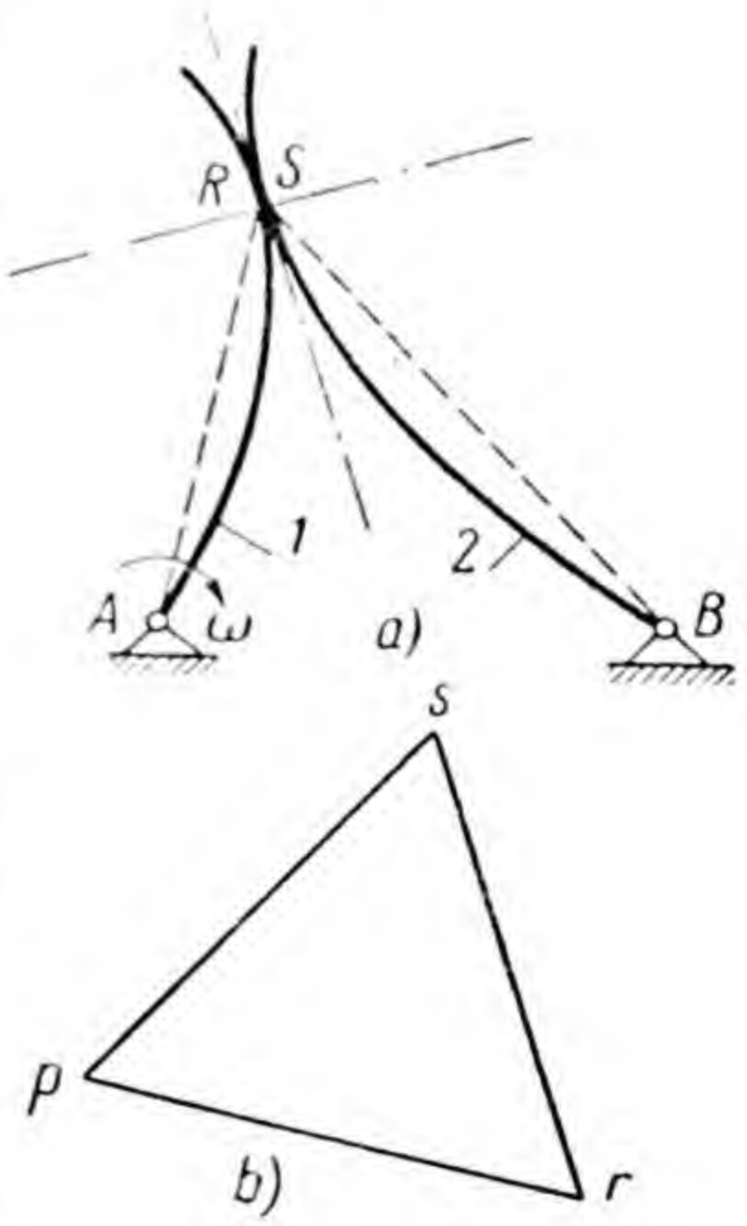

Fig. 47

14. ACCELERATION DIAGRAM

Let us assume that we know from the velocity diagram the velocities of all the points which belong to body BD (Fig. 48, a), and absolute accelerations $\bar{a}_B$ and $\bar{a}_D$ of its two points B and D. It is necessary to determine acceleration $\bar{a}_M$ of point M which belongs to body BD.

Body BD performs compound motion. In examining it as motion together with point B and rotation about point B, in order to determine the total acceleration of point M, we obtain vector equation

$$\bar{a}_M = \bar{a}_B + \bar{a}_{MB},$$

or, since the total relative acceleration $\bar{a}_{MB}$ is the geometric sum of the normal and tangential,

$$a_M = a_B + \bar{a}^n_{MB} + \bar{a}^\tau_{MB},$$

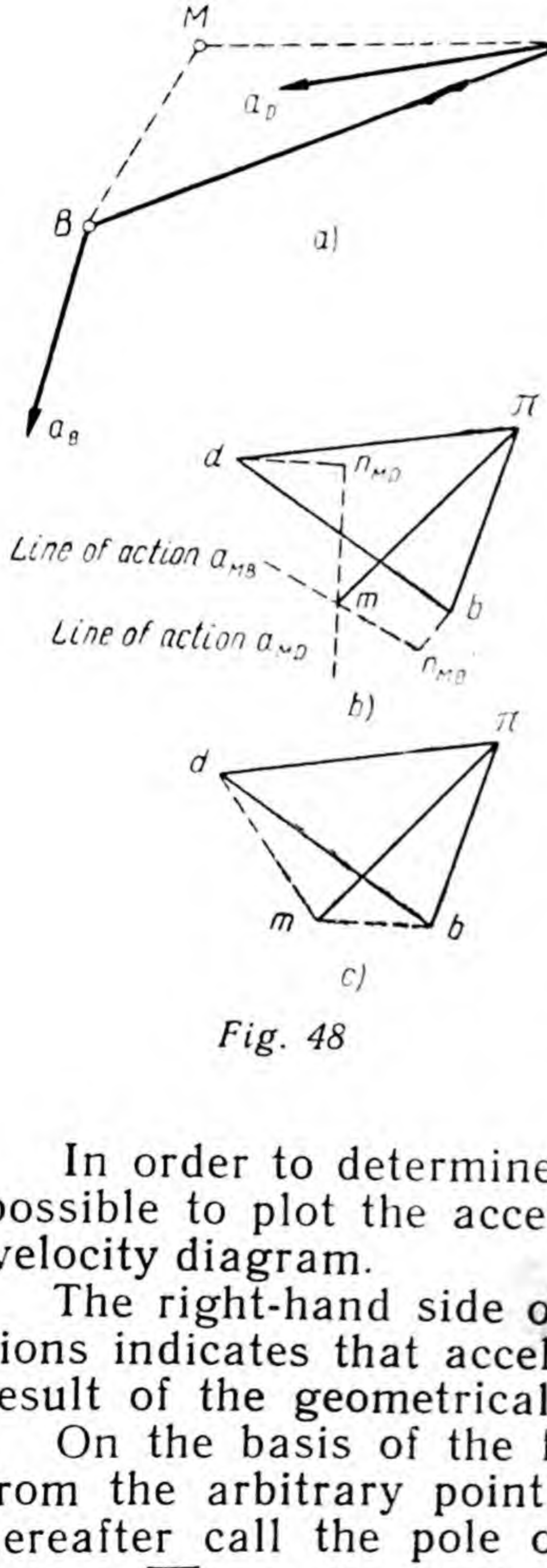

Fig. 48

In this equation acceleration $\bar{a}_B$ is known in magnitude and direction, normal acceleration $\bar{a}^n_{MB}$ is directed from point M to point B and is equal to v^2_{MB}/l_{BM}, the tangential acceleration $\bar{a}^\tau_{MB}$ is directed perpendicular to BM and its magnitude is unknown.

In examining the motion of point M as motion together with point D and motion relative to D, we obtain

$$\bar{a}_M = \bar{a}_D + \bar{a}^n_{MD} + \bar{a}^\tau_{MD},$$

where $\bar{a}_D$ is known in magnitude and direction, $\bar{a}^n_{MD} = v^2_{MD}/l_{MD}$ and is directed along DM from M to D; $\bar{a}^\tau_{MD}$ which is unknown in magnitude is directed perpendicular to DM.

In order to determine the acceleration of point M it is possible to plot the acceleration diagram similarly to the velocity diagram.

The right-hand side of each of the above vector equations indicates that acceleration $\bar{a}_M$ can be obtained as a result of the geometrical addition of three accelerations.

On the basis of the first of these equations we draw from the arbitrary point π (Fig. 48, *b*), which we shall hereafter call the pole of the acceleration diagram, the vector $\overline{\pi b}$ of the first of the geometrical components,

vector $\bar{a}_B$. Vector $\overline{bn}_{MB}$ of the second geometrical component, acceleration $\bar{a}^n_{MB}$, must be drawn to the terminus of this vector. On the body diagram acceleration $\bar{a}^n_{MB}$ is directed from point M to point B, therefore vector $\overline{bn}_{MB}$ from point b must also be directed parallel to MB downwards and to the left. Vector $\overline{bn}_{MB}$ must be laid off to the same scale as vector $\overline{\pi b}$ was laid off.

The scale of the acceleration diagram, which results after drawing vector πb equals

$$\mu_a = \frac{a_B}{\pi b} \text{ m/sec}^2 \times \text{mm},$$

and therefore

$$bn_{MB} = \frac{a^n_{MB}}{\mu_a} \text{ mm}.$$

To the terminus of vector $\overline{bn}_{MB}$, i. e. to point n_{MB}, we must draw the vector of the last geometrical component, acceleration $\bar{a}^\tau_{MB}$. Since this acceleration is known only in direction, we have to confine ourselves to drawing its line of action perpendicular to MB or perpendicular to $\overline{bn}_{BM}$ which is the same thing. Thus, as a result of using the first of the above vector equations we only find that point m, the terminus of vector $\overline{\pi m}$ of absolute acceleration $\bar{a}_M$ of this point, must lie on the line of action of acceleration $\bar{a}^\tau_{MB}$ drawn through point n_{MB}.

In accordance with the second of the above vector equations we draw from pole π vector $\overline{\pi d}$ of acceleration $\bar{a}_D$, and to the terminus of this vector we draw vector $\overline{dn}_{MD}$ of acceleration $\bar{a}^n_{MB}$. The length of vector $\overline{dn}_{MD}$ is equal to $\bar{a}^n_{MD}/\mu_a$, the direction is parallel to MD from point d downwards and to the right, i. e. the same as the direction of acceleration $\bar{a}^n_{MD}$ on the body diagram. Since acceleration $\bar{a}^\tau_{MD}$ is known only in direction, we draw the line of action of this acceleration from point n_{MD} perpendicular to MD or perpendicular to $\overline{dn}_{MD}$, which is the same thing. Point m, which is the terminus of vector $\overline{\pi m}$ of unknown acceleration $\bar{a}_M$, is located at the point of

intersection of both lines of action; this point must be located on each of these lines.

If we were to join point m in Fig. 48, b by means of straight lines with points b and d, we should get triangle bmd which is similar to triangle BMD on the body diagram and is similarly located. Therefore, the position of point m on the acceleration diagram could also be determined as shown in Fig. 48, c, i. e. by plotting on vector $\overline{bd}$ triangle bmd, which is similar to triangle BMD and is similarly

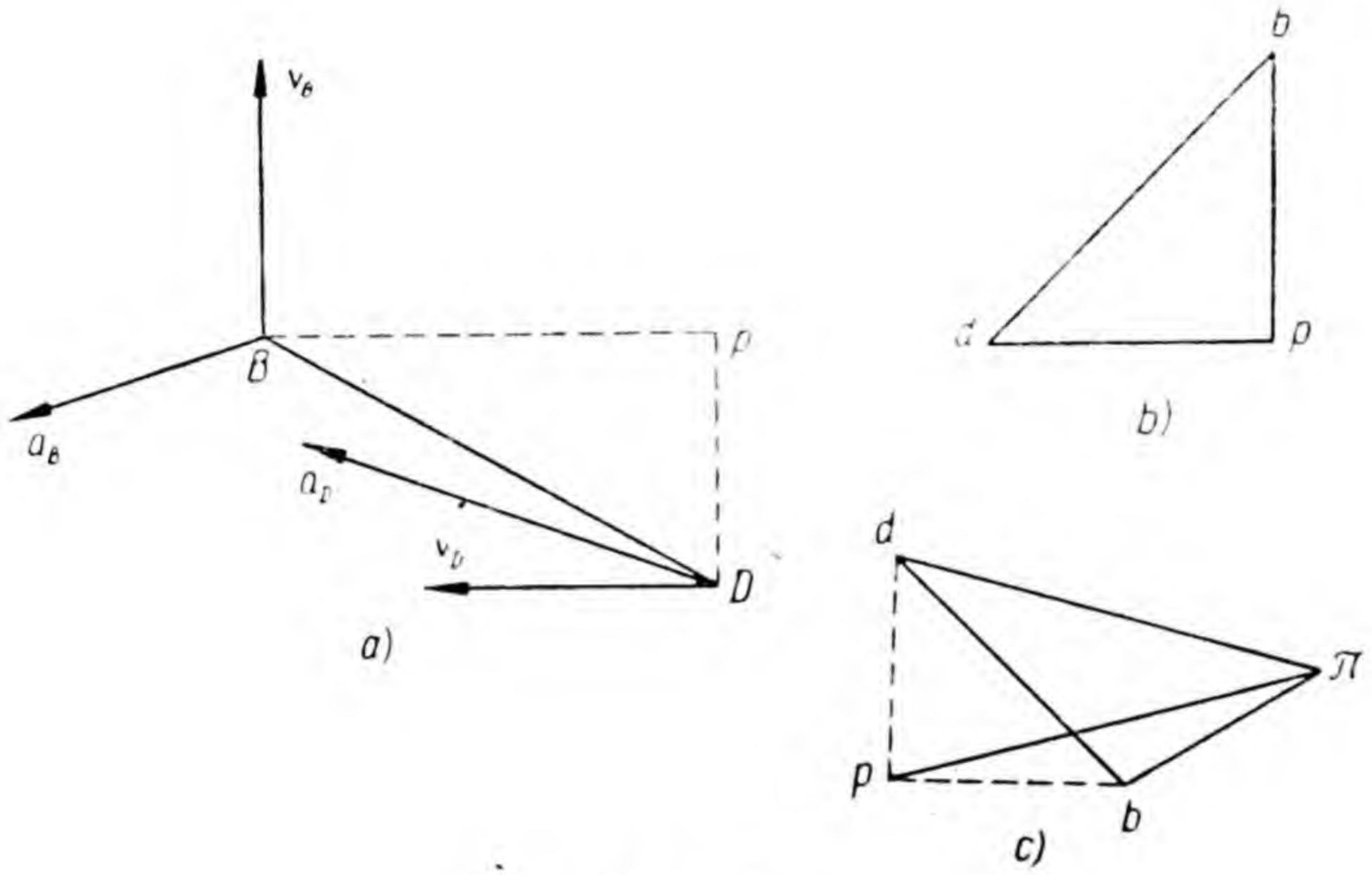

Fig. 49

located. The triangles are similar because the lengths of bd, bm and dm of the vectors of the relative accelerations are proportional to the lengths of segments BD, BM, and DM, which are the radii of rotation during motion of the extreme points of these segments relative to each other.

Example 1. The absolute velocities and accelerations of points B and D of body BD, which performs motion in a parallel plane, are given by the vectors drawn on the diagram (Fig. 49, a). Determine the acceleration of the instantaneous centre of rotation of the body.

We plot the velocity diagram pbd (Fig. 49, b) and the acceleration diagram πbd (Fig. 49, c).

In order to determine the position of the instantaneous centre P of rotation in Fig. 49, a triangle BPD is plotted,

which is similar to triangle bpd in Fig. 49, b and is similarly located. In order to determine on the acceleration diagram the position of point p, which is the terminus of vector $\overline{\pi p}$ of the unknown acceleration $\bar{a}_P$, we plot on vector $\overline{bd}$ triangle bpd, which is similar to triangle BPD (Fig. 49, a) and is similarly located.

Since the three triangles mentioned must be similar and similarly located, there is no necessity to plot triangle BPD in Fig. 49, a: we can confine ourselves to plotting on vector bd of the acceleration diagram (Fig. 49, c) triangle bpd, which is similar to triangle bpd on the velocity diagram (Fig. 49, b) and is similarly located. By joining point p with pole π we obtain vector πp of acceleration $\bar{a}_P$.

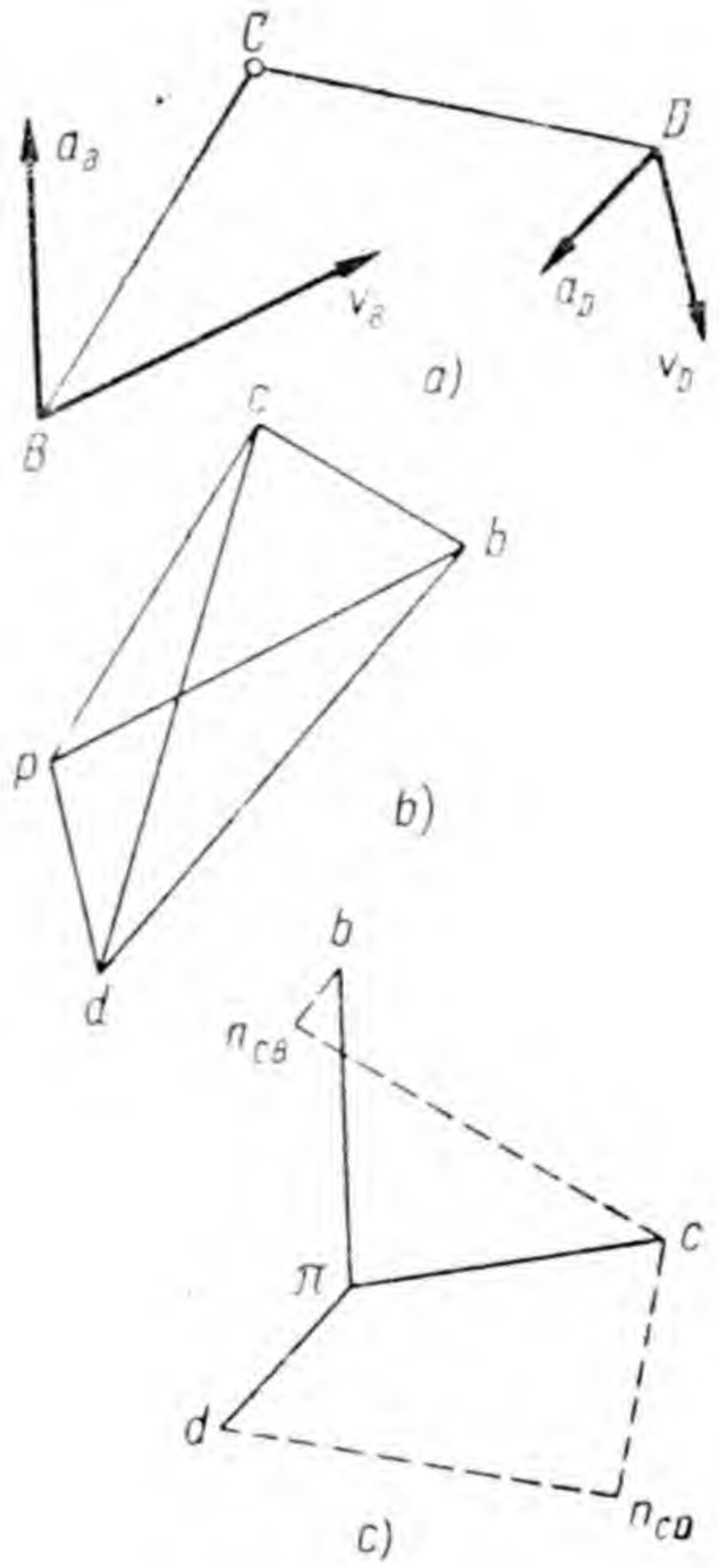

Fig. 50

Example 2. Links BC and CD are connected in turning pair C. Velocities $\bar{v}_B$ and $\bar{v}_D$ and accelerations $\bar{a}_B$ and $\bar{a}_D$ are known. Determine $\bar{a}_C$ (Fig. 50, a).

In order to determine velocities $\bar{v}_{CB}$ and $\bar{v}_{CD}$, which are essential for plotting the acceleration diagram, we plot the velocity diagram (Fig. 50, b).

By considering first the motion of point C as motion together with point B and motion relative to point B, and then as motion with point D and motion relative to point D, we get two vector equations for determining $\bar{a}_C$:

$$\bar{a}_C = \bar{a}_B + \bar{a}^n_{CB} + \bar{a}^\tau_{CB};$$

$$\bar{a}_C = \bar{a}_D + \bar{a}^n_{CD} + \bar{a}^\tau_{CD}.$$

Proceeding from the first equation we draw $\overline{\pi b}$, vector $\bar{a}_B$ (Fig. 50, c). Magnitude $a^n_{CB} = v^2_{CB}/l_{BC} = (bc \times \mu_v)^2/l_{BC}$,

where bc is the length of vector $\bar{v}_{CB}$ on the velocity diagram and μ_v is the scale of the velocity diagram. The direction of $\bar{a}^n_{CB}$ in Fig. 50, *a* is from point *C* to point *B*. Therefore, we draw also vector $\overline{bn}_{CB}$ of this acceleration from point *b* parallel to *BC*. We draw the line of action of acceleration $\bar{a}^\tau_{CB}$, which is unknown in magnitude, from point n_{CB} perpendicular to *BC* and hence to $\overline{bn}_{CB}$.

In accordance with the second equation we draw $\overline{\pi d}$, vector $\bar{a}_D$, then from the terminus of this vector $\overline{dn}_{CD}$, vector $\bar{a}^n_{CD} = v^2_{CD}/l_{CD} = (cd \times \mu_v)^2/l_{CD}$ parallel to *CD* to the right, and from point n_{CD} the line of action $\bar{a}^\tau_{CD}$ perpendicular to *CD*.

Magnitude and direction $\overline{\pi c}$, vector $\bar{a}_C$, are determined from the point of intersection of the lines of action.

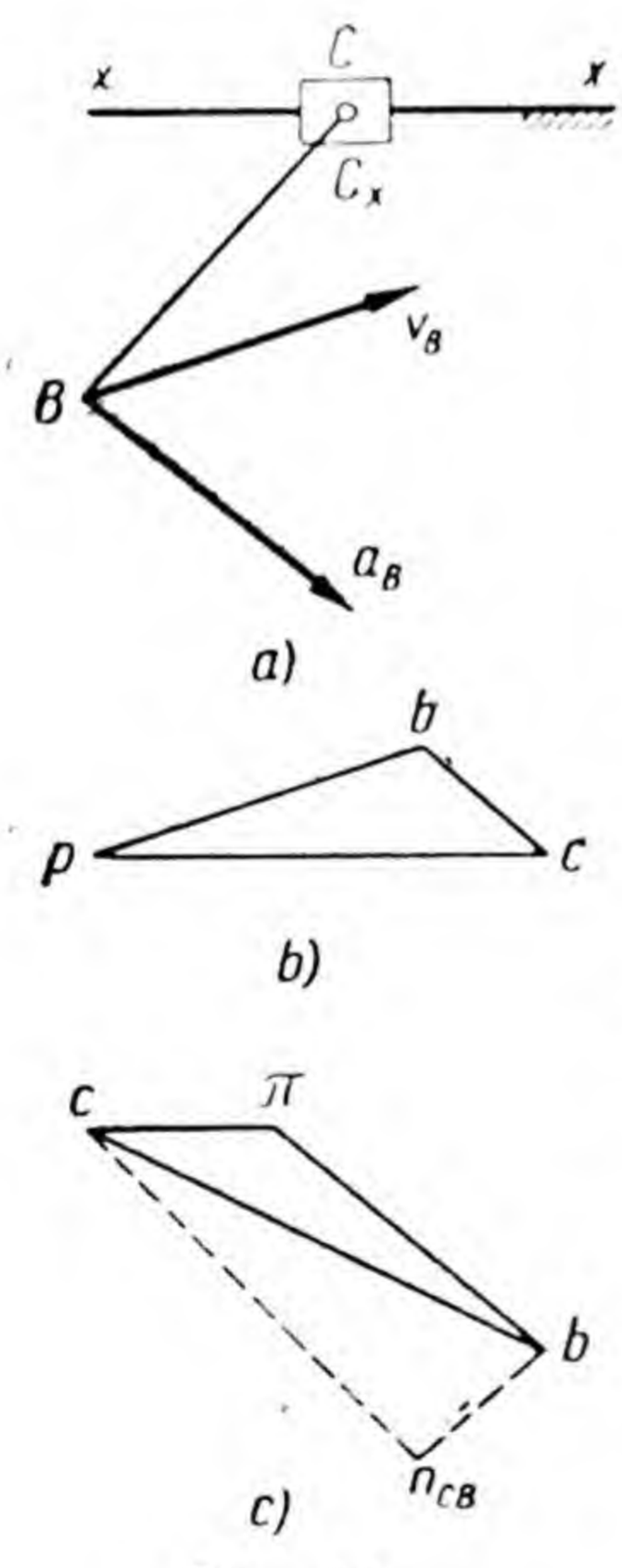

Fig. 51

Example 3. Link *BC* is coupled with the slider, which moves along fixed directrix *xx* (Fig. 51, *a*) in turning pair *C*. In the instant, corresponding to the position presented in Fig. 51, *a* velocity $\bar{v}_B$ and acceleration $\bar{a}_B$ are known. Determine $\bar{a}_C$.

We plot first the velocity diagram which is necessary for plotting the acceleration diagram (Fig. 51, *b*).

By considering first the motion of point *C* as motion together with point *B* and motion relative to point *B*, and then as motion together with point C_x, which is rigidly connected with the directrix, and motion relative to this point (point C_x may be assumed as located on the directrix under point *C*), we obtain two vector equations for determining $\bar{a}_C$:

$$\bar{a}_C = \bar{a}_B + \bar{a}^n_{CB} + \bar{a}^\tau_{CB};$$

$$\bar{a}_C = \bar{a}_{C_x} + \bar{a}^n_{CC_x} + \bar{a}^\tau_{CC_x}.$$

On the basis of the first equation we draw from pole $\overline{\pi b}$ vector $\bar{a}_B$ (Fig. 51, *c*). Magnitude $a^n_{CB} = v^2_{CB}/l_{BC} =$

$=(bc\times\mu_v)^2/l_{BC}$, where bc is the length of vector $\bar{v}_{CB}$ on the velocity diagram, and μ_v is the scale of the velocity diagram. Length $bn_{CB}=a^n_{CB}/\mu_a$, where $\overline{bn}_{CB}$ is vector $\bar{a}^n_{CB}$, and μ_a is the scale of the acceleration diagram. Direction $\bar{a}^n_{CB}$ in Fig. 51, *a* is from point *C* to point *B*, therefore on the acceleration diagram we also draw vector $\overline{bn}_{CB}$ parallel to *BC* from point *b* downwards and to the left. Magnitude $\bar{a}^\tau_{CB}$ is unknown, the direction is perpendicular to *BC* and hence also to $\overline{bn}_{CB}$; in this direction we draw from point n_{CB} the line of action of this acceleration.

On the right-hand side of the second equation, each of the first two geometrical components is zero/a_{C_x}, since point C_x is fixed, and $a^n_{CC_x}=v^2_{CC_x}/\rho$ because radius ρ of the path curvature along which point *C* displaces relative to point C_x is infinity. Acceleration $\bar{a}_{CC_x}$ in Fig. 51, *a* is directed along directrix *xx*, we therefore draw from pole π the line of action of this acceleration parallel to the directrix.

The magnitude and direction $\overline{\pi c}$, vector $\bar{a}_C$, are determined by point *c* of intersection of lines of action $\bar{a}^\tau_{CB}$ and $\bar{a}^\tau_{CC_x}$.

Vector $\overline{\pi c}$ on the acceleration diagram is directed to the left, whereas vector $\overline{pc}$ on the velocity diagram is directed to the right; hence, point *C* in the position, as shown in Fig. 51, *a*, moves more slowly.

Example 4. Plot the acceleration diagram for the mechanism, the diagram of which is given in Fig. 52, *a*.

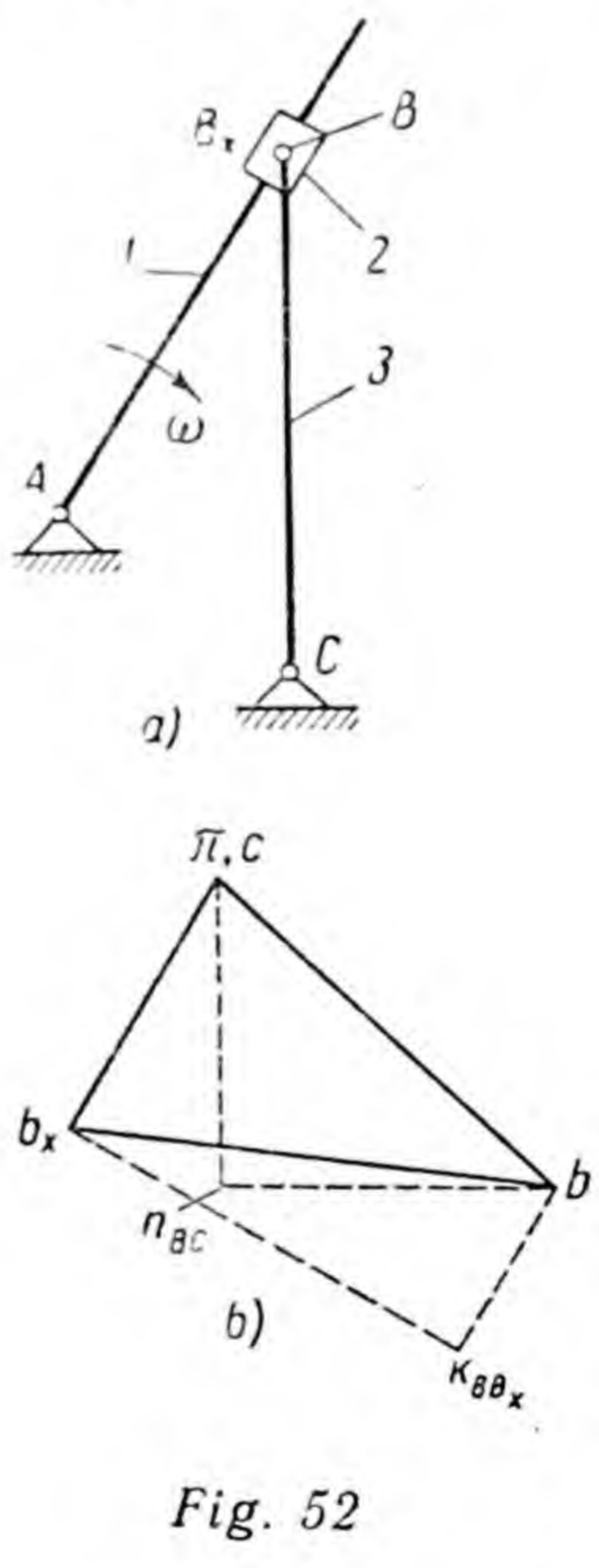

Fig. 52

In constructing the vector equations for determining accelerations $\bar{a}_B$ it is necessary to bear in mind that point *B*, displacing along the turning link, moves with rotary (Coriolis) acceleration which we shall also denote by letter *a* with *k* as the upper index.

In order to determine $\bar{a}_B$ we write two vector equations:

$$\bar{a}_B = \bar{a}_{B_x} + \bar{a}^n_{BB_x} + \bar{a}^k_{BB_x} + \bar{a}^\tau_{BB_x};$$

$$\bar{a}_B = \bar{a}_C + \bar{a}^n_{BC} + \bar{a}^\tau_{BC}.$$

We determine the magnitudes and directions of the geometrical components on the right-hand sides of both equations:

Acceleration	Magnitude	Direction
$\bar{a}_{B_x}$	$v^2_{B_x}/l_{AB_x} = (pb_x \times \mu_v)^2/l_{AB_x}$, where pb_x is the length of vector $\bar{v}_{B_x}$ on the velocity diagram, shown in Fig. 46, *b*, and μ_v is the scale of this diagram	From point B_x (Fig. 52, *a*) to point *A*, since during rotation of link *1* with constant velocity the total acceleration will be normal
$\bar{a}^n_{BB_x}$	$v^2_{BB_x}/\rho = 0$, since $\rho = \infty$	—
$\bar{a}^k_{BB_x}$	$2\omega \times v_{BB_x} = 2\omega(bb_x \times \mu_v)$, where bb_x is the length of vector $\bar{v}_{BB_x}$ on the velocity diagram	Is determined by the vector of velocity $\bar{v}_{BB_x}$, which is turned through 90° in the direction of rotation of link *1*, i. e. in this case clockwise. Velocity $\bar{v}_{BB_x}$ is directed upwards and to the right (see vector $\overline{b_x b}$ in Fig. 46, *b*) parallel to link *1*; hence, acceleration $\bar{a}^k_{BB_x}$ is directed to the right perpendicular to link *1*.
$\bar{a}^\tau_{BB_x}$	Is unknown	Along link *1*
$\bar{a}_C$	Is zero, since point *C* is fixed	—
$\bar{a}^n_{BC}$	$v^2_{BC}/l_{BC} = (cb \times \mu_v)^2/l_{BC}$, where cb is the length of vector $\bar{v}_{BC}$ on the velocity diagram	From point *B* to point *C*
$\bar{a}^\tau_{BC}$	Is unknown	Perpendicular to link *3*

After dividing the magnitudes of accelerations by scale μ_a of the acceleration diagram we determine the lengths of the vectors. Taking into consideration the directions of all vectors as indicated above in accordance

with the first of the above equations, we draw in succession (Fig. 52, *b*) vector πb_x of acceleration $\bar{a}_{B_x}$, vector $\overline{b_x k}_{BB_x}$ of acceleration $\bar{a}^k_{BB_x}$ and the line of action of acceleration $\bar{a}^\tau_{BB_x}$. In accordance with the second equation we draw from point *c*, which coincides with pole π, vector $\overline{cn}_{BC}$ of acceleration $\bar{a}^n_{BC}$ and from the terminus of this vector the line of action of acceleration $\bar{a}^\tau_{BC}$. The terminus of vector πb of acceleration $\bar{a}_B$ is determined from point *b* of intersection of the lines of action of acceleration $\bar{a}^\tau_{BB_x}$ and $\bar{a}^\tau_{BC}$.

Example 5. Plot the acceleration diagram for the four-bar mechanism in the position, shown in Fig. 122, *a* in accordance with the data given on p. 133, and determine accelerations a_{S_1}, a_{S_2} and a_S of the centres of gravity (numerical example).

Example 6. Plot the acceleration diagram for the slider crank mechanism in the position, shown in Fig. 123, *a* in accordance with the data given on p. 141, and determine accelerations a_{S_1}, a_{S_2}, a_C (numerical example).

Example 7. Plot the acceleration diagram for the six-link mechanism shown in Fig. 124, *a* in accordance with the data given on p. 148, and determine accelerations a_{S_1}, a_{S_2}, a_C, a_{S_4} and a_{S_5} and the angular acceleration of link *EF*.

15. KINEMATIC DIAGRAMS

The velocities and accelerations of individual points at various positions of a mechanism are determined by kinematic investigation. Kinematic diagrams in the form of curved paths, velocities and accelerations render a graphic representation of the kinematics of a mechanism. Besides these curves it is necessary in some cases to plot also the paths of individual points.

We shall now study the methods for plotting kinematic diagrams using as an example a four-link slider crank mechanism, which is widespread in engineering.

As we already said, the slider crank mechanism is the basis of various piston engines, piston pumps and com-

pressors, and of a large number of other mechanical devices. In piston engines the motive link of the mechanism is always the slider, in piston pumps and compressors it is the crank, but in the majority of devices, where a slider crank mechanism is applied, the crank, regardless of whether it is a motive one or not, rotates with an angular velocity which is very close to constant velocity. Therefore, in the kinematic investigation of a slider crank mechanism as the driving link (i. e. a link moving in accordance with specified laws of motion) it is convenient to choose a crank also when it is not serving as a motive link.

In a case of constant angular velocity the angles of rotation of the crank from a certain initial position are in direct proportion to the time intervals during which rotations take place; therefore the curves which express the relations of the paths, velocities and accelerations of any of the points of the mechanism to the angle of rotation of the crank are at the same time also the curves which express the time relations of the same magnitudes.

Fig. 53, *a* shows to scale the diagram of a slider crank mechanism with crank *AB* 200 mm in length and connecting rod *BC* 600 mm in length.

The crank rotates with constant angular velocity at 240 r. p. m.

We shall plot the diagrams of the paths, velocities and accelerations of point *C*, which is usually of great importance in the study of slider crank mechanisms.

Accuracy is essential in plotting the curves, from which the magnitudes from 12 to 24 ordinates of each curve are found. We will plot 12 points of each curve. When point *B* is in its extreme left position, point *C* also occupies its extreme left position. Let us consider this position as initial, and on the path of point *B* we shall mark it number *1*. Having divided into 12 equal parts the circle described by point *B*, we mark with successive numbers the different positions of point *B* in the direction of crank rotation, i. e. clockwise. We also mark with the same numbers the respective positions of point *C* on the directrix.

We lay off along the axis of abscissae (Fig. 53, *b*) segment *1-1* and consider its length as the graphic expression of the time interval, which equals 0.25 sec, in the course of which (at 240 r. p. m.) the crank makes one turn. We divide this segment into 12 equal parts, i. e. the same num-

ber of equal parts into which the path of point B is divided in Fig. 53, *a*.

We first plot curve $s=f(t)$, where s is the distance of point C which is read to the right from its initial (extreme

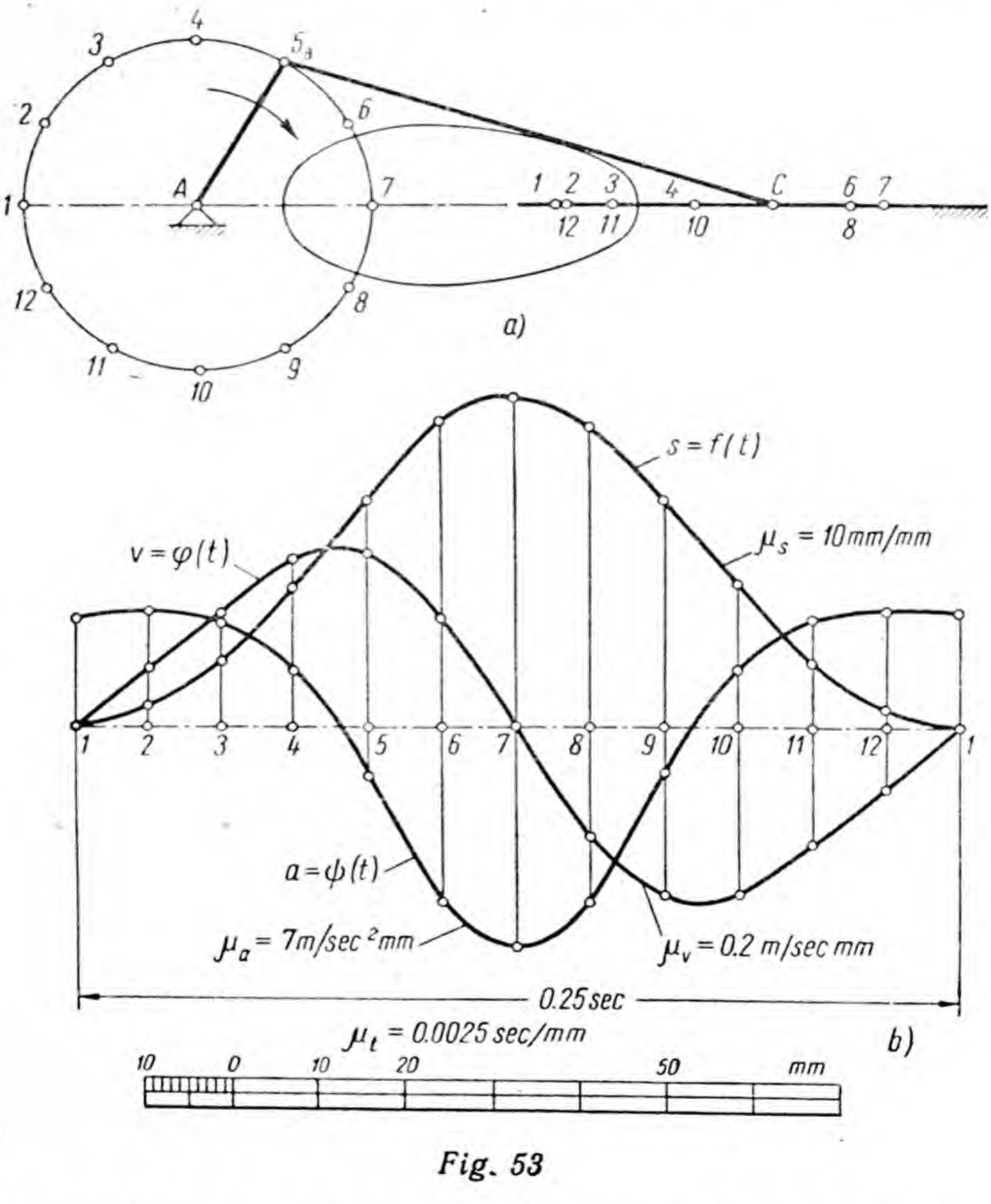

Fig. 53

left) position, and t is the time interval which is read from the initial moment. Since the positions of point C on its path at different positions of point B are determined by invariable distance BC between these points, it is not difficult to find the ordinates of curve $s=f(t)$. By drawing the ordinates in Fig. 53, *b* and joining them with a smooth curve we obtain curve $s=f(t)$.

In order to plot curve $v=\varphi(t)$, where v is the velocity of point C, and t has the same value as in the previous curve, it is necessary to determine the velocities of point C at 12 different positions of point B, and for this purpose, generally speaking, it is necessary to plot the same number of velocity diagrams. Since in this case the mechanism is symmetrical and therefore the location of the curve $s=f(t)$ is also symmetrical relative to the mean ordinate drawn from point 7, the velocities of point C in symmetrical positions relative to this ordinate will be equal in magnitude and opposite in sign. Taking this into consideration we can confine ourselves to plotting the velocity diagrams only for the first seven positions of point B. Two symmetrical branches of the curve $v=\varphi(t)$ are plotted in Fig. 53, *b*. The velocity diagrams which have been plotted for determining the velocities of point C at these positions of point B are not shown. In plotting curve $v=\varphi(t)$ the velocity direction of point C to the right has been considered as positive.

In order to plot curve $a=\psi(t)$, where a is the acceleration of point C, and t is time, it is necessary also to plot the same number of acceleration diagrams as there are different positions planned for point B, but since in this case the two branches of the curve of velocities relative to the mean ordinate are symmetrical we can confine ourselves to plotting the diagrams for the first seven positions only. Curve $a=\psi(t)$ is given in Fig. 53, *b* together with the two preceding curves. The acceleration diagrams, which have been plotted for determining the ordinate of curve $a=\psi(t)$, are not shown. In plotting the curve, the direction of acceleration to the right has been considered as positive.

The curves of velocities and accelerations can equally well be plotted without the help of diagrams. Since the curve of velocities is the first derivative from the curve of paths, it can be plotted by points through graphic differentiation of the path curve. The curve of accelerations, which is the first derivative of the curve of velocities, can also be plotted in a similar manner.

The following scales have been used in Fig. 53, *b*.

The scale of abscissae for all curves $\mu_t=0.0025$ sec/mm (the 100 mm length in Fig. 53, *b* expresses the time interval 0.25 sec, in the course of which the crank makes one turn).

The ordinates of curve $s=f(t)$ are copied directly from Fig. 53, *a*, hence, the scale of ordinates of this curve is $\mu_s=10$ mm/mm.

The ordinates of curve $v=\varphi(t)$ are laid off to scale $\mu_v=0.2$ m/sec×mm, the ordinates of curve $a=\psi(t)$ — to the scale $\mu_a=7$ m/sec²×mm.

We said above that besides the diagrams of paths, velocities and accelerations, in the kinematic analysis of some mechanisms it becomes necessary to plot by points the paths of points belonging to individual links. The mechanism of the dough-making machine, which is shown in Fig. 33, can serve as an example. In the kinematic analysis of this mechanism it is necessary to plot the path of the end point which is rigidly coupled with the connecting rod of the operating member since the capacity of the machine is determined by the shape of this path. In the kinematic analysis of a slider crank mechanism the necessity for finding the paths of individual points arises only in the case of points which are coupled with the connecting rod, since the paths of the points which are connected with the other two moving links are in one case circles, and in the other straight lines. Fig. 53, *a* shows as an example an elliptical path (but not an ellipse) of the connecting rod point, which is located on line *BC* equidistant from points *B* and *C*.

16. ANALYTICAL DETERMINATION OF VELOCITIES AND ACCELERATIONS

The graphical methods which have been presented for determining the velocities and accelerations are lucid, simple, and straightforward. Yet no matter how carefully the plotting of the diagrams is carried out we must always reckon with the shortcoming which is characteristic of graphical methods: the difficulty of ascertaining the accuracy of the results obtained.

In cases where the calculation must be particularly accurate and the degree of accuracy of calculation is specified beforehand, the paths, velocities and accelerations may be determined analytically. Analytical determination of the paths, velocities and accelerations is always possible, since the mechanism in any given position is a closed diagram with sufficient data for the determination

of its sides and angles. However, the equations resulting from analytical methods are often complex and are therefore inconvenient for practical application in the analysis of even the most simple mechanisms.

In the previous section, by using graphical methods, we obtained three curves expressing the paths, velocities and accelerations of point C of the mechanism, diagrammatically shown in Fig. 53, *a*, in functions of the crank angle of rotation or its time of rotation from the initial position. If we apply analytical methods, we must obtain instead of the curves formulae expressing the identical functions as shown by the curves.

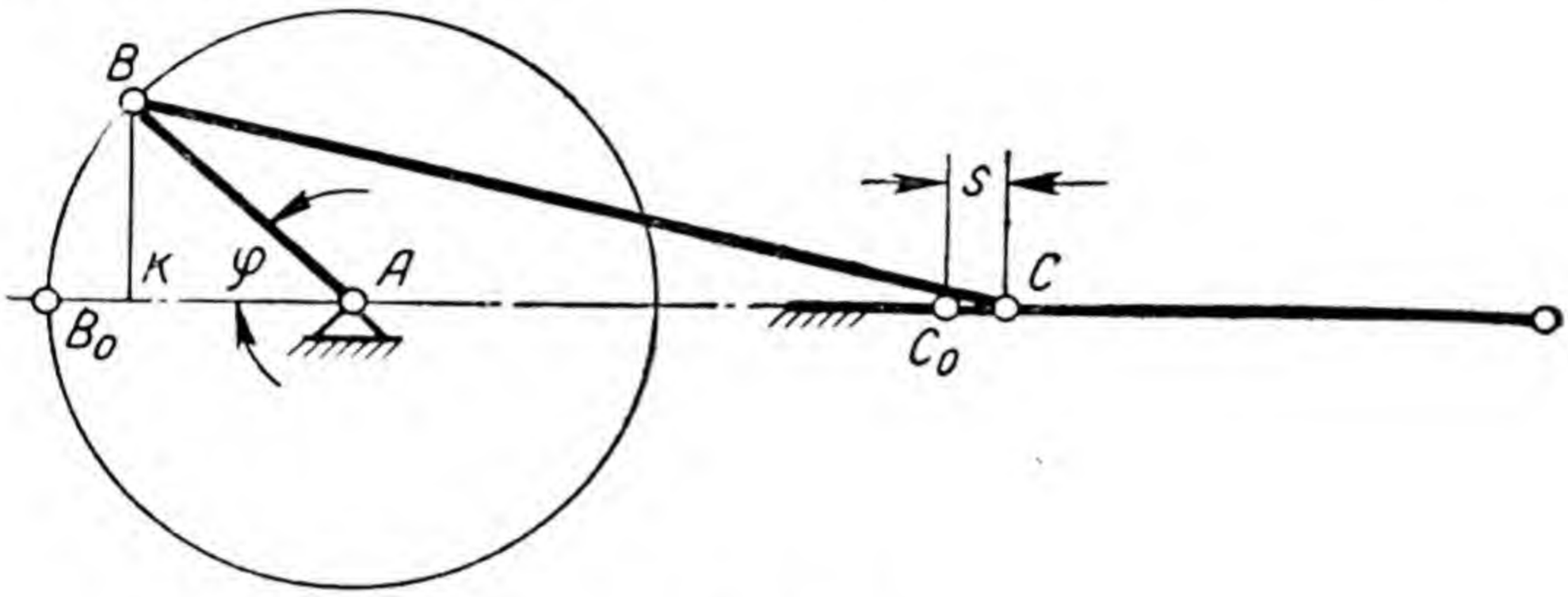

Fig. 54

For the slider crank mechanism shown in Fig. 54 we shall adopt the following symbols:

φ — the angle of crank rotation AB, which is read from the initial position of crank AB_0 clockwise;

l_1 — the length of crank AB;

l_2 — the length of connecting rod BC;

$s = C_0C$ — the path along which point C has passed from initial position C_0 during the time of the crank turn at angle φ.

In order to obtain the equations of the curve of paths we shall express s as function φ:

$$s = C_0C = AC - AC_0 = AC - (l_2 - l_1);$$

$$AC = KC - KA = \sqrt{l_2^2 - l_1^2 \sin^2 \varphi} - l_1 \cos \varphi.$$

Having defined $l_2/l_1 = p$, after simple conversions we obtain

$$s = l_1\left(1 - \cos \varphi + \sqrt{p^2 - \sin^2 \varphi} - p\right).$$

In this equation the path along which point C passes is expressed by the function of the crank angle of rotation. During crank rotation with constant angular velocity at n revolutions per minute the angle of rotation of the crank in radians in the course of t seconds

$$\varphi = \frac{\pi n}{30} t = \omega t,$$

where ω is the angular velocity of rotation in sec^{-1}.

By substituting value φ in the above obtained formula we get the curve of the paths as

$$s = l_1 \left(1 - \cos \omega t + \sqrt{p^2 - \sin^2 \omega t} - p\right).$$

By differentiating this formula we obtain after simplifying the expression for the velocity as a function of time

$$\frac{ds}{dt} = v = l_1 \left(\sin \omega t - \frac{\sin 2\omega t}{2\sqrt{p^2 - \sin^2 \omega t}}\right)\omega.$$

By differentiating this formula we obtain after simplifying the expression for the acceleration as a function of time

$$\frac{dv}{dt} = a = l_1 \left(\cos \omega t - \frac{\cos 2\omega t}{\sqrt{p^2 - \sin^2 \omega t}} - \frac{\sin^2 2\omega t}{4\sqrt{(p^2 - \sin^2 \omega t)^3}}\right)\omega^2.$$

We have chosen as an example one of the simple mechanisms, and in the mechanism we have selected that point for which, not counting the points coupled with the crank, it was easiest to obtain an equation; even so the equations became inconvenient for practical application. Similar equations for various points coupled with the connecting rod and moving along paths that represent curves of the fifth and higher orders would have been much more complex.

In order to avoid the necessity of complex equations for practical calculations, approximate analytical methods are used. For instance, the above equations can be simplified as follows:

$$\sqrt{p^2 - \sin^2 \omega t} = p\left[1 - \left(\frac{\sin \omega t}{p}\right)^2\right]^{\frac{1}{2}} =$$

$$= p\left(1 - \frac{1}{2}\frac{\sin^2 \omega t}{p^2} - \frac{1}{8}\frac{\sin^4 \omega t}{p^4} \cdots\right).$$

Since the series converges quickly, we are able without great error to discard all terms, beginning with the third. In such case we obtain:

$$s = l_1\left(1 - \cos\omega t - \frac{\sin^2\omega t}{2p}\right);$$

$$\frac{ds}{dt} = v = l_1\left(\sin\omega t - \frac{\sin 2\omega t}{2p}\right)\omega;$$

$$\frac{dv}{dt} = a = l_1\left(\cos\omega t - \frac{\cos 2\omega t}{p}\right)\omega^2.$$

Chapter III

PLANE MECHANISMS FOR THE TRANSMISSION OF ROTARY MOTION

17. GENERAL

The elements which serve for the transmission of rotary motion are secured on shafts, which are in most cases cylindrically-shaped rods that rotate in bearings. The shaft that transmits motion is called driving; the shaft that receives motion is called driven.

Transmission of rotary motion is possible between shafts which are situated in space in any position: the axes of the shafts may be parallel, crossing at any angle, and also intersecting at any angle. In practice we most frequently encounter cases where the axes of shafts are parallel, and more rarely where the axes of shafts cross or intersect at right angles. Hereafter we shall deal only with such cases, since all others are less frequently encountered in practice.

Transmission of rotary motion between shafts with parallel axes is performed with the aid of plane mechanisms; in other cases it is performed with the aid of space mechanisms.

Transmission of rotary motion is performed by one of the following means:

1) through direct contact of two bodies, one of which is rigidly coupled with the driving shaft, the other with the driven shaft;

2) by means of flexible bodies, which engage with bodies rigidly coupled with the driving and driven shafts.

The first of these is attained in friction, gear and worm drives, the second in belt and chain drives.

Transmission of rotary motion can be performed by increasing, decreasing or without changing the angular velocity of rotation.

The relation of the angular velocity of the driving shaft to the angular velocity of the driven shaft is termed velocity ratio.*

The velocity ratio during one turn of the driving shaft may or may not vary. In practice we rarely come across mechanisms for the transmission of rotary motion with a variable velocity ratio (i. e. variable during one turn of the driving shaft); we shall therefore not discuss these mechanisms.

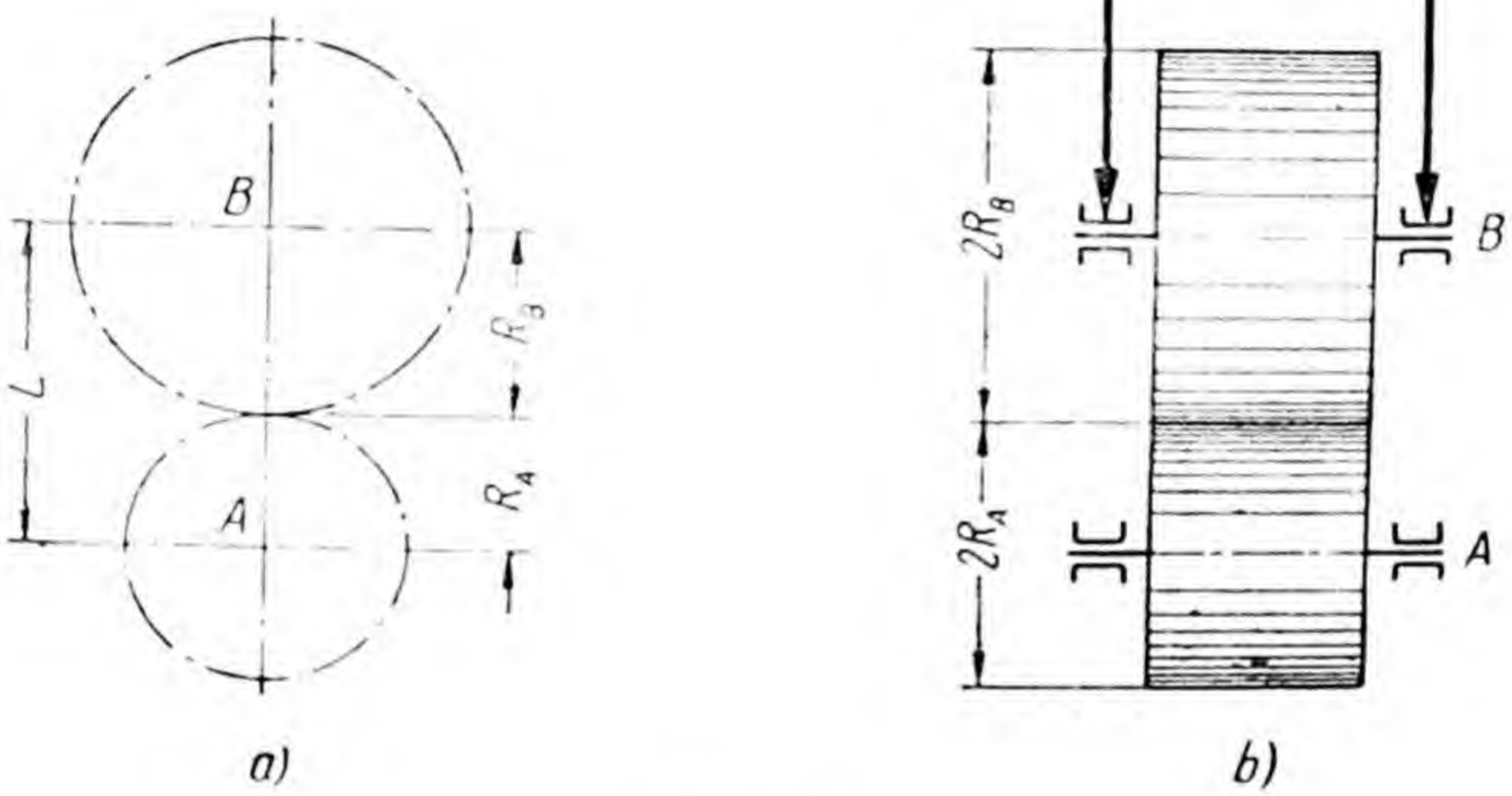

a) *b)*

Fig. 55

If transmission of rotary motion between shafts with parallel axes is performed by direct contact of two bodies, one coupled with one shaft and the second coupled with the other, we can imagine such contacting cylinders coupled with the shafts which, while rotating about the common axes *A* and *B* (Fig 55, *a*) and remaining all the time in contact, do not slip one on another. Such imaginary contacting cylinders are called pitch cylinders. The circles, which we get when the cross-section of the pitch cylinders is made by a plane perpendicular to the axes of the cylinders, are also called pitch circles.

During rotation the pitch cylinders will not slip along each other being that the linear velocities of the points

---

* In some of the popular editions the term velocity ratio stands for transmission ratio which is greater than unity or is unity.

which lie on the surfaces of the cylinders are equal, i. e. when

$$R_A \times \omega_A = R_B \times \omega_B,$$

where R_A and R_B are radii; ω_A and ω_B are the angular velocities of rotation of the pitch cylinders. From this equation follows

$$\frac{R_B}{R_A} = \frac{\omega_A}{\omega_B} = i.$$

Hence, the velocity ratio can be expressed by the relation of the radii of the pitch cylinders.

The design representation of the transmission of rotary motion between parallel shafts is begun by drawing the pitch circles on the diagram. From the given velocity ratio and centre distance (i. e. distance L between the centres of the pitch circles) it is possible to determine the radii of pitch circles after solving the system of two equations:

$$\frac{R_B}{R_A} = i;$$

$$R_A + R_B = L.$$

It follows from the above that the point of contact of the pitch circles divides the line of centres (i. e. the segment AB) into parts, which are inversely proportional to the angular velocities of rotation of the shafts.

18. FRICTION DRIVE

An extremely simple form of plane transmission of rotary motion can be obtained by coupling the driving and driven shafts to cylinders with radii equal to the radii of the pitch cylinders, and by pressing them against each other. Fig. 55, *b* shows this type of transmission, where A is a shaft that rotates on fixed bearings; B is a turning shaft on bearings which can displace in a direction perpendicular to the axes of the shafts; Q is the force which is applied to the bearings of shaft B and which presses the cylinders with radii R_A and R_B against each other.

When the cylinders are pressed against each other along their line of contact (or, to be more exact, on the small surface adjoining the line of contact formed as a result of deformation of the cylinders) a force of friction

develops by means of which rotation is imparted to the driven shaft during rotation of the driving one. Transmission of rotary motion may be effected without one cylinder slipping along the other and, hence, with a velocity ratio equal to the relation of the radii of the cylinders, if the applied force Q ensures sufficient force of friction for this.

This type of transmission is called f r i c t i o n d r i v e. Utilization of the force of friction for meshing of rigidly connected wheels with the shafts, which in a friction drive are termed r o l l e r s, makes transmission simple, and therefore inexpensive, which is very important for industrial installations. The great advantages of a friction drive are that it is noiseless, and that a change of shock load on the driven shaft, i. e. a great and rapid increase in resistance of the driven shaft to rotation cannot result in the breakage of gear elements, since in this case all that would occur is a momentary slippage of the rollers without any significant harm to either roller.

However, this latter advantage of a friction drive is at the same time its disadvantage, which in many cases precludes the possibility of its application. The possibility of one roller slipping along the other does not allow application of the friction drive in cases where an invariable velocity ratio is a requisite condition for proper machine operation, and such cases are frequently encountered in practice. In the evaluation of this disadvantage of the friction drive it is necessary also to bear in mind the fact that slipping of one wheel along the other may occur not only during an increase in resistance to rotation by the driven shaft, but also as a result of a decrease in the force of friction between the rollers. A decrease in the force of friction may occur either as a result of the decrease in the force of pressure of one roller on the other, or as a result of the decrease in the coefficient of friction between the roller rims, for instance, as a result of the penetration of lubricant onto the rims of the rollers.

Another important disadvantage of the friction drive is the use of a device which presses the rollers against each other, while the pressing force is absorbed by the bearings of the rollers; as a result of this in the bearings of the shafts forces of friction develop to overcome which driving forces have to be applied.

Only compound friction drives can relieve the shafts from the action of force which is necessary to keep the rollers pressed against each other. These drives we shall not examine here (such drives are examined in the course on machine elements), but in a simple friction drive, which is effected simply by a pair of wheels, measures can be taken merely to reduce the disadvantage mentioned. It is for this purpose that the rims of metal (cast iron) rollers are frequently made of non-metallic materials (rubber, leather, wood, etc.), by means of which the required force of friction can be obtained with a lesser pressing force and, consequently, with lesser losses of friction in the bearings of the shafts.

Because of these disadvantages of friction drives, the gear drive is being applied much more frequently for the transmission of rotary motion between parallel shafts.

19. GEAR DRIVE

A. General

The gear drive consists of a pair of wheels with teeth which are arranged on the surfaces of circular cylinders. Fig. 56 shows in cross section the arrangement of the teeth of a pair of gears and indicates also the pitch circles with centres O_1 and O_2. During rotation of the driving wheel, the tooth of the driving wheel, pressing on the tooth of the driven wheel, causes the latter to rotate. Before one pair of teeth disengages another pair engages so that the wheels rotate continuously. In the designs currently in use from one to three pairs of teeth may be engaged simultaneously.

Fig. 56 shows the respective positions of a pair of wheels with external toothing, where the centres of the pitch circles are situated on different sides from their point of contact. Gear drives with internal toothing in which the centres of the pitch circles are situated on the same side as the point of contact are also used (Fig. 57). In a drive with external toothing the teeth of each wheel are situated on the outer side of the rim; in drives with internal tothing the teeth of the larger wheel are situated on the inner side of the rim. In a drive with external toothing the wheels rotate in different directions, in a drive with internal

toothing they rotate in the same direction. Hereafter we shall only discuss drives with external toothing, since drives with internal toothing are applied comparatively rarely.

The sides of the teeth are formed by curved surfaces

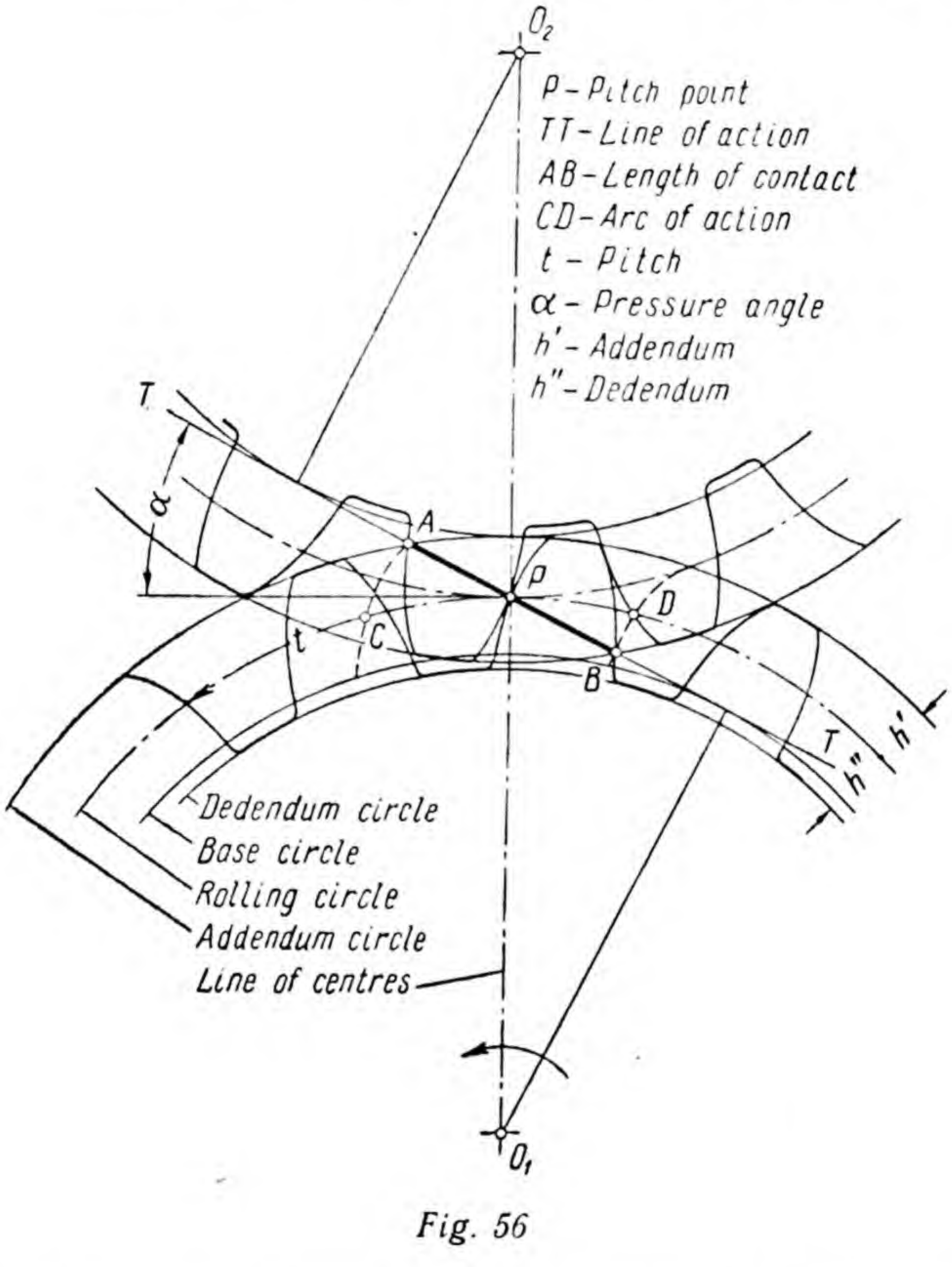

Fig. 56

such as to ensure a constant velocity ratio in the process of engagement of a pair of teeth.

The curve on which the lateral surface of the tooth is plotted as on a directrix is called t h e t o o t h p r o f i l e.

In order to make sure that during rotation of the wheels the teeth of the driving wheel will always coincide with the spaces between the teeth of the driven wheel, it is essential that the distance between the centres of adjacent

teeth should be identical on either wheel. This distance is measured along the pitch circle; it is called p i t c h and is denoted by letter *t*.

The pitch can also be measured from the pitch circle between profiles of adjacent teeth which face the same side.

If we designate the number of wheel teeth with letter *z*, the diameter of the pitch circle with letter d, and express the length of the pitch circle through the diameter on one side and through the number of teeth on the other side we get the equation

$$\pi \times d = z \times t,$$

whence

$$d = z \frac{t}{\pi}.$$

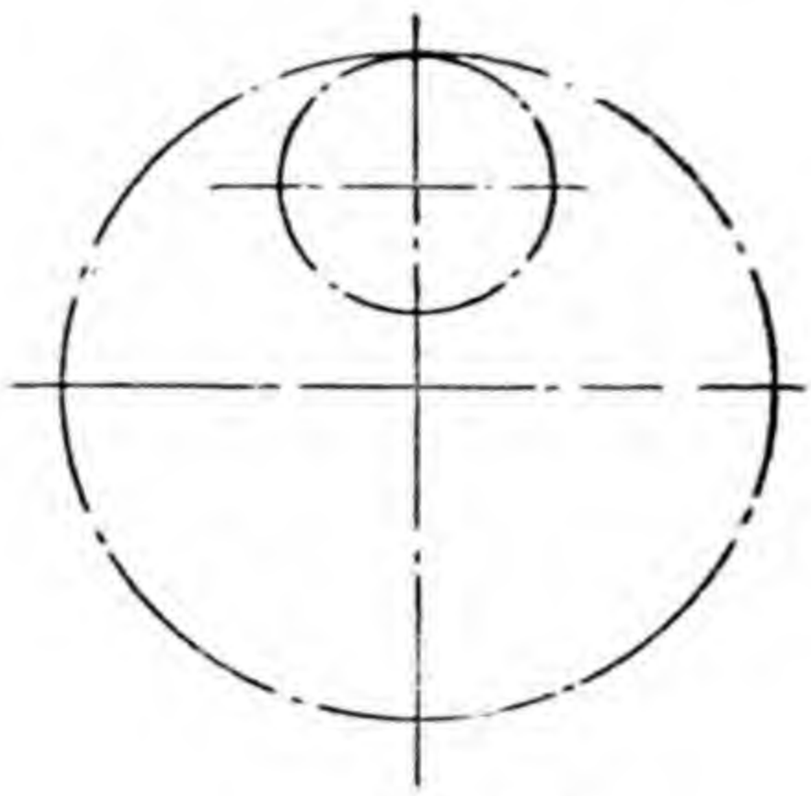

Fig. 57

This equation shows that the diameter and pitch cannot be expressed by commensurable numbers.

For the convenience of manufacturing toothed wheels relation $\frac{t}{\pi}$ is chosen so as to be expressible by a whole number or by a whole number with few decimal places.

Relation $\frac{t}{\pi}$ is called m o d u l e and is denoted by a small *m*.

It will be shown below that provided the teeth profiles are correctly shaped the centre distance O_1O_2 (see Fig. 56) may be to some extent changed during wheel setting without modifying the velocity ratio. In such cases the radii of the pitch circles change.

It follows that the same pair of toothed wheels may be set up differently in such a manner that the wheels will operate at different diameters of the pitch circles, and therefore at different relations of $\frac{t}{\pi}$. It is obvious that the s t a n d a r d m o d u l e s may pertain only to one of the possible pairs of pitch circles. They relate to the nominal pitch circles.

The n o m i n a l p i t c h c i r c l e is an imaginary circle with a diameter equalling zm, where z is the number of teeth in the wheel and m the standard module.

It follows from the above that the nominal pitch circle may coincide with the pitch circle (which happens frequently), but may also differ from it. An understanding of the nominal pitch circle is necessary not only because we have to take its diameter into account in the manufacture of wheels, but also because the term pitch circle applied to one wheel whould have no meaning, since the pitch circles come into being only during the engagement of two wheels.

The nominal pitch circle diameter is considered as the wheel design diameter. The nominal pitch circle divides the tooth into two parts: the tooth portion, which lies outside the nominal pitch circle in wheels with external toothing (and inside the nominal pitch circle in the outer wheel of a drive with internal toothing) and is called addendum h'; the portion of the tooth, which lies between the nominal pitch circle and the wheel body, is called dedendum h''. If the pitch circle does not coincide with the nominal pitch circle the tooth, in accordance with the State Standard, is divided into addendum and dedendum not by the nominal pitch circle, but by the pitch circle.

The dimensions of standard teeth are accepted as follows: the addendum equals the module, the dedendum equals 1.25 of the module. In some cases wheels with stub teeth are used, i. e. the addendum equalling 0.8 module, and the dedendum equalling the module. The tooth thickness, which is measured by the nominal pitch circle, is assumed to equal half of the pitch.

The module is determined as a result of strength and wear resistance calculations, which are discussed in the course on machine elements.

The circle described about the wheel centre and which limits the tooth tops is called addendum circle.

The distance between the profiles of adjacent teeth, which is limited by the addendum circle and the wheel body, is called space. The circle, described about the wheel centre and which limits the spaces from the side of the wheel body, is called dedendum circle.

B. Compound Gearing

A gear drive in the most simple design consists of a driving wheel in engagement with a driven wheel, each of

them rigidly coupled with its shaft which rotates about a fixed axle.

The necessity of a compound gearing arrangement arises when the velocity ratio exceeds that which could practically be achieved by means of one pair of wheels. In such cases use is made of a multistep drive: one or more intermediate shafts (Fig. 58) are arranged between the driving and driven shafts and rotary motion is transmitted in succession from one shaft to another. In this type of drive two wheels are positioned on each of the intermediate shafts (shafts *B* and *C* in Fig. 58); one of them is driven by the motion received from the preceding shaft, while the other is a driving wheel which transmits motion to the next shaft. This type of drive can achieve a high velocity ratio.

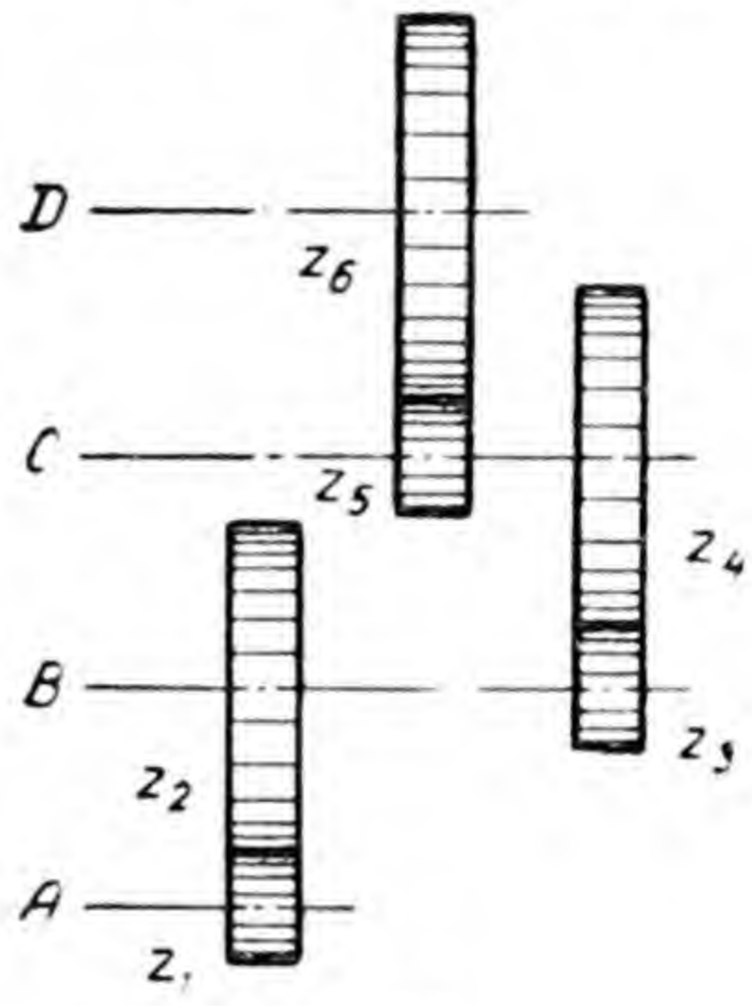

Fig. 58

Denoting the angular velocities of rotation of the shafts by letter ω with a corresponding index, the velocity ratios by letter *i* with two indices, the first of which denotes the driving shaft, and the second the driven shaft, denoting the number of wheel teeth by letter *z* with indices which are given in Fig. 58, and considering shaft *A* as the driving one and shaft *D* as the driven one, and taking into consideration that in a gear drive the velocity ratio can be expressed by the number of teeth of the wheels, since the wheel diameter is equal to the product of the module by the number of teeth, we get:

$$i_{AB} = \frac{\omega_A}{\omega_B} = \frac{z_2}{z_1};$$

$$i_{BC} = \frac{\omega_B}{\omega_C} = \frac{z_4}{z_3};$$

$$i_{CD} = \frac{\omega_C}{\omega_D} = \frac{z_6}{z_5}.$$

By multiplying these equations we obtain after reducing

$$i_{AB} \times i_{BC} \times i_{CD} = \frac{\omega_A}{\omega_D} = i_{AD} = i = \frac{z_2 \times z_4 \times z_6}{z_1 \times z_3 \times z_5}.$$

Hence, in a drive with intermediate shafts, each of which has a driven and driving wheel, the total velocity ratio i equals the product of the intermediate velocity ratios or the relation of the product of the number of teeth on the driven wheels to the product of teeth on the driving wheels (in Fig. 58 the number of teeth on the driven wheels is marked with even indices, and on the driving wheels with odd indices).

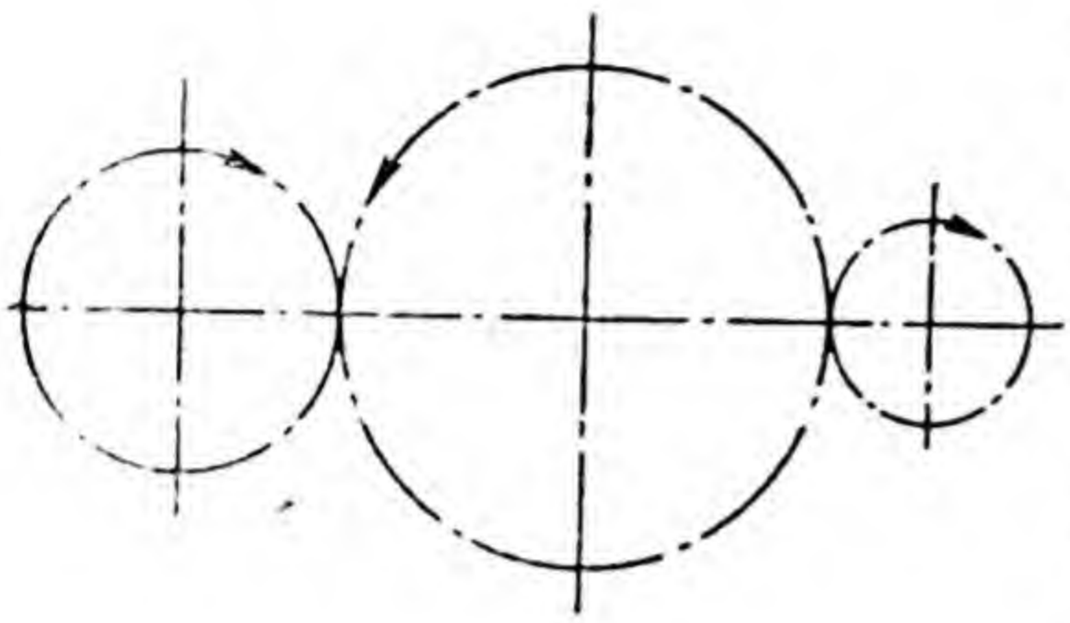

Fig. 59

Fig. 58 shows only two intermediate shafts, but the conclusion reached above will be equally correct for any number of intermediate shafts.

At low velocity ratios, which are achieved by means of one pair of wheels, the arrangement of a compound gearing becomes necessary in those cases where the transmission of rotary motion has to be performed without changing the direction of rotation. If the driving and driven wheels must rotate in one direction, an intermediate (idle) wheel which engages with the driving and driven wheels (Fig. 59), is then fitted between them.

Intermediate wheels also have to be fitted in cases where the distance between the axes of the driving and

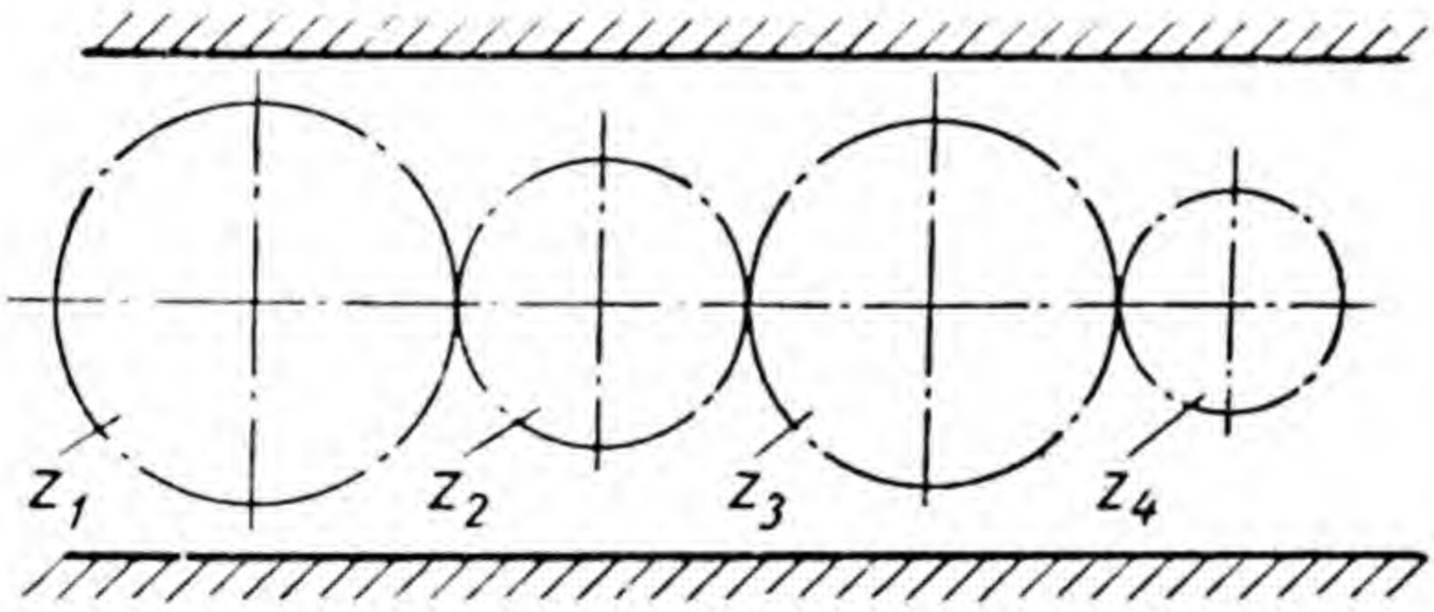

Fig. 60

driven wheels has to be great and for reasons of design it is impossible to fit wheels with large diameters (Fig. 60). Taking the wheel with the number of teeth z_1 (Fig. 60) to be the driving wheel, and the wheel with the number of teeth z_4 to be the driven wheel and determining the total velocity ratio, we will find it to equal $\frac{z_4}{z_1}$, i. e.

the same as it would have been if the transmission had been effected without intermediate wheels. Therefore in drives with intermediate wheels neither the number of these wheels nor the number of teeth in them affect the magnitude of the total velocity ratio. If the driven wheel has to rotate in the same direction as the driving wheel an odd number of intermediate wheels is chosen, if in the opposite direction their number is even.

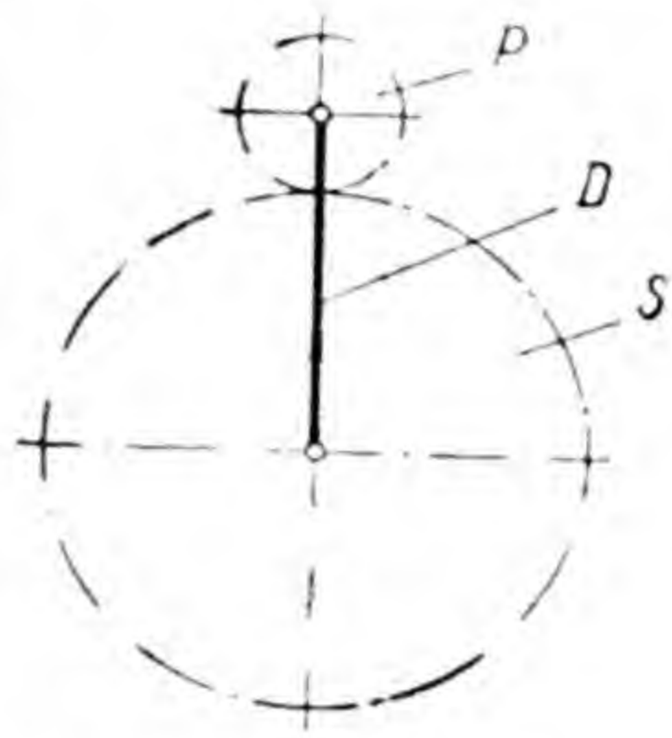

Fig. 61

So far the axles of the driving and driven wheels have been considered as fixed. However frequent use is also made of toothed gears in which the axles of some of the wheels are moving. Fig. 61 shows one of the simplest gears of this type, which consists of toothed wheels S and P and lever D that is called the driver. If wheel S is fixed, during one turn of driver D wheel P will turn about its own axis $\frac{z_S}{z_P}$ times, where z_S and z_P are the number of teeth on wheels S and P, and besides that it will make one more turn about the driver axis. The velocity ratio from the driver to wheel P will therefore equal

$$\frac{z_S}{z_P} + 1.$$

This type of mechanism is usually applied in apparatus where the reactants have to undergo vigorous stirring. In such apparatus the operating members (mixing arms or propellers), which act directly on the processed materials, are secured on the shafts of a few (usually three) wheels P.

The mechanism, shown in Fig. 61, where wheel S is fixed, is called planetary, wheel S is called the sun wheel, wheel P the planet wheel or planet pinion. It is easy to calculate that this mechanism has one degree of movability (two moving links D and P, two turning pairs and one higher pair).

When wheel S is moving the mechanism has two degrees of movability and is called a toothed differential mechanism.

C. Theory of Gearing

The operation of toothed wheels depends to a considerable extent on the machining accuracy of teeth profiles. Before we decide what curves the outlines of the profiles should describe, let us find out what basic requirement these curves must satisfy.

We know that during rotation of engaged toothed wheels, the pitch circles must roll on each other without slipping. This condition can be ensured only if in the process of gearing the tooth profile of the driving wheel is in constant contact with the tooth profile of the driven wheel.

Let points O_1 and O_2 (Fig. 62) be the centres of the pitch circles of the first and second wheels respectively; P is the point of contact of the pitch circles, which is called the pitch point; β_1 is the tooth profile of the first wheel; β_2 is the tooth profile of the second wheel; M is the point of contact of the profiles in the instant corresponding to their respective location, as shown in the diagram.

We shall examine the motion of one wheel: for example, that of the second in relation to the first. During rolling motion of the circle of centre O_2 along the circle of centre O_1, the circle of centre O_2 and profile β_2 which is rigidly connected with it, are turning at this instant about pitch point P, which is the instantaneous centre of rotation. Point M_1, which is connected with profile β_1 and M_2, which is connected with profile β_2, are in contact at point M. When profile β_2 turns about pitch point P the velocity of point M_2 relative to point M_1, given normal functioning of the wheels, can be directed only tangentially to both profiles at point M, as otherwise profile β_2 would either depart from profile β_1 or would press into it. The velocity vector of point M_2 relative to point M_1, which is directed tangentially to both profiles, is the perpendicular to line PM which is the radius of rotation.

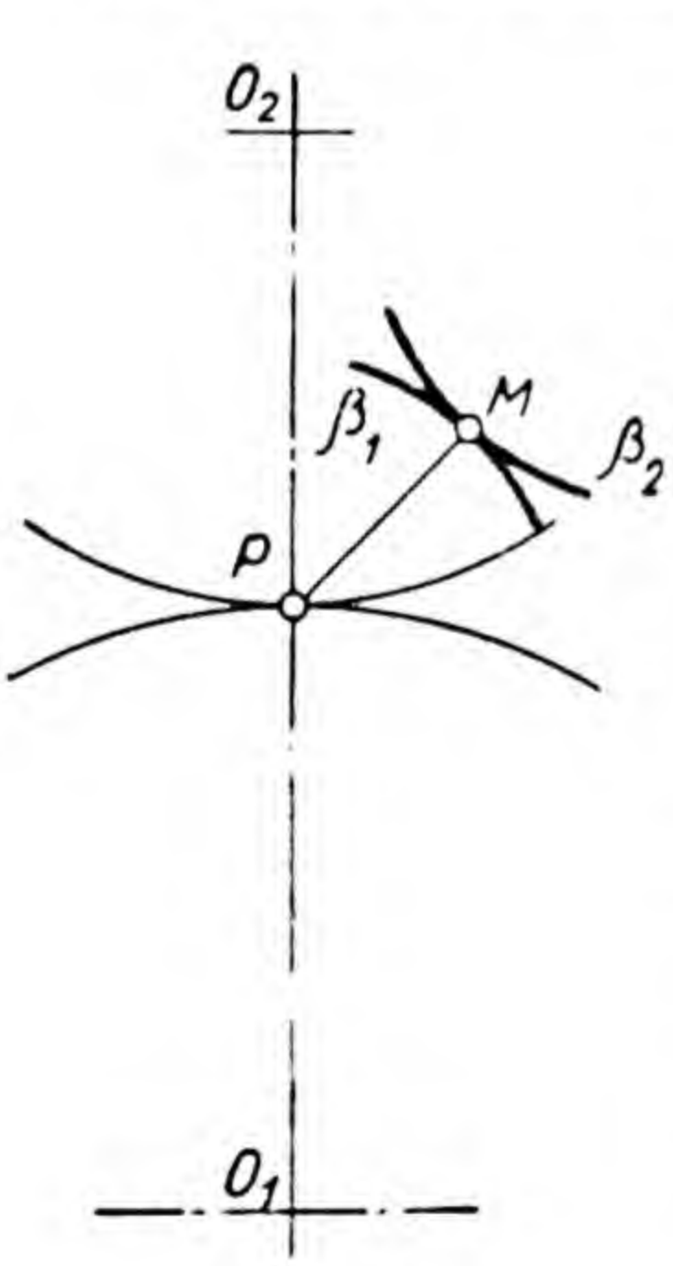

Fig. 62

We come now to requirement which it is important for the profiles of teeth in mesh to satisfy: the common normal to the tooth profiles at the point of contact must pass through the pitch point.

For every given case many profiles satisfying this requirement, can be plotted by specifying an approximate tooth profile for one wheel and plotting a conjugate profile for the tooth of the other wheel. Since in the actual designing of gear drives this is never practised, and the profiles are drawn by mathematical curves, we shall not examine the methods of plotting conjugate profiles by specified approximate profiles.

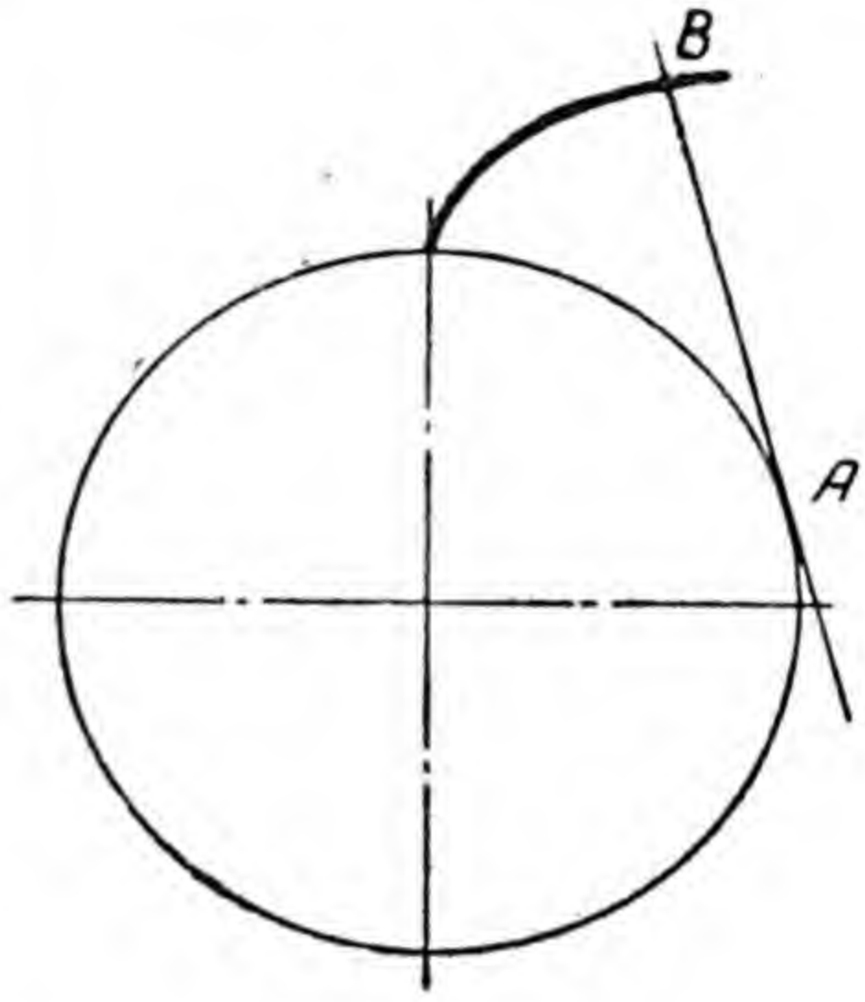

Fig. 63

Historically the first mathematical curves, by which the profiles of teeth were drawn, were the cyclic curves (the cycloid, epicycloid, hypocycloid, pericycloid). Cyclic profiles have great theoretical advantages, but the difficulty of making cyclic teeth made it necessary to abandon completely the production of wheels with such teeth. At present toothed wheels are manufactured only with involute profiles.

In order to evaluate correctly the advantages of involute profiles it is first necessary to find out what properties of the involute are made use of in a gear drive.

The curve described by the point of a straight line which is rolled along the circumference without slipping is called i n v o l u t e. The circle along the circumference of which the straight line rolls, describing with one of its points an involute is called a b a s e c i r c l e; the straight line which rolls along the circumference of the base circle is called a g e n e r a t r i x.

One of the most important properties of the involute is that *the generatrix is normal to the involute.*

This can be easily verified from an examination of Fig. 63. Point A of generatrix AB is the instantaneous centre of rotation, and segment AB is the instantaneous radius of rotation for point B, which describes the involute; segment AB is the normal to the involute at this point,

since it is the perpendicular to the velocity vector of this point which is directed along the tangent to the curve.

We assume in Fig. 64 involute CAB as rigidly connected with the base circle, and tangent TT to the base circle as intersecting the involute at point A. We indicate point B on the involute; segment BB_1 is the segment of the generatrix.

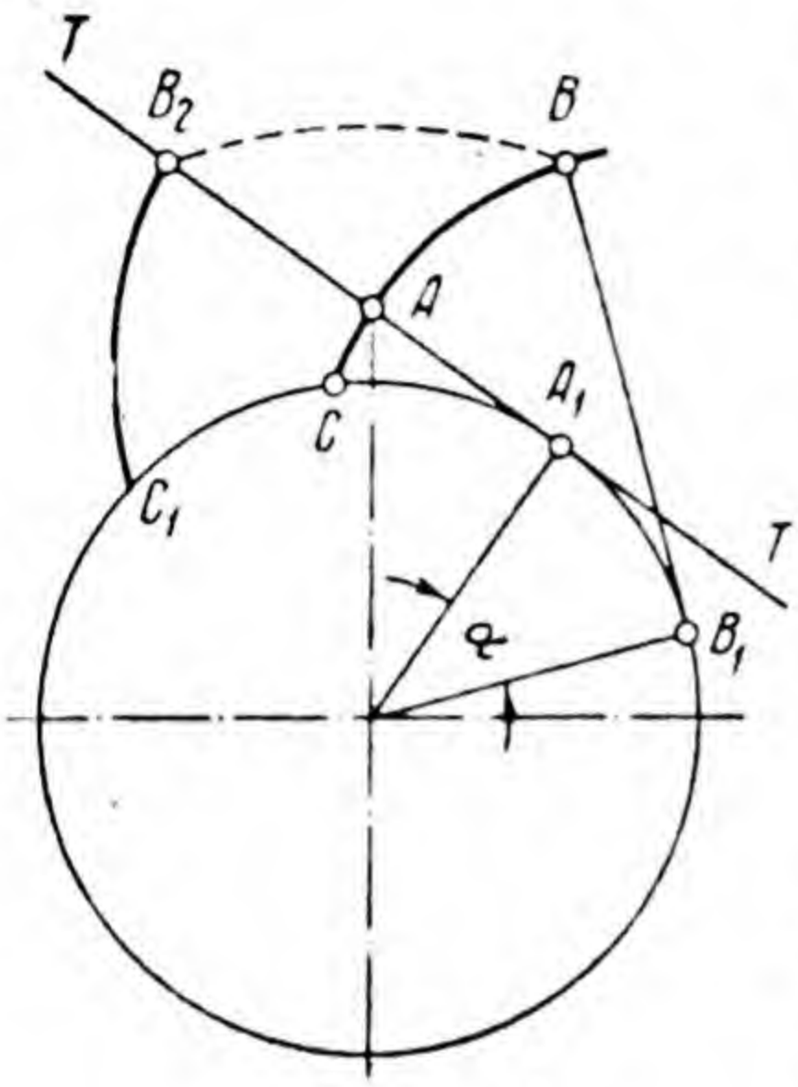

Fig. 64

From the definition of the involute it follows that the length of segment AA_1 equals the length of arc $\overset{\smile}{CA_1}$, and the length of segment BB_1 equals the length of arc $\overset{\smile}{CB_1}$. If we leave line TT stationary, and turn the base circle together with the involute, which is rigidly connected with it, counter-clockwise at angle α so that point B_1 will coincide with point A_1, the involute will pass into position C_1B_2 and segment BB_1 will occupy position B_2A_1 on line TT.

Before the base circle turned together with the involute, the point of involute intersection with line TT occupied position A, during the turn it displaced along line TT, passing in this time the distance AB_2. Path AB_2, along which the point of involute intersection with line TT passes during the turning of the base circle, equals the length of arc $\overset{\smile}{B_1A_1}$ along which point B_1 displaced, since

$$AB_2 = A_1B_2 - AA_1 = BB_1 - AA_1 = \overset{\smile}{CB_1} - \overset{\smile}{CA_1} = \overset{\smile}{B_1A_1}.$$

It follows from this that during rotation of the base circle together with the involute about the centre of the circle the linear velocity of the point of intersection of the involute with any tangent to the base circle (in the direction of this tangent) is equal to the linear velocity of the points which lie on the base circle. This property of the involute allows the transformation of rotary motion with constant angular velocity into translatory motion with constant linear velocity, and vice versa. A simple cam mechanism with the cam outlined by the involute can be utilized for this purpose. This type of mechanism is shown

diagrammatically in Fig. 65, where β is the involute profile of the cam which rotates about the centre of the base circle; K is the base circle for involute β; P is the follower which is directed by bushing B along the straight line of the tangent to the base circle. During counter-clockwise rotation of the cam with constant angular velocity, the involute profile will force the follower upwards with constant linear velocity; conversely, during motion of the follower downwards with constant linear velocity the cam will turn clockwise with constant angular velocity. It is clear from the above that the linear velocity of the follower will be related to the angular velocity of the cam rotation by the following simple function:

$$v = r_0 \times \omega,$$

where v is the linear velocity of the follower, ω is the angular velocity of cam rotation, and r_0 is the radius of the base circle.

Let us imagine (Fig. 66) two cams with contacting involute profiles β_1 and β_2 which rotate about fixed centres O_1 and O_2. Common tangent TT to the base circle is the generatrix for both profiles, and it will therefore be the normal to each of the profiles and must pass through their point of contact.

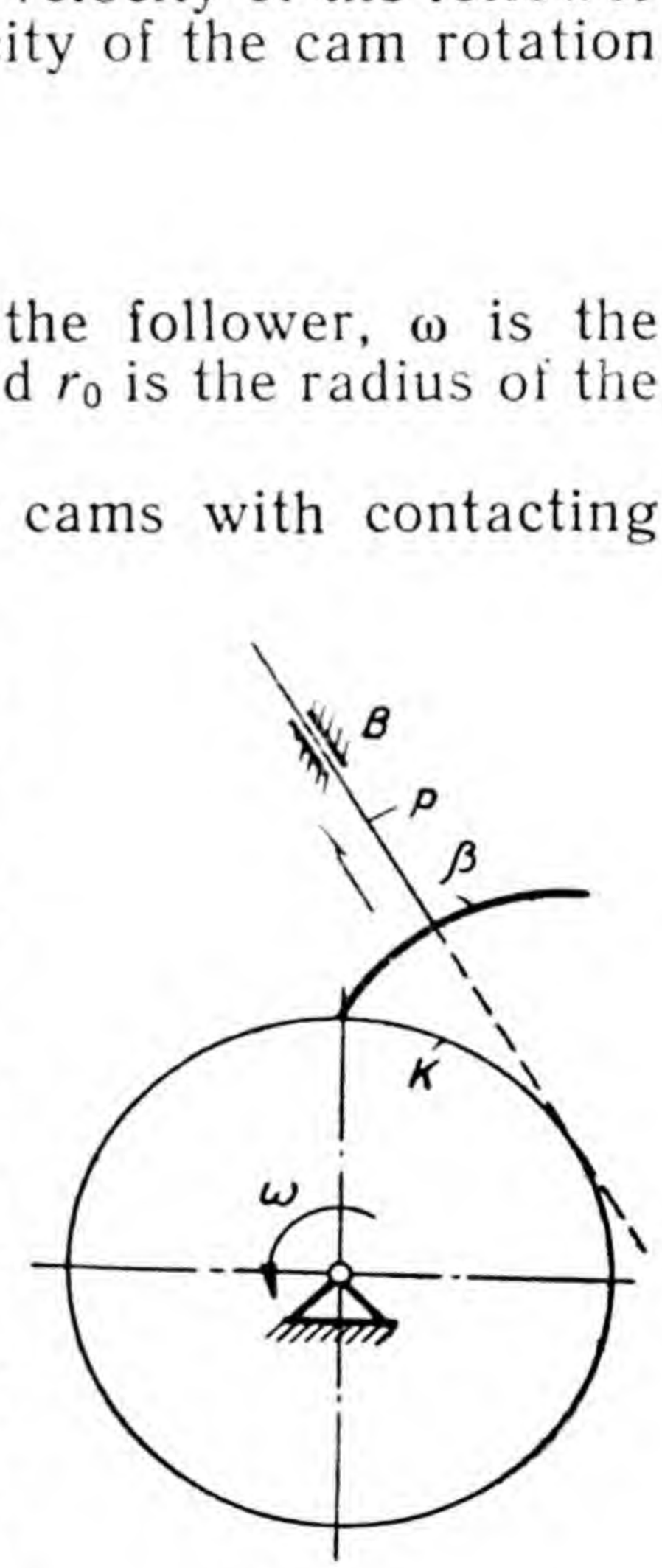

Fig. 65

We shall rotate profile β_1 counter-clockwise with constant angular velocity ω_1. Profile β_1 will force away profile β_2 turning it (together with the base circle) about centre O_2 clockwise. During this interaction of the profiles their point of contact will remain constantly on line TT. The point of intersection of profile β_1 with line TT will displace along this straight line with linear velocity $\omega_1 r_{01}$, and the point of intersection of profile β_2 with line TT will do so with linear velocity $\omega_2 r_{02}$, where r_{01}, and r_{02} are the radii of the base circles. Since both these velocities must be

equal, as otherwise the profiles would depart or press into each other, we get equation

$$\omega_1 r_{01} = \omega_2 r_{02},$$

whence

$$\frac{\omega_1}{\omega_2} = i = \frac{r_{02}}{r_{01}}.$$

Hence, *the relation of the radii of the base circles is equal to the velocity ratio.*

When rotating with constant angular velocity, the driving cam with an involute profile can rotate the driven cam with a similar profile only a small part of a revolution while both cams are in mesh. But if we were to arrange a number of cams about the axes of rotation of both cams in such a manner that at the instant of disengagement of one pair of cams the following pair engaged, the transmission of rotary motion would go on continuously. By proceeding in such a manner we shall get a pair of conjugate wheels, and the interaction of their teeth will in no way differ from the interaction of the conjugate cams, which are shown in Fig. 66.

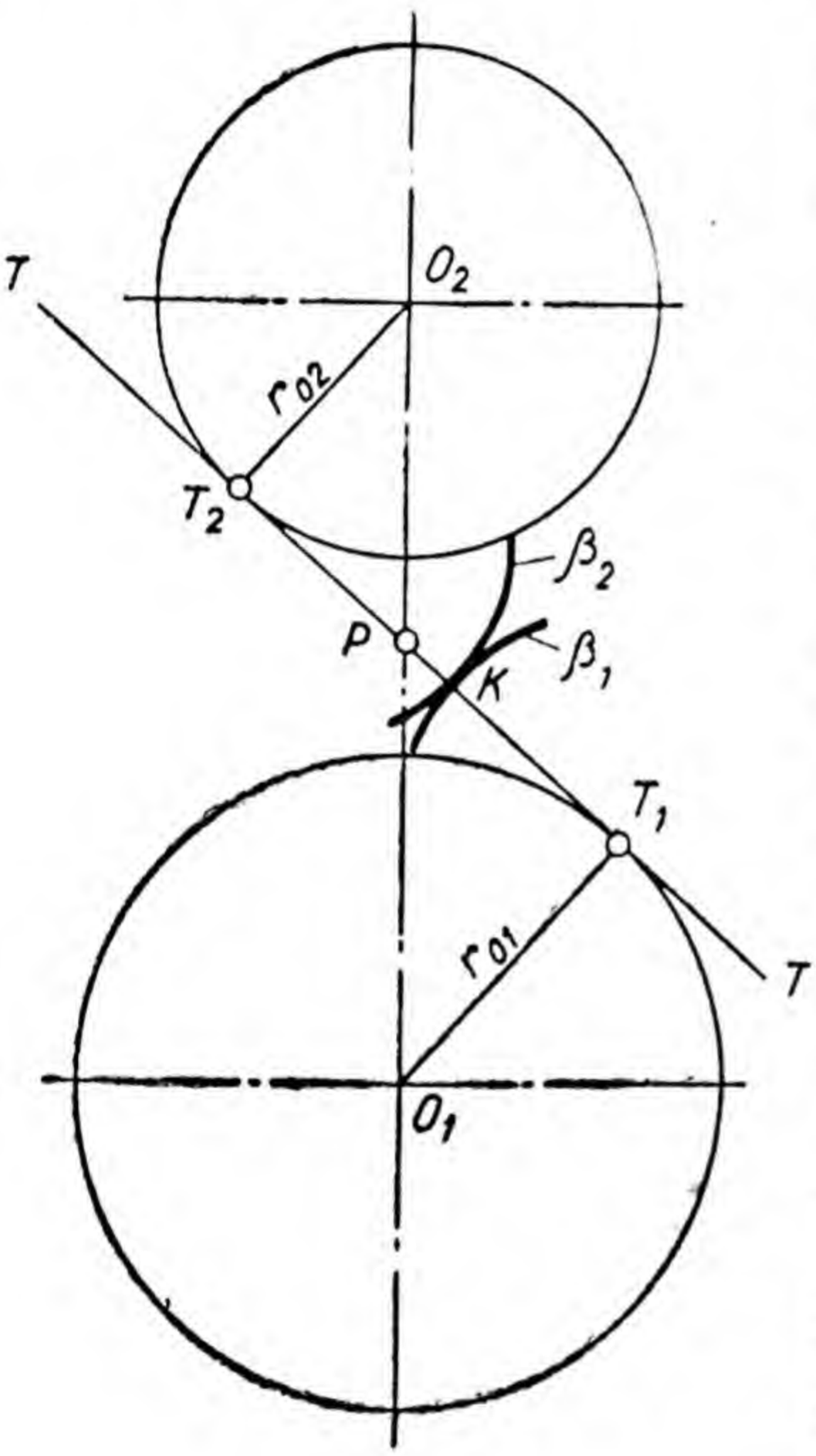

Fig. 66

We have ascertained above that with teeth with involute profiles the profile of the driving tooth will force away the profile of the driven tooth in the direction of the common tangent to the base circles of both profiles with a linear velocity equal to the linear velocity of the points on both base circles; from this it follows that the velocity ratio equals the relation of the radii of the base circles.

We have also ascertained that the common tangent to the base circles is the locus of the contact points of the

involute profiles and is the common normal to the profiles at their point of contact.

We have still to ascertain that this common normal to the profiles at the point of their contact passes through the pitch point, i. e. that the basic requirement for involute profiles is being satisfied and which has already been mentioned as necessary for the proper operation of toothed wheels.

Let us draw in Fig. 66 radii O_1T_1 and O_2T_2, where T_1 and T_2 are the points of contact of line TT with the base circles, and we shall indicate point P of intersection of line TT with line O_1O_2. Segment O_1O_2 is called the line of centres. From the similarity of triangles O_1PT_1 and O_2PT_2, it follows that the relation of segments O_1P and O_2P is equal to the relation of radii O_1T_1 and O_2T_2 of the base circles and equals the velocity ratio.

O_1P and O_2P are thus the radii of the pitch circles, and point P, through which the common normal passes to the profiles at their point of contact, is the pitch point.

Common tangent TT to the base circles, which is the locus of the points of contact of conjugate teeth profiles, is called the line of action.

On the basis of the above considerations we are able now according to centre distance O_1O_2 and given numbers z_1 and z_2 of teeth to plot the teeth of each wheel, proceeding as follows:

1) we divide by point P (see Fig. 56) segment O_1O_2 in relation $\frac{z_1}{z_2}$, determining thus radii O_1P and O_2P of the pitch circles;

2) we determine the module (from calculation of strength);

3) we draw the addendum and dedendum circles, taking into consideration that the radius of the first of them is equal to the radius of the pitch circle, which is enlarged to the module magnitude, and the radius of the second is equal to the radius of the pitch circle reduced by 1.25 module;

4) through pitch point P we draw the line of action at a determined angle to the line of centres O_1O_2;

5) from the centre of the pitch circle we draw a perpendicular to the line of action, determining the length

of the radius of the base circle, and we draw the base circle;

6) by rolling without slipping the line of action along the circumference of the base circle in both directions, we describe with point P the involute section of the profile from the base circle to the addendum circle; the remaining part of the profile which is not utilized in gearing may be drawn along a more or less arbitrary curve;

7) having plotted the tooth thickness by the pitch circle, we plot the profile which limits the tooth from the other side; the latter profile must be, of course, a mirror image of the first one;

8) having divided from point P the pitch circle into parts equal in number to the teeth, we draw also the profiles of the other teeth of the wheel.

In the design of toothed wheels one is faced with the problem of the angle to the line of centres that is to be formed by the line of action. This angle has no special name, but the complementary angle to it, i. e. the angle between the line of action and the perpendicular to the line of centres is called p r e s s u r e a n g l e α (see Fig. 56).

From calculations taking into account the strength and wear resistance of the teeth (the methods for these calculations are explained in the course on machine elements) we obtain the necessary module magnitude. At a certain module it is often desirable, and in some cases essential to adopt for wheels as few teeth as possible. This type of gear will be small in size and cost less in production. But the fewer the teeth in the wheels the harder it is to achieve the necessary condition for the proper operation of the wheels, i. e. that before the final disengagement of one pair of teeth the next pair must already have begun to engage. As a threshold case this condition will be achieved when the a r c o f c o n t a c t, i. e. the path, along which any point of the pitch circle passes during the time of gearing of one pair of teeth, is equal to the pitch. In this case the instants of disengagement of one pair of teeth and of engagement of the next pair will clearly coincide. In gearing designs one must make sure that each of the following pairs of teeth engages not at the final moment of disengagement of the preceding pair, but

before, i. e. that the arc of contact is greater than the pitch. The relation of the arc of contact to the pitch is called the overlap factor and is denoted by a small ε. The overlap factor determines the smoothness of gearing: the greater it is the smoother the drive operation, assuming that the other conditions remain the same.

An increase in the pressure angle necessitates a decrease in the arc of contact and, consequently in the overlap factor; it is therefore necessary to make the pressure angle as small as possible in order to provide for greater smoothness in the drive operation. However when the pressure angle is reduced, the required minimum number of teeth on the smaller wheel increases rapidly; therefore in order to reduce the proportions of wheels and, consequently, to reduce the drive cost, it is necessary to adopt a pressure angle that may possibly be a large one. Guided by such contradictory considerations, it was necessary to establish a pressure angle which would give no difficulties in obtaining a gearing with a sufficient overlap factor, and also would make the use of a large number of teeth unnecessary. The USSR Standard specifies the pressure angle 20°; the tooth-cutting tools are being made in accordance with this pressure angle.

Fig. 56 shows how the pressure angle affects the length of the arc of contact. During counter-clockwise rotation of the driving wheel with centre O_1 gearing starts at point B and the arc of contact at point D, where the tooth profile of the driving wheel intersects the pitch circle at the instant when gearing starts. Gearing begins at point B because at this point the profile of the driving tooth enters into contact with the extreme point of the tooth profile of the driven wheel lying on the addendum circle of this wheel (in Fig. 56 point B coincides with the right-hand profile of the driving wheel tooth; this coincidence is incidental). Gearing ends at point A, which is the point of intersection of the line of action with the addendum circle of the driving wheel. The arc of contact ends at point C, where the profile of the driving tooth, indicated by a dotted line, intersects the pitch circle in the final instant of gearing. The operating portion AB of the line of action, i. e. its segment between the beginning and the end of actual contact of conjugate tooth profiles is called the length of contact.

With a decrease in pressure angle α the line of action TT will turn counter-clockwise in Fig. 56 about pitch point P; as a result point B, the intersection point of the line of action with the addendum circle of the wheel with centre O_2, will move to the right, and point A, the intersection point of the line of action with the addendum circle of the wheel with centre O_1, will move to the left; the arc of contact will then increase because gearing will begin sooner and end later. It is true that in such a case there will be an increase in the diameters of the base circles and as a result the outlines of the profiles will change, and points C and D will be nearer to each other, but this approach will be insignificant compared with the increase in the arc of contact.

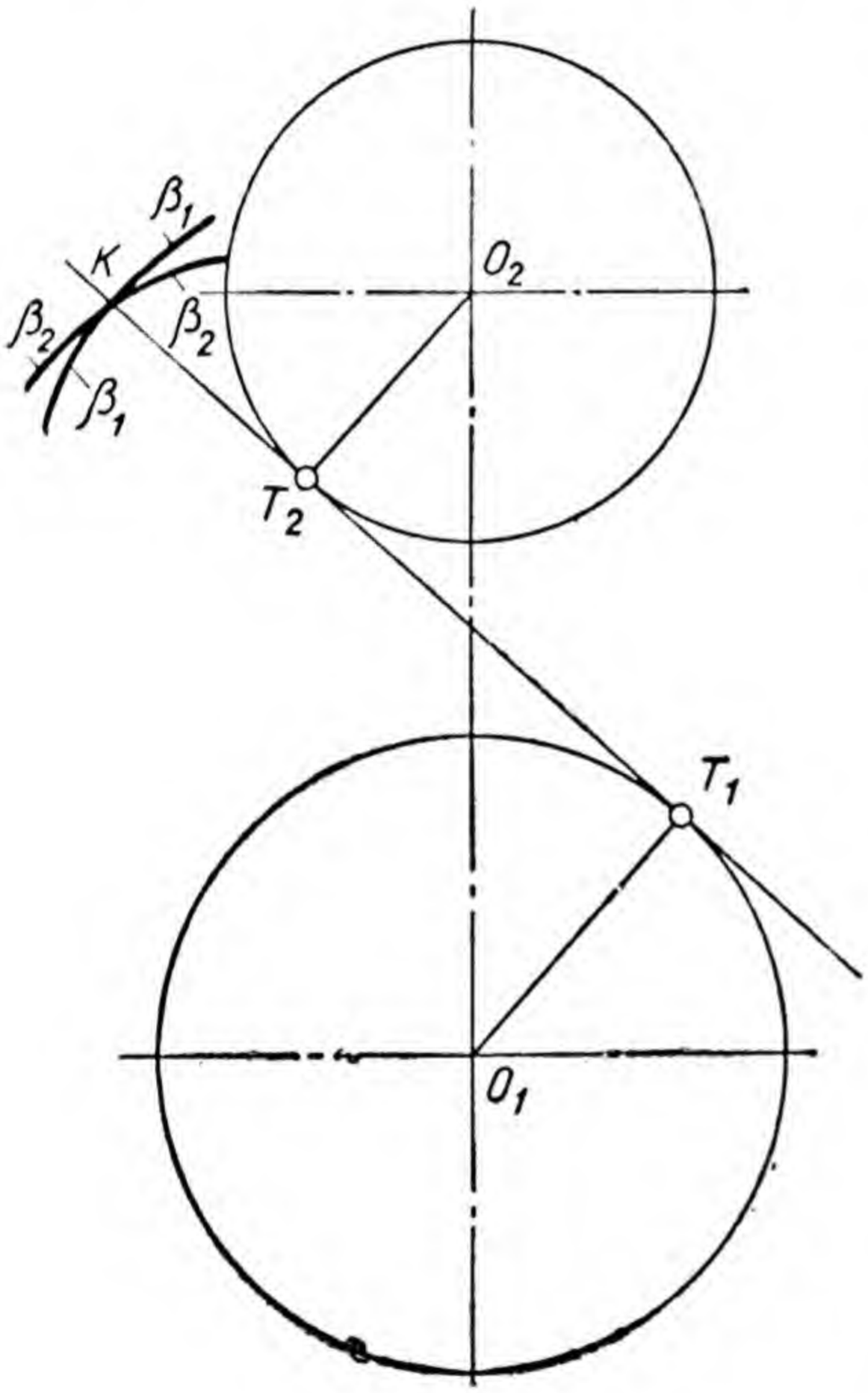

Fig. 67

Let us now discover the minimum number of teeth on the smaller wheel required to facilitate a gear drive at different pressure angles. We shall consider teeth of normal depth, i. e. with an addendum which is equal to the module.

First let us take into consideration the fact that during the operation of wheels the involute profiles may come in contact only on that portion of the line of action which is located between points T_1 and T_2 of contact of this line with the base circles (Fig. 66), since outside this portion the involute profiles cannot come in contact, but can only intersect.

From any point of contact situated on portion T_1T_2 of the line of action, the contacting profiles can be plotted by this point by means of rolling the line of action first along the circumference of one base circle, then along that of the other. For instance, profiles β_1 and β_2 in Fig. 66 can be

plotted by point K. In this case the profiles cannot intersect, since at the point of contact the curvature centres of both profiles (the points of contact of the generatrix with the base circles) are located at different sides from both profiles. The profiles which are so plotted are facing each other with their convex sides.

In drawing profiles by point K, which lies outside portion T_1T_2 of the line of action (Fig. 67), the curvature centres of the profiles at their point of contact will lie on one side of both profiles, as a result of which there can be no profiles facing each other with their convex sides. The curvature of profile β_1, which is traced by point K, decreases to the right of point K since the radius of the curvature increases, and the curvature of profile β_2 increases, since the radius of the curvature decreases gradually during the rolling of the line of action along the circumference of centre O_2; as a result to the right of K profile β_1 is situated higher than profile β_2. To the left of point K the curvature of profile β_2 decreases and the curvature of profile β_1 increases, as a result of which profile β_1 is located lower than profile β_2. It follows from this that it is impossible to use any point lying on the line of action outside portion T_1T_2 to plot two nonintersecting involute profiles by rolling the line of action without slipping first along the circumference or on base circle and then along that of the other.

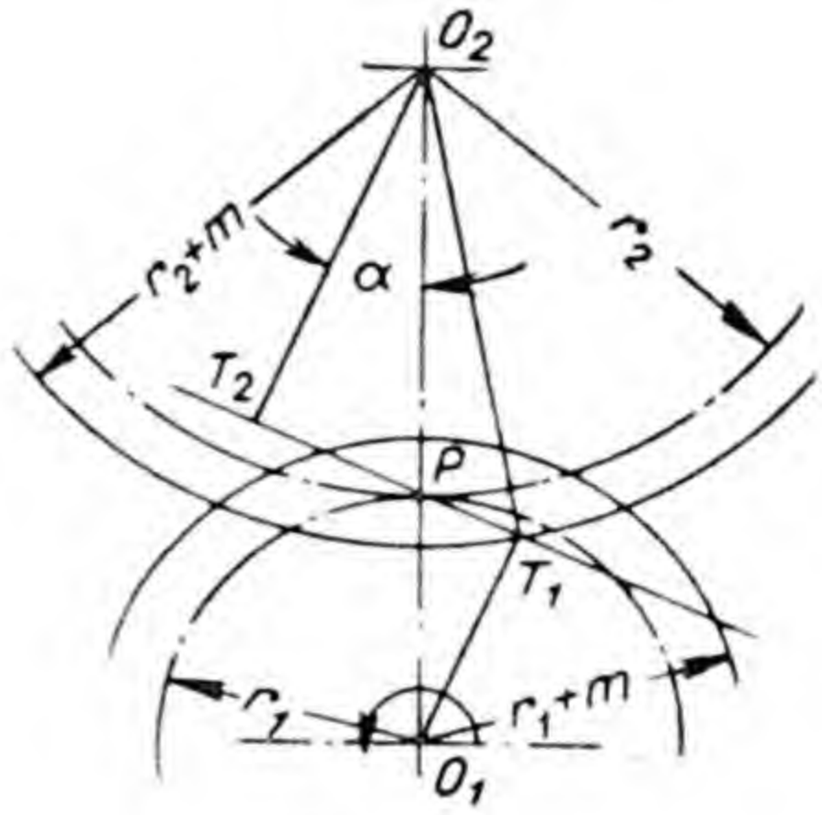

Fig. 68

Let us draw (Fig. 68) the pitch circles of centres O_1 and O_2 and radii r_1 and r_2, the line of action at $90°-\alpha$ angle to the line of centres, the addendum circle of radii r_1+m and r_2+m. Let us drop perpendiculars O_1T_1 and O_2T_2 from centres O_1 and O_2 to the line of action. Segments O_1T_1 and O_2T_2 are radii r_{01} and r_{02} of the base circles.

Let us assume that the driving wheel is the wheel with centre O_1 and that it rotates counter-clockwise.

The quicker the tooth of the driving wheel engages the greater will be the section of the line of action utilized; at the time of gearing the driving wheel will be turning

with one pair of teeth at a large angle and therefore a smaller number of teeth will be sufficient. As we already found with normal teeth the engagement cannot take place on the line of action before point T_1; therefore we will obtain the minimum number of teeth if we assume that engagement starts at point T_1.

Let us draw at point T_1 radius $O_2T_1=r_2+m$ of the larger wheel addendum circle, i. e. the wheel with centre O_2. The length of segment PT_1 of the line of action can be expressed as follows:

$$PT_1=T_1T_2-T_2P=\sqrt{(r_2+m)^2-r_{02}^2}-r_2\sin\alpha.$$

The very same length can also be expressed as follows:

$$PT_1=r_1\sin\alpha.$$

We obtain equation

$$r_1\sin\alpha=\sqrt{(r_2+m)^2-r_{02}^2}-r_2\sin\alpha.$$

Substituting in this equation $r_2=ir_1$, where $i\geqslant 1$, $m=2r_1/z$, where z is the number of teeth of the smaller wheel,

$$r_{02}=r_2\cos\alpha=ir_1\cos\alpha_1,$$

after reducing all members to r_1 and simplifying the equation we get

$$(1+2i)\sin^2\alpha\times z^2-4iz-4=0,$$

whence

$$z=2\,\frac{i+\sqrt{i^2+(1+2i)\sin^2\alpha}}{(1+2i)\sin^2\alpha}.$$

Fig. 69 shows curves that are plotted according to this equation; they express the relations of the practical minimum number of teeth on the pressure angle at different constant velocity ratios.

When $i=\infty$, we obtain a gear rack instead of a larger wheel. By dividing the numerator and the denominator of the right-hand side of the equation obtained above by i, and

then laying $i=\infty$, we get the relation of the minimum number of wheel teeth gearing with the gear rack as

$$z=\frac{2}{\sin^2\alpha}.$$

We stated above that, when the profiles of teeth are correctly produced, the centre distance can be somewhat changed during the setting of the wheels without upsetting the velocity ratio. Now we know that this pertains to involute profiles. Since a change in the centre distance does not change the profiles of teeth, then the diameters of the base circles also remain unchanged, but the direction of the common tangent (i. e. the line of action) to the base

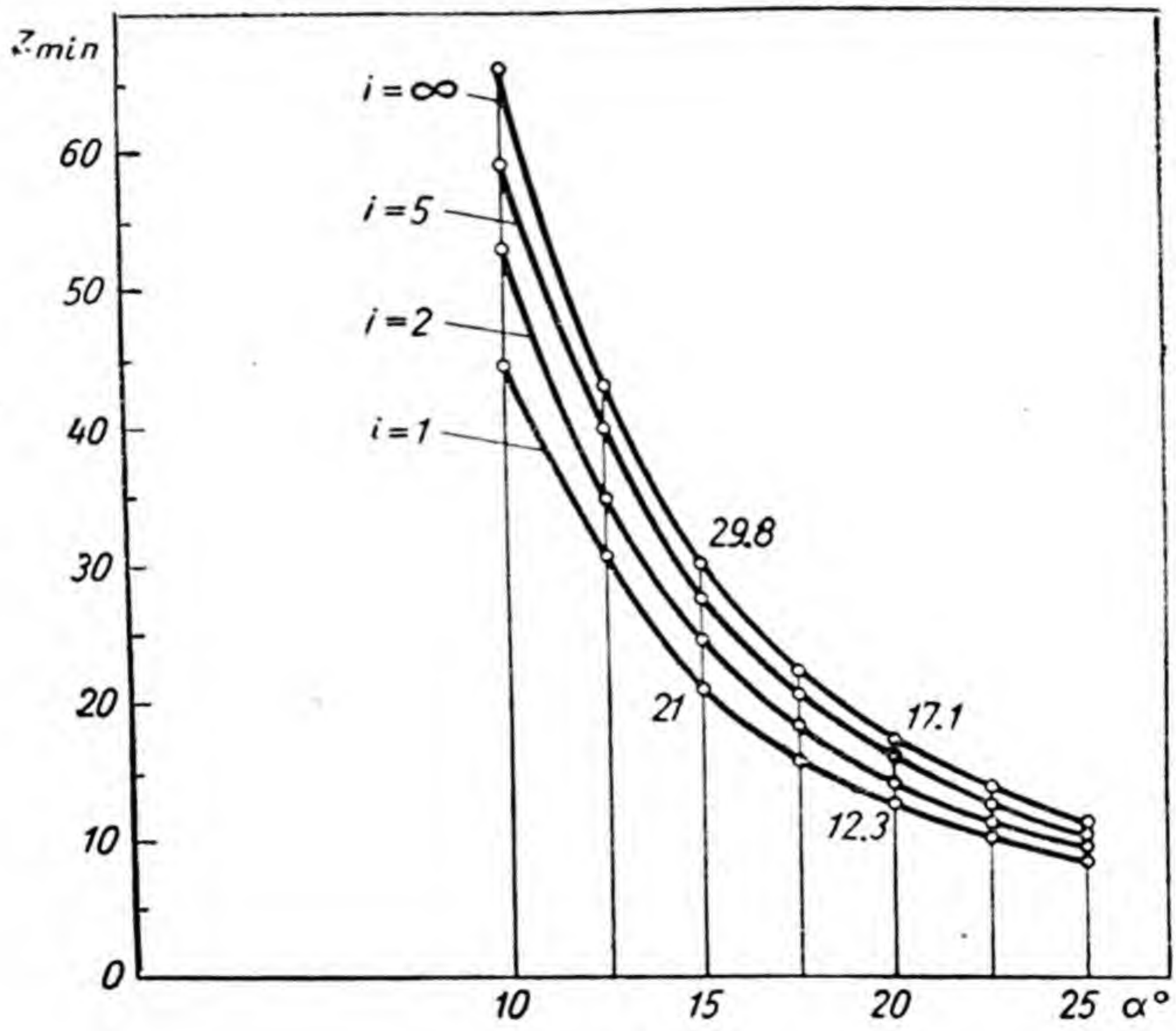

Fig. 69

circles changes, and as a result the position of the pitch point on the line of centres changes. If before changing the centre distance the nominal pitch circles coincided with the pitch circles, then after the pitch point has been moved to a new point on the line of centres with a consequent change in the diameters of the pitch circles, these circles will no longer coincide. A change in the pres-

sure angle (resulting from a change in the direction of the line of action), and also a change in the module (resulting from a change in the diameters of the pitch circles) must necessarily affect the operating conditions of the wheels, in particular, the magnitude of the overlap factor, but the transmission of rotary motion by teeth with involute profiles, when the nominal pitch circles do not coincide with the pitch circles, will be just as correct and with the same velocity ratio as in the case where these circles coincide.

D. The Production of Toothed Wheels

The satisfactory working of toothed wheels can be ensured only if the teeth are accurately manufactured; at high peripheral velocities (of the order of 25 m/sec and over) inaccuracy in profiles of the order of 0.005 mm already affects considerably the drive operation.

The best results in tooth cutting are obtained by applying the g e n e r a t i n g method. For a better understanding of this method it is necessary to find out first how a toothed wheel meshes with the rack, which is a toothed wheel with an infinitely large radius and, therefore, performs rectilinear motion.

Let us draw (Fig. 70) the pitch circle of the wheel of centre *O* and radius *OP*. If *P* is the pitch point, the straight line *SS* is the pitch circle of the rack with an infinitely large radius. Line *SS* is called the m o d u l a r l i n e.

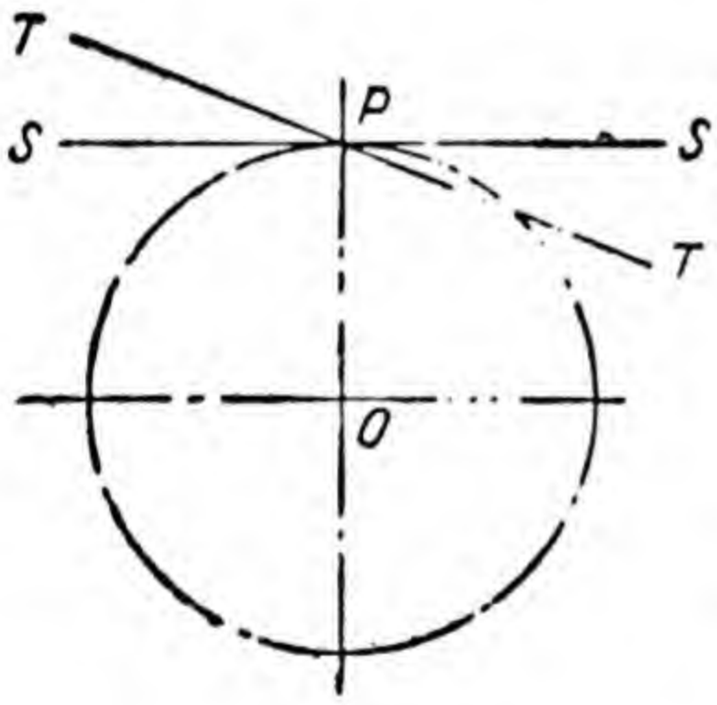

Fig. 70

The line of action, at any respective disposition of the contacting profiles, as determined above, must be normal to both profiles at their point of contact. The tooth profile of the wheel, which rotates about the centre of the base circle, must be outlined by the involute, if the above condition is to be consistently observed during motion of the conjugate tooth profiles of the wheel and rack; on the other hand, the profile of the rack tooth, which moves rectilinearly, will remain perpendicular to the line of action, if the tooth profile is outlined by a straight line perpendicular to the

line of action, since at an infinitely large radius of the base circle the involute becomes a straight line.

The straight-sidedness of the tooth profile of the rack is very important for the technique of toothed wheel manufacture: teeth with a straight-sided profile can be produced with a high degree of precision without particular difficulties, and the precisely manufactured cutting tool can be utilized for accurate machining of teeth with an involute profile, regardless of how many teeth the wheel will consist of.

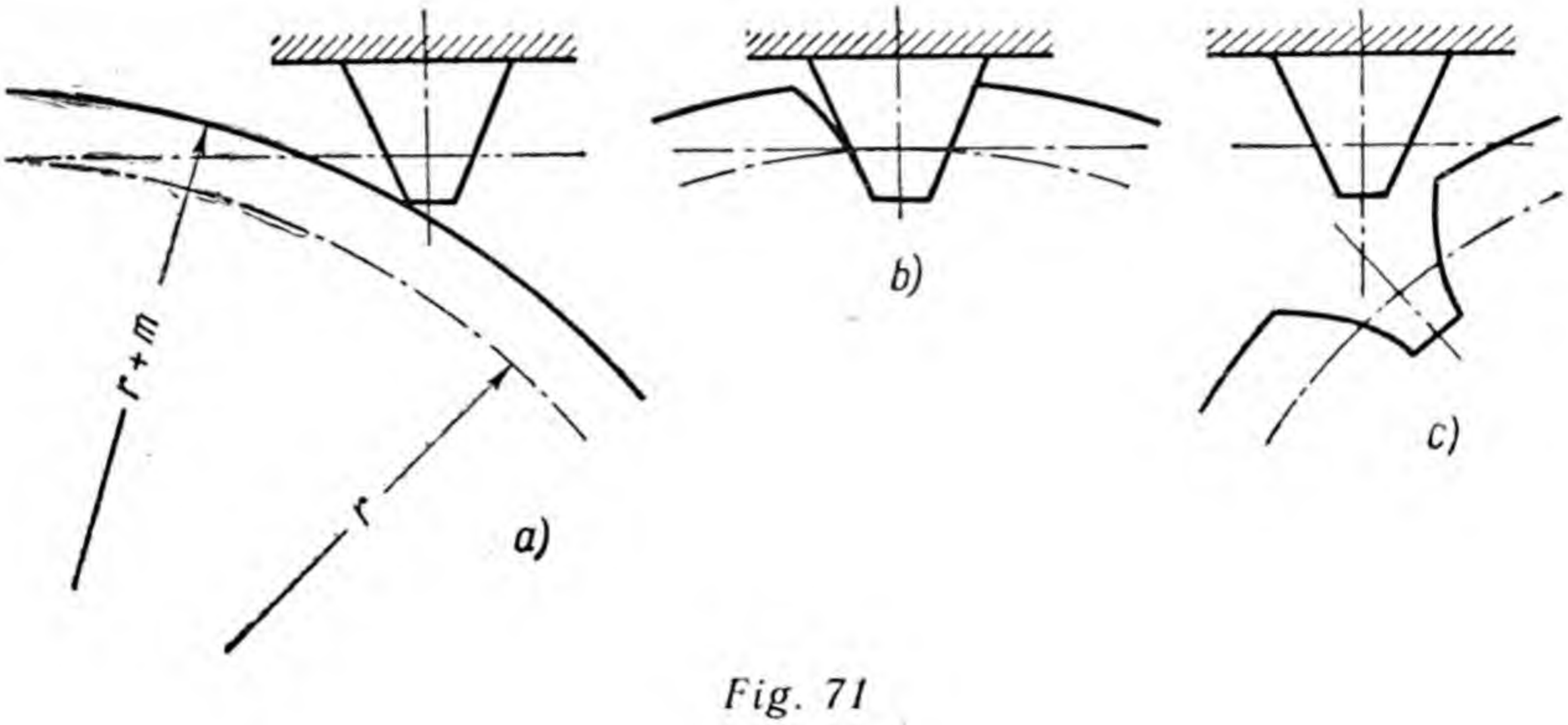

Fig. 71

In order to understand how the involute profile of a wheel tooth is obtained by means of the rack (with teeth of trapezoidal cross section), let us first imagine one tooth of the rack, made of rigid material, and a cylindrical disk made of plastic material, which can easily change its shape under pressure.

Let us arrange the rack tooth and disk, as is shown in Fig. 71, *a*: the lower left angle of the tooth touches the external surface of the disk. The disk radius equals $r+m$, where r is the radius of the wheel nominal pitch circle, and m is the module.

During operation of the wheel and rack the pitch circle of the wheel and the modular line roll over each other without slipping. We shall leave the tooth stationary and roll the nominal pitch circle of the disk along the modular line without slipping. As a result of such rolling the tooth will gradually penetrate into the disk material, making

a space between the adjacent teeth. Fig. 71, *b* shows the respective location of the rack tooth and disk in intermediate position, and Fig. 71, *c* shows the tooth and the space formed after rolling, which is limited by the side surfaces of the adjacent teeth with involute profiles.

It stands to reason that this manner of obtaining a toothed wheel from a cylindrical blank, which is in practice impossible, is given only in order to illustrate the principle of cutting teeth by the generating method. With a steel rack tooth and a metal blank, instead of depressing the rack into the blank, a gradual cutting away of the blank material by the rack tooth is performed, for which purpose the rack is made as a metal-cutting tool whose straight-sided profiles are the profiles of the cutting edges. In this case the rack performs reciprocating motion in a direction perpendicular to the plane of the machined blank, which remains fixed during the working motion of the rack.

Different versions of the generating method are employed in different gear-cutting machines. We shall not examine these versions here.

If the generating method is employed, the profiles of teeth come out involute on the entire length from the addendum circle to the base circle only in those cases, where the number of teeth being cut is not less than the number obtained by the formula given above for determining the minimum possible number of teeth. When the number of teeth is less than that obtained by the formula the profile outline becomes distorted: the tooth point of the rack-tool undercuts part of the involute portion of the profile, which starts at the base circle, during which process the root of the tooth is also undercut, i. e. the portion of the tooth which is situated between the base circle and the dedendum circle. As a result of this the tooth assumes a shape approximately similar to that, shown in Fig. 72. This type of tooth is called undercut.

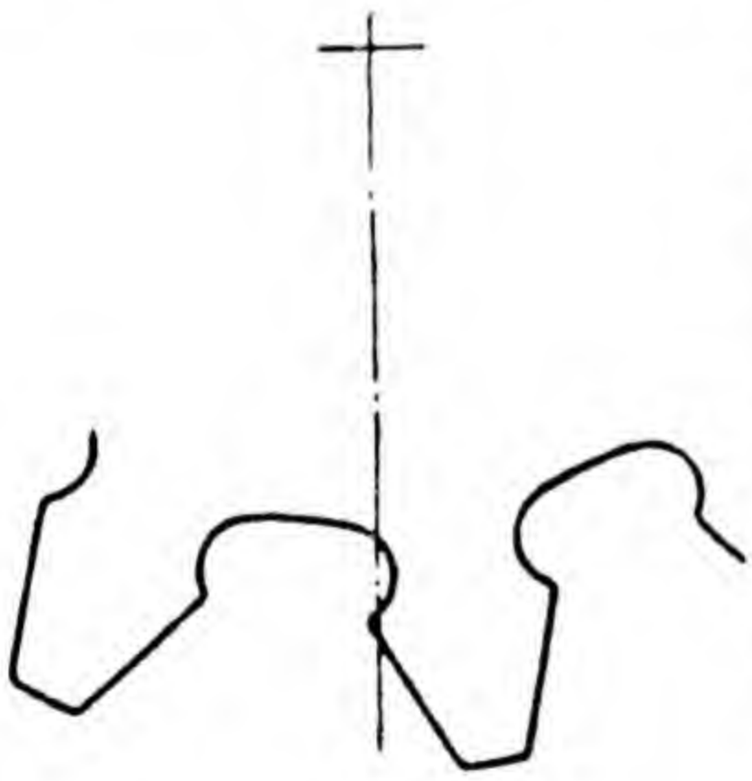

Fig. 72

It should be remembered that the undercutting of teeth to such an extent as to reduce their resistance to bending

occurs only at a significant decrease in the number of teeth, so that the minimum possible number of teeth is of conditional value. For example, by the formula, when $\alpha=20°$, $i=\infty$, $z=17$, the teeth will be undercut, whereas in practice the number of teeth can be accepted as 14 without particularly reducing their strength and this is frequently done.

We assumed above that in cutting teeth the modular line *SS* (see Fig. 70) is directed tangentially to the nominal pitch circle. This is how normal or zero (uncorrected) wheels are manufactured. But in the process of cutting the modular line may be shifted somewhat away from the blank axis (positive shift) or, on the contrary, nearer to the axis (negative shift). In such cases we get so called nonzero (corrected) wheels. Where a shift away from the blank axis takes place, the teeth do not come out undercut when their number is below 17; in such cases the teeth come out thicker at the roots and thinner at the tops in comparison with zero wheels. Where a shift towards the blank axis takes place, the undercutting of teeth is greater than in zero wheels, and this causes a reduction in their strength; shifting towards the blank axis is therefore applied comparatively rarely, mainly in such cases where it is impossible to retain the given centre distance by any other means.

The teeth of a wheel can also be cut by the formed cutter method. This method is effected by means of a cutting tool whose cutting edges are grooved (Fig. 73, *a*). By placing the cutting tool relative to the blank in such a position that the symmetry axis of the cutting edges of the tool is directed along the blank radius, we can make a cavity by moving the tool perpendicular to the blank plane, and by approaching the blank to the tool in the radial direction while the material is cut away. In this method the cutting edges are positioned on a revolving tool, the shape of which is shown in Fig. 73, *b*, and which is called a milling cutter. As this name implies, the process of cutting the blank material is called milling. The cavities are milled in succession, the blank being turned each time at angle $\frac{2\pi}{z}$, where z is the number of teeth.

Since the outline of the involute profile is determined by the pressure angle, by the module and the number

of wheel teeth, it follows that for the production of toothed wheels by the formed cutter method at a standard pressure angle it is necessary to have a special milling cutter for each module and each number of teeth. Since it is in practice impossible to keep large sets of milling cutters at plants, we have to be content with a limited number of cutter sets, utilizing a single cutter for the production of wheels with different numbers of teeth. For example, if we have a set of eight milling cutters, we have to use a single

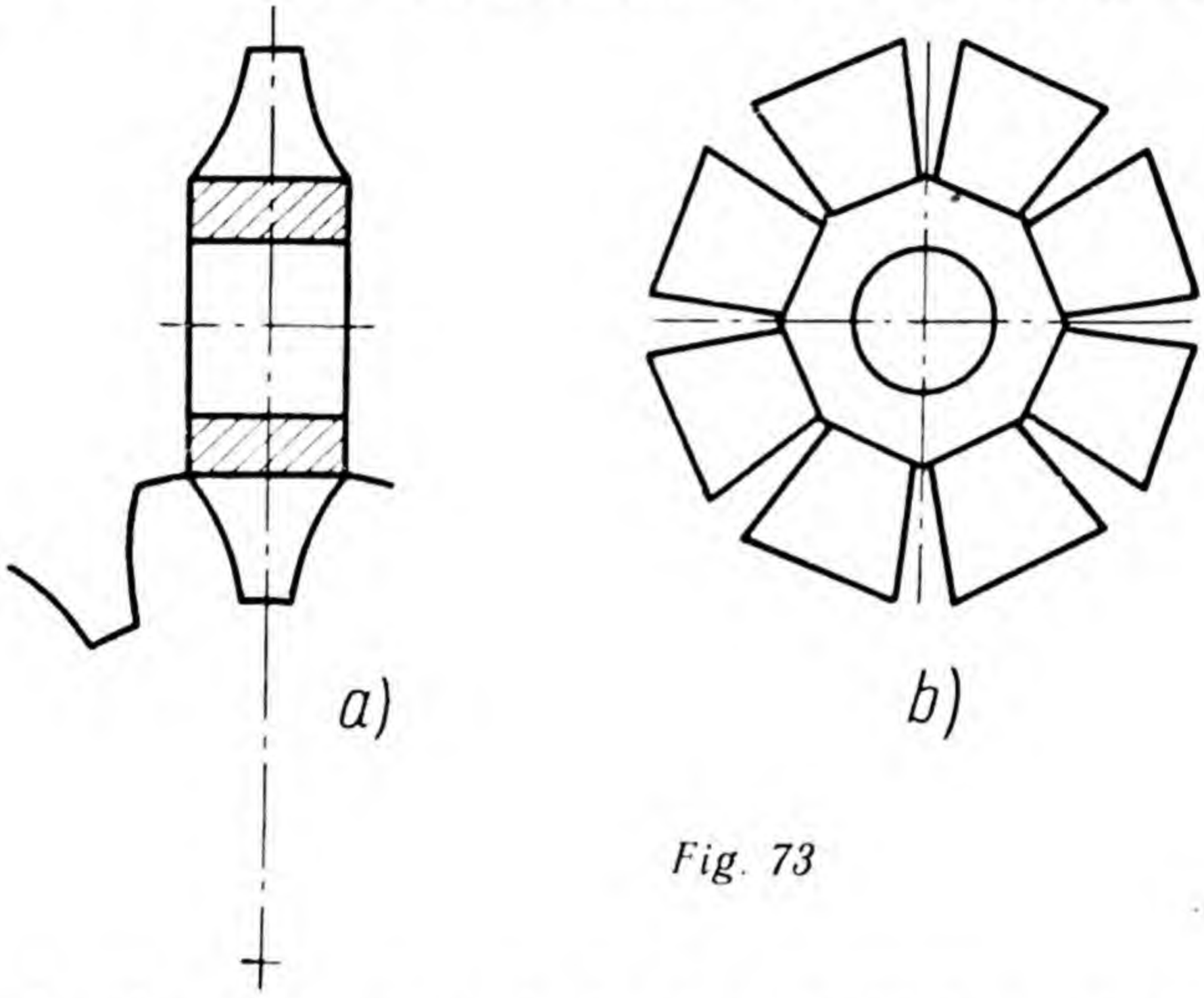

Fig. 73

cutter for the production of wheels with 26-34 teeth, another cutter for the production of wheels with 35-54 teeth, and so on. With each cutter we thus obtain accurate profiles only with one given number of teeth and not very accurate profiles in all other cases. Therefore in the production of toothed wheels intended for operation with high linear velocities on the pitch circles, the formed cutter method is not applied, because the teeth of such wheels must be machined with particularly high precision.

E. Helical and Herringbone Wheels

If we cut a toothed wheel into two equal parts along the plane, which is perpendicular to its axis, and then connect these parts rigidly, drawing them apart relative to each other at an angle smaller than $\frac{2\pi}{z}$, and do the

same to another wheel which is designed to operate in mesh with the first one, we will get two wheels with stepped teeth. The advantage of such wheel complication lies in the fact that at each instant the displaced parts of the teeth relative to each other will work with different portions of the profile, with the result that the wheels will operate more smoothly and with a greater overlap factor: the first portion will come out of contact, and will pass an identical arc of contact as an uncut tooth would have passed, while the other portion will for a certain time remain in contact.

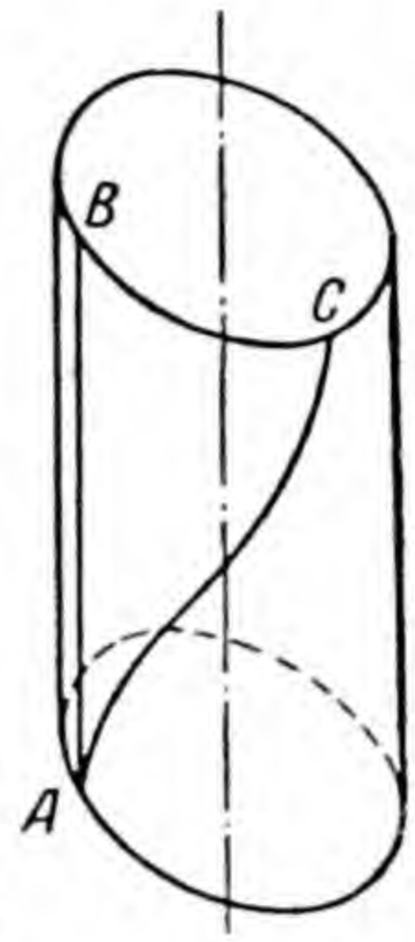

Fig. 74

Wheels with multistep teeth can be produced in a similar way. Despite the advantages mentioned stepped wheels have not, however, found practical application owing to the much greater difficulty of manufacturing them as compared with ordinary straight-tooth wheels.

An increase in the overlap factor and greater smoothness of operation can be obtained by directing the side surfaces of teeth so that the lines of action are located on the pitch cylinder along the helices. This type of wheel is called h e l i c a l.

Fig. 74 shows a pitch cylinder with line AB drawn on it to represent the line of the poles of a straight tooth, and helix AC to represent the line of the poles of the helical tooth. If in a straight-tooth wheel, rotating clockwise, the tooth comes out of contact at the instant when line AB occupies the position, as shown in Fig. 74, then in a wheel with helical teeth at the same instant the tooth is only beginning to come out of contact, and total gearing ends after point B passes arc BC.

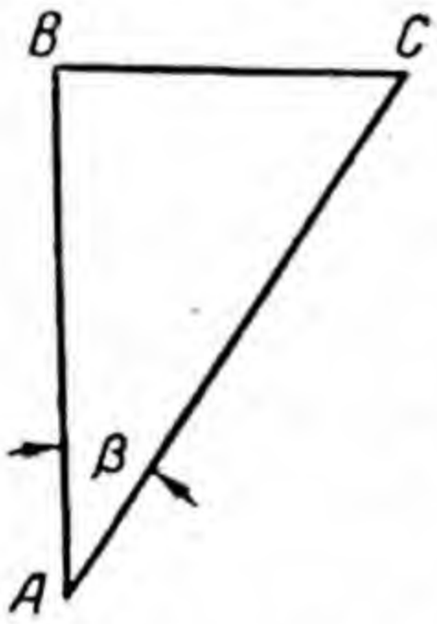

Fig. 75

By developing into plane a portion of the surface of the pitch cylinder, which is limited by lines AB, AC and arc BC, we get triangle ABC (Fig. 75), in which β is the angle of inclination of the line of the poles to the generatrix, which is a complementary angle to the lead angle of the line of the poles, and BC is the auxiliary arc of contact.

Given the length of a straight tooth $AB=b$ and overlap factor ε of straight-tooth wheels, the overlap factor of helical wheels will equal

$$\varepsilon+\frac{BC}{t}=\varepsilon+\frac{b}{t}\tan\beta.$$

Fig. 76 shows a plane development of a pitch cylinder portion with helical lines of the poles marked:

t_s — the circumferential pitch, i. e. the distance along the nominal pitch circle between the profiles turned to one side, of adjacent teeth in the circumferential cross section; relation $t_s/\pi=m_s$ is called the circumferential module;

t_n — the normal pitch, i. e. the shortest distance between the profiles, turned to one side, of adjacent teeth along the pitch cylinder; relation $t_n/\pi=m_n$ is called the normal module;

t_a — the axial pitch, i. e. the distance in a direction parallel to the wheel axis between the profiles, turned to one side, of adjacent teeth along the pitch cylinder.

In comparison with straight-tooth wheels the helical wheels have the following advantages:

1) since helical teeth contact at each instant with different points of the profile they wear out more uniformly than straight teeth;

2) since helical teeth do not come into mesh at once along the entire length, but gradually, they are less sensitive to shocks than straight teeth;

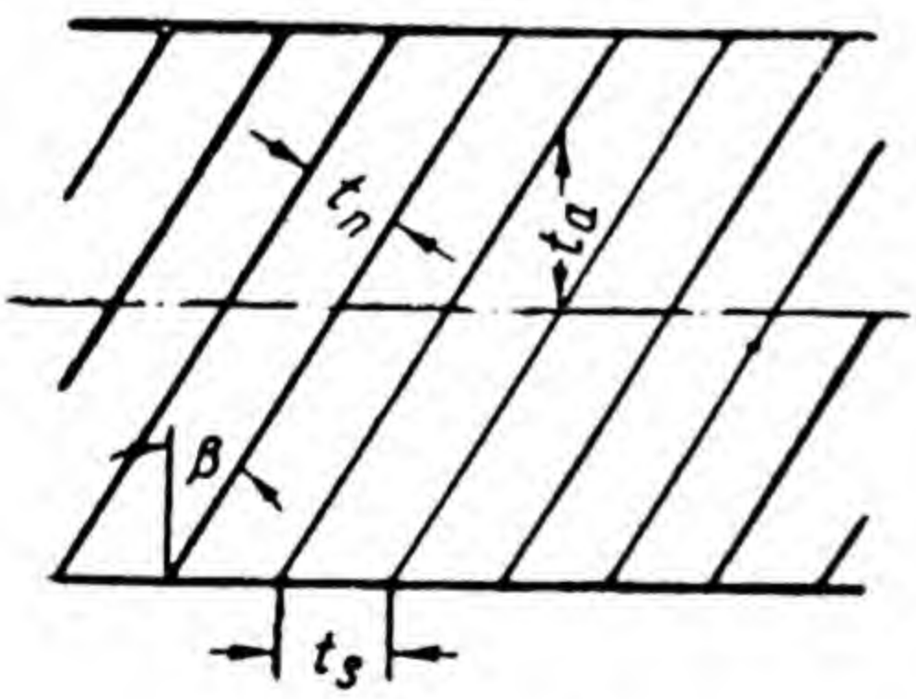

Fig. 76

3) with all other conditions equal, the greater overlap factor makes the minimum possible number of teeth in a helical wheel lower than in a straight-tooth wheel.

The disadvantage of helical wheels is that force P, with which the tooth of one wheel presses on the tooth of another wheel along the common normal to the helices (see Fig. 77, where the helix is shown in developed to plane position), splits into force P_1 which acts in the plane of wheel rotation, and force P_2 which is directed perpendicular to the plane of wheel rotation. Force F_2 creates axial pressure on

the bearings. This brings about additional losses of friction in the bearings, not to mention the resultant complication in the bearing design.

Axial pressures on the bearings can be avoided by placing on one shaft two helical wheels with teeth inclined to different sides or, what is simpler, by positioning on the wheel rim two rows of teeth inclined to different sides. Fig. 78 shows a plane development of a surface portion of the pitch cylinder of this type of wheel with the side helices of the teeth located on the pitch cylinder. For the sake of convenience in the manufacturing of wheels (for the exit of the cutting tool) an intermediate groove of small width is often left between two rows of helical teeth.

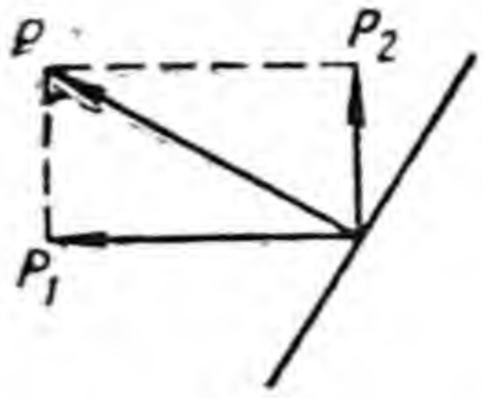

Fig. 77

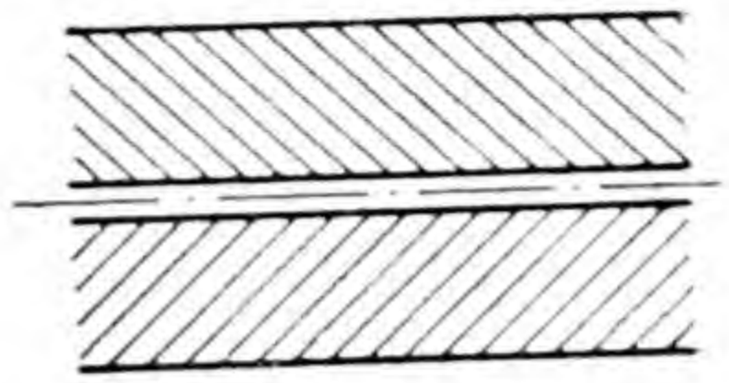

Fig. 78

This type of wheel is called herringbone and is usually used in transmission of large loads and with high linear velocities on the pitch circles of wheels.

In 1954-1955 M. Novikov, Soviet engineer, developed a completely new gearing for helical gears, which is different from the involute and has been successfully mastered.

In Novikov's system the teeth of one wheel are convex and those of the other wheel are concave. The teeth of both wheels are located on the helices in such a way that at any respective position of the wheels the teeth contact at point. The point of contact during operation of the gear displaces in a straight line, which is parallel to the wheel axes and is the line of the poles in this type of gear. Contact of the teeth at point is theoretical; in practice contact takes place on a small area, which results from deformation, and after a short run the gearing wears, so that the contact becomes linear along the whole height of the tooth, and displaces during operation along the tooth length.

Novikov's gearing of helical gears makes possible the transmission of a turning force 2-3 times greater than it was possible with helical gears with involute gearing of the same dimensions and similar material.

20. TRANSMISSION OF ROTARY MOTION THROUGH FLEXIBLE BODIES. BELT DRIVE

Transmission of rotary motion by flexible bodies is accomplished as follows: wheels, whose rims are enveloped by a flexible body, are tightly fitted on the driven and driving shafts; during rotation of the driving shaft and of the wheel fitted to it, the driving wheel entrains the flexible body which in turn entrains the driven wheel. Different types of flexible bodies are employed, such as: belts of various materials, ropes and chains. They are correspondingly classified into belt, rope, and chain drives.

The belt drive is a widely used type of transmission of rotary motion. From the kinematic point of view the rope drive does not differ from the belt drive; the essential difference between these two types of drives is only in the design shapes of the drive elements which are determined by the difference in rope and belt properties. In the past the rope drive was used mainly for the transmission of large loads, but with the growth of electrically operated factory and works equipment it has lost much of its usefulness and is at present hardly applied. In the case of both belt and rope drives the driving wheel entrains the flexible body which in turn entrains the driven wheel with the help of the force of friction. Therefore these two types of drives cannot be applied in those cases where transmission must be effected with an absolutely accurate velocity ratio.

A chain drive is effected by toothed wheels (called "sprockets"), which are enveloped by a chain engaging with the teeth; therefore in distinction from belt and rope drives the velocity ratio in a chain drive, which is equal to the ratio of the number of wheel teeth, remains invariable regardless of fluctuations in the magnitude of transmitted power. The chain drive has two major disadvantages: the heavy weight of the chain (as compared with the weight of a belt) and the gradual stretching of the chain, owing to which the chain has to be shortened from time to time by removing one of its links. These two disadvantages exclude in practice any possibility of using the chain drive where the axes of the driving and driven shafts are a large distance apart. At small distances in

certain mechanical devices application of the chain drive is expedient, particularly when the small distances between the axes of the shafts are too great for a gear drive.

A plane belt drive, i. e. transmission between shafts with parallel axes, is generally shaped as an open-belt drive, shown diagrammatically in Fig. 79, *a*, where O_1 and O_2 are the axes of shafts P_1 and P_2 that are rigidly connected with the wheel shafts, which in a belt drive are called p u l l e y s, and B is the belt which envelops both pulleys. As already mentioned, the transmission of motion from the driving pulley to the belt and from the belt to the driven pulley is effected with the help of the force of friction. With all other conditions equal the force of friction will be greater and transmission better at a greater angle α of contact of the pulley and belt. It is therefore necessary in designing such a drive to position the driving, i. e. the more tensioned portion of the belt, whenever possible, at the bottom, since the slacker driven portion, if positioned on top, increases the angle of belt contact (Fig. 79, *b*), and if placed at the bottom decreases this angle (Fig. 79, *c*).

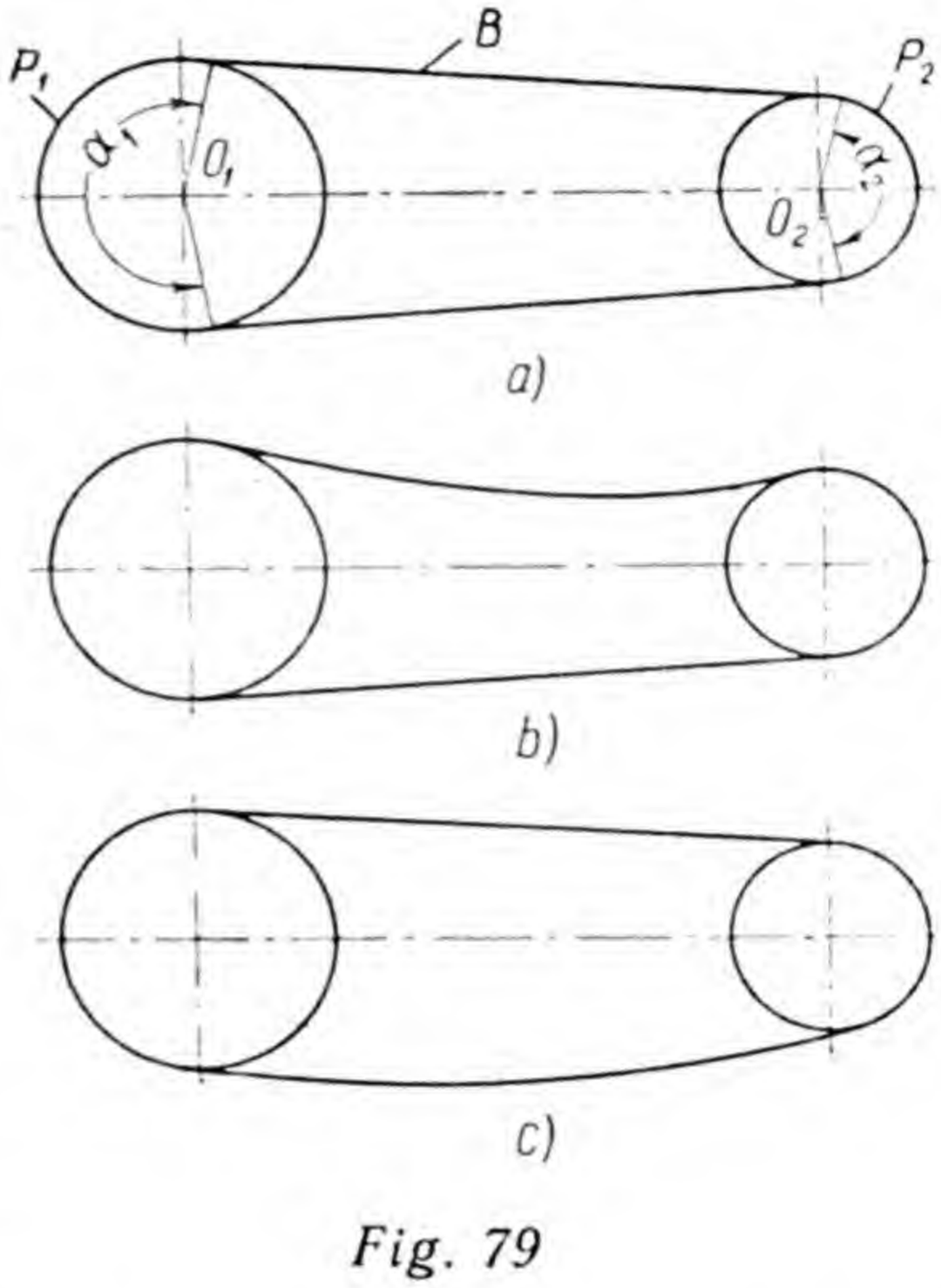

Fig. 79

The distance between the axes of the shafts in an open-belt drive may be considerable, up to 15 m, depending on the width of the belt and other conditions. At exceedingly large distances the belt begins to "whip", i. e. perform vibratory movements in a direction perpendicular to the direction of its motion, using up a part of the power which is transmitted to it by the driving pulley and adversely affecting its service life. With extremely small distances between the axes of the driving and driven shafts the belt slips on the pulleys to a greater extent than is permissible for the satisfactory working of the drive.

In an open-belt drive both pulleys revolve in the same direction. If motion has to be transmitted with a change in the direction of rotation, a crossed belt drive is employed, which is shown diagrammatically in Fig. 80. With identical distances between the axes of the pulleys and identical diameters of the pulleys, the angles of contact of the pulleys and belt are greater in a crossed belt drive than in an open-belt drive, which is an advantage of the crossed belt drive. However, with small distances between the axes of the shafts there is an exceedingly slanted run-off of the belt from the pulleys and as a result of this the belt is not fully utilized. Moreover, in a crossed drive the belt bends in two different planes and at the meeting point of the driving and the driven sides between pulleys, moving in different directions, it is subjected to wear. These disadvantages of crossed belt drives become more expressed the greater the belt width and the greater the linear velocity of the belt.

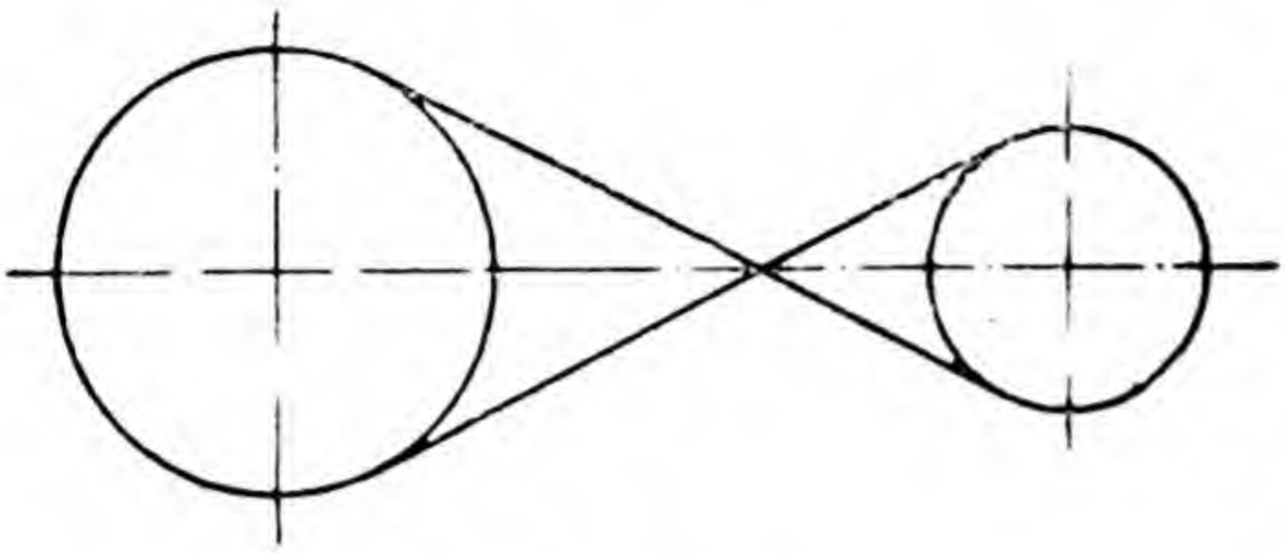

Fig. 80

If it were possible to construct a belt drive in such a way that the belt would not slip on the pulleys, the velocity ratio would be determined from the relation

$$\omega_1 R_1 = \omega_2 R_2,$$

whence

$$\frac{\omega_1}{\omega_2} = \frac{R_2}{R_1} = i,$$

i. e. the velocity ratio would be equal to the relation of the radii of the pulleys.

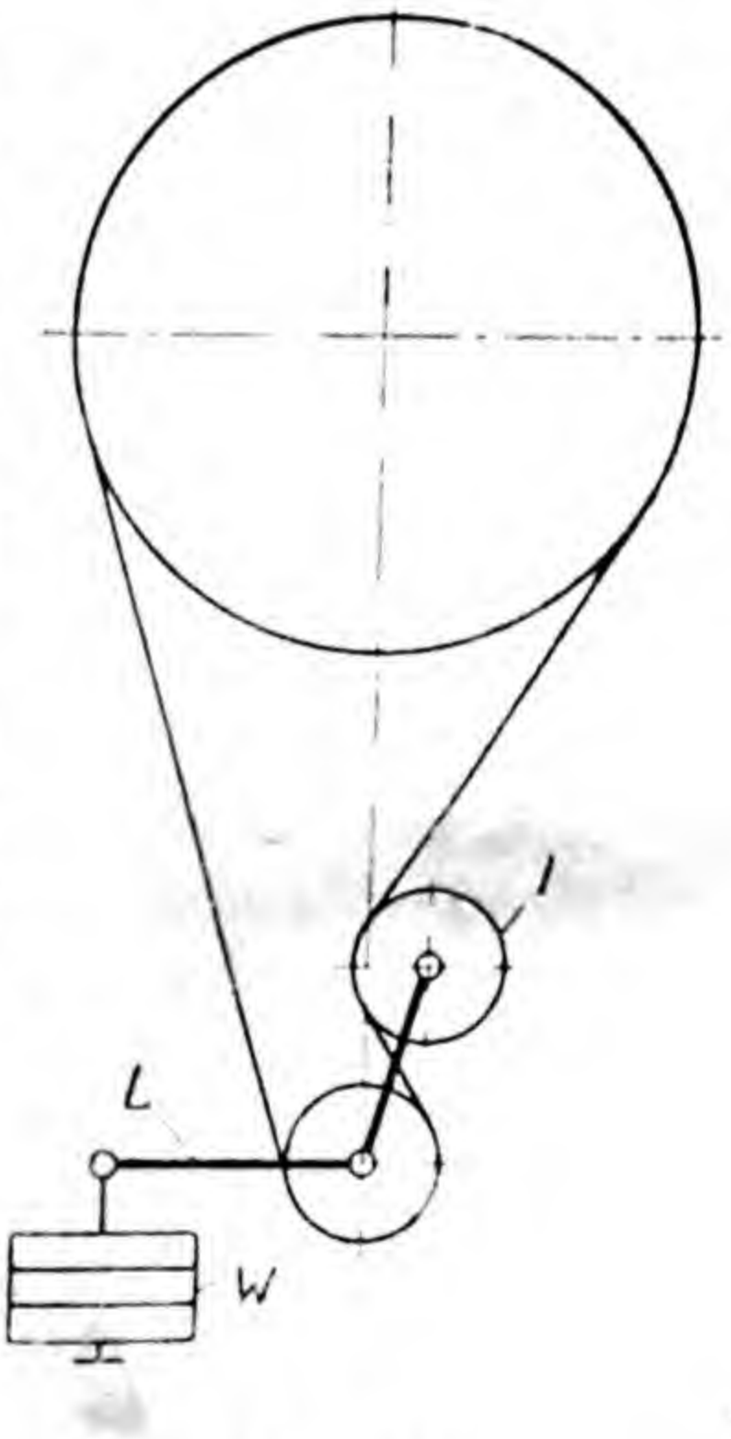

Fig. 81

However, in the work transmission the belt will necessarily slip on the pulleys, no matter how accurately the drive is constructed, since its driving portion is stretched more than its driven portion. Practice shows that

owing to the inevitable slip of the belt on the pulleys the speed of the driven pulley, given satisfactory drive operation, will be 1.5-2.5 per cent less than it would have been if there had been no slip. With all the other conditions equal the slip will be greater the greater the power transmitted.

The impossibility of achieving accurate velocity ratios is a disadvantage of the belt drive. However, in many cases this disadvantage is of no significance for practical purposes.

The belt slip exceeds the permissible limit and the operation of a belt drive becomes unsatisfactory where there is a very large velocity ratio or too small a distance between the axes of the driving and driven shafts, since either of these unfavourable conditions renders insufficient the angle of contact of the belt on the smaller pulley. In such cases the belt drive is provided with an idler pulley or with a countershaft.

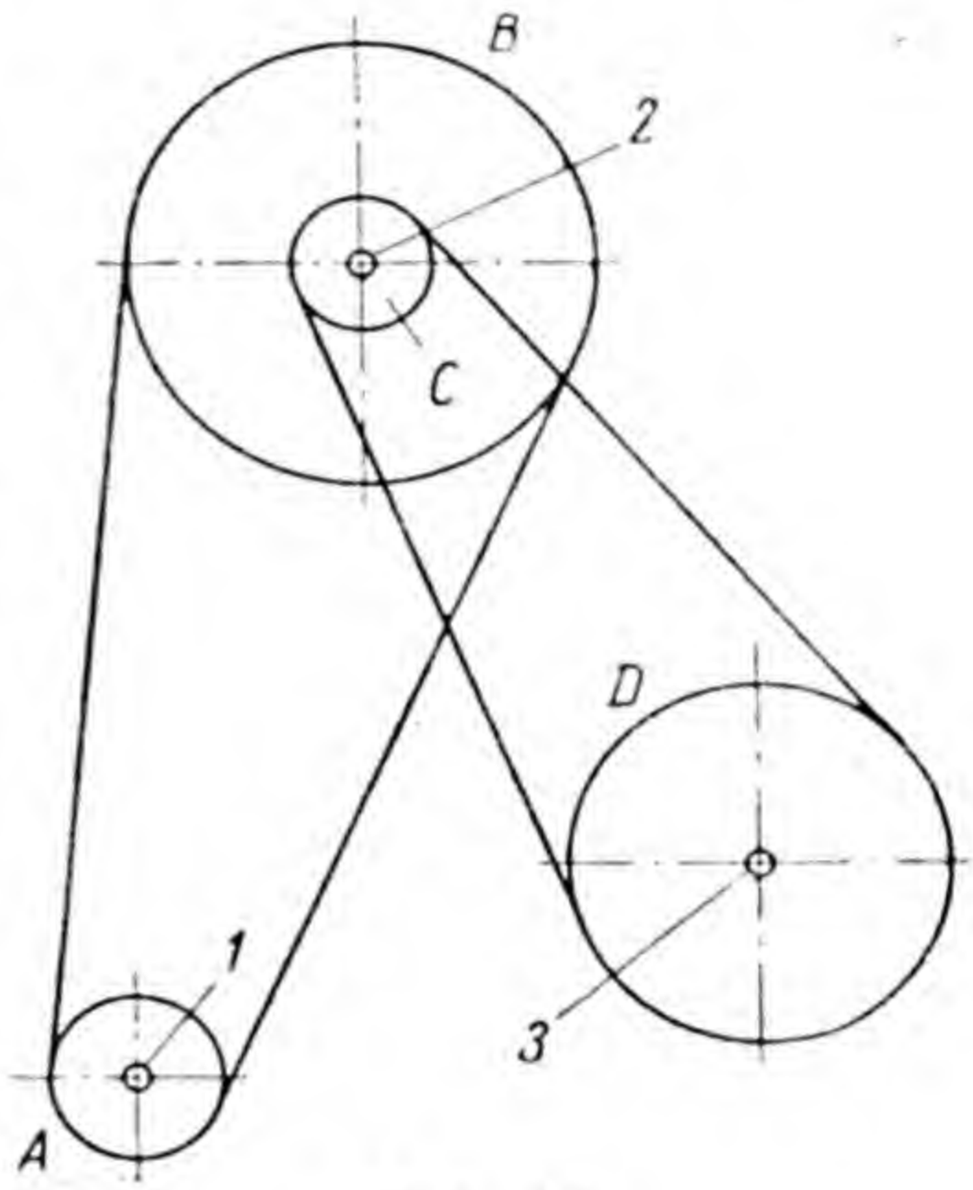

Fig. 82

A drive with an idler pulley is shown diagrammatically in Fig. 81. In this type of drive idler pulley *I*, which rotates freely on the axis of double-arm lever *L*, presses with a certain force on the driven part of the belt and by deflecting it increases considerably the angle of contact of the smaller pulley and belt. Lever *L* rests freely on the axis of the smaller pulley and is under the action of weight *W* or a spring. The force with which the idler pulley presses on the belt can be easily adjusted by changing the weight or tightening the spring. A drive with an idler pulley can operate satisfactorily even with large velocity ratios and small distances between the axes of the driving and driven shafts.

A drive with a countershaft (Fig. 82) is a drive with an intermediate shaft, in which the total velocity ratio from driving shaft *1* to driven shaft *3* is performed in two stages: from pulley *A* motion is transmitted to pulley *B*, which is located on shaft *2*, and from pulley *C*, which is

rigidly connected with the same shaft *2*, to pulley *D*. In each of the stages, which are ordinary open drives, the velocity ratio must not exceed the limit beyond which the belt is likely to slip over the pulley; it is therefore expedient to install two or more intermediate shafts in the case of a very high velocity ratio. A drive with a countershaft is at times employed even if there is no necessity to break up a large velocity ratio into two smaller ones: a countershaft may be called for if the

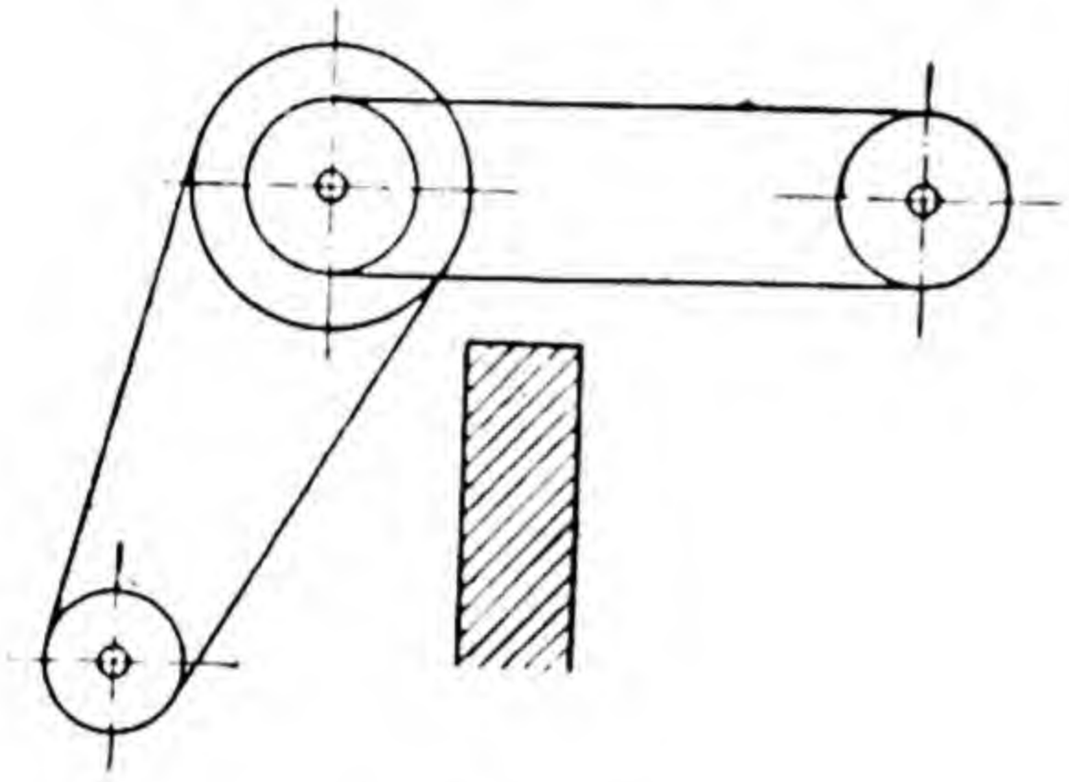

Fig. 83

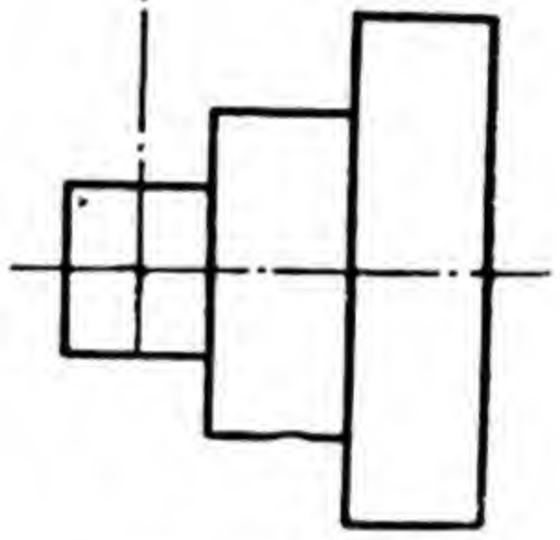

Fig. 84

local conditions do not allow direct transmission from the driving to the driven shaft (Fig. 83).

It is frequently necessary to effect transmission to machines at varied velocity ratios. This is achieved by means of stepped pulleys (Fig. 84). The diameters of

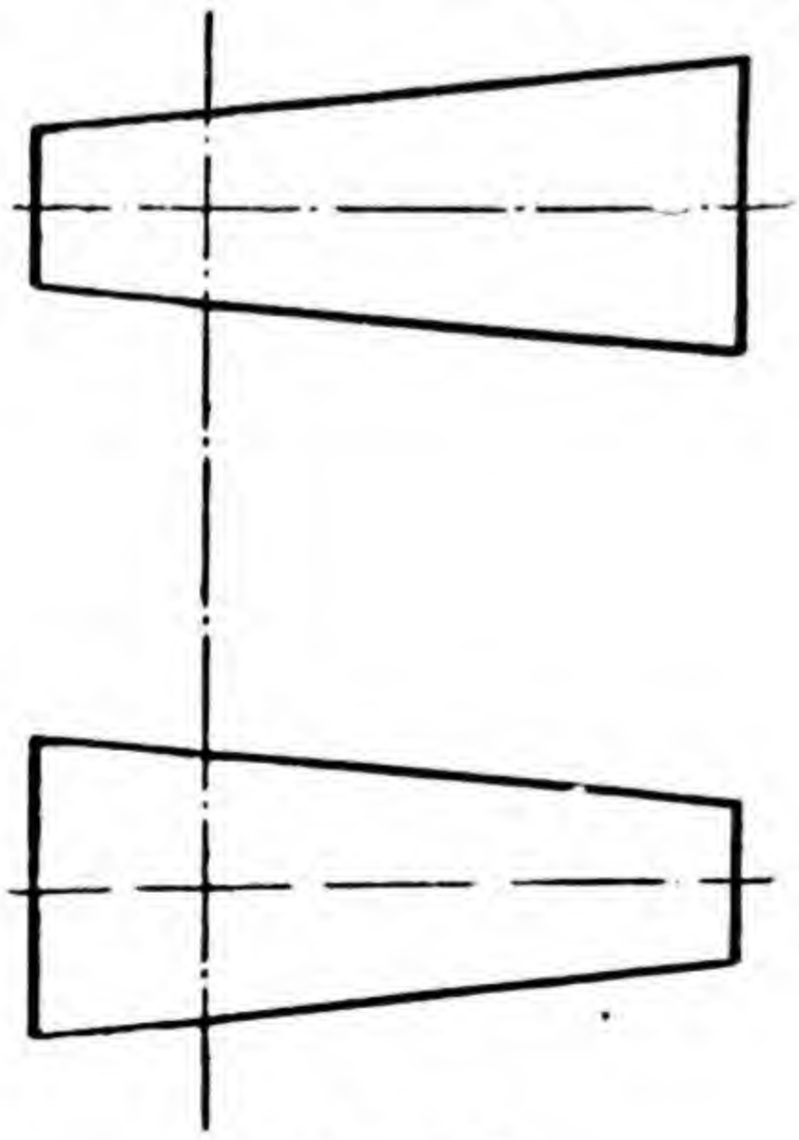

Fig. 85

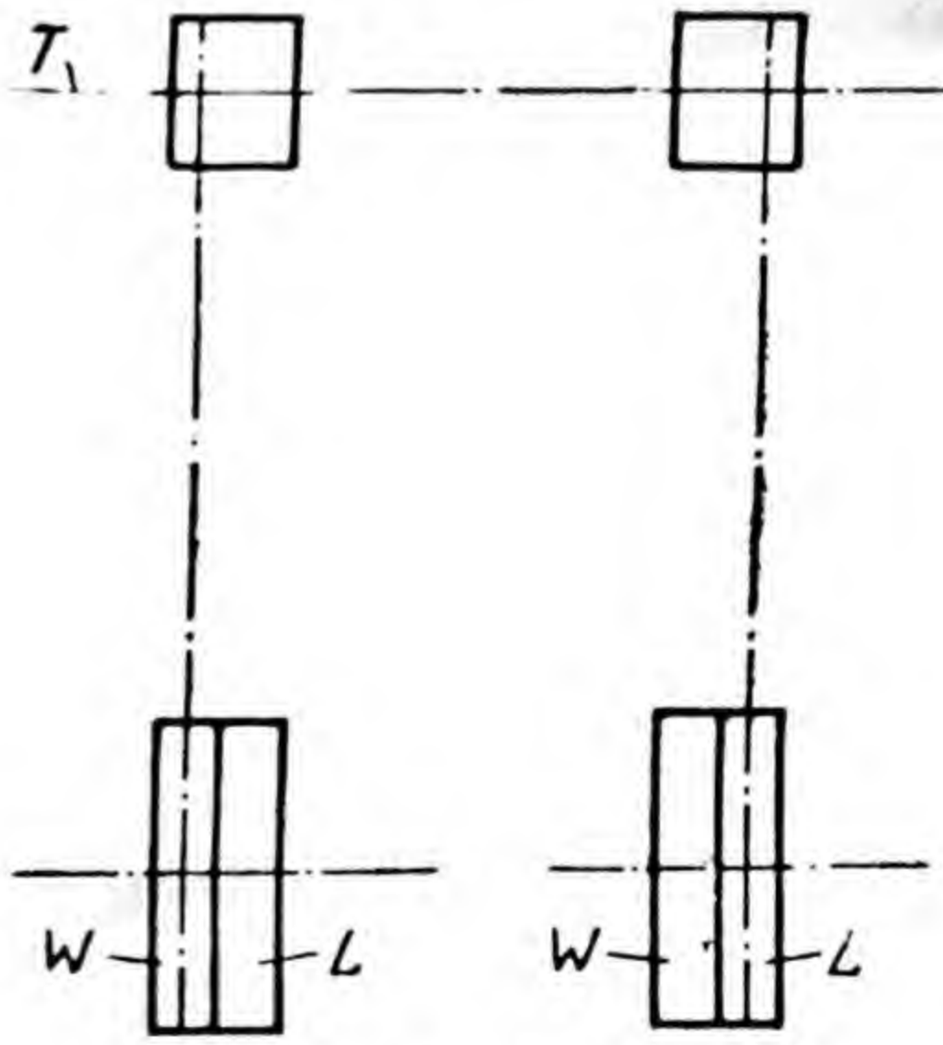

Fig. 86

stepped pulleys should be so chosen that an identical length of belt is required on each step. If cone pulleys are employed (Fig. 85), the velocity ratio can be smoothly changed within certain limits, depending on the maximum and minimum diameters of the pulleys, without stopping the drive operation while changing the velocity ratio.

In cases where the pulleys of a number of machines or apparatuses are driven from one driving shaft and where it is necessary to be able to stop transmission of rotary motion to any of them, without stopping transmission to the others, loose pulley *L*, which revolves freely on the shaft, is placed on the driven shaft of each machine or apparatus next to the working pulley *W* (Fig. 86), which is rigidly connected with the driven shaft. By placing on driving shaft *T* a pulley of double width it is possible, while maintaining constant rotation of the driving shaft, to actuate or stop the driven shaft by shifting the belt from the loose pulley onto the working one and vice versa with the help of a simple device called shifter.

Chapter IV

SPACE MECHANISMS FOR THE TRANSMISSION OF ROTARY MOTION

21. FRICTION DRIVE

A space friction drive is produced between shafts with intersecting axes. This drive can take place at different angles between the axes of the shafts, but most frequently it is employed between shafts with axes intersecting at right angles. We will discuss here only this type of drive.

In the transmission of rotary motion between shafts with parallel axes (at a constant velocity ratio) the pitch cylinders roll over each other without slip; this type of drive is therefore called spur gear. In transmission between shafts with intersecting axes (at a constant velocity ratio)

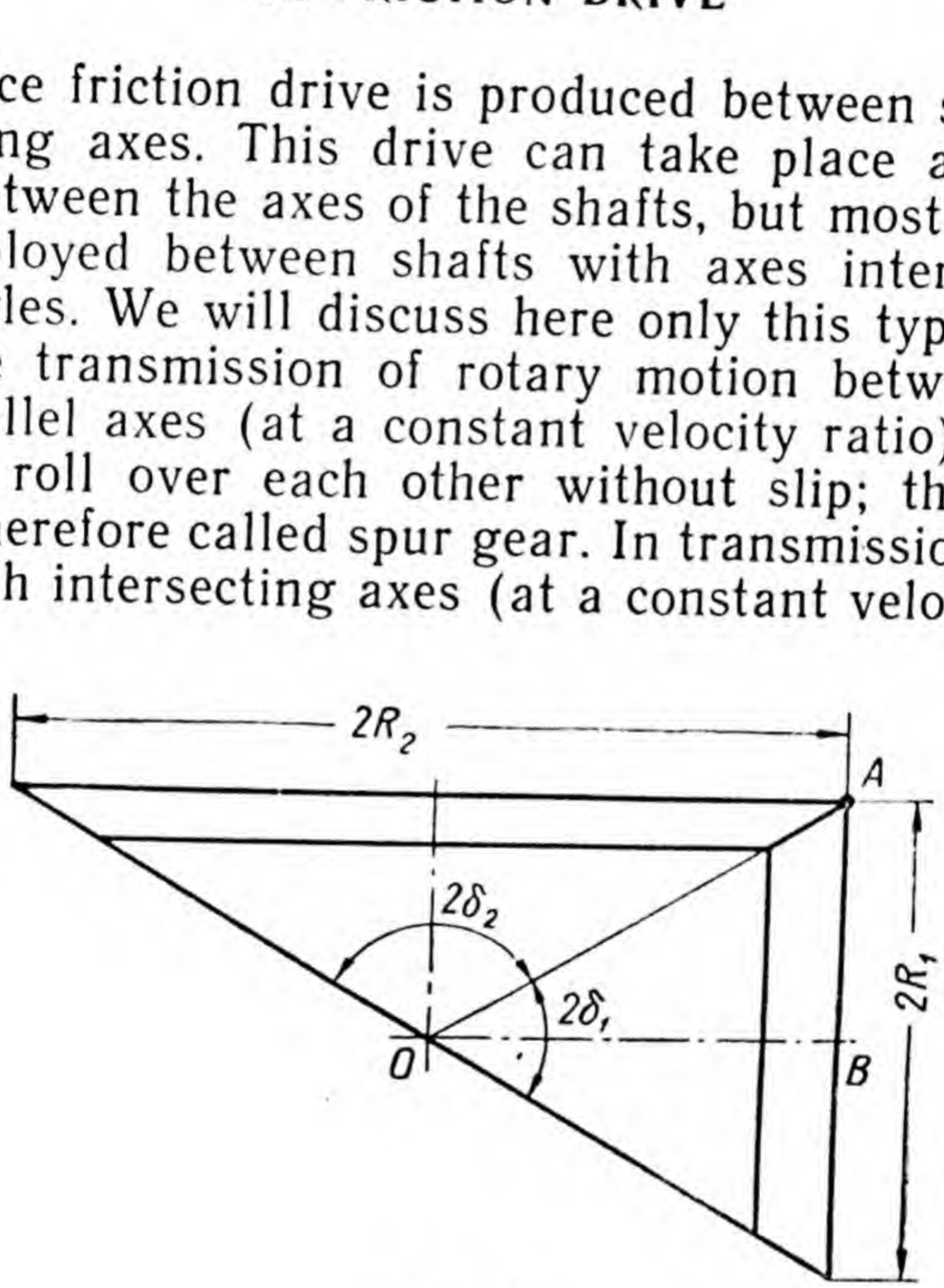

Fig. 87

the pitch cones roll over each other (Fig. 87); this type of drive is therefore called b e v e l g e a r d r i v e.

In a spur gear the velocity ratio can be expressed by the relation of the radii of the pitch cylinders, in a bevel gear drive by the relation of the radii of the pitch cone bases, as can be easily seen from the following.

The linear velocity of point A (Fig. 87), which belongs to one of the cones, during rotation of the cone about axis OB is equal to $\omega_1 R_1$, where ω_1 and R_1 are the angular velocity of rotation and the radius of the cone base; the linear velocity of point A, which belongs to another cone, is equal to $\omega_2 R_2$, where ω_2 and R_2 are the angular velocity of rotation and the radius of this cone's base. With the rolling of one cone on the other without slip the following equation should be correct

$$\omega_1 R_1 = \omega_2 R_2,$$

whence

$$\frac{\omega_1}{\omega_2} = i = \frac{R_2}{R_1}.$$

In a bevel gear drive the velocity ratio can also be expressed differently. Denoting by δ_1 and δ_2 the half angles at cone apices, we get

$$\frac{R_2}{R_1} = \tan \delta_2 = \cot \delta_1,$$

i. e. the velocity ratio of a bevel gear drive can be expressed by the tangent of the half angle of the apex of one of the pitch cones or by the tangent of the half angle of the apex of the other cone.

In a spur friction gear the surfaces of the pitch cylinders are the outer surfaces of the rollers. Similarly in a bevel friction gear drive the surfaces of the pitch cones are the outer surfaces of the bevel rollers which, as in the spur gear drive, must be pressed against each other with sufficient force.

Pressure of one roller against the other is achieved in a spur gear by positioning the shaft of one of the rollers on bearings which move in the radial direction, and maintained by the motion of the bearings together with the shaft and roller in the radial direction. In a bevel gear the shafts are positioned on fixed bearings, and pressure is effected by force (usually from a spring) which is directed along the axis of one of the rollers.

In an ordinary bevel friction gear drive the velocity ratio is constant. In the disk gear, shown diagrammatically in Fig. 88, the velocity ratio may vary within certain limits by changing the distance k from the disk axis B to the

centre plane of roller *A*. There are simple devices that can secure roller *A* at any point on its shaft in order to change this distance.

The disk gear is one type of variable-speed drives. Variable-speed drives are called mechanisms for the smooth, i. e. stepless change of the angular velocity of the driven shaft at constant velocity of the driving shaft. In a bevel friction drive the shafts press on the bearings not only in the radial direction, as is the case in a spur gear drive, but also in the axial direction. Otherwise the advantages and disadvantages of a bevel friction gear drive determining the sphere of its application are the same as those in a spur gear drive.

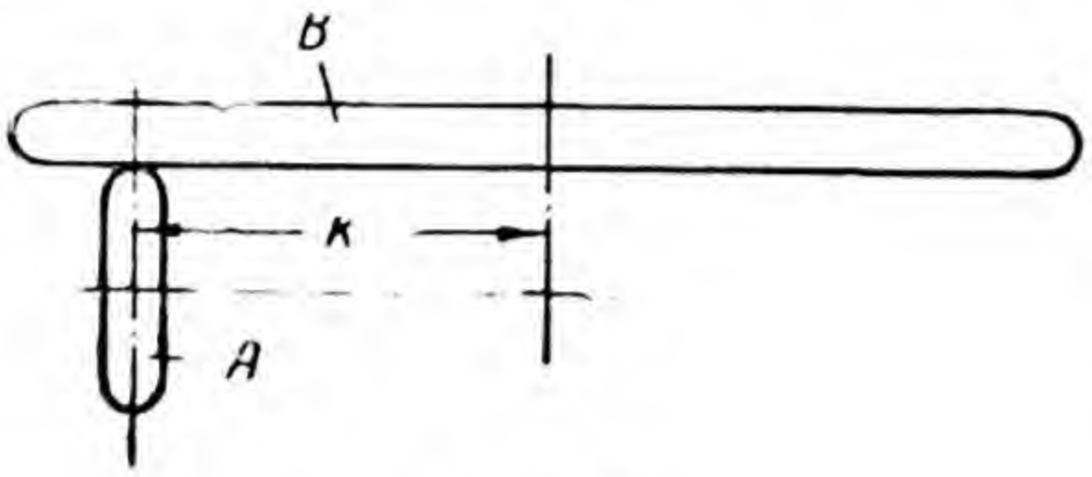

Fig. 88

22. GEAR DRIVE

A space gear drive, like a space friction drive, takes place between shafts with intersecting axes and is similarly employed mainly between shafts with axes that cross at right angles. We shall discuss only this type of drive.

As is the case with the pitch cylinders in a spur gear drive the pitch cones in a bevel gear drive are imaginary. The proportions of the teeth in height and thickness and the pitch and module in a bevel wheel change in proportion to the distance from the cone apex. The module of a bevel wheel, which should be approximated to the State Standard when designing a drive, is considered the module on the larger base of the pitch cone.

As is the case with a bevel friction drive the velocity ratio in a bevel gear drive can be expressed by the relation of the base radii of the pitch cones or by the tangent of the half angle at the apex of one of the pitch cones (or by the cotangent of the half angle at the apex of the other).

In a spur gear drive the meshing of a pair of conjugate profiles takes place on one plane, and thus both profiles can be drawn on a plane with the necessary accuracy (in practice they are produced by cutting on gear-cutting machines without preliminary drawing).

In a bevel gear drive the meshing of a pair of conjugate profiles takes place on a spherical surface, and since a spherical surface cannot be developed into plane, the accurate drawing of the profiles of bevel wheels on plane is impossible. When the execution has been accurate, the profiles of bevel wheel teeth should be spherical involutes. but the production of wheels with such profiles is in practice very difficult with existing machines.

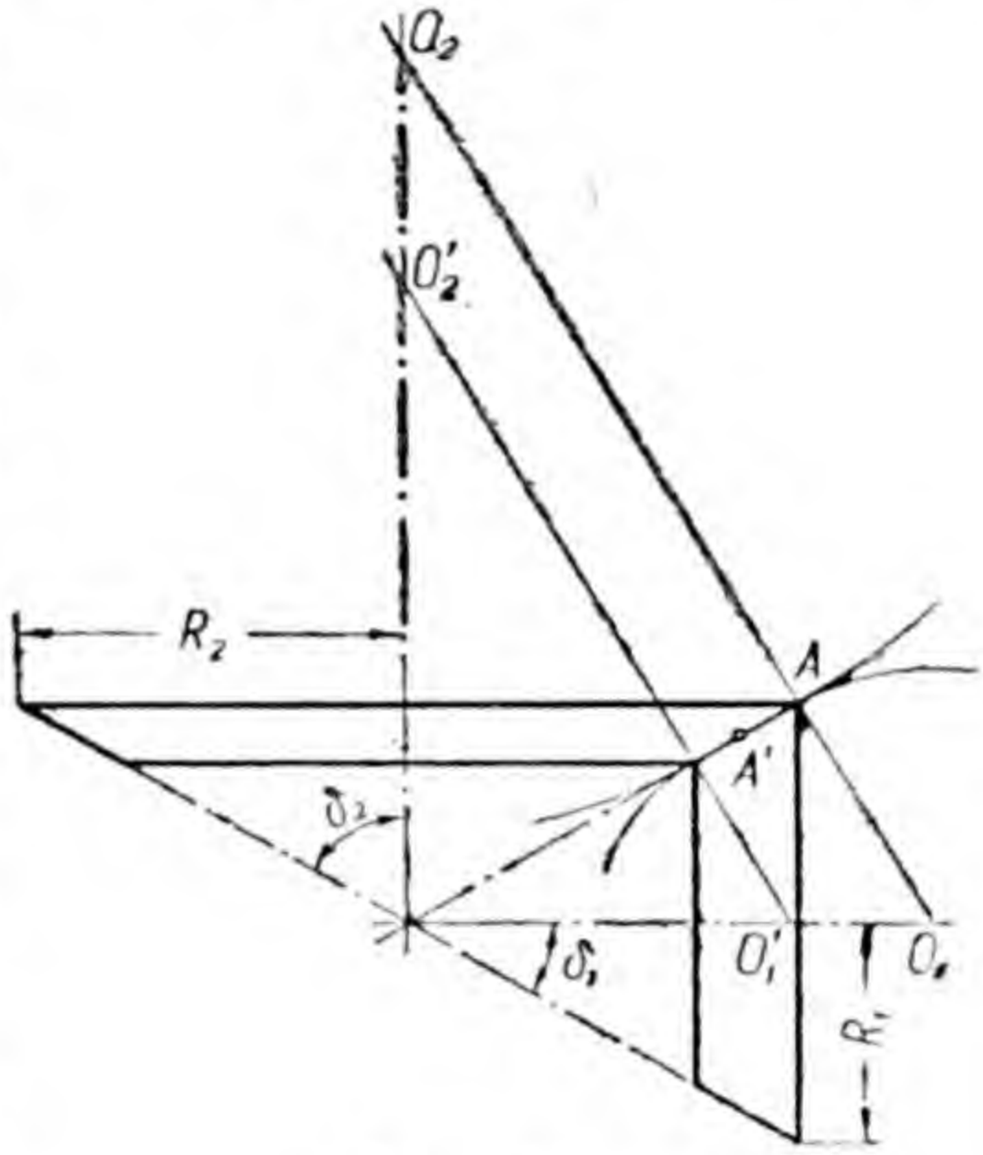

Fig. 89

An approximate method for designing bevel gearing was proposed as long ago as 100 years. According to this method drawing of the profiles of bevel wheel teeth on plane is performed as follows (Fig. 89):

1) the pitch cones are plotted;

2) from point A of the common generatrix of the pitch cones we draw a perpendicular to this generatrix; point O_1 and O_2 of intersection of this perpendicular with the axes of the pitch cones are the apices of auxiliary cones;

3) segments O_1A and O_2A are the generatrices of the auxiliary cones; the circular arcs of radii O_1A and O_2A are the developments of the bases of the auxiliary cones;

4) on the developments of the bases of the auxiliary cones, similar to the pitch circles, the teeth profiles are plotted as in a spur gear drive.

The circular arcs of radii O'_1A' and O'_2A' are similarly obtained and on them are plotted the teeth profiles for the small bases of the pitch cones as on the pitch circles.

Development into plane of the auxiliary cone does not represent a complete circle, but only a portion of a circle limited by the arc which is equal to $2\pi R$, where R is the radius of the base of the pitch and auxiliary cones. On this arc are plotted as many profiles as are to be located on the circle of the pitch cone base, and on the circle of radius $\frac{R}{\cos \delta}$, which is circumscribed by the generatrix of the auxiliary

cone, can be arranged $\frac{z}{\cos\delta}$ profiles, where z is the number of teeth of the bevel wheel, and δ is the half angle at the apex of the pitch cone. Therefore, when the other conditions remain unchanged a pair of bevel wheels with z number of teeth of the smaller wheel operates with the same overlap factor as a pair of spur wheels operating with the number of teeth on the smaller wheel equal to $\frac{z}{\cos\delta}$. The number $\frac{z}{\cos\delta}$ is called the imaginary (reduced) number of teeth of the bevel wheel.

In modern gear-cutting machines the profiles of bevel wheel teeth are shaped differently from both the spherical involutes and the profiles which result from plotting by the simplified method discussed above.

23. WORM GEAR DRIVE

The worm gear drive is a modification of the space kinematic pair, i. e. the screw drive.

If the screw were to be retained from translatory motion (Fig. 90, *a*) and the nut from rotary motion, then by turning the screw the nut will get translation. The motion of the nut will not change if only a portion and not the entire nut is in contact with the screw (Fig. 90, *b*). On the cut-off nut, as given in Fig. 90, *b*, will be shown only the

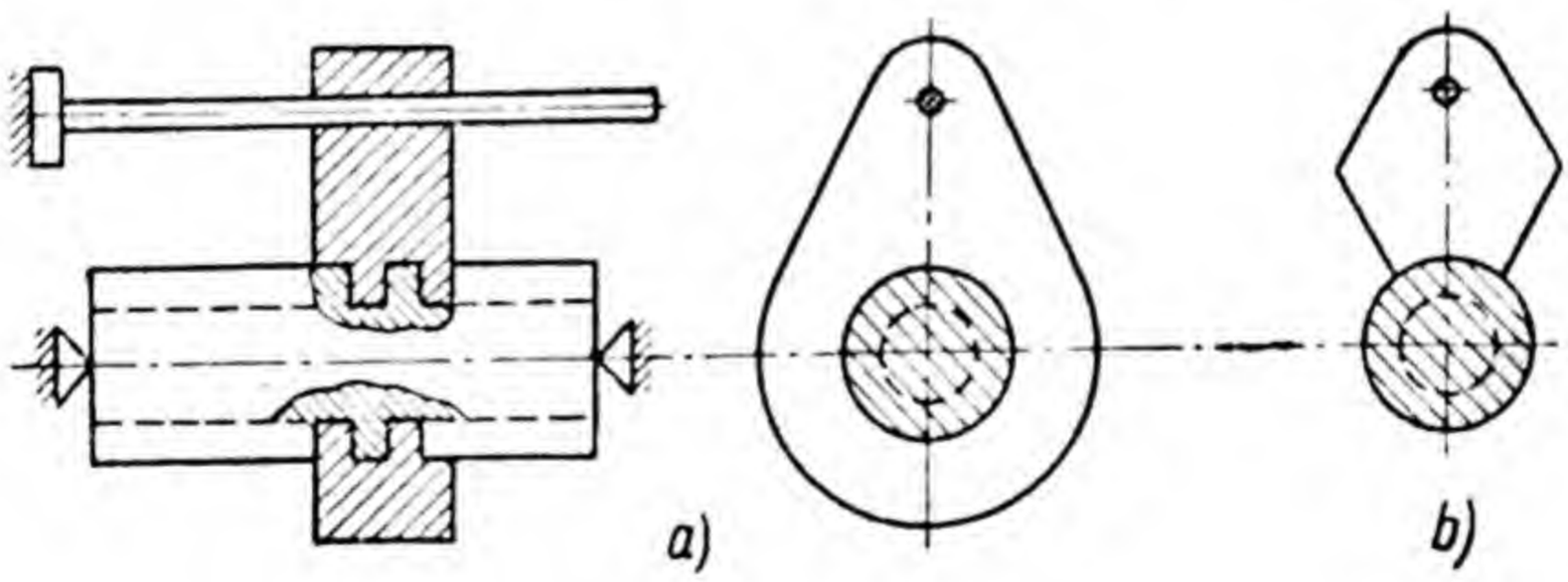

Fig. 90

thread portions of the screw thread which will have the shape of helical teeth.

By turning the screw we displace the threads of the cut-off nut translatory; translation can be examined as rotation about a circle of an infinitely large radius. If the nut threads are located on the wheel rim, a corresponding change in their shape will result in a worm gear, as shown

in Fig. 91, where the nut is called worm and the wheel, worm wheel.

When the section of a worm gear is performed by plane which is perpendicular to the wheel axis and passes through the axis of the worm, we get, as can be observed in Fig. 92, the same as in a section by plane perpendicular to the axis of a straight-tooth wheel which

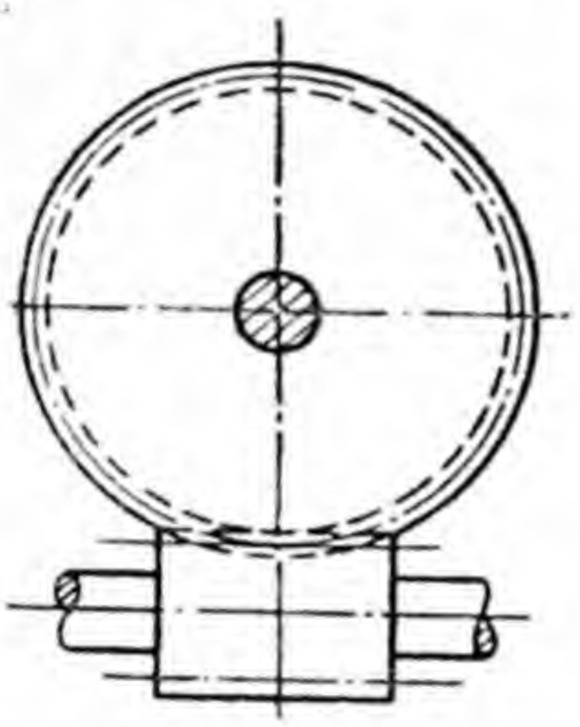

Fig. 91

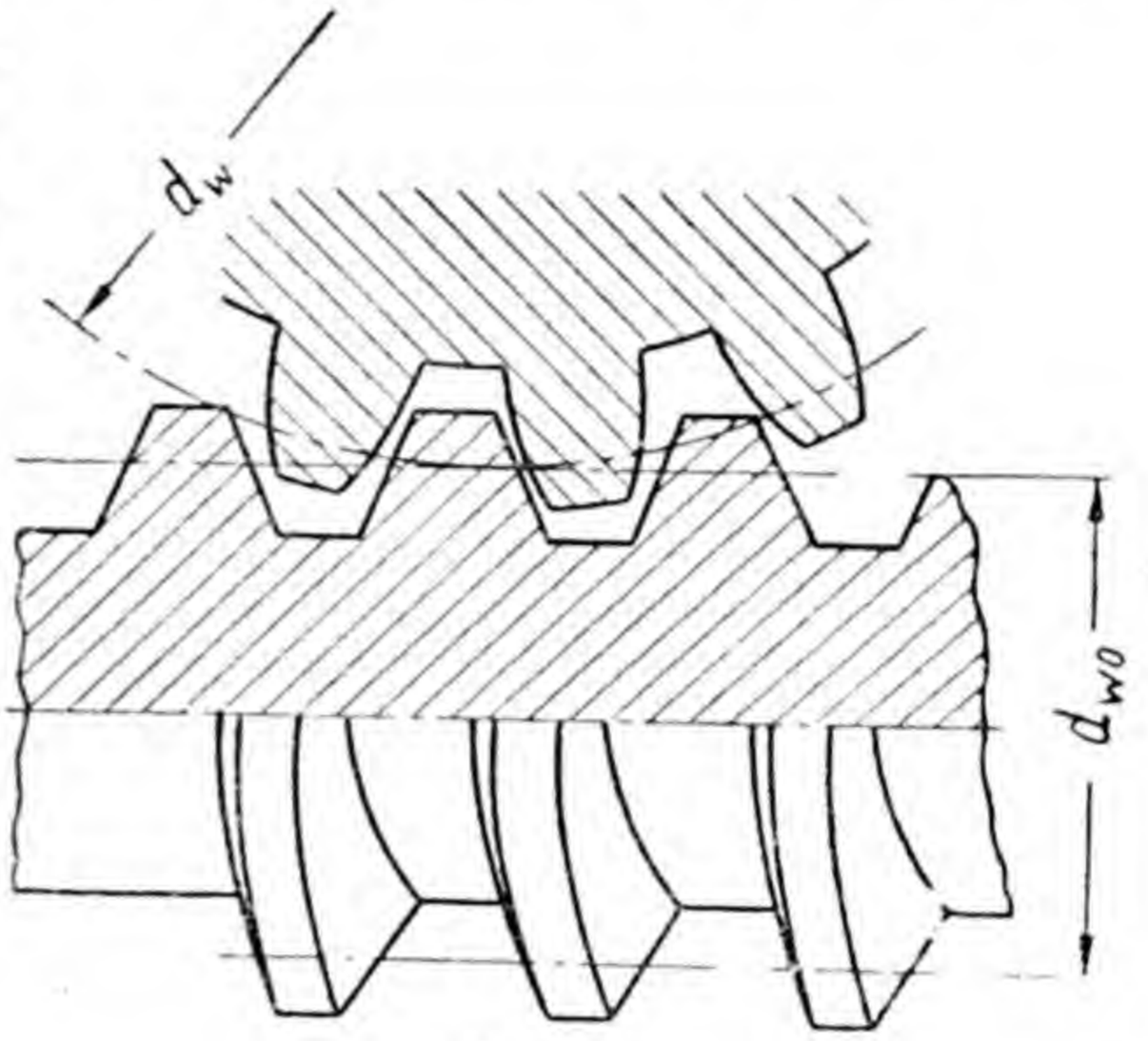

Fig. 92

is in mesh with the rack. The tooth profile of the rack, as we have previously explained, is straight-sided, and therefore the worm thread in longitudinal section is a trapezoid. Worms with involute profiles are also employed.

The distance between adjacent points of intersection of the helix on the worm pitch cylinder with the cylinder generatrix is called the helix lead. The helix lead is usually denoted by a small *s*.

The helix of the worm thread on the pitch cylinder is called the helix centre line.

In the development of the worm pitch cylinder together with the helix centre line by plane we get two straight lines, one of which is the development of the nominal pitch circle and the other is the development of the helix. Angle λ between these lines is equal to the lead angle of the worm along the pitch cylinder (Fig. 93).

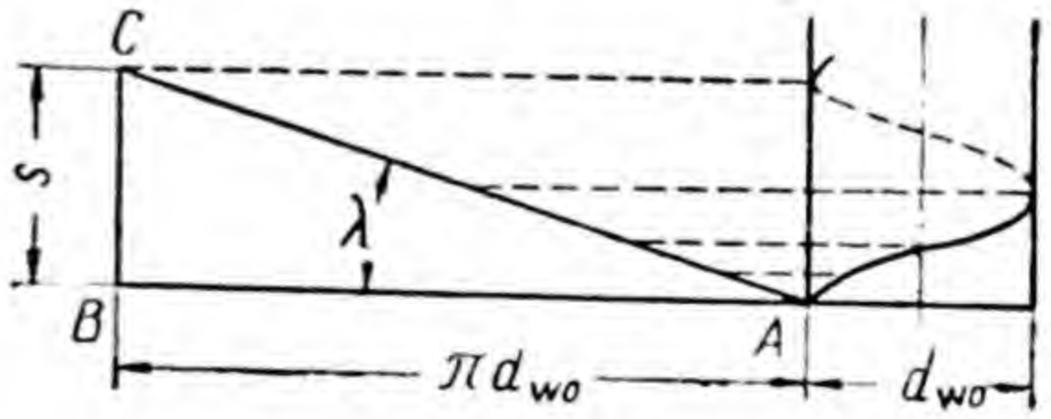

Fig. 93

The lead angle of the worm along the pitch cylinder is

called the acute angle between the tangent to the helix centre line and the tangent to the nominal pitch circle at the same point.

By laying off from point A (Fig. 93) length AB, which is equal to the lenght of the nominal pitch circle, and laying off on the perpendicular to AB the length BC, which is equal to lead s of the helix centre line, we get from the triangle ABC the following relation between angle λ by lead s of the helix and the diameter d_{wo} of the worm pitch cylinder:

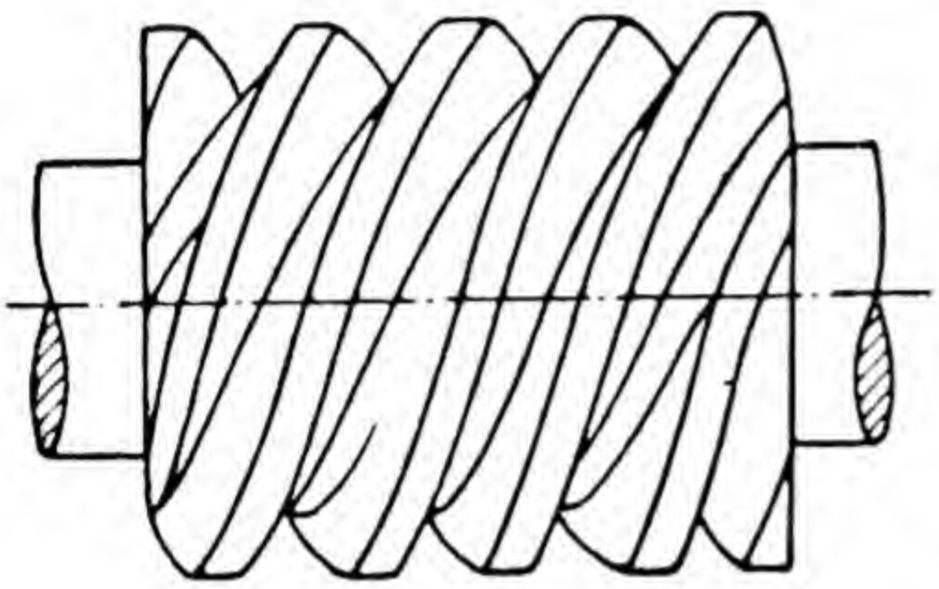

Fig. 94

$$\tan \lambda = \frac{s}{\pi d_{wo}}.$$

A number of threads which are at an equal distance from each other can be located on a worm. Fig. 94 shows a worm with three threads of this kind. If a worm has z_{wo} of such threads it is called z_{wo}-thread worm.

The number z_{wo} of worm starts is called the number of worm threads which are intersected by the plane perpendicular to its axis.

The distance between profile surfaces of adjacent threads that are facing one side and measured parallel to the worm axis is called the worm a x i a l p i t c h. The worm axial pitch is always denoted by a small t.

Fig. 95 shows the longitudinal section of a triple-thread worm, denoting by figures *1*, *2* and *3* the different starts, the helix lead by s, and the axial pitch by t. From what has been previously said we obtain the following relation between s and t:

$$s = z_{wo} \times t.$$

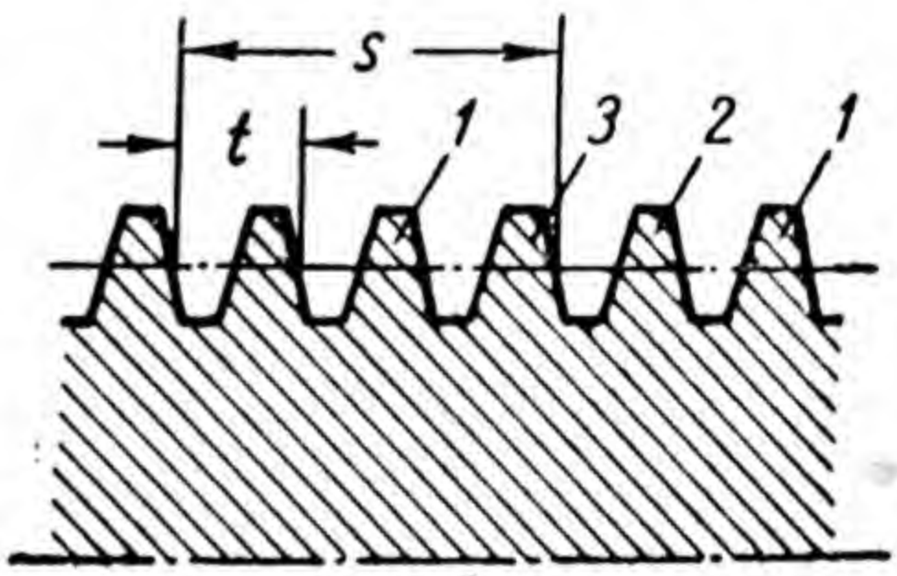

Fig. 95

Taking this into consideration we obtain

$$\tan \lambda = \frac{s}{\pi d_{wo}} = \frac{z_{wo} \times t}{\pi d_{wo}} = \frac{z_{wo} \times \pi m}{\pi d_{wo}} = \frac{z_{wo}}{q},$$

where m is the module and $q = d_{wo}/m$ is the number of modules in the diameter of the worm pitch cylinder.

The numbers q, which should be accepted in the design of worm gears, are specified by the State Standard. In addition provision is made for the following modules and numbers q at various modules, although these are not advisable according to the State Standard:

m=	3	4	5	6	8	10	12	16	20 mm
q=	12	11	10	9	8	8	8	9	8

When z_{wo} equals from 1 to 4 and q equals from 12 to 8 the angle λ changes within the limits from arc tan $\frac{1}{12}$ = $=4°23'55''$ to arc tan $\frac{4}{8}=26°33'54''$.

The pressure angle $\alpha=20°$ is standardized in the circumferential cross-section of the wheel, i. e. in the section by plane which is perpendicular to the wheel axis. With a standard pressure angle the minimum possible number of teeth in the wheel is 14; however in order to get a drive of satisfactory operation it is not advisable to adopt less than 26 teeth for a wheel.

The linear velocity on the wheel pitch circle

$$v_w=\frac{\pi d_w n_w}{60},$$

where d_w and n_w are the diameter of the pitch circle and the wheel revolutions per minute.

The linear velocity of the nut, which is in gear with the worm and moves translatory at worm rotation, would be equal to

$$v_{wo}=\frac{sn_{wo}}{60}.$$

Since $v_w=v_{wo}$, then

$$\pi d_w n_w=sn_{wo},$$

whence we get the velocity ratio i as

$$i=\frac{n_{wo}}{n_w}=\frac{\pi d_w}{s}=\frac{\pi z_w m}{z_{wo}\pi m}=\frac{z_w}{z_{wo}},$$

i. e. i is equal to the relation of the number of wheel teeth to the number of worm starts.

The velocity ratios of worm gears employed in heavy engineering number more than 50, and in gears of low power applied in fine mechanics up to 300 and over.

The proportions of worm wheel teeth in section by plane, which is perpendicular to the wheel axis, are the same as those adopted in a gear drive. The same is true for the proportions of the threads of the worm in section by plane, which passes through its axis.

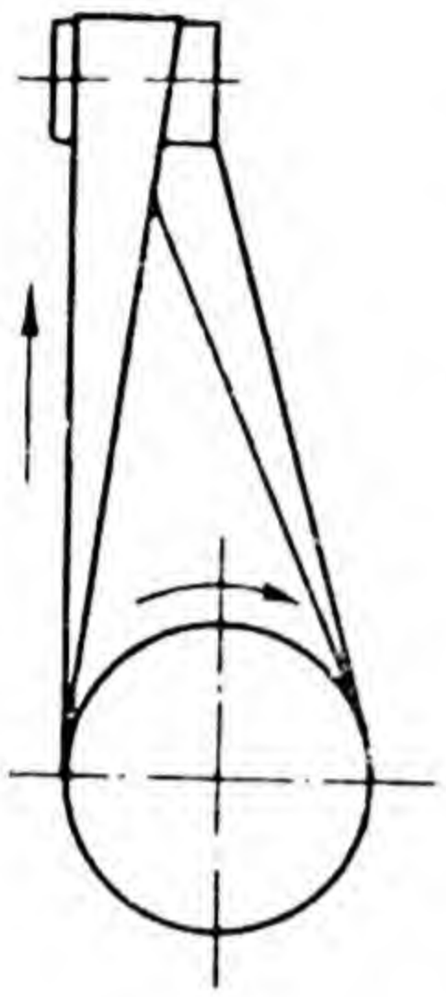

Fig. 96

Depending on the angular velocity of worm rotation the worm gears are classified as high-speed gears and low-speed gears. The high-speed gears are employed mainly for power transmission from electric engines. In such cases the worm shaft is connected by means of a clutch to the engine shaft, which revolves with high angular velocity, and the wheel shaft is connected with the shaft of the operating mechanism which rotates with low angular velocity. Low-speed gears are used mainly in hand-driven devices for gaining force, for example, in manually operated hoisting mechanisms.

The driving link in a worm gear is most frequently the worm. Worm gears with a driving wheel are seldom used and only in low-power devices.

24. BELT DRIVE

Compared with a plane drive a space belt drive is rarely used.

Transmission between shafts, the axes of which lie in different planes and intersect at right angles, is effected by a quarter-twist belt drive, as shown in Fig. 96. In the arrangement of this type of drive the following conditions must be observed: the belt must move onto the pulley in a straight line, so that the axis of the oncoming side of the belt onto the pulley is in the direction coinciding with the pulley centre plane, and so that the running off side of the belt from the pulley does not deviate sideways by an angle exceeding 25°. Therefore, a quarter-twist belt drive can function during belt motion only in one direction, i. e. it is not reversible. Likewise a plane drive will work

satisfactorily only when the belt moves onto the pulley in a straight line, but in this case it is unnecessary to dwell on this point since in a correctly mounted drive it is naturally observed during belt motion in any direction.

A belt drive may be performed between shafts positioned in any spatial relationship to each other by using guide rollers, which revolve freely on their axes. The axes of the guide rollers, as well as those of the driving and driven pulleys, must be arranged to conform with the above condition. But such drives are already obsolete.

Chapter V

CAM GEARS

25. DESIGNING OF CAM GEARS

A simple cam gear is a three-link mechanism with a higher pair, and is mainly used for the transformation of rotary motion by the driving link into motion of the driven link by given law. There are many types of cam gears with a wide field of application but in this brief chapter we shall not examine all the widely used types.

Figs. 39 and 40 show the kinematic diagram of two cam gears. In the gear of Fig. 39 during rotation of the driving link *C*, which is of a more or less intricate profile and is called a cam, the driven link *F*, called a follower, moves alternately in both directions by translation. In the other gear (Fig. 40) the driven link turns about a fixed axis at small angles also alternately in both directions. In both gears the closing of the higher pair links, i. e. their constant contact, is usually ensured by a spring which presses the driven link onto the driving one.

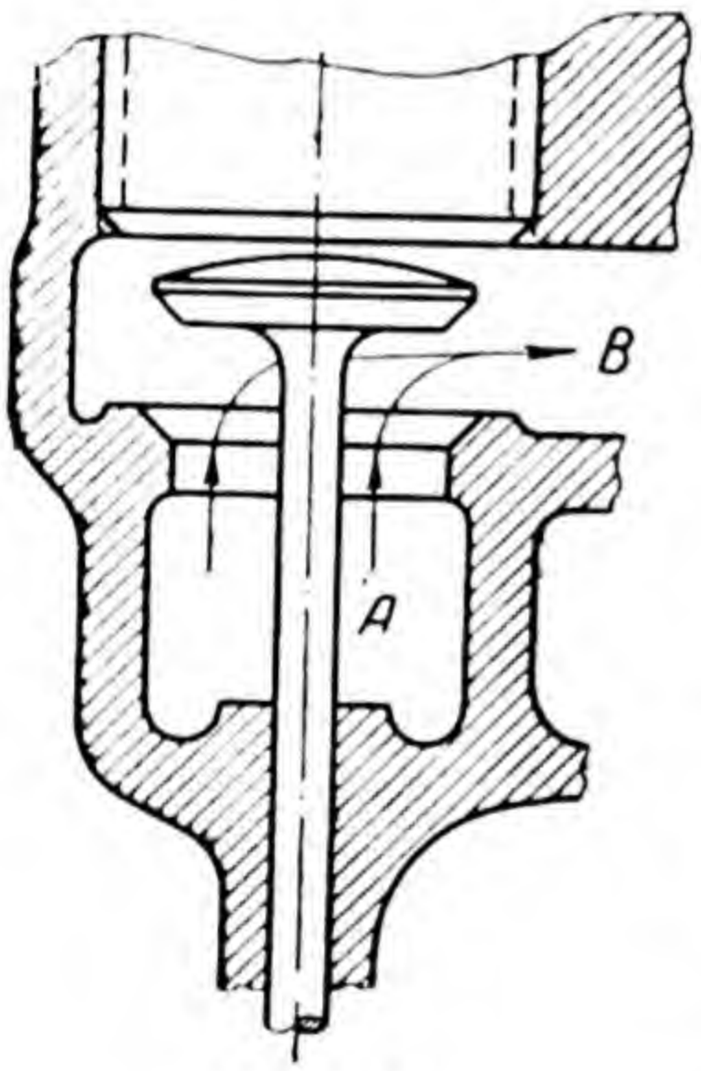

Fig. 97

In designing a cam gear it is necessary to determine first the law of motion of the driven link, taking into consideration its function in the arrangement incorporating the cam gear. The considerations by which one has to be guided can be well illustrated by concrete example.

Let us imagine a cam gear, which is plotted according to the diagram, shown in Fig. 39, and designed to keep open the hole for communication between spaces *A* and *B* (Fig. 97) at cam rotation with constant angular velocity in

the course of one quarter turn of the cam, and to keep it closed during the other turning portion. This function is fulfilled by a cam gear in an internal-combustion engine; through the hole, which is overlapped by a cam gear, a mixture of benzine vapours and air flows from space *A* into space (duct) *B*, and through a hole positioned in a different part of the engine, and overlapped by another cam gear, the combustion products from space *B* are discharged into the atmosphere. In this case the cam gear follower is called a valve.

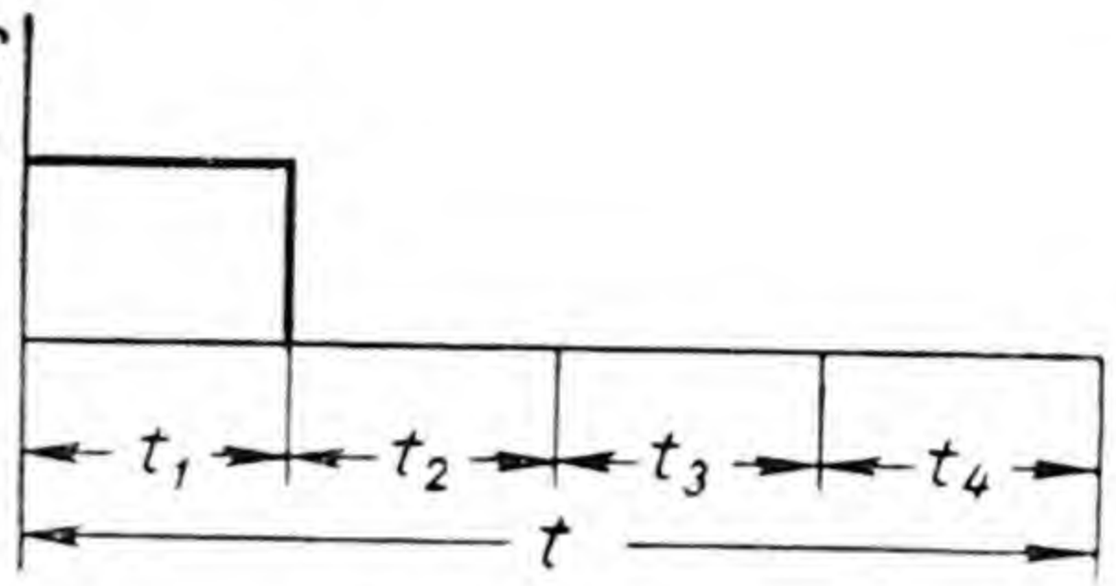

Fig. 98

The valve is lifted by a cam which is not shown in the drawing.

The cam profile must not only ensure the lifting and lowering of the valve onto the seat within certain strict time intervals, but also ensure a maximum opening of the hole from the moment of valve lifting to the moment of its lowering on the seat, so that the valve creates the least resistance to the flow of gases. In addition, the cam profile must ensure an even greater smoothness and shockless movement of the valve in order to avoid rapid wear of the contacting surfaces of the valve and seat as well as of the follower and cam. The fulfillment of these conditions depends on the law of motion of the follower selected as a basis in plotting of the cam profile.

If we only consider the function fulfilled by the valve, we will get an ideal graph of the follower, as shown in Fig. 98, where by the axis of abscissae the time interval t is laid off in four equal parts and during this time interval the cam makes one turn; and the distance of the valve from its lower position in which it closes the hole fully is laid off by the axis of ordinates. The graph provides for the instantaneous transition of the valve from its lower to the extreme upper position, at the beginning of the first quarter turn of the cam for remaining in this position while the cam completes the first quarter of the turn, then for the instantaneous transition into the lower position and remaining there during the time interval $t_2+t_3+t_4$, i. e. up

to the beginning of the following turn of the cam. This graph is ideal because from the beginning and up to the end of the first quarter turn the hole stays fully open all the time, giving the minimum possible resistance to the flow of gases.

However, this graph is in practice unsuitable: the very rapid (not to mention the instantaneous) transitions of the valve from one position to another and the mass connected with it would call for extremely high accelerations as a result of which exceedingly great forces of inertia and shocks would occur.

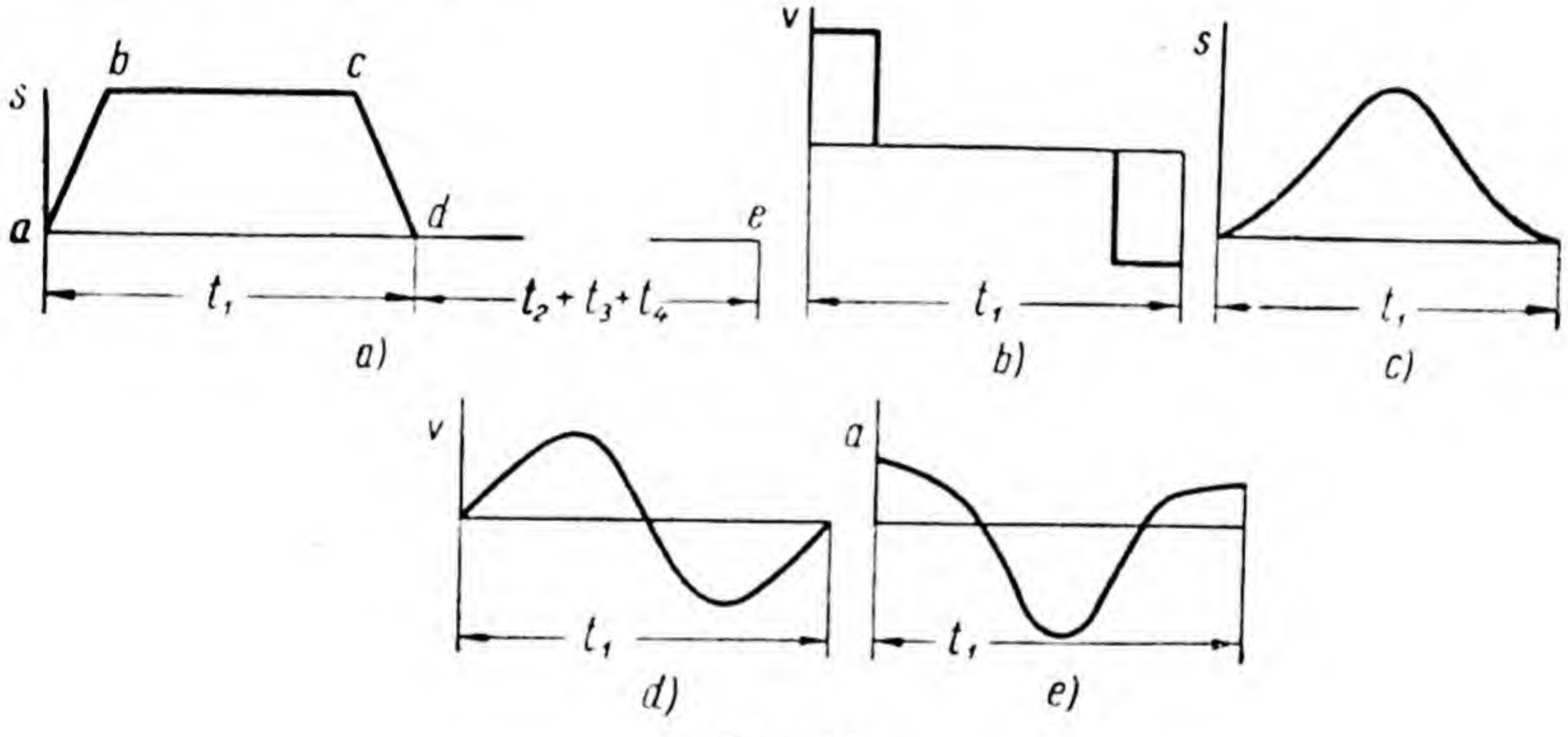

Fig. 99

Taking this into consideration, we have to provide for a gradual transition of the driven link from the lower position to the upper and vice versa and outline a graph such, as shown in Fig. 99, *a*. The following four phases assume this form in the graph: 1) phase of departure (along line *ab*); 2) upper position phase (along line *bc*); 3) phase of approach (along line *cd*); 4) lower position phase (along line *de*).

However, this graph, which is also of the driven link paths and consists of four straight-line portions, cannot serve as a basis for a cam gear, as is easily shown by plotting the velocity diagram (Fig. 99, *b*) in accordance with this graph, from the velocity diagram it can be seen that at points *a, b, c*, and *d* of the graph of paths the velocity change is instantaneous and therefore theoretically changes its magnitude at infinitely high accelerations.

In order to avoid rigid shocks, i. e. shocks at infinitely

high accelerations, it becomes necessary to produce the graph of paths approximately, as shown in Fig. 99, *c*, i. e. to provide for a smooth transition from one phase to another. With this graph of paths the velocity diagram will resemble the one, shown in Fig. 101, *d* and the acceleration diagram, the one in Fig. 99, *e*. Shocks are especially to be avoided at the moment the valve begins to lift and when it returns onto the seat. The graph in Fig. 99, *e* shows that movement of the driven link of the gear will not be accompanied by rigid shocks. However, the softer the shocks at the transition instants from one phase to another the greater is the mean resistance during the passage of gases through the hole inadequately opened by the valve.

On the basis of these and similar considerations we choose the most expedient law of motion of the follower.

In order to prevent the rapid wear of the contact points of the follower and cam the follower end is shaped as a roller freely revolving on an axle. The diameter of the roller axle and the diameter of the roller proper are determined after wear resistance calculations and according to considerations of design, which we shall not dwell on; but the presence of the roller must be considered in the designing of a cam gear, because with a follower and roller instead of the theoretical cam profile indicated in the kinematic diagram, along which the follower moves relative to the cam, we shall have a practical profile along which the roller moves. Let us discuss the method of plotting a practical cam profile.

For plotting a practical cam profile it is necessary to have a graph of the follower paths, where the follower path is expressed in relation to the angle of cam rotation. If we have a graph where the follower path is expressed in a function of time, then with constant angular velocity of cam rotation the graph may be used after recalculation of the scale by the axis of abscissae. With variable angular velocity of cam rotation the graph can be easily reconstructed, when the dependence of the angular velocity of cam rotation on time is taken into consideration.

Let us assume (Fig. 100) that the follower with its roller is in the lower position phase and that point *O* is the centre of the cam profile rotation. We assume that the cam rotates counter-clockwise. We draw from centre *O* the circle which is tangent to the follower roller. On this

circle must be drawn the part of the cam profile against which the roller must rest in the lower position phase.

Let us turn the cam through angle φ counter-clockwise. In the course of this turn centre *A* of the roller profile displaces upwards by distance *s*, which we know from the graph of paths, and the roller is placed in the position relative to the turned cam, as is shown in Fig. 100 by a dotted line. A similar relative position of cam and roller results also in cases when the cam is left stationary and the follower with the roller are turned about point *O* through angle φ clockwise. This position of the roller is shown in Fig. 100 by an unbroken circle. In this position, as well as in any other (which will result in accordance with the graph of paths when turning the follower with roller through different angles in a direction, which is opposite to cam rotation), the roller must contact the cam profile. When we have plotted a sufficient number of roller positions at various turning angles of the follower, we get the cam profile as a curve enveloping various positions of the roller profile that were drawn in the way previously discussed.

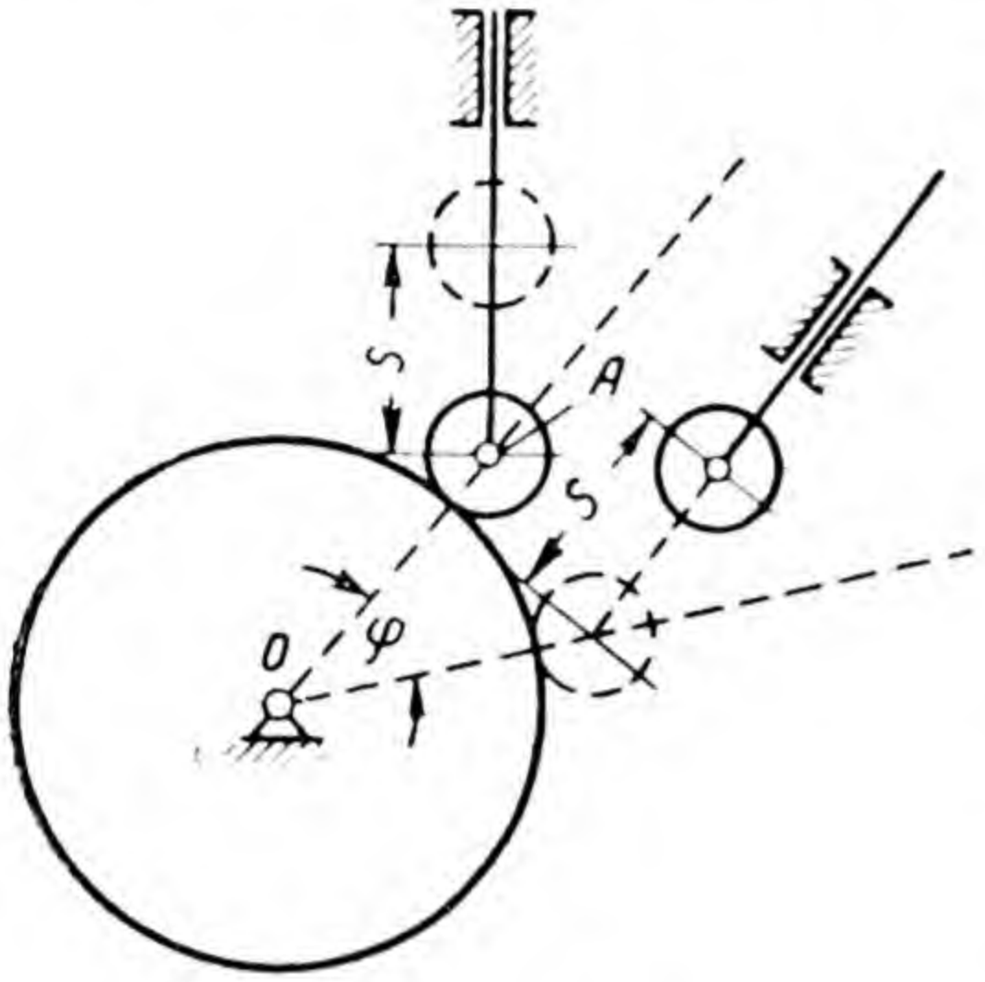

Fig. 100

Fig. 101 shows a specified graph of follower paths, and Fig. 102 shows

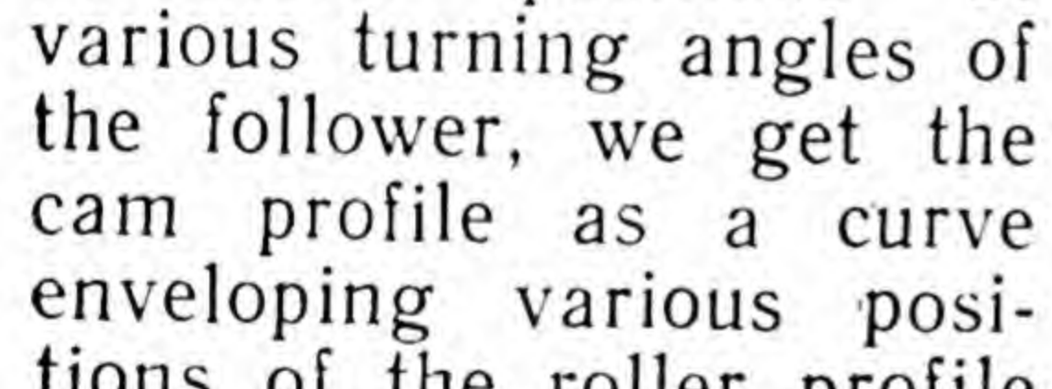

Fig. 101

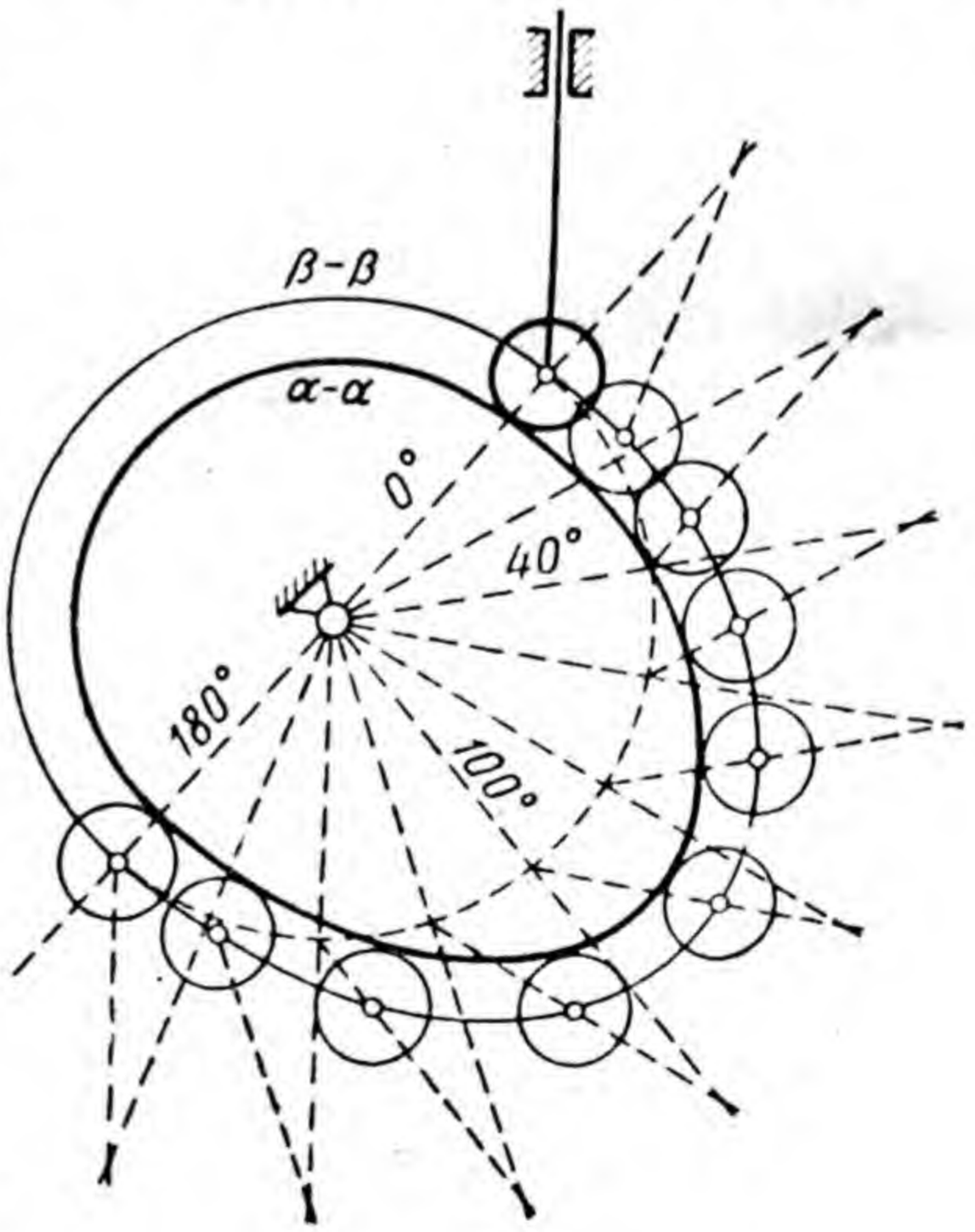

Fig. 102

the practical profile $\alpha - \alpha$ of the cam which has been constructed in accordance with this graph. During motion of the roller along a cam with this profile the centre of the roller profile will move along curve $\beta - \beta$. If the cam profile were to be traced along curve $\beta - \beta$, and the follower without roller were to rest against this profile, the follower motion would proceed in exactly the same way as with a roller resting against the practical profile $\alpha - \alpha$. The curve $\beta - \beta$ is called the theoretical profile.

The theoretical and practical profiles are equidistant curves, i. e. curves that are remote from each other at an identical distance at all points, which are located on the common normals to both curves. The distance

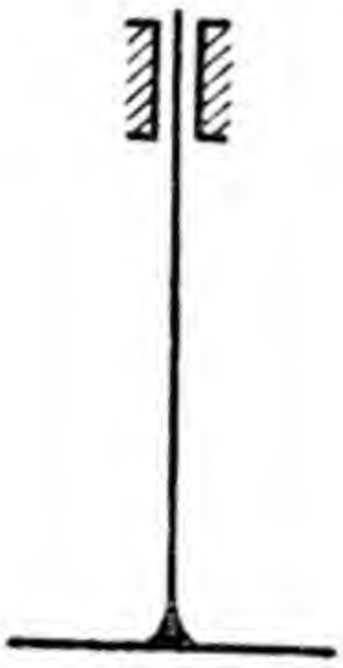

Fig. 103

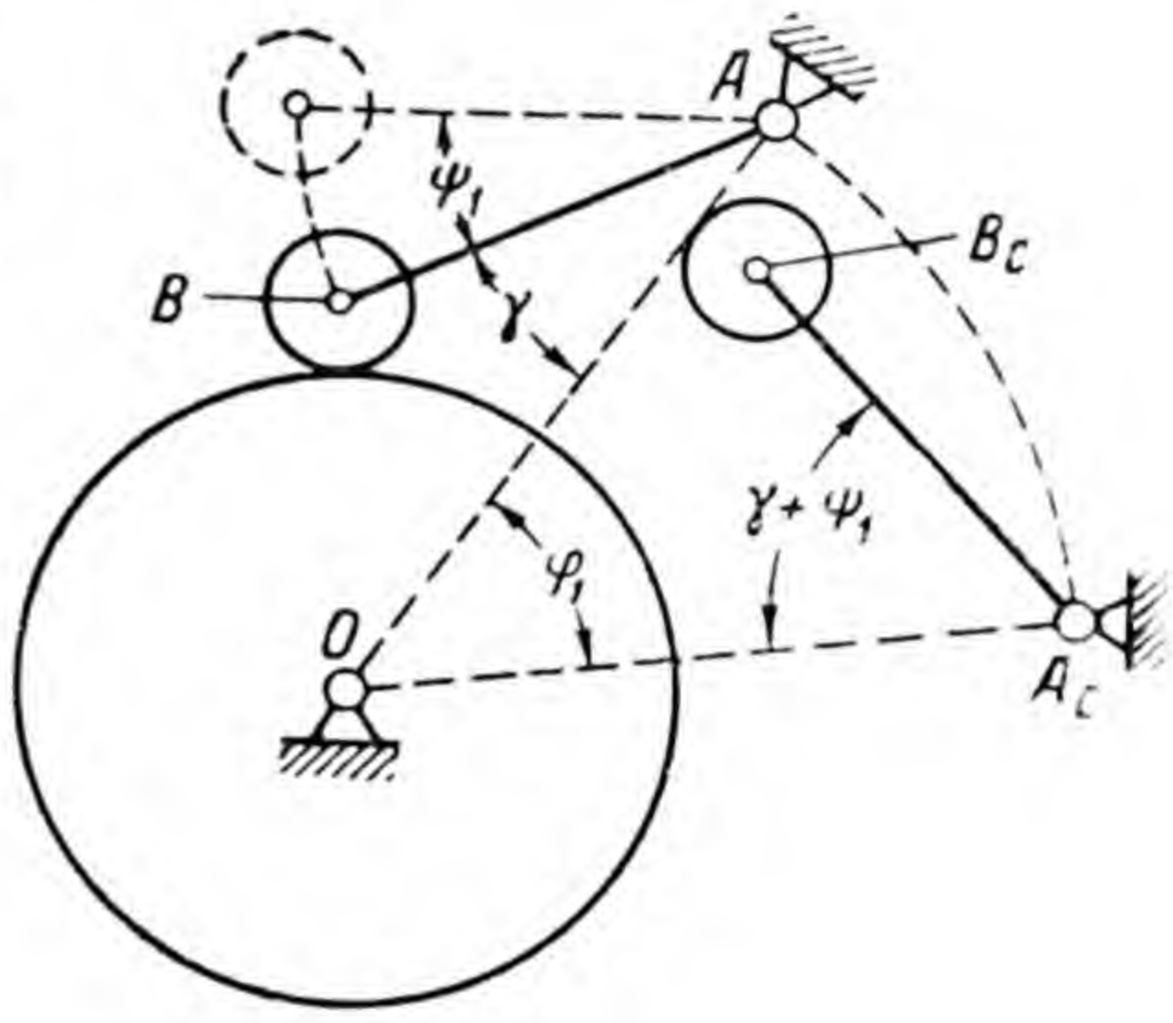

Fig. 104

between both profiles will obviously be equal to the roller radius.

Taking this into consideration it is possible to get a practical cam profile by constructing a whole series of circles of radius equal to the roller radius and with centres located on the theoretical profile. The envelope of all of these circles gives us the practical profile.

In some cases the follower end is shaped not as a roller, but as a plate (Fig. 103). Since the plate is both a design and kinematic element, the cam profile in the shape of a curve which envelops the plate in its different positions relative to the cam is both a theoretical and practical one.

In order to plot the practical cam profile of the gear with rotating driven link AB (Fig. 104) it is necessary to have the graph in which the angle of rotation ψ of rod AB

is expressed in the function of angle φ of cam rotation. In this case as well the graph must provide for such motion of the driven link that excludes extremely high accelerations.

In this case as well as in the previous one, the practical cam profile can be plotted by the method of reversed motion. Let point *O* be the centre of cam profile rotation (Fig. 104), point *A*, the centre of rod *AB* rotation, point *B*, the centre of cylindrical roller profile, and γ, the angle between lines *OA* and *AB* in the initial position of rod *AB*. We assume the cam rotation as counter-clockwise.

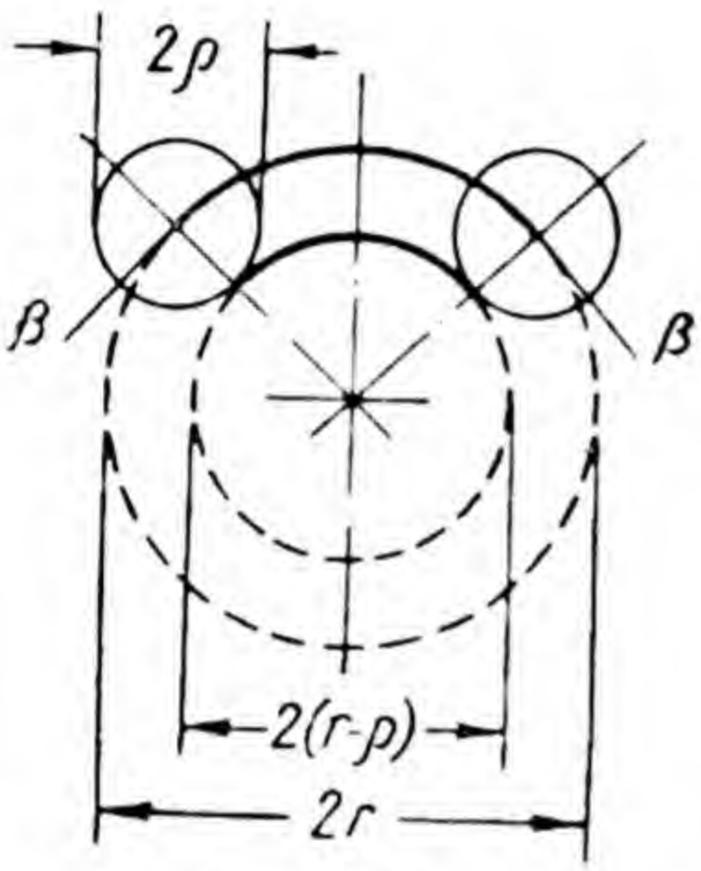

Fig. 105

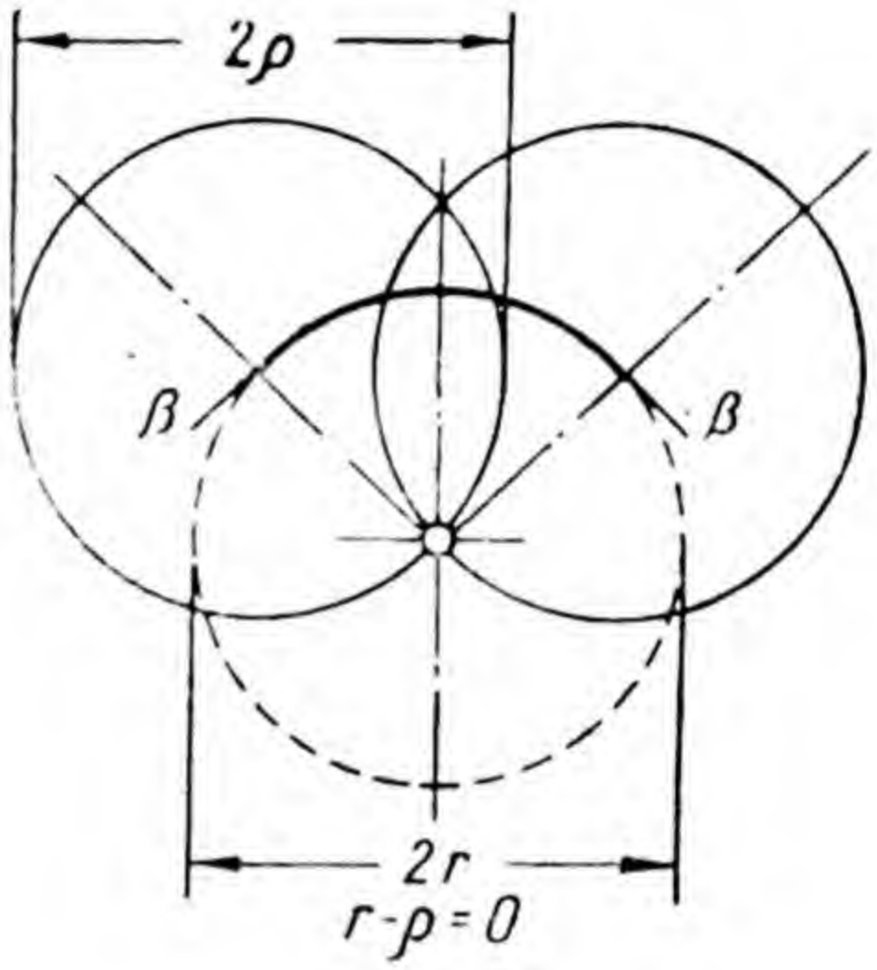

Fig. 106

When the cam turns counter-clockwise through angle φ_1 the rod *AB* in conformity with the graph (not shown in the drawing) must turn about centre *A* through angle ψ_1 and, consequently, be located to line *OA* at the angle $\gamma+\psi_1$; the roller in this case must take up the position which is shown in Fig. 104 by a dotted line. We will obtain a similar position for the roller relative to the cam, if leaving the cam stationary, we turn line *OA* through angle φ_1 shifting it clockwise into position OA_c, and then place the rod *AB* with the roller at angle $\gamma+\psi_1$ to line OA_c, after which the roller profile will assume the position B_c. By turning line *OA* clockwise through different angles, i. e. in the direction opposite to that of cam rotation, we will obtain different positions of the roller profile relative to the practical cam profile. The practical cam profile will be shaped as a curve enveloping the roller profile in its various positions. The theoretical profile, as well as for the gear with follower, will be shaped as an equidistant curve,

remote from the practical profile by a distance which is equal to the roller radius.

In designing cam gears it is necessary to make sure that the roller radius does not exceed the radius of curvature at any point of the theoretical profile which is facing the roller with the convex side, as otherwise no practical profile can be obtained. One can easily see this by imagining the convex portion β—β of the theoretical profile in the shape of a circular arc of radius r, being greater than radius ρ of the roller (Fig. 105), of radius r being equal to radius ρ (Fig. 106), and radius r being smaller than ρ (Fig. 107). In the first case the practical profile is possible, in the second case it has the form of a point, and in the third, the form of a self-intersecting curve.

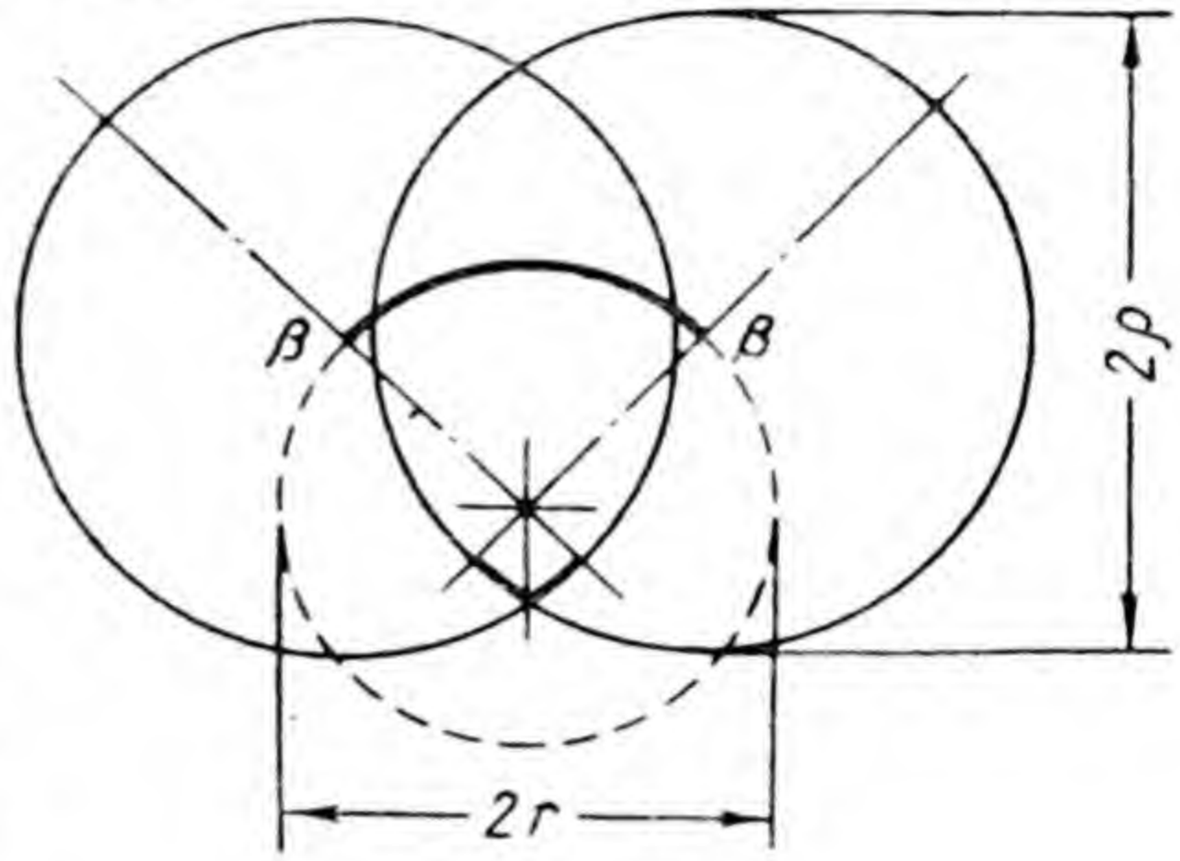

Fig. 107

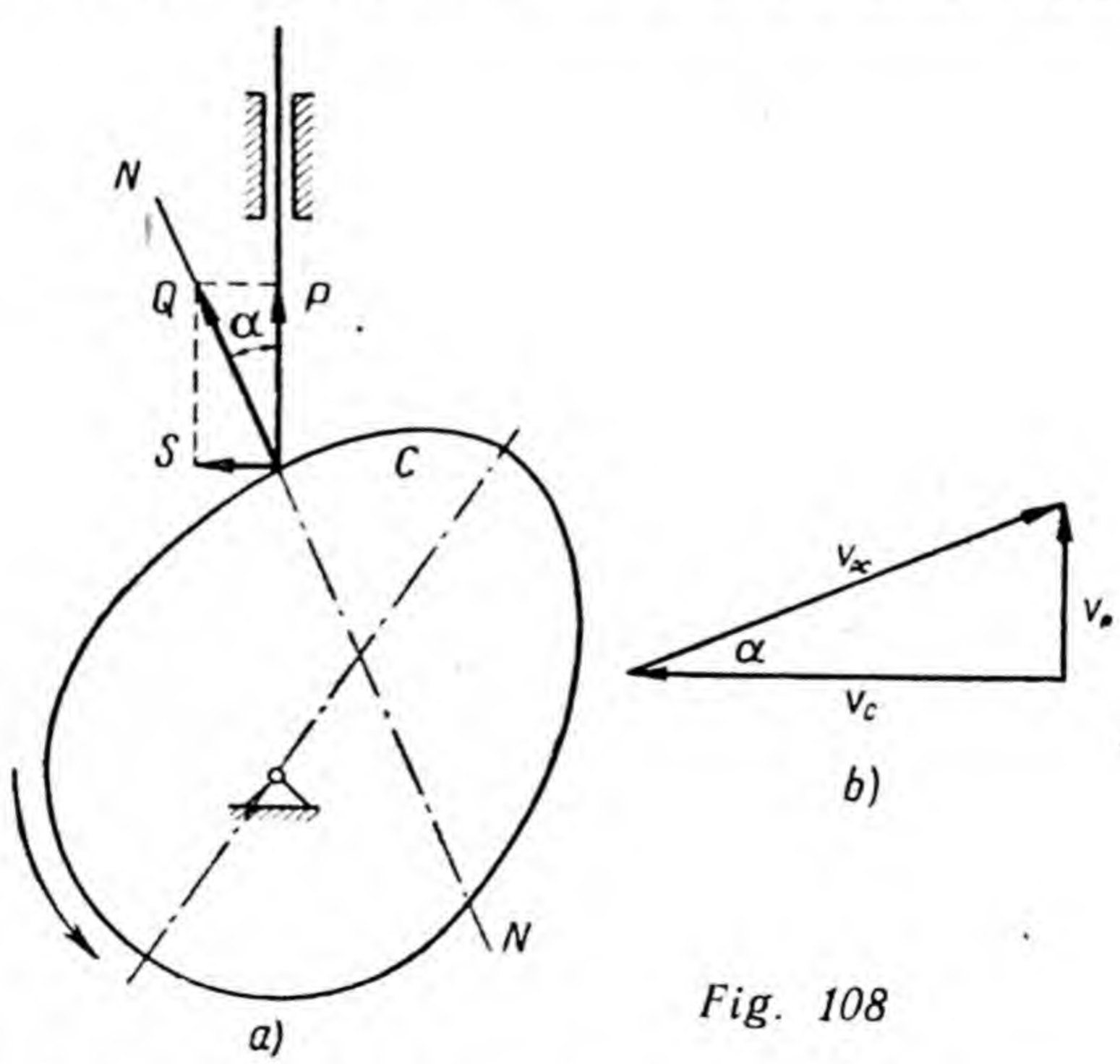

Fig. 108

In the designing of a cam gear we also have to solve the problem of the most expedient proportions of the cam. For instance, if the cam is too large the gear with the

follower will be bulkier than is actually needed; if the cam is too small the gear will operate unsatisfactorily and there may even occur jamming of the follower on the cam or in the guide. In the operation of such a gear the magnitude of angle of pressure α (Fig. 108, *a*) plays an important role; this is the angle between the follower axis and the normal NN to the cam profile at the point of cam and follower contact. The magnitude of this angle depends also on the cam proportions. The force Q from the side of the cam onto the follower, which is directed along the normal NN, may be resolved into force $P=Q\cos\alpha$, which raises the follower, and lateral force $S=Q\sin\alpha$. The smaller the angle α the greater is force P and the lesser is force S; hence, from the dynamic point of view it is more expedient to have a possibly smaller angle of pressure. But, on the other hand, the relation of velocity v_P of follower lift and velocity v_c, which belongs to the cam point of contact with the follower, is expressed as follows (Fig. 108, *b*):

$$v_P=v_c\tan\alpha.$$

Therefore from the kinematic point of view it is more expedient to have a possibly larger angle of pressure.

The proper choice of the angle of pressure magnitude is therefore accompanied by certain difficulties.

26. KINEMATIC ANALYSIS OF CAM GEARS

The velocities and accelerations in a kinematic analysis of cam gears can be determined either by means of graphic differentiation or by plotting velocity and acceleration diagrams.

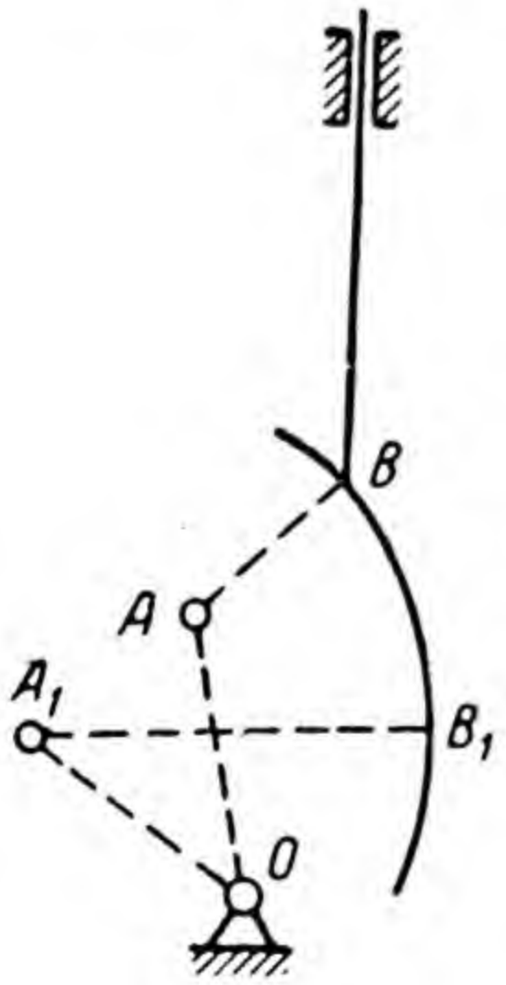

Fig. 109

In plotting the velocity and acceleration diagrams the cam gear, as well as any other mechanism with a higher pair, must be replaceable by a mechanism which has only lower pairs. When replacing a higher pair by one link with lower pairs it is necessary to know the curvature radii of the link profiles of the higher pair at their points of contact; in cases when the profiles are traced by non-mathematical curves, we have to use approximate magnitudes of curvature radii.

When replacing cam gears by mechanisms with lower pairs it is necessary to proceed from the kinematic diagram of the mechanisms. On the kinematic diagram of each of them the theoretical cam profile must be given, against which the driven link must thrust with the point which coincides with the centre of the cylindrical roller profile. Depending on the type of curve used to trace the theoretical cam profile we can have replacing mechanisms of various types and mechanisms of the very same type, but with the links differing in length in certain positions. Let us examine this by means of examples.

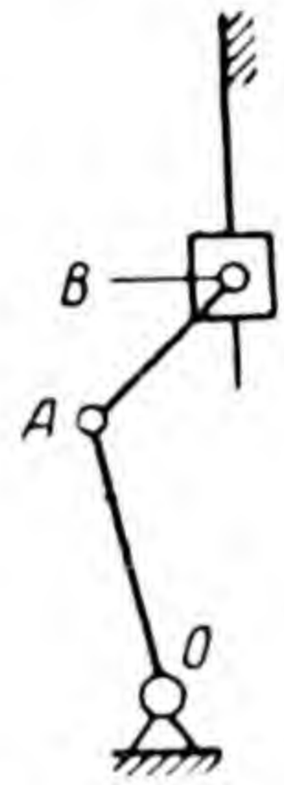

Fig. 110

Fig. 109 shows the curvilinear portion of the cam profile and the follower which rests against the cam profile by point. The follower profile is point B; hence, the curvature centre of the follower profile is located at point B. Point A is the curvature centre of the cam profile at point B; point O is the centre of the turning pair in which the cam is connected with the frame. The replacing mechanism has the shape of a crank gear, as shown in Fig. 110, where the follower has the form of a slider, link OA, that of a crank and link AB that of a connecting rod. At the approach of point B_1 of the cam profile (Fig. 109) to the follower the form of the replacing mechanism remains unchanged, but the lengths of crank OA and connecting rod AB are different owing to the change in proportions of radius A_1B_1 of the curvature.

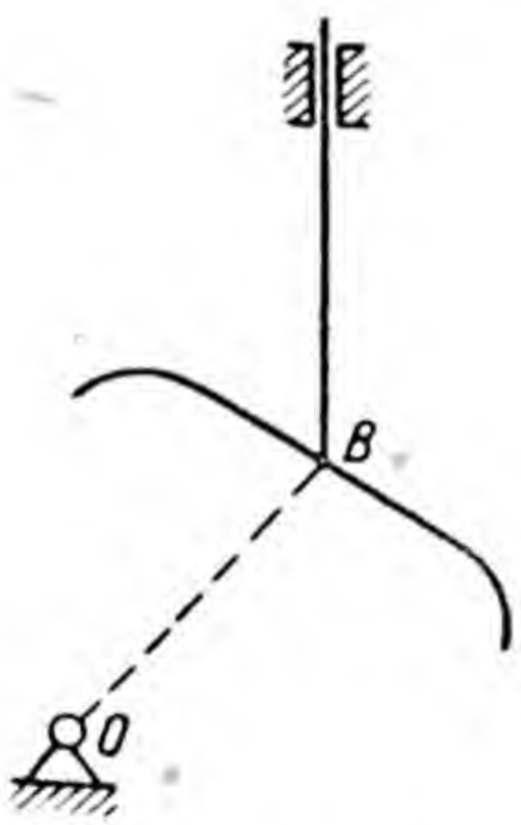

Fig. 111

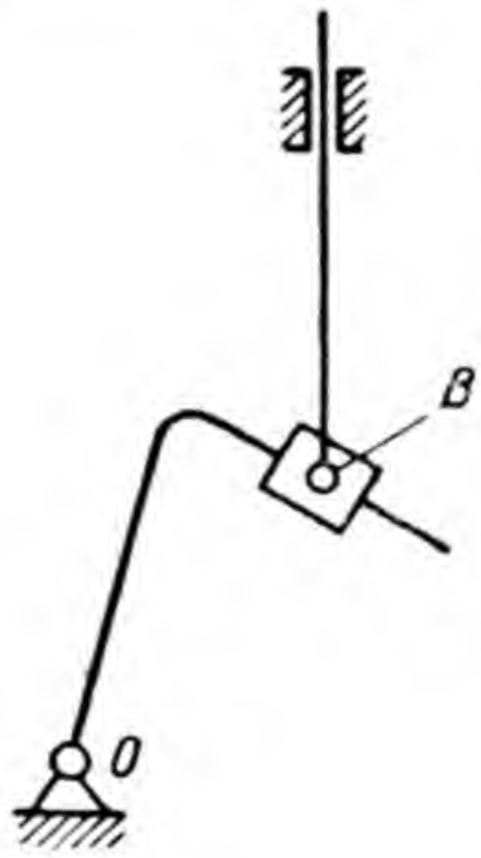

Fig. 112

Fig. 111 shows the straight-line portion of the cam profile and the follower which rests against the cam profile by point B. The radius of curvature of the cam profile at point B is infinity, therefore on the straight-line portion we get a link of a sliding pair and the replacing mechanism in the form,

shown in Fig. 112, with two turning and two sliding pairs.

Fig. 113 shows the curvilinear portion of the cam profile and rod *BC* rotating about centre *C* which thrusts against the cam profile by point. We obtain the replacing mechanism in the form of *OABC*, where centre *A* of the cam profile curvature at point *B* is the centre of the turning pair, in which crank *OA* and connecting rod *AB* are connected; rod *BC* is the rocker arm in this

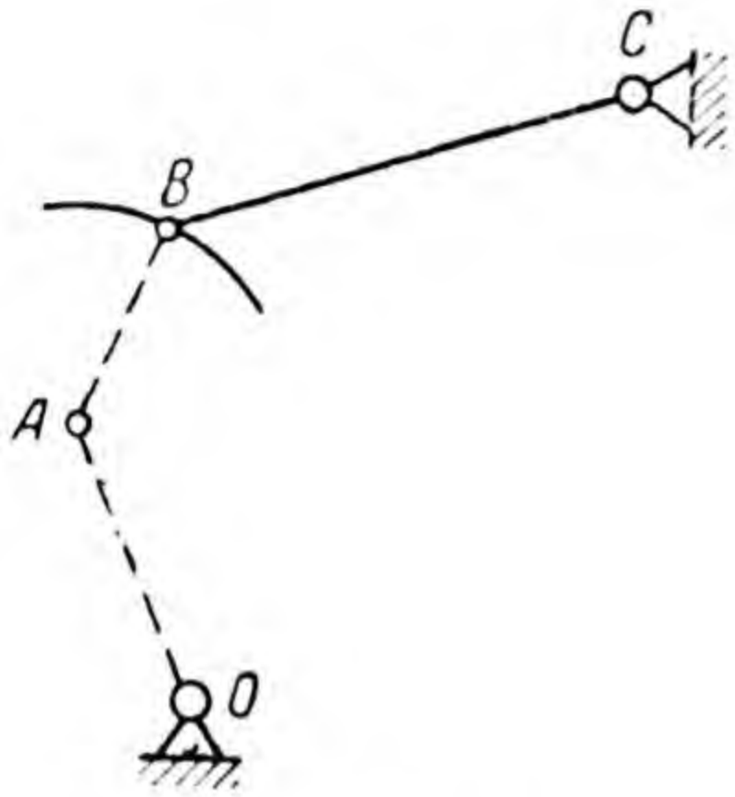

Fig. 113

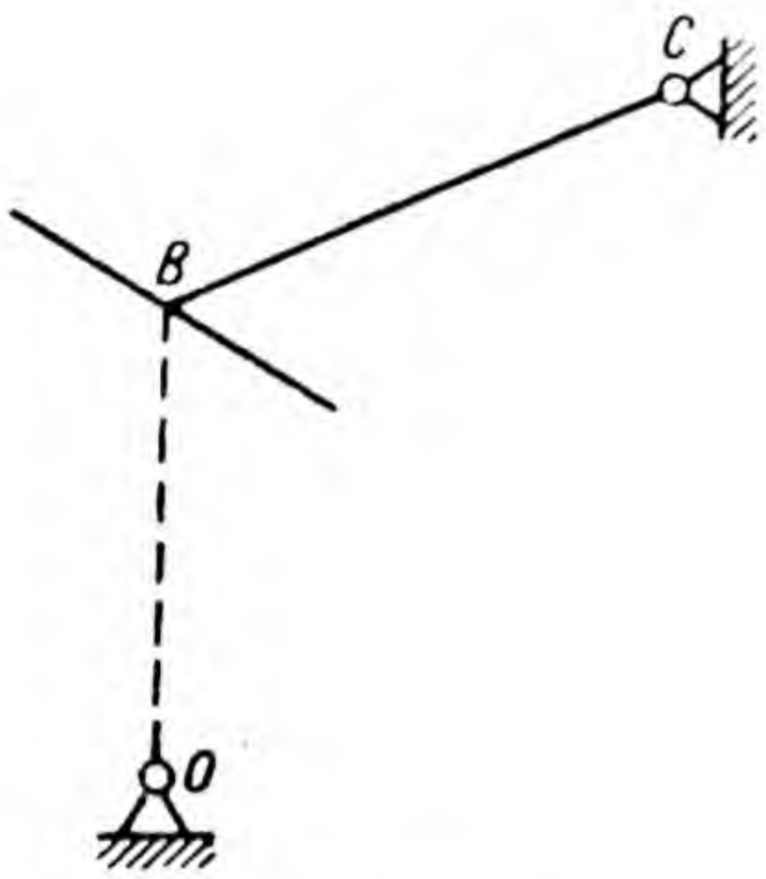

Fig. 114

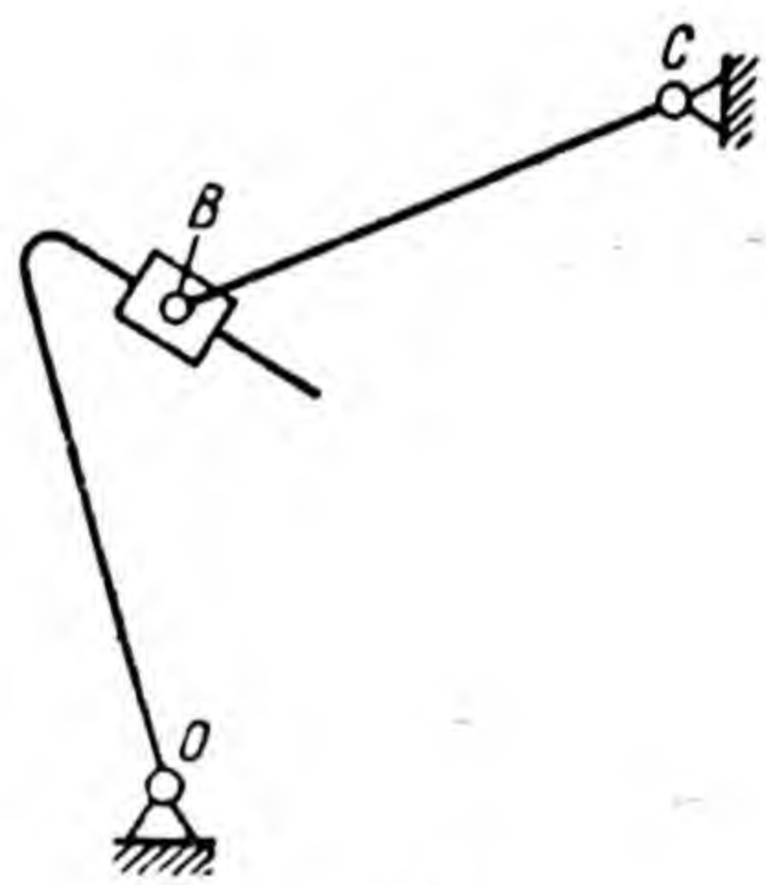

Fig. 115

mechanism. If rod *BC* were to rest on the straight-line portion of the cam profile (Fig. 114), the replacing mechanism would take a different form (Fig. 115).

Chapter VI

COMBINED STATIC AND INERTIA-FORCE ANALYSIS OF PLANE MECHANISMS

27. INTRODUCTORY

During the operation of a mechanism forces of inertia develop in its links owing to the action of external forces, and in the bearings of the links, i. e. kinematic pairs, reacting forces develop.

The magnitudes, directions and points of application of the external forces which act on the mechanism are considered in the theory of mechanisms and machines as specified, and therefore the methods of their determination will not be examined.

The methods for calculating links and bearings of links for strength are also not discussed in the theory of mechanisms and machines, but the required information for strength calculation as regards the forces of inertia and reacting forces in kinematic pairs that develop during the operation of a mechanism is found by the methods which are presented in the theory of mechanisms and machines. Of all the methods for determining these forces we shall examine the most expedient one, the combined static and inertia-force analysis. The essence of this method consists in the following.

If body A, acting on body B, imparts acceleration to the latter, body B, reacting to body A, acts on it with a force which is called the force of inertia.

The force of inertia acts on the body which imparts acceleration, but not on the accelerated body. For example, if body B, which is held by cord A, rotates about a certain axis, it is not body B that is subjected to the action of the forces of inertia (called centrifugal force), but cord A, which continuously deflects body B from rectilinear motion, thereby imparting acceleration to body B. From the instant cord A breaks under the action of the centrifugal

force the movement of body B will proceed not in the radial direction, i. e. not along the line of action of the centrifugal force, but along the tangent to the path along which body B moved prior to the breaking of the cord, since neither before breaking nor in the instant of breaking was body B under the action of centrifugal force.

The force of inertia can be transferred to the accelerated body only conditionally. If all the forces of inertia are transferred conditionally to the accelerated body of a moving system, then according to d'Alembert's principle the moving system can be considered at the instant of examination as stationary in a state of equilibrium under the action of the forces, including the force of inertia. It is on this principle that the combined static and inertia-force analysis is based. This method is called the combined static and inertia-force analysis because the forces in the links and the pressures in the kinematic pairs of a mechanism, which develop by the action of external forces applied to the mechanism, are determined first through kinematic analysis of a mechanism which has the accelerations that are required for the determination of the forces of inertia, and then by a static calculation.

28. DETERMINATION OF THE FORCES OF INERTIA

During the motion of the link of a mechanism all the material points which move with accelerations act with the forces of inertia on the adjacent material points. Stresses in the links develop owing to the combined action of the external forces and elementary forces of inertia. The forces which act on the links are balanced by the reacting forces which develop in the bearings of the links, i. e. in the kinematic pairs.

The stresses which develop in links under the action of forces are not examined in the theory of mechanisms and machines, because, as mentioned above the methods of calculation of links for strength are not discussed in the theory of mechanisms and machines. In future the forces of inertia will therefore be taken into consideration only in determining pressures in kinematic pairs.

At the same time the infinite number of elementary forces of inertia which act in links have to be replaced by resultant forces and couples. We shall explain below by

what kind of resultant forces and couples all the elementary forces of inertia acting in the links can be replaced.

In replacing the elementary forces by resultant forces it should always be kept in mind that there are no actual resultant forces either in nature or in engineering: the resultant force is an imaginary force which, if it were existent and acting by itself, would create the same pressures on the bearings of the link as are actually developed by all the acting elementary forces.

In determining the resultant force we have to find out its magnitude, its line of action and direction. The point of application of the resultant on its line of action is of no significance in determining the pressures in the link bearings, since along the line of action the resultant can be transferred to any point. This transfer of the point of application can influence neither the magnitudes and directions of the moments developed by the resultant relative to different points of the link, nor the magnitudes and directions of the reacting forces in kinematic pairs.

In certain cases it is convenient to transfer the line of action of the resultant by a certain distance parallel to itself. Such a transfer will fail to influence the magnitudes and directions of the reacting forces in kinematic pairs only if the magnitude and direction of the resultant couple moment is changed correspondingly. By transferring the resultant line of action of the elementary forces of inertia in such a manner we can reduce the combined action on the link of the force and the couple to the action of only one force.

In determining the magnitudes, directions and lines of action of resultant forces of inertia in various types of plane motion we shall in future proceed from the assumption that the moving body has at least one plane of symmetry, i. e. a plane on both sides of which all the forces of inertia are located symmetrically. In representing the body on the drawing we shall depict the plane of symmetry and shall assume that all points of the body move on planes which are parallel to this plane. Marking on the drawing the point of application of the elementary force of inertia, we shall assume that all the elementary forces of inertia, acting at points located on the line that is perpendicular to the plane of symmetry at this point, are transferred parallel to themselves to this point. For

example, the body, shown in two projections in Fig. 116, will have one plane of symmetry when moving parallel to the plane of the drawing in Fig. 116, *a* or perpendicular to the plane of the drawing in Fig. 116, *b*. In this case the elementary force of inertia, which is applied at point *x* (Fig. 116, *a*), should be understood as the sum of all the elementary forces of inertia, which act at all material points on the line *x*—*x* (Fig. 116, *b*) and are transferred parallel to themselves on the plane of symmetry. Fig. 116, *a* shows the section of a body by plane of symmetry, and in Fig, 116, *b* the line *a*—*a* is the line of intersection of the drawing plane with the plane of symmetry.

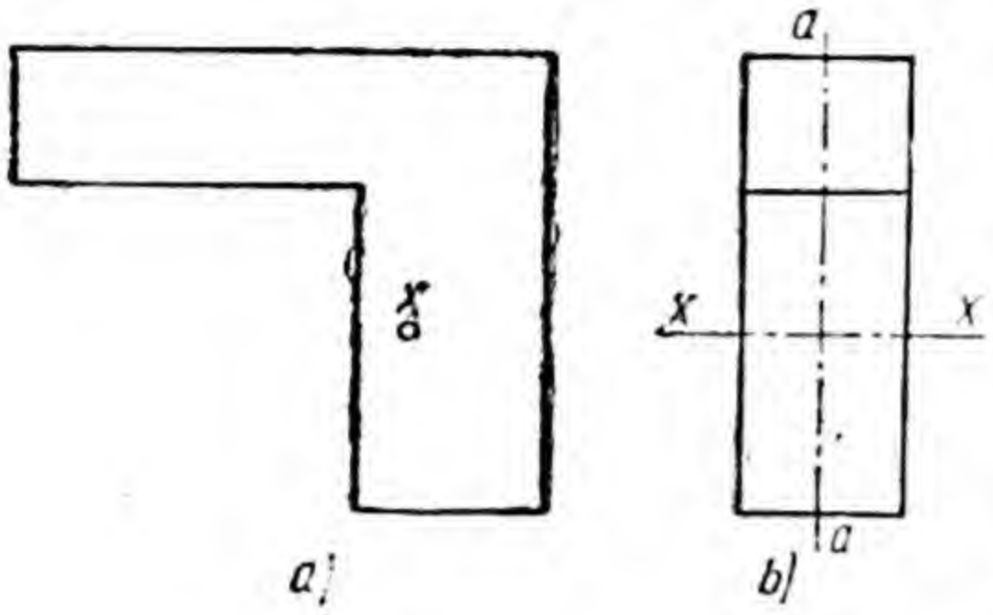

Fig. 116

During the motion of this body in a direction perpendicular to the drawing plane (see Fig. 116, *a*), the moving body will have no plane of symmetry.

Determination of the forces of inertia developing during the motion of bodies which have more than one plane of symmetry is beyond the scope of the present course.

The link of a plane mechanism may move with translatory motion, rotate about a fixed axis, or perform compound motion. In all these cases the force of inertia, as explained in the course on theoretical mechanics, is equal to the product of link mass on the acceleration of its centre of gravity and is directed to the side which is opposite to the acceleration of the centre of gravity.

During translatory motion the line of action of the force of inertia passes through the centre of gravity, during rotary motion with variable angular velocity it passes through the centre of oscillation, which lies on the extension of the line connecting the centre of gravity with the centre of rotation, and is at distance r_O from the centre of rotation, where

$$r_O = r_S + \frac{J_S}{mr_S} = r_S + \frac{\rho^2}{r_S},$$

where r_S is the radius of rotation of the centre of gravity;

J_S is the inertia moment of the link relative to the centre of gravity;
m is the link mass;

ρ is the radius of inertia, which equals $\sqrt{\frac{J_S}{m}}$.

During rotary motion with constant angular velocity the total acceleration of the centre of gravity is equal to normal, and therefore the line of action of the force of inertia coincides with the radius of rotation of the centre of gravity.

Compound motion of the link can be examined as motion with acceleration of any chosen point of the link and rotation about this point. In this case the total force $\bar{P}_I$ of inertia is obtained as a geometric sum of two forces — force $\bar{P}'_I$ of inertia in motion with acceleration of the chosen point, and force $\bar{P}''_I$ of inertia during rotation of the link about this point. By drawing through the centre of gravity of the link a line of action of force $\bar{P}'_I$ parallel to the acceleration vector of the chosen point, and through the centre of oscillation the line of action of force $\bar{P}''_I$ parallel to acceleration of the centre of gravity in rotary motion of the link about the chosen point, we shall obtain at the point of intersection of these lines a point, through which the line of action of the total force $\bar{P}_I$ of inertia passes. The vector of this force must be directed parallel to the vector of absolute acceleration of the centre of gravity to the side which is opposite from the direction of this vector.

Example. Link BC (Fig. 117, a) performs compound motion. Determine the magnitude of the force of inertia, its line of action and the direction by the following data: 1) by mass m of the link; 2) the moment of inertia J_S of the link relative to the centre of gravity; 3) accelerations $\bar{a}_B$ and $\bar{a}_C$; 4) the position of centre of gravity S.

By given accelerations $\bar{a}_B$ and $\bar{a}_C$ we plot the acceleration diagram (Fig. 117, b). Having determined the position of point s on the acceleration diagram by drawing on line bc the triangle bsc, which is similar to triangle BSC of the link and located similarly to triangle BSC, we get vectors $\overline{bs}$ and $\overline{cs}$ of relative accelerations. We draw the vector $\overline{\pi s}$ of absolute acceleration $\bar{a}_S$ of the centre of gravity.

Compound motion of link BC we consider as motion with point B and rotation about this point. The total force $\bar{P}_I$ of inertia will be obtained as a result of the geometrical addition of the force of inertia in the link motion with point B and force $\bar{P}_I''$ of inertia at rotation of the link about point B.

The first of the components equals

$$P_I' = -ma_B.$$

We multiply the link mass by acceleration a_B, but not by acceleration a_S, since in translatory motion with point B

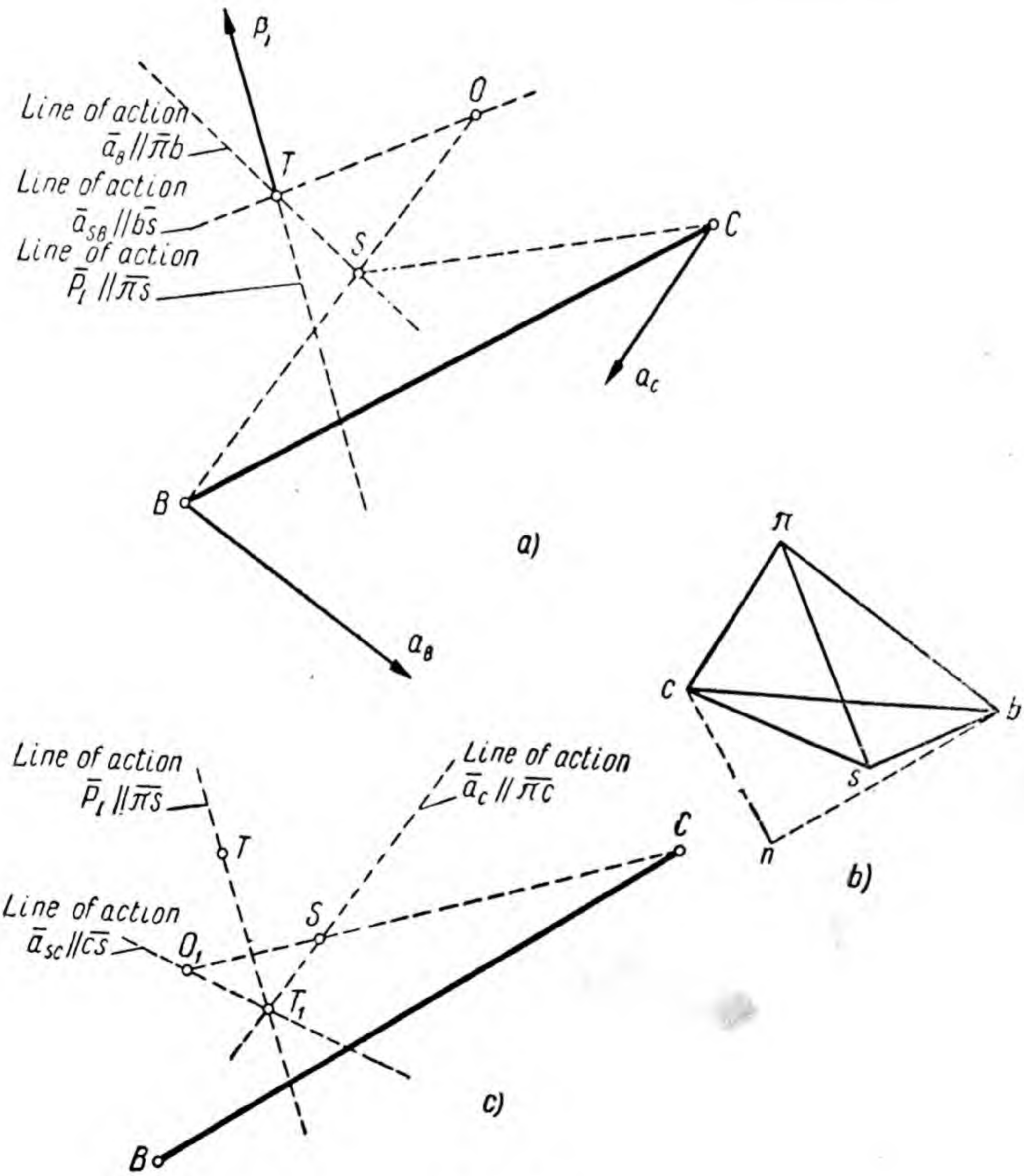

Fig. 117

the accelerations of all points of the link, including also the acceleration of the centre of gravity, are equal to the acceleration of point B.

Force $\bar{P}_I'$ must be applied in the centre of gravity. Without calculating the magnitude of this force we draw through centre of gravity S a line of its action parallel to vector $\overline{\pi b}$ of acceleration a_B (Fig. 117, b).

The second component equals

$$P_I'' = -ma_{SB}.$$

This force must be applied in the centre of oscillation O (Fig. 117, a), which is located on the extension of line BS at distance l_{SO} from point S, which equals

$$l_{SO} = \frac{J_S}{ml_{BS}},$$

where l_{BS} is the length of segment BS.

Without calculating the magnitude of force P_I'', we draw through centre of oscillation O the line of action of this force parallel to vector $\overline{bs}$ of acceleration $\bar{a}_{SB}$.

The lines of action of forces $\bar{P}_I'$ and $\bar{P}_I''$ intersect at point T. In order to obtain the magnitude, direction and point of application of the resultant $\bar{P}_I$ we would have to transfer the vectors of these forces along the lines of their action up to point T, which we obtained without calculating the vector lengths. Having determined the point of application of the resultant $\bar{P}_I$, we draw the vector of this force from point T parallel and opposite in direction to vector $\overline{\pi s}$ (Fig. 117, b) of absolute acceleration $\bar{a}_S$ of the centre of gravity. The magnitude $P_I = -ma_S$.

The line of action and the direction of force $\bar{P}_I$ we obtained in Fig. 117, a, having resolved the compound motion of link BC into translatory motion together with point B and rotary motion about point B. By resolving the compound motion of link BC into translatory motion together with point C and rotary motion about point C, we get centre of oscillation O_1 on the extension of line CS (Fig. 117, c) at distance l_{SO_1} from the centre of gravity S, which equals

$$l_{SO_1} = \frac{J_S}{ml_{CS}}.$$

By drawing through point S the line of action of acceleration $\bar{a}_C$ parallel to vector $\overline{\pi c}$ of the acceleration diagram and through point O_1 the line of action of acceleration $\bar{a}_{SC}$ parallel to vector $\overline{cs}$, we get point T_1 of their intersection on the same line of action of force $\bar{P}_I$, which was also obtained in the previous construction in Fig. 117, *a*.

If we take instead of points B and C any other point connected with link BC (except the centre of gravity), we obtain the point of intersection of the lines of action of forces $\bar{P}_I'$ and $\bar{P}_I''$ in a new place, but on the same line of action of force P_I as in the other two constructions. But if the motion of link BC were resolved into translatory motion with the centre of gravity and rotation about the centre of gravity, then all the elementary forces of inertia could not be reduced to only one resultant. In this case force $P_I' = -ma_S = P_I$ must be applied to the centre of gravity and force P_I'' is zero, since during rotation about the centre of gravity the elementary forces of inertia, as explained in the course on theoretical mechanics, apply only to a couple with moment $J_S\varepsilon$, where ε is the angular acceleration of the link.

Angular acceleration ε of link BC can be determined by resolving acceleration $\bar{a}_{CB}$ (vector $\overline{bc}$ in Fig. 117, *b*) into normal acceleration $\bar{a}_{CB}^n$ (vector $\overline{bn}$ in Fig. 117, *b*, which is parallel to link BC) and tangential acceleration $\bar{a}_{BC}^{\tau}$ (vector $\overline{nc}$ in Fig. 117, *b*, which is perpendicular to link BC) and taking into consideration

$$\varepsilon = a_{CB}^{\tau}/l_{BC} = (nc)\mu_a/l_{BC},$$

where μ_a is the scale of the acceleration diagram, and l_{BC} is the length of link BC.

The direction of the angular acceleration is found by transferring vector $\overline{nc}$ parallel to itself at point C in Fig. 117, *a*; by joining point n of the vector with point C in Fig. 117, *a* we obtain the counter-clockwise direction of the angular acceleration.

29. DETERMINATION OF PRESSURES IN KINEMATIC PAIRS

Since every mechanism of class I order 2 comprises a mechanism of class I order 1 and one or a number of two-arm groups connected to it in succession, determination of pressures in pairs should be carried out by separating the two-arm groups in succession, beginning with the last one attached. In determining the pressure in pairs of individual groups the action of links in destroyed joints is replaced by forces. Thus, for instance, if we have to determine the pressure in pairs of an eight-link mechanism, as shown in Fig. 118, it is necessary to begin with the last group attached, group $B''C''D''$. After determining the pressure in the pairs of this group and subsequently replacing the action of links $B''C''$ and $C''D''$ by links BC and $B'C'$ with forces, which are applied in points B'' and D'', it is then necessary to proceed to group $B'C'D'$. In determining the pressures in the pairs of this group, besides the specified forces, attention should be paid to the force at point D'' from the side of link $C''D''$ of the previous group. After separating group $B'C'D'$ pressures in the pairs of the separated group BCD must be determined with consideration of the forces in points B'' and B' from the side of the links of the previous groups.

After separating the group BCD and determining the pressures in the pairs of this group it is necessary to examine crank AB. After applying at point B of this link the force with which link BC acts on crank AB, it only remains to determine the magnitude of the moment which has to balance the action of link BC on the crank and determine the pressure in the last pair A.

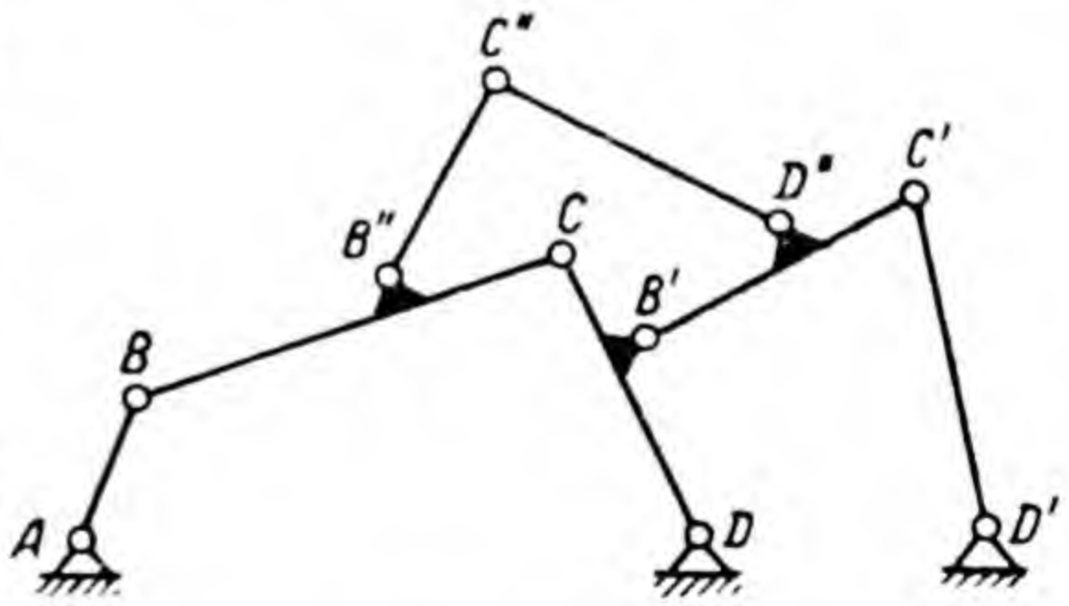

Fig. 118

Thus the task of determining the pressure in pairs of even a compound mechanism of class I order 2 comes down to the determination of pressures in pairs which are separated in succession from a mechanism of two-arm groups. Determination of pressures in pairs of a two-arm group does not create difficulties, since a group with two links and three lower

pairs is a system which is determinable from the static point of view, because in order to determine six unknown (two unknown in every kinematic pair) six equations of equilibrium can be used (three equations for each of the two links). For each of the lower pairs we have the following two unknown: for a turning pair the point of application of the force (the joint centre) is known, but the magnitude and direction of the force are unknown; for a sliding pair the direction of the force (perpendicular to the directrix) is known, but the magnitude and point of application of the force are unknown.

Determination of pressures in pairs of a two-arm group is performed simply by the method of diagrams of forces. Let us examine how this method is used in determining pressures in pairs of a group with three turning pairs and a group with two turning pairs and one sliding pair.

A. A Group with Three Turning Pairs

If several forces and several couples act on a link, all the forces and couples can be reduced to one force and one couple by addition. If the link is under the action of force P and couple with moment M, then the action of the couple and the force on the link can be replaced, as we know from theoretical mechanics, by the action of one force. In determining the magnitude, line of action and direction along the line of action of which all the forces and couples, including the forces of inertia, have been considered, we shall therefore in future make the general assumption that each of the links in a group is under the action of one force.

Denoting by P_2 (Fig. 119, *a*) the force which acts on link BC, and by P_3 the force that acts on link CD, we will determine the pressures in pairs B, C and D. The index of letter P indicates the link number on which the external specified force acts. The force from one link onto the other we shall denote by letter P and two indices, the first to indicate the number of the link from which the force is acting, and the second to indicate the number of the link which is under action.

For example, P_{23} denotes the force from link *2* onto link *3*, P_{32} denotes the force from link *3* onto link *2*. We assume the group to be connected at point B with link *1*

which is not shown in the figure, and at point D with link *4*, and we shall accordingly denote the forces at points B and D by P_{12} and P_{43} or P_{21} and P_{34}, depending from the side of which links the action of forces is to be examined.

Being incorporated in the mechanism, the group BCD is in motion, but since in determining forces P_2 and P_3 the forces of inertia were considered and transferred conditionally to the links of the group, it follows that at the moment corresponding to the position of the group, as shown in Fig. 119, *a*, the group can be considered, in accordance with d'Alembert's principle, as being in

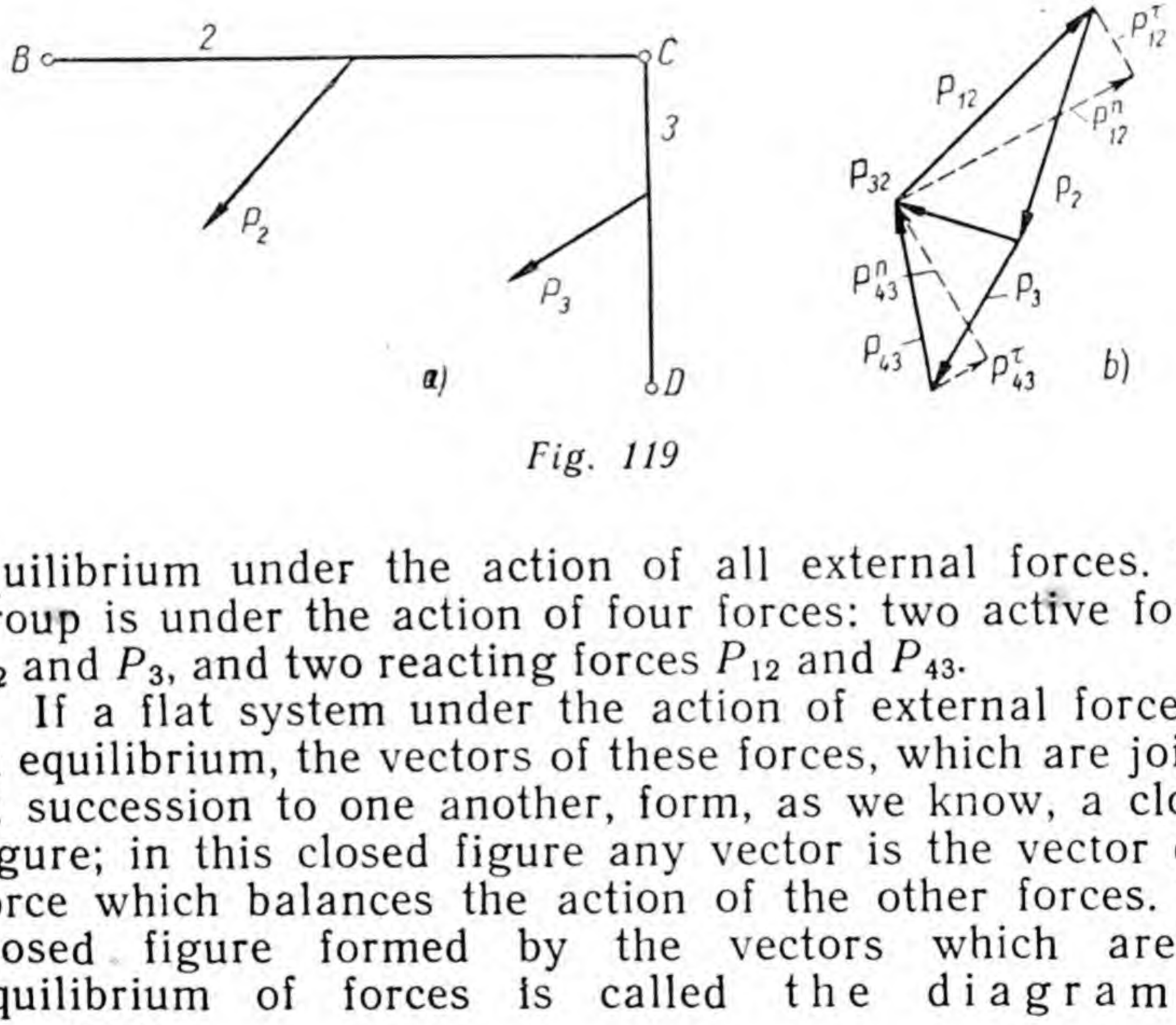

Fig. 119

equilibrium under the action of all external forces. The group is under the action of four forces: two active forces P_2 and P_3, and two reacting forces P_{12} and P_{43}.

If a flat system under the action of external forces is in equilibrium, the vectors of these forces, which are joined in succession to one another, form, as we know, a closed figure; in this closed figure any vector is the vector of a force which balances the action of the other forces. The closed figure formed by the vectors which are in equilibrium of forces is called the diagram of forces.

We cannot plot immediately the diagram of forces for group BCD, since we do not know the magnitudes and directions of the reacting forces P_{12} and P_{43}, but this difficulty can be overcome as follows.

Without knowing the magnitudes and directions of force P_{12}, we can determine the component of this force in the direction perpendicular to link BC. Denoting this component by P_{12}^{τ} and by P_{12}^{n} the component in the

direction along link BC, we determine the magnitude of force P_{12}^{τ} from the equation of moments relative to point C: since the moment of force P_{12}^{n} directed along link BC is zero, the moment of force P_2 is balanced only by the moment of force P_{12}^{τ}. Therefore

$$P_{12}^{\tau} l_{BC} = P_2 h_2,$$

whence $P_{12}^{\tau} = P_2 \frac{h_2}{l_{BC}}$, where h_2 is the arm of force P_2, which is determined according to the drawing.

The moment of force P_2 tends to rotate link BC about point C counter-clockwise, therefore the moment of force P_{12}^{τ} must be directed clockwise and, consequently, force P_{12}^{τ} must be directed perpendicular to link BC upwards.

By resolving force P_{43} to force P_{43}^{τ}, which is directed perpendicular to link CD, and force P_{43}^{n}, directed along link CD, from the equation of moments relative to point C we get

$$P_{43}^{\tau} = P_3 \frac{h_3}{l_{CD}},$$

where h_3 is the arm of force P_3, which is determined according to the drawing.

After resolving each of the forces P_{12} and P_{43} into two components and determining the magnitudes and directions of forces P_{12}^{τ} and P_{43}^{τ} we get six forces under the action of which group BCD must be in equilibrium. The vectors of four of these forces, P_2, P_3, P_{12}^{τ}, and P_{43}^{τ}, are known in magnitude and direction, but the vectors of forces P_{12}^{n} and P_{43}^{n} are known only by the lines of action. Having these data we can plot the diagram of forces in accordance with the following vector equation:

$$\bar{P}_2 + \bar{P}_3 + \bar{P}_{43}^{\tau} + \bar{P}_{43}^{n} + \bar{P}_{12}^{n} + \bar{P}_{12}^{\tau} = 0.$$

Plotting can be done in the following manner (Fig. 119, *b*):

1. Starting from arbitrary point *f* in the drawing, which we shall term the pole of the diagram, we draw in succession the first three components of the vector equation, i.e. we join vectors $\bar{P}_2$, $\bar{P}_3$ and $\bar{P}_{43}^{\tau}$ in succession to one another.

2. Since the magnitude of force $\bar{P}^n_{43}$ is unknown and only its line of action is known, we draw from the terminus of the last vector, vector $\bar{P}^\tau_{43}$, the line of action of vector $\bar{P}^n_{43}$; this line must be parallel to link CD and therefore perpendicular to vector $\bar{P}^\tau_{43}$.

3. Since we are unable to continue plotting the diagram of forces in the order that we have chosen, i.e. the order which is determinable by the order of components of the vector equation, we proceed to the end members of the equation and draw the vector $\bar{P}^\tau_{12}$; since this vector is the last one in the equation and must therefore close the figure, we direct the vector arrow to the pole.

4. The last vector but one in the equation, $\bar{P}^n_{12}$, is known only by the line of action, therefore from the origin of vector $\bar{P}^\tau_{12}$ we draw the line of action $\bar{P}^n_{12}$ parallel to link BC or perpendicular to vector $\bar{P}^\tau_{12}$, which is the same thing.

Since the group BCD is in equilibrium, the vectors must form a closed figure, therefore the point of intersection of the lines of action of vectors $\bar{P}^n_{43}$ and $\bar{P}^n_{12}$ is the terminus of vector $\bar{P}^n_{43}$ and the origin of vector $\bar{P}^n_{12}$. In this way the unknown magnitudes of forces $\bar{P}_{12}$ and $\bar{P}_{43}$ are determined.

The pressure in pair B from the side of the first link onto the second is obtained as a result of the geometrical addition of forces $\bar{P}^n_{12}$ and $\bar{P}^\tau_{12}$; we will get the resultant vector of these forces by joining on the diagram of forces the origin of vector $\bar{P}^n_{12}$ with the terminus of vector $\bar{P}^\tau_{12}$ and placing on the segment obtained an arrow opposite to the arrows of vectors $\bar{P}^n_{12}$ and $\bar{P}^\tau_{12}$.

The pressure in pair D will be obtained as a result of the geometrical addition of vectors $\bar{P}^\tau_{43}$ and P^n_{43}: the line that joins the terminus of the last of these vectors with the origin of the first, and the arrow, which is directed opposite to the arrows of the added vectors, is the vector of force $\bar{P}_{43}$.

Both external forces $\bar{P}_2$ and $\bar{P}_3$ and reacting forces $\bar{P}_{12}$ and $\bar{P}_{43}$ which act on group BCD must form a closed figure

with arrows in one direction; this is in fact what happens on the diagram of forces that we have plotted.

Having plotted the diagram of forces we have still not found on it the pressure in pair C because the force which acts from the side of one link on the other is not an external force acting on group BCD, since inside the group force $\bar{P}_{23}$ is balanced by force $\bar{P}_{32}$ which is equal to it and is oppositely directed. In order to determine the magnitude and direction of the force with which one of the links in the group presses on the other link, it is necessary to plot a diagram of forces for any one of the links.

Link BC is in equilibrium under the action of three forces: $\bar{P}_2$, $\bar{P}_{12}$ and as yet unknown force $\bar{P}_{32}$. The diagram of forces for link BC should represent a triangle, which is formed by the vectors of these forces. Since we have plotted the first two vectors on the diagram of forces we can also draw vector $\bar{P}_{32}$ on the same diagram, joining the terminus of vector $\bar{P}_2$ with the origin of vector $\bar{P}_{12}$ and placing an arrow on the segment obtained, the arrow being turned in the same direction as the arrows of vectors $\bar{P}_2$ and $\bar{P}_{12}$. By turning vector $\bar{P}_{32}$ through 180° we shall get vector $\bar{P}_{23}$. We shall obtain the same vectors $\bar{P}_{23}$ and $\bar{P}_{32}$ in examining the equilibrium of one link CD.

In plotting the diagram of forces it is expedient to draw the vectors in the same order as has been indicated above. It can easily be seen that if we join to the terminus of vector $\bar{P}_3$ vector $\bar{P}'_{12}$ instead of vector $\bar{P}'_{43}$ and the latter vector to pole f, then for determining the pressure in pair C we shall have to plot a separate diagram of forces for any one of the links.

B. A Group with Two Turning and One Extreme Sliding Pair

This group (Fig. 120, a) is incorporated in a slider crank mechanism, which, as stated above, is widely applied in engineering.

Denoting by P_2 the force which acts on the second link (link BC), and by P_3 the force which acts on the third link (slider), we shall determine the pressures in pairs

B, C and in sliding pair CC_x, where C_x is the point on the fixed directrix $x—x$, which belongs to the fixed fourth link not incorporated in the group.

Forces P_2 and P_3 are given and are therefore known in magnitude, lines of action and direction along the lines of action. Reaction P_{12} in pair B is unknown both in magnitude and direction, but the point of its application is known. Reaction P_{43}, i. e. the force from the side of the directrix on to the slider, can be directed only along the perpendicular to the directrix; its magnitude and point of application are unknown.

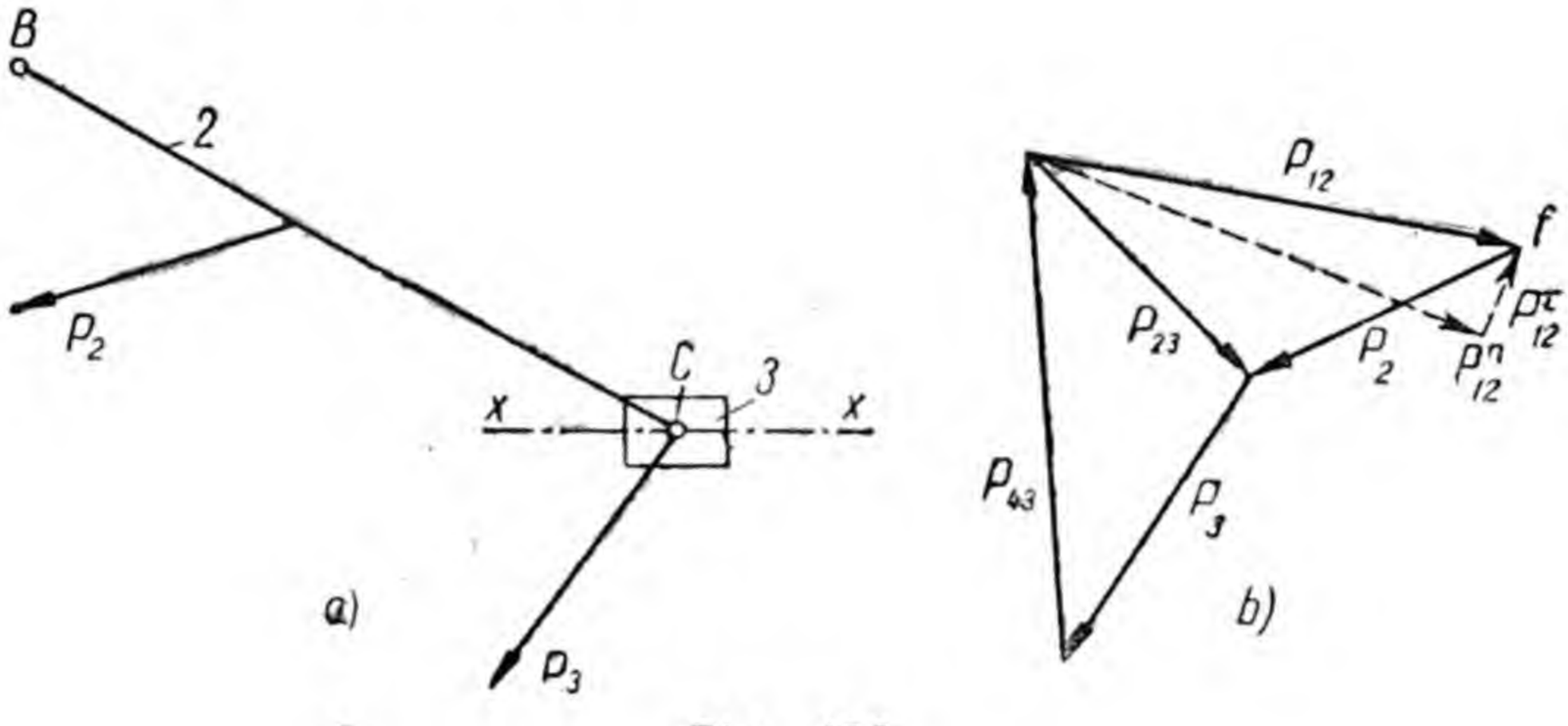

Fig. 120

By resolving force $\bar{P}_{12}$ into forces $\bar{P}^{\tau}_{12}$ and $\bar{P}^{n}_{12}$ and by determining the magnitude and direction of force $\bar{P}^{\tau}_{12}$, as we did above, from the condition of equilibrium of the group we get the vector equation

$$\bar{P}_2+\bar{P}_3+\bar{P}_{43}+\bar{P}^{n}_{12}+\bar{P}^{\tau}_{12}=0,$$

in which the first, second and last vectors are known in magnitude and direction, whereas the third and fourth are known only in direction.

We plot the diagram of forces in the following order (Fig. 120, *b*):

1) we draw vectors $\vec{P}_2$ and $\vec{P}_3$ from pole f;

2) from the terminus of vector $\bar{P}_3$ we draw the line of action of force $\bar{P}_{43}$ perpendicular to the directrix $x—x$;

3) to the origin of vector $\bar{P}_2$ (point f) we join vector $\bar{P}^{\tau}_{12}$; the arrow of this vector must be turned to the origin

of vector $\bar{P}_2$ (point f), since this last vector in the equation must close the figure;

4) to the origin of vector $\bar{P}_{12}^{\tau}$ we join the line of action of force $\bar{P}_{12}^{n}$ perpendicular to vector $\bar{P}_{12}^{\tau}$.

At the point of intersection of the lines of action vector $\bar{P}_{43}$ ends and vector $\bar{P}_{12}^{n}$ begins.

We obtain vector $\bar{P}_{12}$ (pressure in pair B) by joining the origin of vector $\bar{P}_{12}^{n}$ with the terminus of $\bar{P}_{12}^{\tau}$. On the segment obtained the arrow must be placed opposite to the arrows of both vectors. Vector $\bar{P}_{43}$ is the vector of force from the side of the directrix to the slider.

The pressure in pair C can be determined, as indicated above, from the condition of equilibrium of link BC or the slider.

C. Combined Static and Inertia-force Analysis of a Crank

After determining the pressures in pairs of driven links of the mechanism we determine the magnitude and direction of force $\bar{P}_{21}$ with which the link connected to the crank acts on the crank.

In most cases the power that is consumed by a mechanism is supplied from the engine to shaft A (Fig. 121) of the crank, so that on the one hand, the crankshaft must be in equilibrium under the action of moment from the engine and the resultant moment of all the external forces applied to the crank, including force $\bar{P}_{21}$, on the other. If the crank is under the action of only force $\bar{P}_{21}$ and the centrifugal force of inertia is conditionally transferred to it, the moment from the side of the engine will be equal to $M = -\bar{P}_{21} \times h_{21}$, where h_{21} is the arm of force P_{21}.

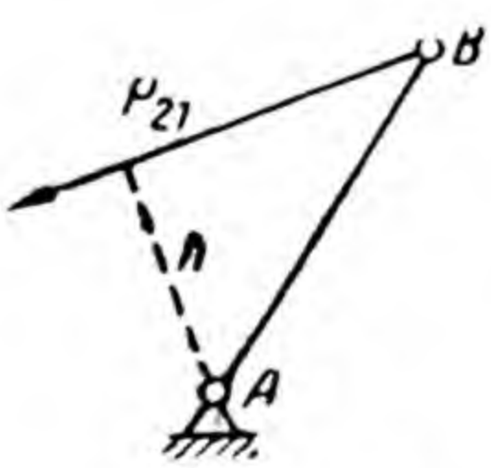

Fig. 121

In determining the pressure in pair A, i. e. force $\bar{P}_{41}$ from the side of the fixed (fourth) link onto the crank (first link), vector $\bar{P}_{21}$ must be drawn on the diagram of forces, and the vectors of all the given forces which act on the crank and the force of inertia must be conditionally transferred onto

the crank. The vector of force $\overline{P}_{41}$, which is to be determined, must join the terminus of the last of the vectors with the origin of the first.

D. Numerical Examples of Kinematic Analysis and of Combined Static and Inertia-force Analysis

Example 1. Determine the pressures from the forces of inertia in the kinematic pairs of the four-bar mechanism

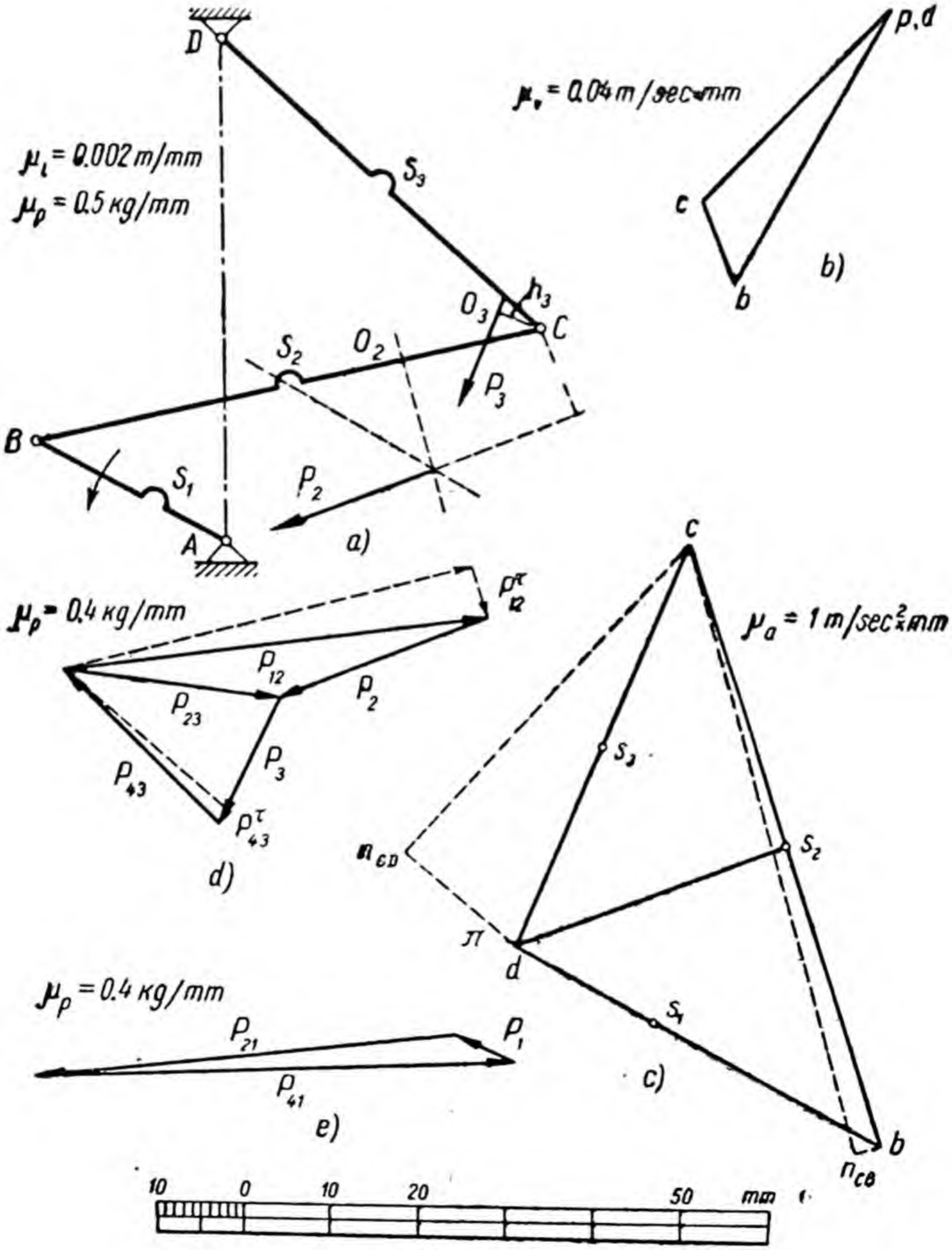

Fig. 122

in the position, as shown in Fig. 122, *a*, given the following data:

1) the lengths of links:

$l_{AB}=50$ mm, $l_{BC}=120$ mm, $l_{CD}=100$ mm, $l_{AD}=120$ mm;

2) the positions of centres of gravity S of the links:

$$l_{AS_1}=20 \text{ mm}, \quad l_{BS_2}=60 \text{ mm}, \quad l_{DS_3}=50 \text{ mm};$$

3) moments of inertia J of the second and third links relative to the axes which pass through the centres of gravity:

$$J_2=J_3=5\times10^{-4} \text{ kg}\times\text{m}\times\text{sec}^2;$$

4) weights G of the links:

$$G_1=1.5 \text{ kg}, \quad G_2=3 \text{ kg}, \quad G_3=2.5\text{kg};$$

5) the number of revolutions of crank AB, which rotates counter-clockwise with constant velocity $n=300$ r.p.m.

The number of links is indicated in Fig. 122, *a*.

We shall determine the pressure in pairs by the method of diagrams of forces. In order to plot the diagrams of forces it is first necessary to determine the magnitudes, lines of action and directions along the lines of action of the forces of inertia in the links. In order to determine the forces of inertia it is necessary to plot the acceleration diagram, while in order to obtain the data required to plot this diagram it is necessary to plot the velocity diagram. The graphic calculation must therefore be started by plotting the velocity diagram.

1. VELOCITY DIAGRAM

Absolute velocity of point B:

$$v_B=l_{AB}\times\omega_1=0.05 \text{ m}\times\frac{\pi\times300}{30} \text{ sec}^{-1}=1.57 \text{ m/sec}.$$

Choosing the scale $\mu_v=0.04$ m/sec$\times$mm, we determine the length of vector $\overline{pb}$ of velocity $\bar{v}_B$:

$$pb=v_B/\mu_v=1.57 \text{ m/sec}/0.04 \text{ m/sec}\times\text{mm}=39.25 \text{ mm}.$$

We determine the velocity of point C by two vector equations:

$$\bar{v}_C=\bar{v}_B+\bar{v}_{CB};$$
$$\bar{v}_C=\bar{v}_D+\bar{v}_{CD}.$$

In accordance with the first equation we draw vector $\overline{pb}$ perpendicular to AB from pole p downwards and to the left (Fig. 122, b), and from the terminus of this vector we draw the line of action $\bar{v}_{CB}$ perpendicular to BC.

In accordance with the second equation we place the terminus of vector $\overline{pd}$ of velocity $\bar{v}_D$ at the pole, since $v_D=0$. Then from the pole we draw the line of action of velocity $\bar{v}_{CD}$ perpendicular to CD. At point c, the point of intersection of the lines of action, we get the terminus of vector pc of velocity v_C. The velocity diagram thus assumes the shape of triangle pbc.

Using the velocity diagram we determine the velocity magnitudes which are required for plotting the acceleration diagram:

$$v_{CB}=bc\times\mu_v=10\text{ mm}\times0.04\text{ m/sec}\times\text{mm}=0.4\text{ m/sec},$$
$$v_{CD}=pc\times\mu_v=33\text{ mm}\times0.04\text{ m/sec}\times\text{mm}=1.32\text{ m/sec}.$$

2. ACCELERATION DIAGRAM

We determine the magnitudes which are required for plotting the acceleration diagram:

$$a_B=a_B^n=v_B^2/l_{AB}=(1.57\text{ m/sec})^2/0.05\text{ m}=49\text{ m/sec}^2;$$
$$a_{CB}^n=v_{CB}^2/l_{BC}=(0.4\text{ m/sec})^2/0.12\text{ m}=1.3\text{ m/sec}^2;$$
$$a_{CD}^n=v_{CD}^2/l_{CD}=(1.32\text{ m/sec})^2/0.1\text{ m}=17.4\text{ m/sec}^2.$$

Choosing the scale $\mu_a=1\text{ m/sec}^2\times\text{mm}$, we calculate the lengths of the vectors:

$$\pi b=a_B/\mu_a=49\text{ m/sec}^2/1\text{ m/sec}^2\times\text{mm}=49\text{ mm};$$
$$bn_{CB}=a_{CB}^n/\mu_a=1.3\text{ m/sec}^2/1\text{ m sec}^2\times\text{mm}=1.3\text{ mm};$$
$$\pi n_{CD}=a_{CD}^n/\mu_a=17.4\text{ m/sec}^2/1\text{ m/sec}^2\times\text{mm}=17.4\text{ mm}.$$

We determine the acceleration of point C by two vector equations:

$$\bar{a}_C=\bar{a}_B+\bar{a}_{CB}^n+\bar{a}_{CB}^\tau;$$
$$\bar{a}_C=\bar{a}_D+\bar{a}_{CD}^n+\bar{a}_{CD}^\tau.$$

In accordance with the first equation we draw (Fig. 122, *c*) vector $\overline{\pi b}$ parallel to *AB*, directing it from the pole downwards and to the right, since the acceleration of point *B* in the mechanism is directed from point *B* to point *A*. From point *b* we draw vector $\overline{bn_{CB}}$, directing it parallel to *BC* downwards and to the left, since acceleration $\bar{a}^n_{CB}$ is directed in the mechanism from point *C* to point *B*. From point n_{CB} we draw the line of action of acceleration $\bar{a}^\tau_{CB}$.

In accordance with the second equation we place the terminus of vector $\overline{\pi d}$ at the pole, since acceleration $\underline{a_D}$ of fixed point *D* is zero. From the pole we draw vector $\overline{\pi n_{CD}}$ parallel to *CD*, directing it upwards and to the left, since acceleration $\bar{a}^n_{CD}$ is directed in the mechanism from point *C* to point *D*. From point n_{CD} we draw the line of action of acceleration $\bar{a}^\tau_{CD}$ up to its intersection with the line of action of acceleration $\bar{a}^\tau_{CB}$ at point *c*.

By joining point *c* with points π and *b* we get the acceleration diagram in the form of triangle πbc.

In order to determine the accelerations of the centres of gravity of the links we first determine the positions of points s_1, s_2 and s_3 on the vectors of the acceleration diagram:

$$\pi s_1 = \pi b \times \frac{l_{AS_1}}{l_{AB}} = 49 \times \frac{20}{50} = 19.6 \text{ mm};$$

$$\pi s_2 = bc \times \frac{l_{BC_2}}{l_{BC}} = 76 \times \frac{60}{120} = 38 \text{ mm};$$

$$\pi s_3 = \pi c \times \frac{l_{DS_3}}{l_{DC}} = 53 \times \frac{50}{100} = 26.5 \text{ mm}$$

By drawing vector $\overline{\pi s_2}$ we get its length as 34.5 mm. Accelerations of the centres of gravity:

$$a_{S_1} = \pi s_1 \times \mu_a = 19.6 \text{ mm} \times 1 \text{ m/sec}^2 \times \text{mm} = 19.6 \text{ m/sec}^2;$$

$$a_{S_2} = \pi s_2 \times \mu_a = 34.5 \text{ mm} \times 1 \text{ m/sec}^2 \times \text{mm} = 34.5 \text{ m/sec}^2;$$

$$a_{S_3} = \pi s_3 \times \mu_a = 26.5 \text{ mm} \times 1 \text{ m/sec}^2 \times \text{mm} = 26.5 \text{ m/sec}^2.$$

The masses of the links:

$$m_1 = 1.5 \text{ kg}/9.8 \text{ m/sec}^2 = 0.153 \text{ kg} \times \text{sec}^2/\text{m};$$

$$m_2 = 3 \text{ kg}/9.8 \text{ m/sec}^2 = 0.306 \text{ kg} \times \text{sec}^2/\text{m};$$

$$m_3 = 2.5 \text{ kg}/9.8 \text{ m/sec}^2 = 0.255 \text{ kg} \times \text{sec}^2/\text{m}.$$

The magnitudes of the forces of inertia:

$$P_1 = m_1 \times a_{S_1} = 0.153 \times 19.6 = 3 \text{ kg};$$

$$P_2 = m_2 \times a_{S_2} = 0.306 \times 34.5 = 10.6 \text{ kg};$$

$$P_3 = m_3 \times a_{S_3} = 0.255 \times 26.5 = 6.75 \text{ kg}.$$

Acceleration $\bar{a}_{S_1}$ of the centre of gravity S_1 of link AB, which rotates with constant velocity, is directed along line AB to the centre of rotation. The force of inertia $\bar{P}_1$ is therefore directed along line AB upwards and to the left, i. e. to the side which is opposite to acceleration $\bar{a}_{S_1}$. The vector of force $\bar{P}_1$ in Fig. 122, *a* is not drawn.

Link BC performs compound motion, which we consider as translatory motion with acceleration of point B and rotary motion about that point. The force of inertia $\bar{P}_2$ of link BC we therefore obtain as the geometric sum of two forces: force of inertia P_2' in translatory motion and force of inertia P_2'' in rotary motion. Since in translatory motion of the link the accelerations of all of its points are equal and parallel, then $P_2' = m_2 \times a_B$, where a_B is the acceleration of the centre of gravity S_2 in translatory motion with point B. Force $P_2'' = m_2 \times a_{S_2 B}$, where $a_{S_2 B}$ is the acceleration of the centre of gravity S_2 in rotary motion. The line of action of force P_2 passes through the centre of gravity S_2, the line of action of the force $\bar{P}_2''$ passes through the centre of oscillation O_2, which is located at distance l_{BO_2} from the centre of rotation, i. e. point B, where:

$$l_{BO_2} = l_{BS_2} + \frac{J_2}{m_2 \times l_{BS_2}} = l_{BS_2} + \frac{5 \times 10^{-4}}{0.306 \times 0.06} =$$

$$= 0.06 \text{ m} + 0.027 \text{ m} = 87 \text{ mm}.$$

We obtain at the point of intersection the point of application of resultant $\bar{P}_2'$ by drawing through point S_2 the line of action of force $\bar{P}_2'$, which is parallel to vector $\overline{\pi b}$ of the acceleration diagram, and through point O_2 the line of action of force $\bar{P}_2''$, which is parallel to vector $\overline{bs_2}$. The magnitude of P_2 has already been determined, its line of action is parallel to vector $\overline{\pi s_2}$ of acceleration $\bar{a}_{S_2}$, and the direction along the line of action is opposite to acceleration $\bar{a}_{S_2}$.

Link CD performs rotary motion with variable velocity. Force $\bar{P}_3$ is directed along the line of action parallel to vector $\overline{\pi s_3}$ of acceleration $\bar{a}_{S_3}$ to the side which is opposite to this acceleration. The point of application of force P_3 is the centre of oscillation O_2, which is located at a distance l_{DO_3} from the centre of rotation, i. e. point D, where:

$$l_{DO_3}=l_{DS_3}=\frac{J_3}{m_3\times l_{DS_3}}=l_{DS_3}+\frac{5\times 10^{-4}}{0.255\times 0.05}=$$

$$=0.05\text{ m}+0.039\text{ m}=89\text{ mm}.$$

4. PRESSURES IN KINEMATIC PAIRS

The external forces which act on group BCD must satisfy the vector equation

$$\bar{P}_2+\bar{P}_3+\bar{P}_{43}+\bar{P}_{12}=0.$$

We cannot plot the diagram of forces in accordance with this equation, since forces $\bar{P}_{43}$ and $\bar{P}_{12}$ are known only by their points of application, while their magnitudes and directions are unknown. We therefore resolve each of these forces into a tangential component, which is directed perpendicular to the link, and a normal component which is directed along the link. In this case the vector equation is expressed as follows:

$$\bar{P}_2+\bar{P}_3+\bar{P}_{43}^{\tau}+\bar{P}_{43}^{n}+\bar{P}_{12}^{n}+\bar{P}_{12}^{\tau}=0.$$

We determine the magnitude of P_{43}^{τ} from the equation of the moments of the forces acting on link CD relative to point C. The moments of forces P_{23} and P_{43}^{n} are each zero,

since the lines of action of these forces pass through point C; therefore the equation of moments is obtained in the form

$$P_3 h_3 = P_{43}^{\tau} l_{CD},$$

where h_3 is the arm of force P_3, which is determined by the drawing (Fig. 122, a). Since the length of h_3 equals 10 mm, the force P_{43}^{τ} is equal to

$$P_{43}^{\tau} = P_3 \times h_3 / l_{CD} = 6.75 \text{ kg} \times 10 \text{ mm} / 100 \text{ mm} = 0{,}675 \text{ kg}.$$

We determine the magnitude of P_{12}^{τ} in a similar manner from the equation of the moments of the forces, acting on link BC, relative to point C:

$$P_{12}^{\tau} = C_2 \times h_2 / l_{BC} = 10.6 \text{ kg} \times 24 \text{ mm} / 120 \text{ mm} = 2.12 \text{ kg}.$$

Choosing the scale $\mu_P = 0.4$ kg/mm, we determine the lengths of the vectors of forces:

$$\overline{P}_2 = 10.6 \text{ kg} / 0.4 \text{ kg/mm} = 26.5 \text{ mm};$$

$$\overline{P}_3 = 6.75 \text{ kg} / 0.4 \text{ kg/mm} = 16.9 \text{ mm};$$

$$\overline{P}_{43}^{\tau} = 0.675 \text{ kg} / 0.4 \text{ kg/mm} = 1.69 \text{ mm};$$

$$\overline{P}_{12}^{\tau} = 2.12 \text{ kg} / 0.4 \text{ kg/mm} = 5.3 \text{ mm}.$$

We plot the diagram of forces: we draw the vectors of forces $\overline{P}_2$ and $\overline{P}_3$ (Fig. 122, d), then from the terminus of the latter we draw vector $\overline{P}_{43}^{\tau}$, directing it perpendicular to CD upwards and to the right, since by directing it so the force $\overline{P}_{43}^{\tau}$ creates a moment which counteracts the moment of force $\overline{P}_3$ relative to point C; from the terminus of vector $\overline{P}_{43}^{\tau}$ we draw the line of action of force $\overline{P}_{43}^{n}$ parallel to CD. Since we cannot join the vector $\overline{P}_{43}^{n}$ whose length is as yet unknown, with the vector $\overline{P}_{12}^{n}$ we join to vector $\overline{P}_2$ the vector $\overline{P}_{12}^{\tau}$, the last one in the equation, directing it perpendicular to BC downwards and to the right, since in so directing it a moment is created by force $\overline{P}_{12}^{\tau}$ which counteracts the moment of force $\overline{P}_2$ relative to point C. From the origin of vector $\overline{P}_{12}^{\tau}$ we draw the line of action $\overline{P}_{12}^{n}$ up to its point of intersection with the line of

action $\bar{P}_{43}^{n}$. By joining the point of intersection of the lines of action $\bar{P}_{43}^{n}$ and $\bar{P}_{12}^{n}$ with the origin of vector $\bar{P}_2$ and the terminus of vector P_3 we get the diagram of forces, which corresponds to the vector equation

$$\bar{P}_2+\bar{P}_3+\bar{P}_{43}+\bar{P}_{12}=0.$$

After measuring the lengths of vectors $\bar{P}_{12}$ and $\bar{P}_{43}$, we get

pressure in pair B $P_{12}=50\text{ mm}\times 0.4\text{ kg/mm}=20\text{ kg}$;

pressure in pair D $P_{43}=26\text{ mm}\times 0.4\text{ kg/mm}=10.4\text{ kg}$.

In order to determine the pressure in pair C it is necessary to plot the diagram of forces for link BC or CD. The diagram of forces for link CD should be plotted by the vector equation

$$\bar{P}_3+\bar{P}_{43}+\bar{P}_{23}=0.$$

The first two vectors in Fig. 122, *d* are already drawn; it remains to draw vector P_{23} which closes the triangle of forces. After drawing this vector and measuring its length, we get pressure in pair C

$$P_{23}=25\text{ mm}\times 0.4\text{ kg/mm}=10\text{ kg}.$$

The diagram of forces for the crank should be drawn by equation

$$\bar{P}_1+\bar{P}_{21}+\bar{P}_{41}=0.$$

After drawing vectors $\bar{P}_1$ and $\bar{P}_{21}$ (force $\bar{P}_{21}$ is equal to force $\bar{P}_{12}$ and is opposite in direction), and after joining the origin of the first of them with the terminus of the second, we get the vector of force $\bar{P}_{41}$. After measuring the length of this vector, we obtain pressure in pair A

$$P_{41}=56\text{ mm}\times 0.4\text{ kg/mm}=22.4\text{ kg}.$$

Example 2. Determine the pressures in the kinematic pairs of the slider crank mechanism in the position, as shown in Fig. 123, *a*, given the following data:

1) the lengths of links $l_{AB}=60$ mm, $l_{BC}=190$ mm;

2) the positions of the centres of gravity S of the links: $l_{AS_1}=30$ mm, $l_{BS_2}=50$ *mm*; the centre of gravity of the slider is at point C;

3) the moment of inertia of connecting rod BC relative to the centre of gravity $J_2=5\times10^{-4}$ kg×m×sec^2;

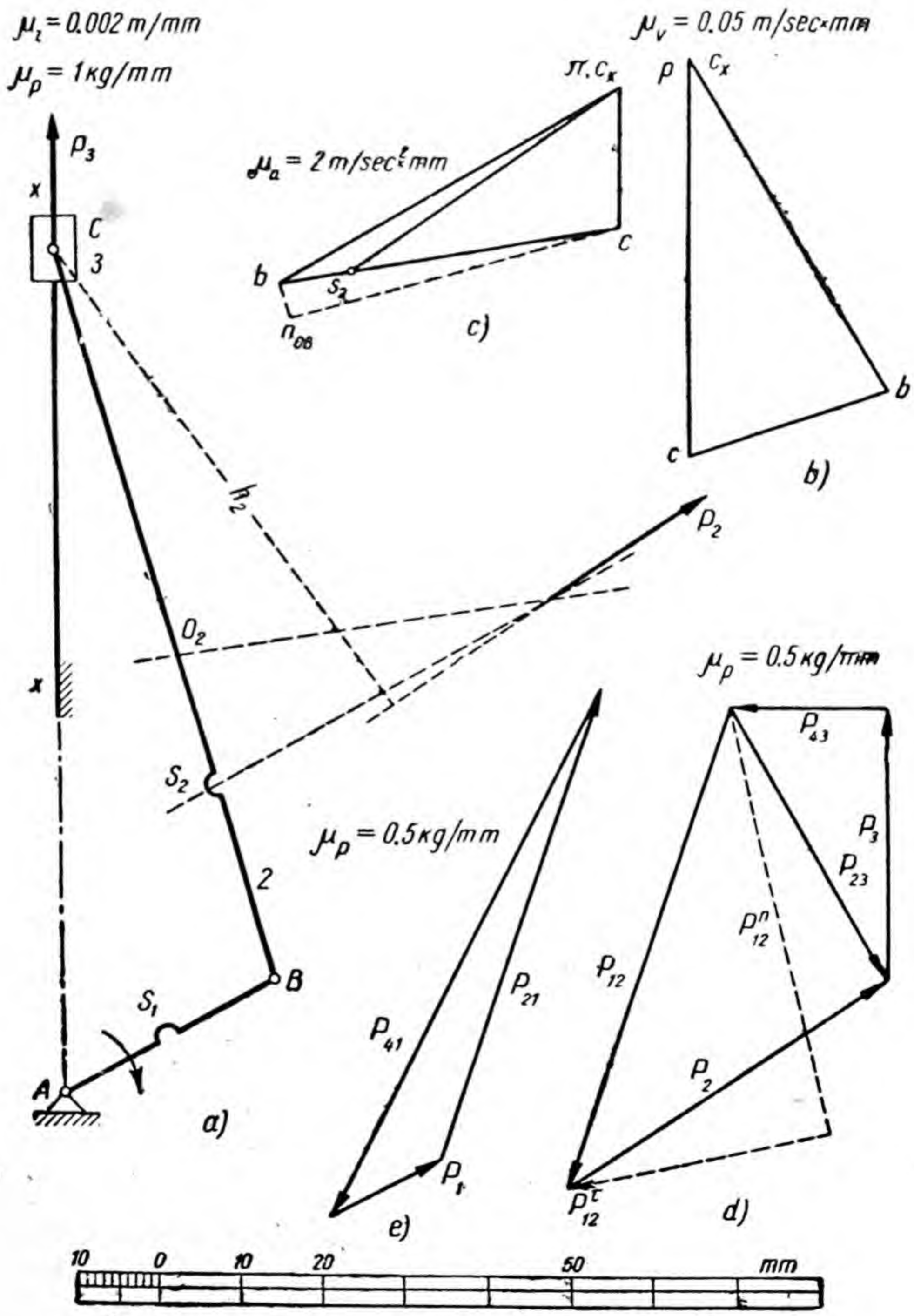

Fig. 123

4) weight G of the links: $G_1=1.57$ kg, $G_2=2.94$ kg, $G_3=4.9$ kg;

5) the number of revolutions of crank AB, which rotates clockwise with constant velocity, $n=382$ r. p. m.

The number of links is shown in Fig. 123, *a*.

1. VELOCITY DIAGRAM

Absolute velocity of point B:

$$v_B=l_{AB}\times\omega_1=0.06\text{ m}\,\frac{\pi\times382}{30}\text{sec}^{-1}=2.4\text{ m/sec.}$$

We plot the diagram to the scale $\mu_v=0.05$ m/sec×mm. The length of velocity vector $\bar{v}_B$

$$pb=\bar{v}_B/\mu_v=2.4\text{ m/sec}/0.05\text{ m/sec}\times\text{mm}=48\text{ mm.}$$

We determine the velocity of point C by two vector equations:

$$v_C=v_B+v_{CB};$$

$$\bar{v}_C=\bar{v}_{C_x}+\bar{v}_{CC_x}.$$

In accordance with the first equation we draw vector $\overline{pb}$ perpendicular to AB from pole p downwards and to the right (Fig. 123, *b*) and from the terminus of this vector we draw the line of action $\bar{v}_{CB}$ perpendicular to BC.

In accordance with the second equation we place the terminus of vector $\overline{pc_x}$ of velocity $\bar{v}_{C_x}$ of the fixed point C_x, which lies on the directrix x—x, at the pole, since $v_{C_x}=0$; we then draw from the pole the line of action of velocity $\bar{v}_{CC_x}$ parallel to the directrix. At the point of intersection of the lines of action we get the terminus of vector $\overline{pc}$ of the velocity of point C. We get the velocity diagram in the form of triangle pbc.

Using the diagram constructed we determine the magnitude of velocity v_{CB}, which is required for plotting the acceleration diagram:

$$v_{CB}=bc\times\mu_v=25\text{ mm}\times0.05\text{ m/sec}\times\text{mm}=1.25\text{ m/sec.}$$

2. ACCELERATION DIAGRAM

We determine the magnitudes which are required for plotting the acceleration diagram:

$$a_B = a_B^n = v_B^2/l_{AB} = (2.4 \text{ m/sec})^2/0.06 \text{ m} = 96 \text{ m/sec}^2;$$

$$a_{CB}^n = v_{CB}^2/l_{BC} = (1.25 \text{ m/sec})^2/0.19 \text{ m} = 8.2 \text{ m/sec}^2.$$

Choosing the diagram scale $\mu_a = 2 \text{ m/sec}^2 \times \text{mm}$, we calculate the lengths of the vectors:

$$\pi b = a_B/\mu_a = 96 \text{ m/sec}^2/2 \text{ m/sec}^2 \times \text{mm} = 48 \text{ mm};$$

$$bn_{CB} = a_{CB}^n/\mu_a = 8.2 \text{ m/sec}^2/2 \text{ m/sec}^2 \times \text{mm} = 4.1 \text{ mm}.$$

We determine the acceleration of point C by two vector equations:

$$\bar{a}_C = \bar{a}_B + \bar{a}_{CB}^n + \bar{a}_{CB}^\tau;$$

$$\bar{a}_C = \bar{a}_{C_x} + \bar{a}_{CC_x}^n + \bar{a}_{CC_x}^\tau.$$

In accordance with the first equation we draw (Fig. 123, *c*) the vector $\overrightarrow{\pi b}$ parallel to AB, directing it from the pole downwards and to the left, then from point b the vector $\overrightarrow{bn_{CB}}$ parallel to BC downwards and to the right. The magnitude of acceleration $\bar{a}_{CB}^\tau$ is as yet unknown, therefore we draw from point n_{CB} the line of action of this acceleration perpendicular to BC.

In accordance with the second equation we place the terminus of vector $\overrightarrow{\pi c_x}$, which is zero, of acceleration a_{C_x} of the fixed point C_x at the pole.

Normal acceleration $\bar{a}_{CC_x}^n$ of point C, which moves along a rectilinear path, is also zero, since the radius of curvature of the path is infinity. Acceleration $\bar{a}_{CC_x}^\tau$ is known only by its line of action, which is along the directrix. By drawing from the pole a line of action of this acceleration parallel to the directrix up to its point of intersection with the line of action $\bar{a}_{CB}^\tau$, we get point c and vector $\overrightarrow{\pi c}$ of acceleration $\bar{a}_C$. We get the acceleration diagram in the form of triangle πbc.

In order to determine the accelerations of the centres of gravity of the links we first have to determine the positions on the diagram of points s_1 and s_2, the vector termini of absolute accelerations $\bar{a}_{S_1}$ and $\bar{a}_{S_2}$:

$$\pi s_1 = \pi b \times \frac{l_{AS_1}}{l_{AB}} = 48 \times \frac{30}{60} = 24 \text{ mm};$$

$$bs_2 = bc \times \frac{l_{BS_2}}{l_{BC}} = 41.5 \times \frac{50}{190} = 9 \text{ mm};$$

$$\pi s_2 = 39 \text{ mm}; \ \pi c = 17 \text{ mm}.$$

Accelerations of the centres of gravity:

$$\pi s_2 = 39 \text{ mm}; \ \pi c = 17 \text{ mm}.$$

$$a_{S_1} = \pi s_1 \times \mu_a = 24 \text{ mm} \times 2 \text{ m/sec}^2 \times \text{mm} = 48 \text{ m/sec}^2;$$

$$a_{S_2} = \pi s_2 \times \mu_a = 39 \text{ mm} \times 2 \text{ m/sec}^2 \times \text{mm} = 78 \text{ m/sec}^2;$$

$$a_C = \pi c \times \mu_a = 17 \text{ mm} \times 2 \text{ m/sec}^2 \times \text{mm} = 34 \text{ m/sec}^2.$$

3. FORCES OF INERTIA

The masses of the links:

$$m_1 = 1.57 \text{ kg}/9.8 \text{ m/sec}^2 = 0.16 \text{ kg} \times \text{sec}^2/\text{m};$$

$$m_2 = 2.94 \text{ kg}/9.8 \text{ m/sec}^2 = 0.3 \text{ kg} \times \text{sec}^2/\text{m};$$

$$m_3 = 4.9 \text{ kg}/9.8 \text{ m/sec}^2 = 0.5 \text{ kg} \times \text{sec}^2/\text{m}.$$

The magnitudes of the forces of inertia:

$$P_1 = m_1 \times a_{S_1} = 0.16 \text{ kg} \times \text{sec}^2/\text{m} \times 48 \text{ m/sec}^2 = 7.7 \text{ kg};$$

$$P_2 = m_2 \times a_{S_2} = 0.3 \text{ kg} \times \text{sec}^2/\text{m} \times 78 \text{ m/sec}^2 = 23.4 \text{ kg};$$

$$P_3 = m_3 \times a_C = 0.5 \text{ kg} \times \text{sec}^2/\text{m} \times 34 \text{ m/sec}^2 = 17 \text{ kg}.$$

The force of inertia P_1 is directed along the line of action of acceleration $\bar{a}_{S_1}$ in the opposite direction to that of the acceleration, i. e. in Fig. 123, *a*, along link *AB* upwards and to the right. The vector of this force is not drawn in Fig. 123, *a*.

By resolving the compound motion of link BC into translatory motion with acceleration of point B and rotary motion about this point, we get the total force of inertia as the geometric sum of two components: the force of inertia $\bar{P}_2'$ in translatory motion, and the force of inertia $\bar{P}_2''$ in rotary motion. The line of action of force $\bar{P}_2'$ passes through the centre of gravity S_2 parallel to vector $\overline{\pi b}$ of the acceleration diagram, since in translatory motion with point B the acceleration of the centre of gravity is equal to the acceleration of point B. Force $\bar{P}_2''$ passes through the centre of oscillation O_2, which is located at distance l_{BO_2} from the centre of rotation, i. e. from point B, where:

$$l_{BO_2} = l_{BS_2} + \frac{J_2}{m_2 \times l_{BS_2}} = l_{BS_2} + \frac{5 \times 10^{-4}}{0.3 \times 0.05} =$$

$$= 0.05 \text{ m} + 0.033 \text{ m} = 83 \text{ mm}.$$

The line of action $\bar{P}_2''$ is parallel to vector $\overline{bs_2}$ of the acceleration of centre of gravity S_2 in rotary motion about point B.

At the intersection of the lines of action of forces $\bar{P}_2'$ and $\bar{P}_2''$ we get a point through which the line of action of the total force of inertia $\bar{P}_2$ passes. The line of action of this force is parallel to vector $\overline{\pi s_2}$ of acceleration $\bar{a}_{S_2}$ of the centre of gravity in compound motion of link BC. The magnitude of force P_2 has already been determined.

Force $\bar{P}_3$ passes through point C and is directed along the line of action of acceleration $\bar{a}_C$ in the opposite direction.

4. PRESSURES IN KINEMATIC PAIRS

After resolving force $\bar{P}_{12}$ into normal and tangential components we plot the diagram of forces for the group BCC_x in accordance with the vector equation

$$\bar{P}_2 + \bar{P}_3 + \bar{P}_{43} + \bar{P}_{12}^n + \bar{P}_{12}^\tau = 0.$$

We determine the magnitude of force P_{12}^τ from the equation of moments of forces relative to point C, which act on link BC. The moments of forces $\bar{P}_{32}$ and $\bar{P}_{12}^n$ are

zero, because the lines of action of these forces pass through point C. The arm of force $\bar{P}_{12}^{\tau}$ is equal to $l_{BC}=190$ mm; the arm h_2 of force $\bar{P}_2$ which is determined by the drawing (Fig. 123, a) equals 141. The force $\bar{P}_{12}^{\tau}$ will equal

$$P_{12}^{\tau}=P_2\times h_2/l_{BC}=23.4 \text{ kg}\times 141 \text{ mm}/190 \text{ mm}=17.5 \text{ kg}.$$

Choosing the scale $\mu_P=0.5$ kg/mm, we calculate the lengths of the vectors of the forces

$$\bar{P}_2=23.4 \text{ kg}/0.5 \text{ kg/mm}=46.8 \text{ mm};$$
$$\bar{P}_3=17 \text{ kg}/0.5 \text{ kg/mm}=34 \text{ mm};$$
$$\bar{P}_{12}^{\tau}=17.5 \text{ kg}/0.5 \text{ kg/mm}=35 \text{ mm}.$$

We draw (Fig. 123, d) the vectors of forces $\bar{P}_2$ and $\bar{P}_3$ and from the terminus of the last vector the line of action of force $\bar{P}_{43}$ perpendicular to the directrix, since only along this line of action can the directrix press on the slider. After we have drawn the vector of force $\bar{P}_{12}^{\tau}$ perpendicular to BC downwards to the left to the origin of vector P_2, since by this direction the moment of force $\bar{P}_2$ is balanced by the moment of force $\bar{P}_{12}^{\tau}$, we draw from the origin of vector $\bar{P}_{12}^{\tau}$ the line of action of force $\bar{P}_{12}^{n}$ up to its point of intersection with the line of action of force $\bar{P}_{43}$. We get the vectors of forces $\bar{P}_{12}$ and $\bar{P}_{43}$ by joining the point of intersection of the lines of action with the origin of the vector of force $\bar{P}_2$.

After measuring the lengths of the vectors, we get:
the pressure in pair B $P_{12}=64$ mm$\times 0.5$ kg/mm$=32$ kg;
the pressure in the sliding pair $P_{43}=19$ mm$\times 0.5$ kg/mm$=9.5$ kg.

The pressure in pair C can be determined according to the diagram of forces, which is plotted by the vector equation for the slider,

$$\bar{P}_3+\bar{P}_{43}+\bar{P}_{23}=0.$$

The first two vectors in Fig. 123, d are already drawn. Closing the triangle of forces by vector $\bar{P}_{23}$ and measuring the length of this vector, we get

pressure in pair C $P_{23}=39$ mm$\times 0.5$ kg/mm$=19.5$ kg.

The pressure in pair A can be determined according to the diagram of forces for crank AB, which is plotted by the vector equation

$$\bar{P}_1+\bar{P}_{21}+\bar{P}_{41}=0.$$

The magnitude and direction of force $\bar{P}_1$ have already been determined. Force $\bar{P}_{21}$ is equal to force $\bar{P}_{12}$ and opposite to it in direction. By drawing the vectors of these forces (Fig. 123, *e*) and closing the triangle by vector P_{41}, we get the pressure in pair A $P_{41}=76$ mm$\times 0.5$ kg/mm$=$ $=38$ kg.

Example 3. Determine the pressures in the kinematic pairs, the angular velocity and angular acceleration of link EF of the six-link mechanism in the position, as shown in Fig. 124, *a*, given the following data:

1) the lengths of the links: $l_{AB}=50$ mm, $l_{BC}=180$ mm, $l_{BD}=120$ mm, $l_{DE}=180$ mm, $l_{EF}=100$ mm, $l_{AF}=250$ mm;

2) the positions of the centres of gravity S of the links: $l_{AS_1}=25$ mm, $l_{BS_2}=90$ mm, $l_{DS_4}=90$ mm, $l_{FS_5}=40$ mm; the centre of gravity of the slider is at point C;

3) weights G of the links: $G_1=1.96$ kg, $G_2=5.88$ kg, $G_3=9.8$ kg, $G_4=3.92$ kg, $G_5=2.94$ kg (the number of the links is indicated in Fig. 124, *a*);

4) the moments of inertia J of the links relative to their centres of gravity: $J_2=6\times 10^{-4}$ kg$\times$m$\times$sec^2, $J_4=5\times$ $\times 10^{-4}$ kg$\times$m$\times$sec^2, $J_5=3\times 10^{-4}$ kg/m$\times$sec^2;

5) the number of revolutions of crank AB, which rotates clockwise with constant velocity, $n=300$ r. p. m.

1. VELOCITY DIAGRAM

$$v_B=l_{AB}\times\omega_1=0.05\text{ m}\times\frac{\pi\times 300}{30}\text{ sec}^{-1}=1.57\text{ m/sec}.$$

The length of vector $\bar{v}_B$

$$pb=v_B/\mu_v=1.57\text{ m/sec}/0.04\text{ m/sec}\times\text{mm}=39.2\text{ mm},$$

where the scale of the velocity diagram is $\mu_v=0.04$ m/sec$\times$ $\times$mm.

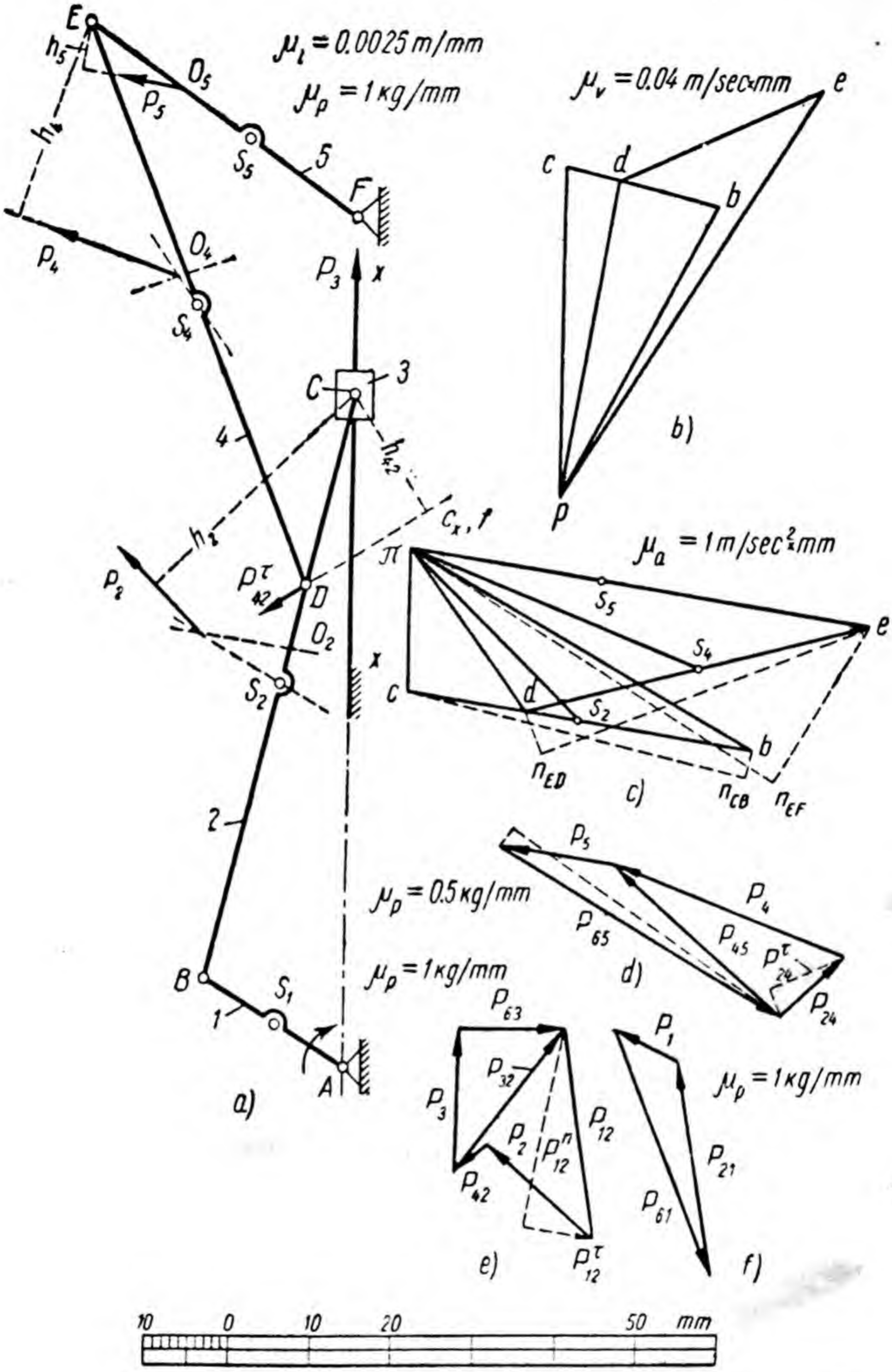

Fig. 124

We plot the velocity diagram (Fig. 124, *b*):

1) we draw the vector $\overline{pb}$ perpendicular to AB, directing it upwards and to the right in the direction of the velocity of point B;

2) in order to determine velocity $\bar{v}_C$ we have two vector equations:

$$\bar{v}_C = \bar{v}_B + \bar{v}_{CB};$$

$$\bar{v}_C = \bar{v}_{C_x} + \bar{v}_{CC_x},$$

where C_x is the point on the fixed directrix x—x, which is located under point C; by drawing the line of action $\bar{v}_{CB}$ from point b perpendicular to BC and the line of action $\bar{v}_{CC_x}$ parallel to directrix x—x from the pole (because $v_{C_x}=0$, and point c_x, therefore, coincides with the pole), we get at the point of intersection of the lines of action the point c, the terminus of vector $\overline{pc}$ of velocity $\bar{v}_C$;

3) dividing the segment bc by point d in relation $bd/bc = l_{BD}/l_{BC}$, we draw $\overline{pd}$, the vector $\bar{v}_D$;

4) for determining $\bar{v}_E$ we have two vector equations:

$$\bar{v}_E = \bar{v}_D + \bar{v}_{ED};$$

$$\bar{v}_E = \bar{v}_F + \bar{v}_{EF},$$

by drawing from point d the line of action v_{ED} perpendicular to DE and from the pole (since $v_F=0$, and point f, therefore, coincides with the pole) the line of action $\bar{v}_{EF}$ perpendicular to EF, we get at the point of intersection of the lines of action the point e, the terminus of vector $\overline{de}$ of velocity $\bar{v}_{ED}$, and the terminus of vector $\overline{pe}$ of velocity $\bar{v}_E$.

By the plotted diagram we determine the velocities required for plotting the acceleration diagram:

$$v_{CB} = bc \times \mu_v = 19.5 \text{ mm} \times 0.04 \text{ m/sec} \times \text{mm} = 0.78 \text{ m/sec};$$

$$v_{ED} = de \times \mu_v = 28 \text{ mm} \times 0.04 \text{ m/sec} \times \text{mm} = 1.12 \text{ m/sec};$$

$$v_{EF} = pe \times \mu_v = 58 \text{ mm} \times 0.04 \text{ m/sec} \times \text{mm} = 2.32 \text{ m/sec}.$$

The angular velocity of rotation of link EF (link No. 5)

$$\omega_5 = v_E/l_{EF} = 2.32 \text{ m/sec}/0.1 \text{ m} = 23.2 \text{ sec}^{-1}.$$

The direction of ω_5 is clockwise, which becomes clear after vector $\overline{pe}$ is transferred parallel to itself before joining points p and E in Fig. 124, *a*.

$$a_B = a_B^n = v_B^2/l_{AB} = (1.57 \text{ m/sec})^2/0.05 \text{ m} = 49.3 \text{ m/sec}^2.$$

Choosing the scale $\mu_a = 1$ m/sec$^2 \times$mm, we get the length of vector $\bar{a}_B$ to equal

$$\pi b = a_B/\mu_a = 49.3 \text{ m/sec}^2/1 \text{ m/sec}^2 \times \text{mm} = 49.3 \text{ mm}.$$

We draw (Fig. 124, *c*) from pole π the vector $\overline{\pi b}$, directing it parallel to AB downwards, since acceleration $\bar{a}_B$ is directed in the mechanism from point B to point A (Fig. 124, *a*).

We determine the acceleration $\bar{a}_C$ by two vector equations:

$$\bar{a}_C = \bar{a}_B + \bar{a}_{CB}^n + \bar{a}_{CB}^\tau;$$

$$\bar{a}_C = \bar{a}_{C_x} + \bar{a}_{CC_x}^n + \bar{a}_{CC_x}^\tau.$$

The magnitude of acceleration $a_{CB}^n = v_{CB}^2/l_{BC} =$ $= (0.78 \text{ m/sec})^2/0.18 \text{ m} = 3.36 \text{ m/sec}^2$; the vector length of this acceleration $bn_{CB} = a_{CB}^n/\mu_a = 3.36 \text{ m/sec}^2/1 \text{ m/sec}^2 \times$ $\times$mm $= 3.36$ mm.

From point b we draw the vector $\overline{bn_{CB}}$, directing it parallel to BC downwards, since acceleration $\bar{a}_{CB}^n$ is directed in the mechanism along line BC from point C to point B. From point n_{CB} we draw the line of action of acceleration $\bar{a}_{CB}^\tau$ perpendicular to BC.

Going over to the second equation we place point c_x at the pole, since acceleration $a_{C_x} = 0$ (point C_x is stationary). Acceleration $a_{CC_x}^n$ is also zero, since point C moves along a rectilinear path, whose radius of curvature is infinity. Therefore we draw the line of action $\bar{a}_{CC_x}^\tau$ from the pole parallel to the directrix x—x. At the point of intersection of the lines of action we get the terminus of vector πc of acceleration $\bar{a}_C$.

By joining points b and c and dividing the segment bc by point d in relation $bd/bc = l_{BD}/l_{BC}$ and joining point d with the pole, we get the vector $\overline{\pi d}$ of acceleration $\bar{a}_D$.

We determine the acceleration $\bar{a}_E$ by two vector equations:

$$\bar{a}_E = \bar{a}_D + \bar{a}_{ED}^n + \bar{a}_{ED}^\tau;$$

$$\bar{a}_E = \bar{a}_F + \bar{a}_{EF}^n + \bar{a}_{EF}^\tau.$$

We determine the magnitudes of the normal components of relative accelerations:

$$a^n_{ED} = v^2_{ED}/l_{ED} = (1.12 \text{ m/sec})^2/0.18 \text{ m} = 6.97 \approx 7 \text{ m/sec}^2;$$

$$a^n_{EF} = v^2_{EF}/l_{EF} = (2.32 \text{ m/sec})^2/0.1 \text{ m} \approx 53.8 \text{ m/sec}^2.$$

We determine the vector lengths of accelerations $\bar{a}^n_{ED}$ and $\bar{a}^n_{EF}$:

$$dn_{ED} = a^n_{ED}/\mu_a = 7 \text{ m/sec}^2/1 \text{ m/sec}^2 \times \text{mm} = 7 \text{ mm};$$

$$\pi n_{EF} = a^n_{EF}/\mu_a = 53.8 \text{ m/sec}^2/1 \text{ m/sec}^2 \times \text{mm} = 53.8 \text{ mm}.$$

In accordance with the first equation we draw from point d, the terminus of the vector $\overline{\pi d}$, which is already drawn, the vector $\overline{dn_{ED}}$, directing it parallel to ED downwards, since acceleration $\bar{a}^n_{ED}$ is directed in the mechanism from point E to point D, and from the terminus n_{ED} of this vector the line of action of acceleration $\bar{a}^\tau_{ED}$ perpendicular to DE.

In accordance with the second equation we place point f, the vector terminus of acceleration a_F, which is zero, at the pole, and from the pole we draw vector $\overline{\pi n_{EF}}$ and from the point n_{EF} the terminus of this vector, the line of action $\bar{a}^\tau_{EF}$ up to its point of intersection with the line of action $\bar{a}^\tau_{ED}$ at point e.

Joining point e with points d and π, we get vector $\overline{de}$ of acceleration $\bar{a}_{ED}$ and vector $\overline{\pi e}$ of acceleration $\bar{a}_{EF} = \bar{a}_E$.

By means of the plotted acceleration diagram we determine the accelerations of the centres of gravity of the links, which are necessary for determining the forces of inertia:

1) by dividing by point s_1 the vector $\overline{\pi b}$ in relation $\pi s_1/\pi b = l_{AS_1}/l_{AB}$, we get the length of vector $\pi s_1 = 24.65$ mm and acceleration $a_{S_1} = \pi s_1 \times \mu_a = 24.65 \text{ mm} \times$ $\times 1 \text{ m/sec}^2 \times \text{mm} = 24.65 \text{ m/sec}^2$;

2) by dividing by point s_2 the vector $\overline{bc}$ in relation $bs_2/bc = l_{BS_2}/l_{BC}$ and joining point s_2 with the pole, we get the length of vector $\pi s_2 = 30$ mm, and acceleration $a_{S_2} =$ $= \pi s_2 \times \mu_a = 30 \text{ mm} \times 1 \text{ m/sec}^2 \times \text{mm} = 30 \text{ m/sec}^2$;

3) the length of vector $\pi c = 17.5$ mm; therefore acceleration $a_C = \pi c \times \mu_a = 17.5 \text{ mm} \times 1 \text{ m/sec}^2 \times \text{mm} = 17.5 \text{ m/sec}^2$;

4) by dividing by point s_4 the vector $\overline{de}$ in relation $ds_4/de = l_{DS_4}/l_{DE}$ and joining point s_4 with the pole, we get the length of vector $\pi s_4 = 39$ mm, and acceleration $a_{S_4} = \pi s_4 \times \mu_a = 39 \text{ mm} \times 1 \text{ m/sec}^2 \times \text{mm} = 39 \text{ m/sec}^2$;

5) by dividing by point s_5 the vector $\overline{\pi e}$ in relation $\pi s_5/\pi e = l_{FS_5}/l_{FE}$, we get the length of vector $\pi s_5 = 23.6$ mm, and acceleration $a_{S_5} = \pi s_5 \times \mu_a = 23.6 \text{ mm} \times 1 \text{ m/sec}^2 \times \text{mm} = 23.6 \text{ m/sec}^2$.

We get the angular acceleration of link ε_5 (link No. 5) by dividing the tangential acceleration $\bar{a}_E^{\tau}$ of point E by the radius of rotation of this point, i. e. by the length $l_{FE} = 0.1$ m.

The length of vector $n_{EF}e = 25$ mm, acceleration $a_E^{\tau} = n_{EF}e \times \mu_a = 25 \text{ mm} \times 1 \text{ m/sec}^2 \times \text{mm} = 25 \text{ m/sec}^2$. Hence,

$$\varepsilon_5 = 25 \text{ m/sec}^2/0.1 \text{ m} = 250 \text{ sec}^{-2}.$$

The direction of acceleration ε_5 is clockwise; this becomes clear after vector $\overline{\pi n_{EF}}$ is transferred parallel to itself before joining point π with point E in Fig.124, *a*.

3. FORCES OF INERTIA

The masses of the links:

$m_1 = 1.96 \text{ kg}/9.8 \text{ m/sec}^2 = 0.2 \text{ kg} \times \text{sec}^2/\text{m}$;

$m_2 = 5.88 \text{ kg}/9.8 \text{ m/sec}^2 = 0.6 \text{ kg} \times \text{sec}^2/\text{m}$;

$m_3 = 9.8 \text{ kg}/9.8 \text{ m/sec}^2 = 1.0 \text{ kg} \times \text{sec}^2/\text{m}$;

$m_4 = 3.92 \text{ kg}/9.8 \text{ m/sec}^2 = 0.4 \text{ kg} \times \text{sec}^2/\text{m}$;

$m_5 = 2.94 \text{ kg}/9.8 \text{ m/sec}^2 = 0.3 \text{ kg} \times \text{sec}^2/\text{m}$.

The magnitudes of the forces of inertia:

$P_1 = m_1 \times a_{S_1} = 0.2 \text{ kg} \times \text{sec}^2/\text{m} \times 24.65 \text{ m/sec}^2 = 4.93 \text{ kg}$;

$P_2 = m_2 \times a_{S_2} = 0.6 \text{ kg} \times \text{sec}^2/\text{m} \times 30 \text{ m/sec}^2 = 18 \text{ kg}$;

$P_3 = m_3 \times a_C = 1.0 \text{ kg} \times \text{sec}^2/\text{m} \times 17.5 \text{ m/sec}^2 = 17.5 \text{ kg}$;

$P_4 = m_4 \times a_{S_4} = 0.4 \text{ kg} \times \text{sec}^2/\text{m} \times 39 \text{ m/sec}^2 = 15.6 \text{ kg}$;

$P_5 = m_5 \times a_{S_5} = 0.3 \text{ kg} \times \text{sec}^2/\text{m} \times 23.6 \text{ m/sec}^2 = 7 \text{ kg}$.

The following are the lines of action of the forces of inertia and directions along the lines of action.

The line of action of force P_1 coincides with the line of action of acceleration $\bar{a}_B^n$, i. e. with the line AB. The direction of force $\bar{P}_1$ is opposite to that of acceleration $\bar{a}_{S_1}$, i. e. upwards and to the left. The vector $\bar{P}_1$ is not drawn in Fig. 124, *a*.

We consider the compound motion of link BC as translatory motion with acceleration of point B and rotary motion about point B. The line of action of force P_2 in translation passes through the centre of gravity S_2 parallel to vector $\overline{\pi b}$, the acceleration vector $\bar{a}_B$ of the centre of gravity S_2 in translatory motion. The line of action of force $\bar{P}_2''$ in rotary motion about point B passes parallel to vector $\overline{bs_2}$ of acceleration $\bar{a}_{S_2B}$ in this motion through the centre of oscillation O_2, which is located at distance l_{BO_2} from point B, where:

$$l_{BO_2}=l_{BS_2}+\frac{J_2}{m_2\times l_{BS_2}}=l_{BS_2}+\frac{6\times10^{-4}}{0.6\times0.09}=0.09\text{m}+0.011\text{m}=101\text{mm}.$$

Through the point of intersection of the lines of action of forces $\bar{P}_2'$ and $\bar{P}_2''$ there passes the line of action of force $\bar{P}_2$, which is parallel to vector $\overline{\pi s_2}$ of absolute acceleration $\bar{a}_{S_2}$ of the centre of gravity S_2 of link BC. The direction of force $\bar{P}_2$ along the line of action is opposite to that of acceleration $\bar{a}_{S_2}$.

Force $\bar{P}_3$ is directed along the directrix x—x in the opposite direction to that of vector $\overline{\pi c}$ of acceleration $\bar{a}_C$.

We consider the compound motion of link DE as translatory motion with acceleration of point D and rotary motion about point D. We accordingly draw through the centre of gravity S_4 the line of action of force $\bar{P}_4'$ in translation and through the centre of oscillation O_4, which is located at distance l_{DO_4} from point D, where:

$$l_{DO_4}=l_{DS_4}+\frac{J_4}{m_4\times l_{DS_4}}=l_{DS_4}+\frac{5\times10^{-4}}{0.4\times0.09}=$$

$$=0.09\text{ m}+0.014\text{ m}=104\text{ mm},$$

we draw the line of action of force $\bar{P}_4''$ in rotary motion

parallel to vector $\overline{ds}_4$ of acceleration $\bar{a}_{S_4 D}$ of the centre of gravity S_4 in this motion.

From the point of intersection of the lines of action of forces $\bar{P}_4'$ and $\bar{P}_4''$ we draw the vector of force $\bar{P}_4$, directing it parallel and opposite to vector $\overline{\pi s}_4$ of acceleration $\bar{a}_{S_4}$.

Link EF performs rotary motion with variable velocity. The point of application of force $\bar{P}_5$ is the centre of oscillation O_5, which is located at distance l_{FO_5} from point F, where:

$$l_{FO_5} = l_{FS_5} + \frac{J_5}{m_5 \times l_{FS_5}} = l_{FS_5} + \frac{3 \times 10^{-4}}{0.3 \times 0.04} =$$

$$= 0.04 \text{ m} + 0.025 \text{ m} = 65 \text{ mm}.$$

We draw from the centre of oscillation O_5 the vector of force $\bar{P}_5$, directing it parallel to vector $\overline{\pi s}_5$ of acceleration $\bar{a}_{S_5}$ and opposite to it in direction.

4. PRESSURES IN KINEMATIC PAIRS

It is necessary first to determine the pressures in the pairs of the group which has been attached last, the group FED.

The links of this group, in the position, as shown in Fig. 124, *a*, are under the action of forces $\bar{P}_4$, $\bar{P}_5$, $\bar{P}_{65}$ and $\bar{P}_{24}$. After resolving forces $\bar{P}_{65}$ and $\bar{P}_{24}$ into normal and tangential components, we plot the diagram of forces by the vector equation

$$\bar{P}_4 + \bar{P}_5 + \bar{P}_{65}^{\tau} + \bar{P}_{65}^{n} + \bar{P}_{24}^{n} + \bar{P}_{24}^{\tau} = 0.$$

Link EF is under the action of forces $\bar{P}_5$, $\bar{P}_{45}$, $\bar{P}_{65}^{n}$ and $\bar{P}_{65}^{\tau}$. The moments of forces $\bar{P}_{45}$ and $\bar{P}_{65}^{n}$ relative to point E are zero (the lines of action of these forces pass through point E). The moment of force P_5 is equal to $P_5 \times h_5$, where h_5 is the arm of force P_5, which is determined by the drawing and equals 15 mm (Fig. 124, *a*). From the equation of moments

$$P_{65}^{\tau} \times l_{EF} = P_5 \times h_5$$

we get

$$P_{65} = P_5 \times h_5 / l_{EF} = 7 \text{ kg} \times 15 \text{ mm} / 100 \text{ mm} \approx 1 \text{ kg}.$$

Link DE is under the action of forces $\bar{P}_4$, $\bar{P}_{54}$, $\bar{P}^n_{24}$ and $\bar{P}^\tau_{24}$. The moments of forces $\bar{P}_{54}$ and $\bar{P}^n_{24}$ relative to point E are zero (the lines of action of these forces pass through point E). The moment of force P_4 is equal to $P_4 \times h_4$, where h_4 is the arm of this force, which is determined by the drawing and equals 57 mm. From the equation of moments

$$P^\tau_{24} \times l_{DE} = P_4 \times h_4$$

we get

$$P^\tau_{24} = P_4 h_4 / l_{DE} = 15.6 \text{ kg} \times 57 \text{ mm} / 180 \text{ mm} \approx 5 \text{ kg}.$$

Choosing the scale $\mu_P = 0.5$ kg/mm, we determine the vector lengths of the forces:

$$\bar{P}_4 = 15.6 \text{ kg} / 0.5 \text{ kg/mm} = 31.2 \text{ mm};$$

$$\bar{P}_5 = 7 \text{ kg} / 0.5 \text{ kg/mm} = 14 \text{ mm};$$

$$\bar{P}^\tau_{65} = 1 \text{ kg} / 0.5 \text{ kg/mm} = 2 \text{ mm};$$

$$\bar{P}^\tau_{24} = 5 \text{ kg} / 0.5 \text{ kg/mm} = 10 \text{ mm}.$$

We draw in succession (Fig. 124, *d*) the vectors of forces $\bar{P}_4$ and $\bar{P}_5$, then vector $\bar{P}^\tau_{65}$ perpendicular to FE upwards and to the right and from its terminus the line of action of force $\bar{P}^n_{65}$ parallel to FE. To the origin of vector $\bar{P}_4$ we join the vector of force $\bar{P}^\tau_{24}$ and from its origin we draw the line of action of force $\bar{P}^n_{24}$ up to its point of intersection with the line of action of force $\bar{P}^n_{65}$. After joining the point of intersection of the lines of action with the terminus of vector $\bar{P}_5$ and the origin of vector $\bar{P}_4$, we get the diagram of forces which corresponds to the vector equation

$$\bar{P}_4 + \bar{P}_5 + \bar{P}_{65} + \bar{P}_{24} = 0.$$

After measuring the vector lengths, we get

pressure in pair F $P_{65} = 41$ mm $\times 0.5$ kg/mm $= 20.5$ kg;

pressure in pair D $P_{24} = 10$ mm $\times 0.5$ kg/mm $= 5$ kg.

Pressure in pair E can be determined by the diagram of forces which has been plotted for link DE or link FE. Link FE is under the action of forces P_5, P_{65} and P_{45}. The

vectors of the first two of these forces in Fig. 124, *d* are already drawn; after joining the terminus of vector $\bar{P}_{65}$ with the origin of vector $\bar{P}_5$, we get the vector of force $\bar{P}_{45}$. After measuring the length of this vector, we get

pressure in pair E $P_{45}=28$ mm$\times 0.5$ kg/mm$=14$ kg.

The group BCC_x is under the action of forces $\bar{P}_2$, $\bar{P}_{42}$, $\bar{P}_3$, $\bar{P}_{63}$ and $\bar{P}_{12}$. After resolving the last of these into normal and tangential components, we plot the diagram of forces by the vector equation

$$\bar{P}_2+\bar{P}_{42}+\bar{P}_3+\bar{P}_{63}+\bar{P}^n_{12}+\bar{P}^\tau_{12}=0.$$

Link BC is under the action of forces $\bar{P}_2$, $\bar{P}_{42}$, $\bar{P}_{32}$, $\bar{P}^n_{12}$ and $\bar{P}^\tau_{12}$. Since the moments of forces $\bar{P}_{32}$ and $\bar{P}^n_{12}$ relative to point C are zero (the lines of action of these forces pass through point C), the equation of moments relative to point C will be

$$P^\tau_{12}\, l_{BC}=P_2h_2+P_{42}h_{42},$$

where $h_2=85$ mm is the arm of force P_2, which is determined by the drawing, and $h_{42}=42.5$ mm is the arm of force P_{42} (Fig. 124, *a*). From this equation we get

$$P^\tau_{12}\,\frac{P_2h_2+P_{42}h_{42}}{l_{BC}}=\frac{18\text{ kg}\times 85\text{ mm}+5\text{ kg}\times 42.5\text{ mm}}{180\text{ mm}}=9.7\text{ kg}.$$

Choosing the scale $\mu_P=1$ kg/mm, we determine the vector lengths of the forces:

$$\bar{P}_2=18\text{ kg}/1\text{ kg/mm}=18\text{ mm};$$

$$\bar{P}_{42}=5\text{ kg}/1\text{ kg/mm}=5\text{ mm};$$

$$\bar{P}_3=17.5\text{ kg}/1\text{ kg/mm}=17.5\text{ mm};$$

$$\bar{P}^\tau_{12}=9.7\text{ kg}/1\text{ kg/mm}=9.7\text{ mm}.$$

We draw in succession (Fig. 124, *e*) the vectors $\bar{P}_2$, $\bar{P}_{42}$, $\bar{P}_3$ and from the terminus of the last one the line of action of force P_{63}. After joining to the origin of vector $\bar{P}_2$ the vector $\bar{P}^\tau_{12}$, which is directed perpendicular to BC and to the right, we draw from its origin the line of action of force $\bar{P}^n_{12}$ up to its point of intersection with the line of

action of force $\bar{P}_{63}$. Having joined the point of intersection of the lines of action with the origin of vector $\bar{P}_2$, we get the diagram of forces which corresponds to the vector equation

$$\bar{P}_2+\bar{P}_{42}+\bar{P}_3+\bar{P}_{63}+\bar{P}_{12}=0.$$

After measuring the lengths of vectors P_{12} and P_{63}, we get:

pressure in pair B $P_{12}=27$ mm$\times 1$ kg/mm$=27$ kg;

pressure in the sliding pair $P_{63}=13$ mm$\times 1$ kg/mm$=$ $=13$ kg.

Pressure in pair C is determined from the diagram of forces for link BC, which was plotted by the vector equation

$$\bar{P}_{12}+\bar{P}_2+\bar{P}_{42}+\bar{P}_{32}=0.$$

The first three vectors in Fig. 124, *e* are already drawn. By joining the terminus of vector P_{42} with the origin of vector P_{12}, we get the vector of force P_{32}. After measuring the length of this vector we get:

pressure in pair C $P_{32}=22$ mm$\times 1$ kg/mm$=22$ kg.

Pressure in pair A we determine from the diagram of forces for the crank, which is plotted by the vector equation

$$\bar{P}_{21}+\bar{P}_1+\bar{P}_{61}=0.$$

The magnitude and direction of force $\bar{P}_1$ have already been determined. Force $\bar{P}_{21}$ is equal in magnitude to force P_{12} and is opposite to it in direction. By drawing the vectors of these forces to the scale $\mu_P=1$ kg/mm (Fig. 124, *f*) and measuring the length of vector $\bar{P}_{61}$, which closes the triangle of forces, we get:

pressure in pair A $P_{61}=34$ mm$\times 1$ kg/mm$=34$ kg.

Chapter VII

FRICTION IN KINEMATIC PAIRS

30. KINDS OF FRICTION

Friction always takes place when any given bodies— solids, fluids or gases, — which are in contact with each other, move relative to each other or are under the action of forces that strive to bring about their relative motion. In the subsequent discussion we shall consider only friction on the surfaces of contacting solids.

Experience shows that in the relative motion of two contacting solid bodies, pressed against each other by a certain force, a resisting force to the relative motion acts on the contact surfaces. This force is called the force of friction.

During relative motion of two contacting solid bodies both the sliding and rolling of one body on the other may take place. As a result either sliding friction or rolling friction develops, or both kinds of friction occur simultaneously.

Experience also shows that the force of sliding friction decreases when the contacting surfaces of solids are lubricated with a liquid. If the lubricant separates fully the surfaces of the bodies, the friction is called liquid friction; when there is no lubricant the friction is called dry friction. When the lubricant does not fully separate the body surfaces the friction is called semifluid or semidry, depending on which kind of friction is predominant.

31. SLIDING FRICTION OF UNLUBRICATED BODIES

A. The Direction and Magnitude of the Force of Friction. Coefficient of Friction

Experience shows that the force of friction on the contact surface of two solid bodies is always directed against the side which is opposite to the relative velocity

of motion or, when both bodies are in a state of rest, against the side opposite to the force striving to move one of the contacting bodies.

The many factors on which the magnitude of the force of friction depends present great difficulties in their calculation. In many cases with an accuracy sufficient for practical purposes, Coulomb's formula may be used to determine the magnitude of the force of friction.

$$F = fQ, \tag{6}$$

where F is the force of friction, Q is the normal force to the contact surface by which body *1* is pressed to body *2* (Fig. 125), and f is the proportion factor, which is called the coefficient of sliding friction.

Thus, if body *1* moves relative to body *2* with a certain velocity v_{12}, this motion is resisted by the force of friction F, which is directed against the side opposite from velocity v_{12}, and is determined by formula (6).

Experience shows that with the very same bodies *1* and *2*, with the same force Q and with the other conditions identical the force of friction F_0, which has to be overcome in order to move one of the bodies that is in a state of rest relative to the other, is greater than that force of friction F which resists body *1* in its motion relative to body *2*. It is therefore necessary, in determining the force of friction by the formula given above, to take into consideration the difference between the magnitudes of the coefficient of sliding friction f and the coefficient of friction of rest f_0.

Since the force of friction is a reactive force, magnitude Qf_0 of the force of friction of rest which is determined by formula (6) is the maximum possible, able to resist force P that strives to move one of the contacting bodies relative to the other, but when $P < Qf_0$, the force of friction is exactly equal to force P.

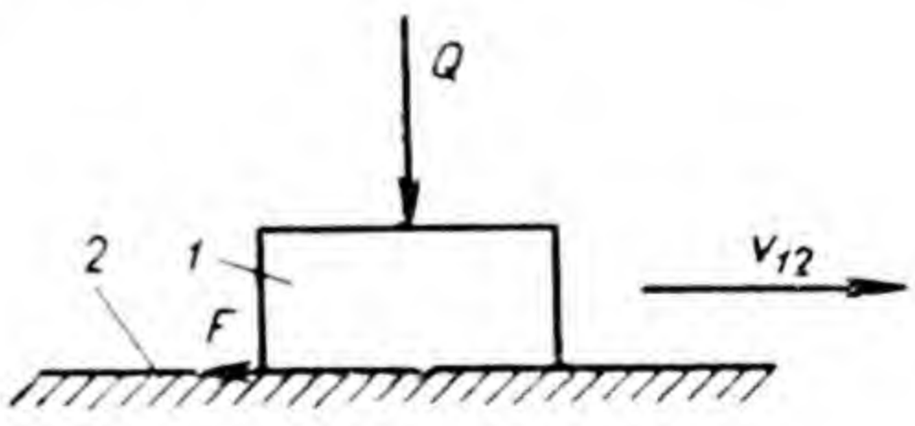

Fig. 125

The coefficient of sliding friction is a dimensionless magnitude which is quoted in engineering reference books in other cases of a particular nature, where only the materials of friction bodies and the finish of their contacting surfaces are taken into account. In using the reference

magnitude of the coefficient of friction and determining the magnitude of the force of friction by the formula given above, we assume that the magnitude of the coefficient of friction depends only on the material and the surface finish, and not on the sliding speed, nor on the specific pressure, nor on the time during which sliding takes place. It should be remembered that this assumption is only approximately correct and only within the limits of sliding speeds, specific pressures and sliding duration used by Coulomb during the experiments which produced the above formula. The following were the limits within which Coulomb carried out experiments in 1785, and which Moran verified in 1834: sliding speed — from 0.3 to 3 m/sec, and pressure on the surface of contact — not more than 10 kg/cm^2. This has to be taken into consideration since in modern engineering we frequently deal with much greater speeds and pressures on friction surfaces. Sliding duration was not considered at all in Coulomb's experiments.

The experiments, which have been carried out by various researchers since Coulomb's and Moran's experiments, have shown that beyond the mentioned limits the magnitude of the coefficient of friction changes considerably as a result of the sliding speed and the pressure on the friction surface and because of sliding duration. For example, it was shown that by increasing the sliding speed from 2.13 to 26.8 m/sec the magnitude of the coefficient of friction decreased almost sixfold, and at the very same speed it decreased almost threefold after 25 seconds from the beginning of the experiment.

The above should be considered when determining the magnitudes of the forces of friction in technical calculations, which are based on the utilization of reference data concerning the magnitudes of the coefficients of friction.

B. Angle of Friction and Friction Cone

If body *1* (Fig. 126) is pressed to body *2* by force Q_{12}, then in the absence of the frictional force reaction Q_{21}, from the side of body *2* to body *1* is directed along the normal to the surface of contact. In the presence of frictional force F reaction R is the resultant of normal reaction Q_{21} and the force of friction F. Angle φ, through which the

resultant R deflects from the normal reaction Q_{21}, is called the angle of friction.

From Fig. 126 follows that

$$\tan \varphi = \frac{F}{Q_{21}}.$$

Therefore, in accordance with equation (6) we get

$$\tan \varphi = f, \tag{7}$$

i. e. the coefficient of friction is equal to the tangent of the angle of friction.

Thus, the angle of friction is the angle between the normal reaction and the resultant force of friction and the normal reaction or, in other words, the angle whose tangent is equal to the coefficient of friction.

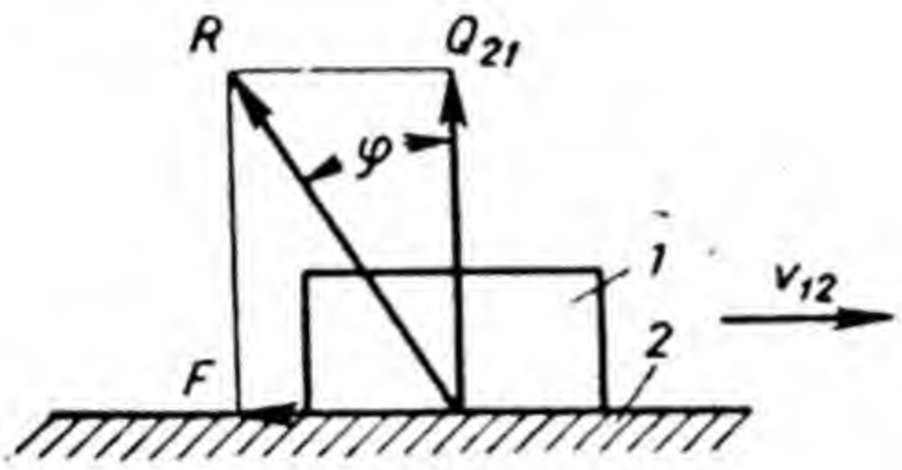

Fig. 126

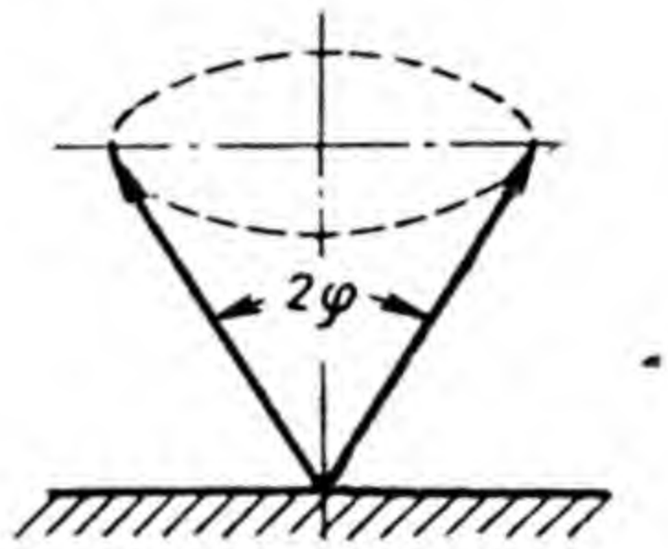

Fig. 127

During motion of body *1* in different directions on the plane resultant R of reactions will deflect from normal reaction Q_{21} at angle φ to the side, which is opposite to the relative velocity of motion, always remaining on the surface of the cone with angle 2φ at the apex which is formed by the rotation of resultant R about the normal reaction (Fig. 127). This cone is called the friction cone.

In other words, a friction cone is a surface circumscribed by the resultant of the force of friction and the normal reaction at its rotation about the normal reaction or, a cone with an angle at the apex equal to the double angle of friction.

C. Friction on the Horizontal Plane

The motion of a body on the plane can be examined under the action of one force only, since in all cases a number of forces that act on the body can be reduced to one resultant.

Let us assume that force Q acts on the body (Fig. 128) at angle λ to the perpendicular to the plane of contact.

We will transfer force Q to the point of its intersection of the vector with the perpendicular to the plane of contact and resolve it along two perpendicular directions respective to each other. The normal component Q^n, pressing the body to the plane, creates the reacting force of friction of rest F_0 to the body motion; the tangential component Q^τ strives to move the body.

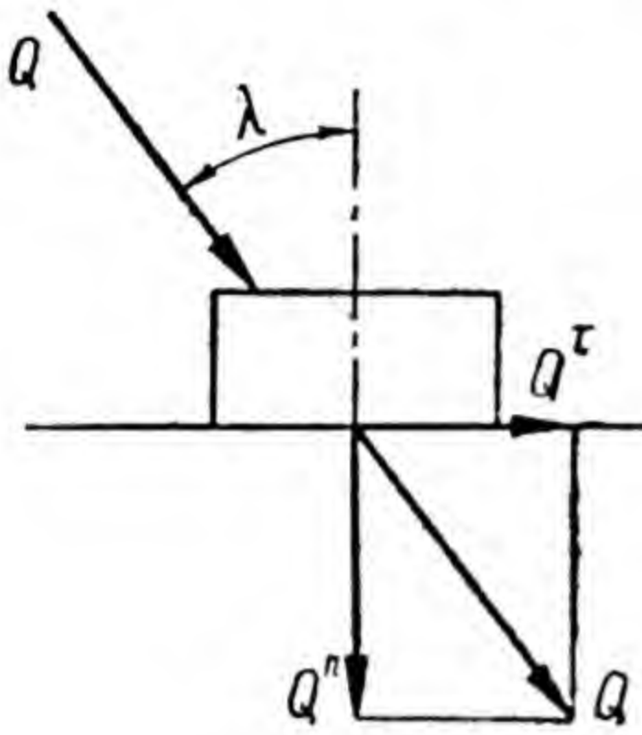

Fig. 128

To produce motion it is necessary to observe the following condition:

$$Q^\tau > F_0.$$

Since

$$Q^\tau = Q \sin \lambda,$$

$$F_0 = f_0 Q^n = f_0 Q \cos \lambda,$$

where f_0 is the coefficient of friction of rest, then

$$Q \sin \lambda > f_0 Q \cos \lambda,$$

whence

$$\tan \lambda > f_0$$

or on the basis of formula (7)

$$\tan \lambda > \tan \varphi_0;$$

$$\lambda > \varphi_0,$$

where φ_0 is the angle of friction of rest.

It follows from this that regardless of its magnitude the force acting inside the friction cone cannot move the body.

By substituting in the above inequalities F for F_0, f and φ for f_0 and φ_0, and by replacing in all inequalities the sign $>$ by sign $\geqslant$, we find that motion of the body on the horizontal plane is possible only by observing the condition, where $\lambda \geqslant \varphi$.

Where $\lambda = \varphi$, we obtain $Q^\tau = F$ and motion with constant velocity;

where $\lambda > \varphi$, we obtain $Q^\tau > F$ and motion with acceleration.

Where $\lambda < \varphi_0$, the development of motion as previously shown is impossible; where $\lambda < \varphi$, the motion of the body, brought about by certain forces and continuing by inertia, will be retarded under the action of force Q, since in this case the force of friction created by force Q^n and counteracting motion will be greater than force Q^τ sustaining motion.

From what has been previously said it follows that the problems, concerning the possibility of developing the motion of one of the contacting bodies relative to the other and concerning the possibility of motion with constant velocity or acceleration, are solved identically, with the single difference that in one case we have to take into consideration the coefficient f_0 and angle φ_0 of friction of rest, and in the other, the coefficient f and angle φ of sliding friction.

D. Friction on the Inclined Plane

Let us first examine a case where on the body located on the plane inclined at angle λ to the horizon acts one force which is perpendicular to the plane base (Fig. 129), for instance, the force of weight.

In this case motion is possible only downwards.

The angle between the vector Q and the perpendicular to the plane is equal to the angle λ of inclination of the plane.

In accordance with what we have said above concerning the possibility of motion it is necessary to observe the condition

$$\lambda \geqslant \varphi.$$

Where $\lambda < \varphi$ under the action of the force, which is perpendicular to the plane base, motion, regardless of the force magnitude, cannot develop nor continue without delay.

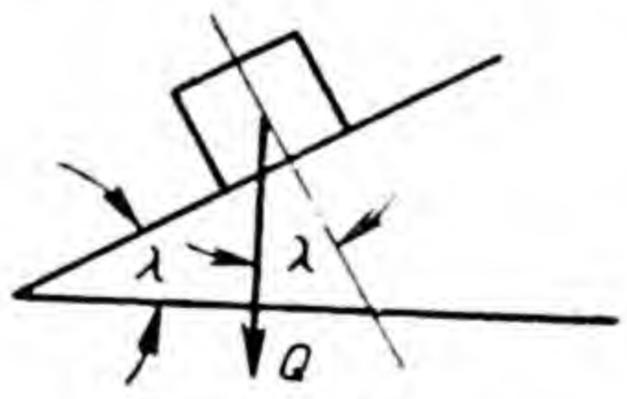

Fig. 129

A plane with an angle of inclination smaller than the angle of friction is called s e l f - b r e a k i n g. The self-breaking effect is very widely used in different devices in engineering. Let us now examine a case where two forces act on a body, which is located on the plane inclined at λ to the horizon; one of these forces is perpendicular and the other is parallel

to the plane base. In this case the body can move in both directions. Let us find the conditions for the possibility of motion in each of the two directions.

a) **Motion of the body upwards on the inclined plane** (Fig. 130). In this case force P, which is parallel to the plane base, must be directed to the right. For the possibility of moving upwards on the plane it is necessary for resultant R of forces P and Q to form angle β with a perpendicular to the plane not smaller than the angle φ of friction, i. e. it is essential to observe the condition

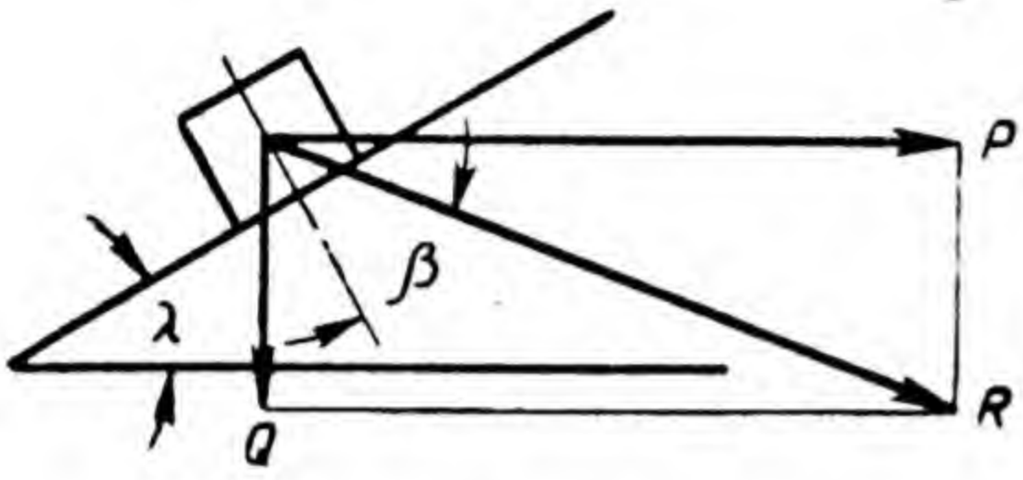

Fig. 130

$$\beta \geqslant \varphi.$$

From the construction follows

$$P = Q \tan (\lambda + \beta).$$

From the above inequality and equality follows the condition for the possibility of body motion upwards on the inclined plane:

$$P \geqslant Q \tan (\lambda + \varphi). \qquad (8)$$

b) **Motion of the body downwards on the inclined plane** (Fig. 131). In this case resultant R from the construction equals

$$P = Q \tan (\lambda - \beta)$$

and, hence, the motion downwards on the inclined plane is possible at $\beta \geqslant \varphi$ by observing the condition

$$P \leqslant Q \tan (\lambda - \varphi). \qquad (9)$$

In Fig. 131 the force P is directed to the right and is therefore a force which counteracts the motion. The force P directed to the left (Fig. 132) will be required for moving the body downwards only in the case where motion will not take place under the action of only one force Q, i. e. in the case of $\lambda \leqslant \varphi$.

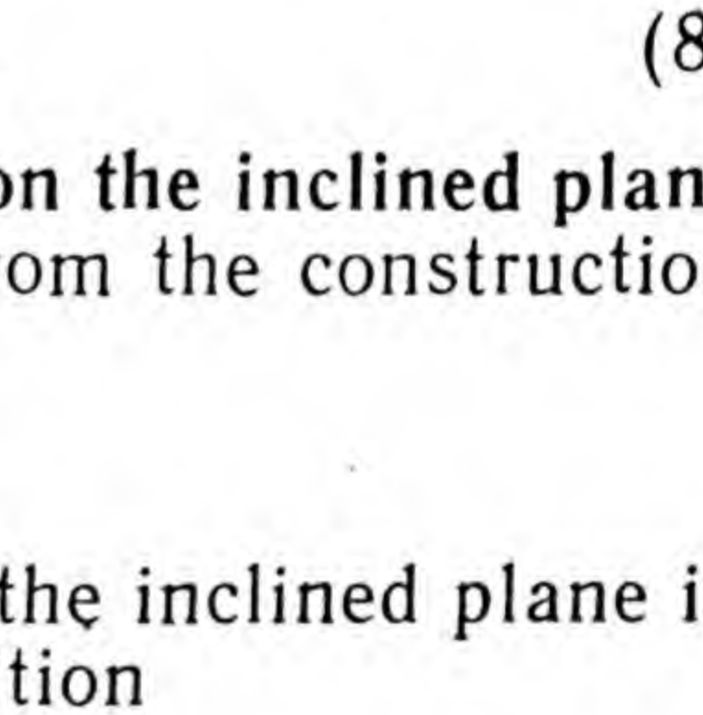

Fig. 131

From the construction (Fig. 132) we get

$$P = Q \tan (\beta - \lambda).$$

Where $\beta \geqslant \varphi$ and the direction of force P indicated in Fig. 132, the required magnitude of force P must satisfy the condition

$$P \geqslant Q \tan (\varphi - \lambda). \qquad (10)$$

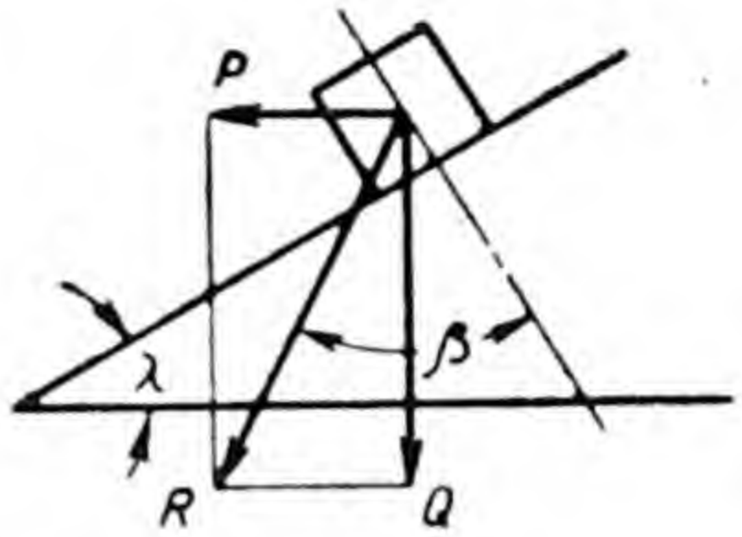

Fig. 132

E. Friction of V-Shaped Slider

In all previous cases we assumed that the force, which presses the body to the plane of friction, is directed perpendicular to this plane. In these cases, in accordance with equation (6) we obtained the magnitude of the force of friction by multiplying the force pressing the body to the plane by the coefficient of friction.

Fig. 133 shows a V-shaped slider in cross section shaped like a trapezium and pressed by force Q to two friction surfaces, each of which is inclined to the line of action of force Q at angle γ. During motion of the V-shaped slider in the direction which is perpendicular to the drawing plane the magnitude of the force of friction in accordance with formula (6) will equal

$$F = 2Nf,$$

where N is the force which is perpendicular to the plane of friction.

Knowing that the sum of the projections of forces to the vertical is zero, we obtain

$$2N = \frac{Q}{\sin \gamma}.$$

By introducing the designation $\frac{f}{\sin \gamma} = f'$, we obtain

$$F = Qf', \qquad (11)$$

where magnitude f' is called the imaginary or reduced coefficient of friction.

In technical calculations we have to deal with the imaginary coefficient of friction as well as with the im-

aginary angle of friction φ', which is determined from the equation $\tan\varphi'=f'$, in cases where the force which presses one body to the other is not directed by the normal to the surface of friction. Since $f'>f$, then in cases where it is desirable to obtain a possibly greater force of friction, at a definite force to press one body to another, the friction surfaces are sometimes not arranged at right

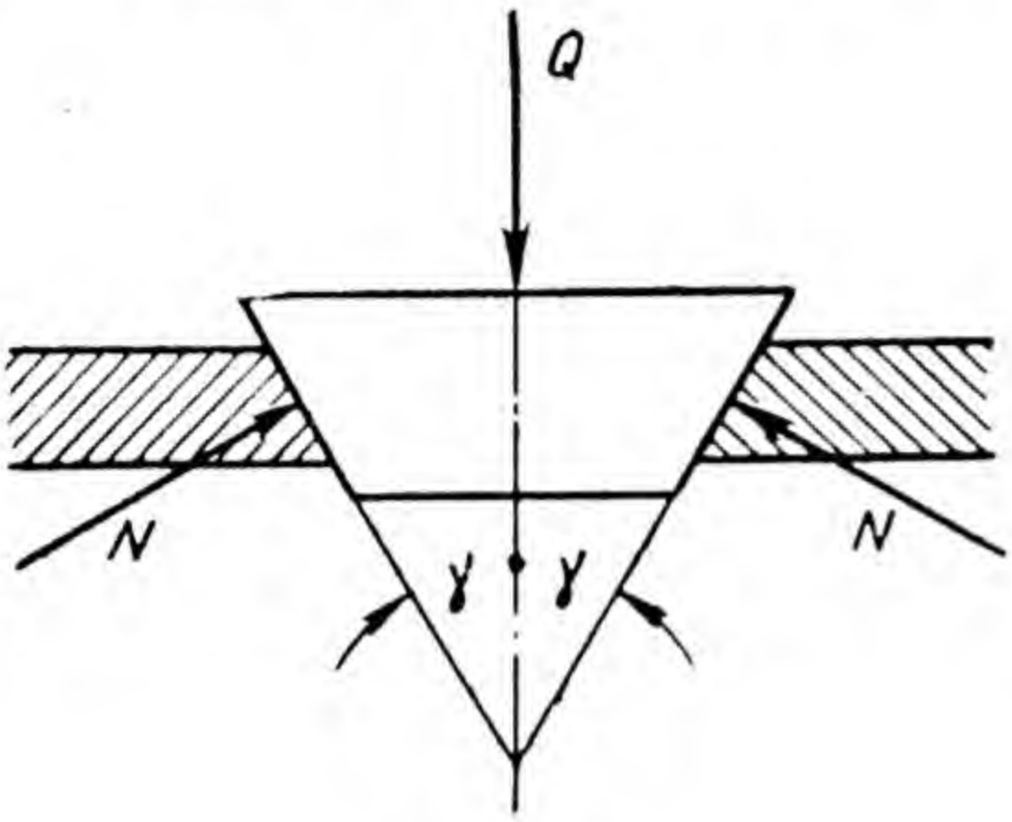

Fig. 133

Fig. 134

angles to the line of action of the pressing force. For example, in order to reduce the force which presses one of the friction wheels to the other, the wheel rims are sometimes made V-grooved (Fig. 134). We shall deal with another example in the following paragraph.

If instead of a V-shaped slider, which moves in the direction perpendicular to the drawing plane, we imagine a solid frustum (Fig. 133), which is pressed by force Q to the inner surface of the hollow frustum, then the magnitude of the force of friction, counteracting the rotation of the solid cone in the hollow one, will also have to be determined by equation (11).

F. Friction in Screws

In determining the magnitude of the force of friction on the contact surface of a screw and nut it is assumed that the developed helical surface of the screw is an inclined plane with the nut as a load on the inclined plane, or, on the contrary, that the inclined plane is the developed helical surface of the nut and the screw is the load on this inclined plane.

In making this assumption it is necessary to bear in mind that the developed helical surface is not in fact an inclined plane with a definite angle of inclination. We

shall get the helical surface by moving segment AB of the straight line (Fig. 135) with point A along the helix and maintaining it during this motion normal to the cylinder surface or, what is the same thing, perpendicular to the cylinder axis. During one turn about the cylinder axis, when segment AB will pass into position A_1B_1, all points of the segment will displace along the cylinder axis by the same pitch t, but all the points will pass the paths along the cylinders with different diameters: one end point A of the segment will pass along the cylinder with diameter d_1, the other end point B, along the cylinder with diameter d, which is not shown in Fig. 135. The lead angle λ_A, along which point A will pass, will be equal to $\lambda_A = \arctan\frac{t}{nd_1}$, lead angle λ_B, along which point B will pass, will be equal to $\lambda_B = \arctan\frac{t}{\pi d}$. Since $d_1 < d$, then $\lambda_A > \lambda_B$.

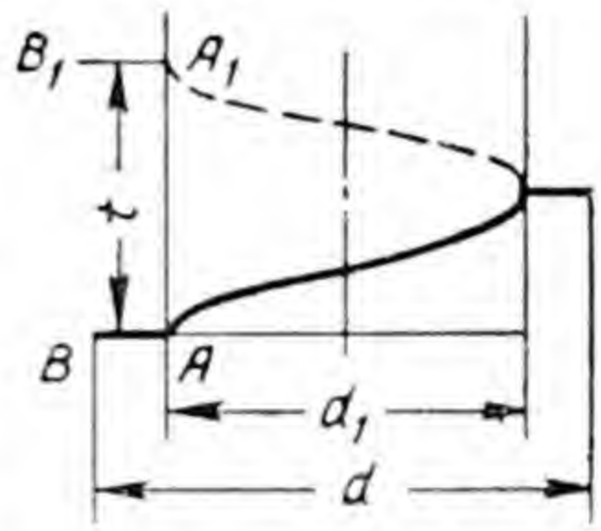

Fig. 135

Assuming that the developed helical surface is an inclined plane with one definite angle of inclination, angle λ_A or λ_B, we will allow for an inaccuracy which will be of no practical significance, if the length of segment AB is small by comparison with the diameter d_1 or d, which is the usual case in machine building. We shall allow for an even less important inaccuracy, if we assume that the developed helical surface is an inclined plane with the angle of inclination equal to the lead angle on the mean diameter, i. e. to the angle which is determined by the equation

$$\tan\lambda = \frac{t}{\pi\frac{d_1+d}{2}}.$$

The screw thread can be imagined in the motion of points A and A_1 of the thread profile as rectangle ABB_1A_1 (Fig. 136) or triangle ABA_1 (Fig. 137) along the helices, which are located on the cylinder with diameter d_1; during such motion segment AA_1 must remain all the time parallel to the cylinder axis. Practically the screw thread is, of course, obtained by removing the material from the cylinder with diameter d with the help of a cutting tool. In

similar manner we can imagine the formation and practical production of a nut thread.

If we imagine the contacting surfaces of a screw and nut and one of the links of the screw pair as an inclined plane, we can assume the other link as a point load on this plane, proceeding from the fact that according to formula (6) the force of friction does not depend on the magnitude of the contact surface. In this way we can use formulae (8), (9) and (10), which establish the relations between forces P and Q that act on the body located on the inclined plane. In applying these formulae to a screw pair, angle λ in these formulae will be the lead angle on the mean diameter, force Q, the force which is directed along the pair axis, and force P, the force which is directed along the tangent to the circle of a radius equal to the mean radius of the thread. If r is the mean radius of the thread and M is the moment, which rotates the moving link of the screw pair (screw or nut), then $P = \frac{M}{r}$.

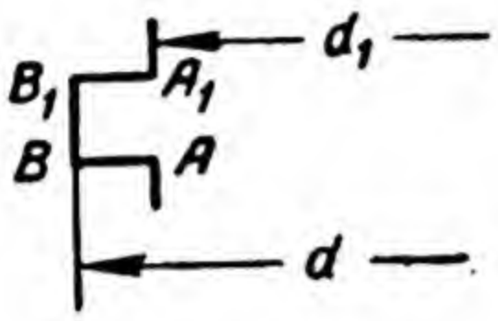

Fig. 136

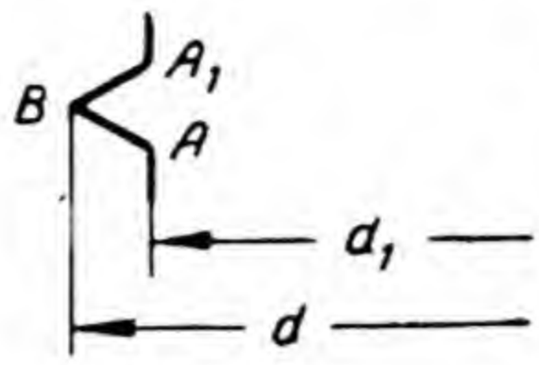

Fig. 137

For example, if P_0 is the force which is applied to the spanner by the operator when screwing the nut on or off (Fig. 138), and l is the distance from the point of application of force P_0 to the axis of the screw pair, then $P = P_0 \frac{l}{r}$.

The above formulae can be used to determine the forces P and Q only in screws with square thread (Fig. 139). By resolving the axial load Q (on an inclined plane the force which is perpendicular to the plane base, see Fig. 140), we get the component, that presses the links of the screw pair against each other, which equals $Q \cos \lambda$. In a square thread this force is normal to the friction surface (Fig. 141) and therefore generates a force of friction which equals $fQ \cos \lambda$. In an oblique-angled thread (Fig. 142) force

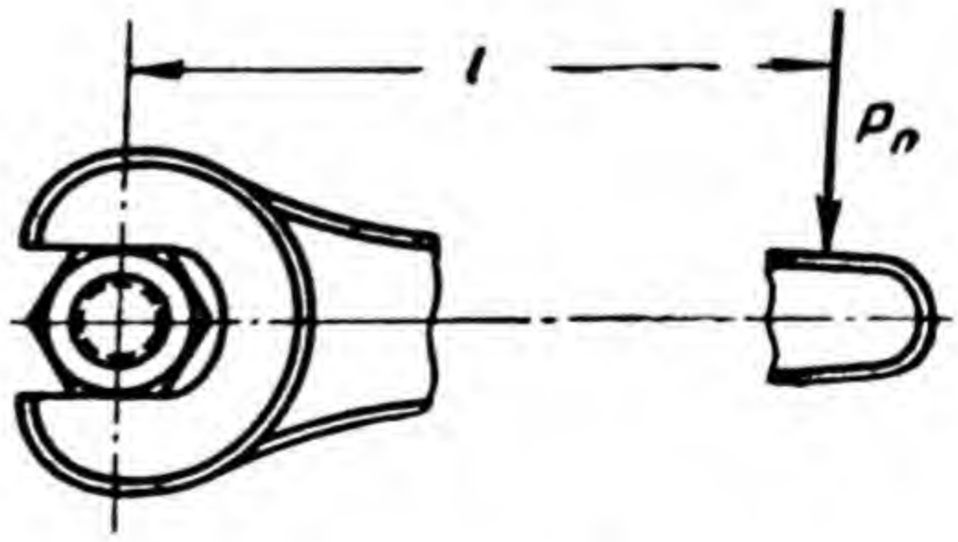

Fig. 138

$Q \cos \lambda$ is not normal to the friction surface (Fig. 143), and therefore in determining the magnitude of the force of friction which is generated by this force, the force $Q \cos \lambda$ should be multiplied by the imaginary coefficient of friction f', which equals $f' = \frac{f}{\cos \beta}$, where β is the half angle at the profile apex of the oblique-angled thread. Therefore, in applying formulae (8), (9) and (10) to screws with oblique-angled thread the angle φ of friction, which is a

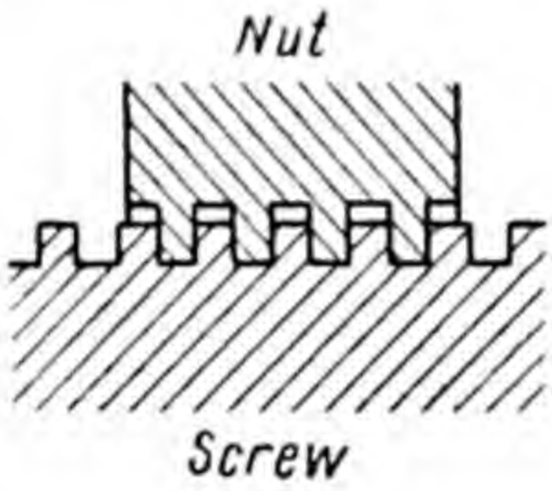

Fig. 139

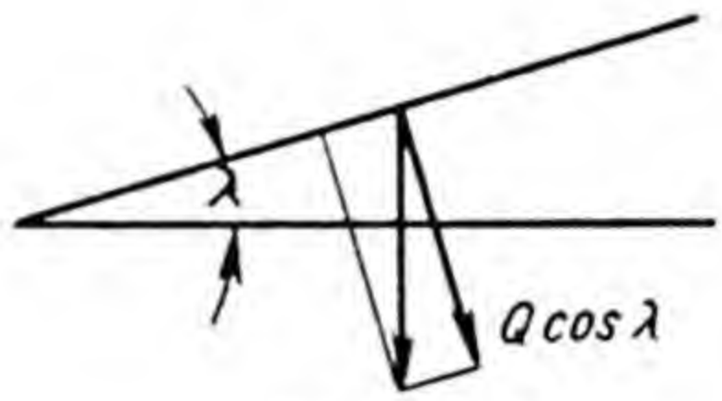

Fig. 140

part of the formulae, should be replaced by the imaginary angle of friction φ'.

Since the force of friction is greater in a screw with oblique-angled thread than in a screw with square thread when all other conditions are equal, it is advisable to use an oblique-angled thread in fasteners (bolts, studs, screws), where it is desirable to have a possibly greater force of

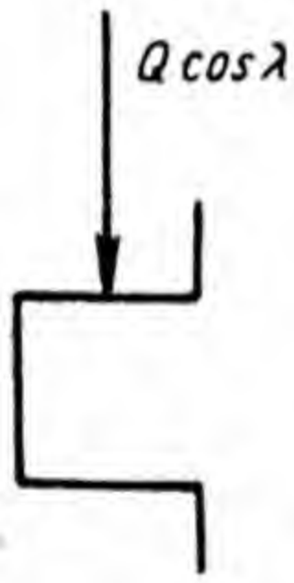

Fig. 141

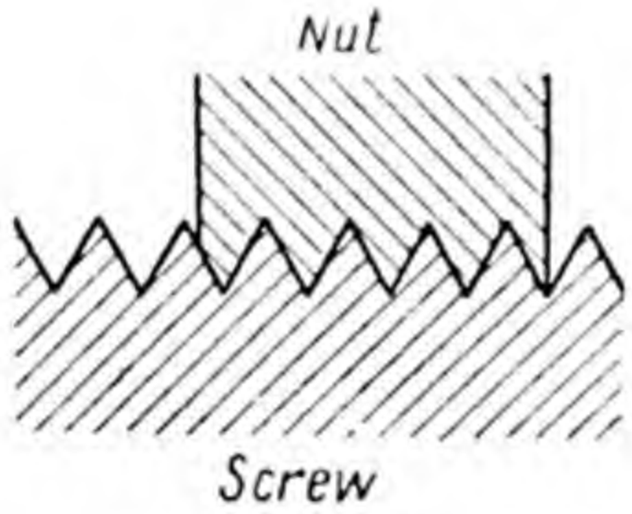

Fig. 142

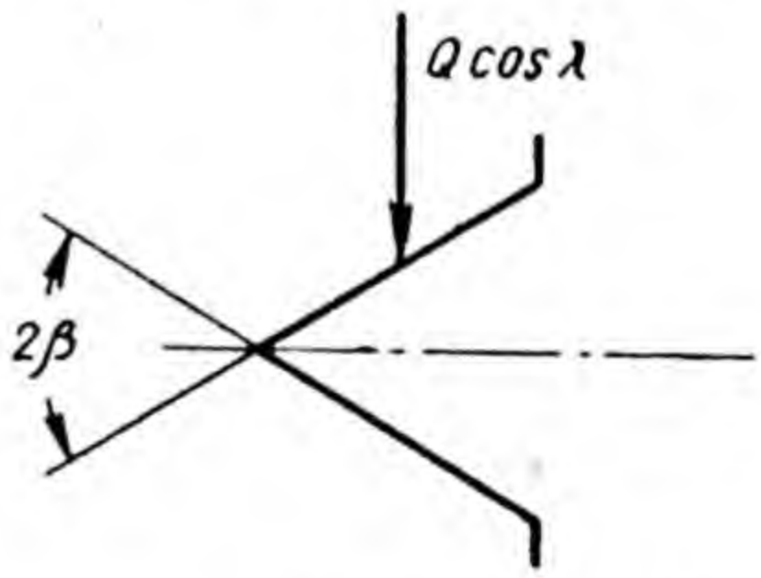

Fig. 143

friction, and square thread for screws which are intended for the transmission of motion.

For screw fasteners the thread, as specified by the USSR Standard, has a profile in the shape of an equilateral triangle. Owing to practical considerations, instead of a square thread for screws transmitting motion, the Standard specifies a thread with trapezoidal profile (Fig. 144) with

a 30° angle at the profile apex. The increase of the force of friction in a trapezoidal thread is insignificant compared with a square thread, since the cosine of the half angle at the profile apex is near unity (cos 15°=0.966), and therefore the difference between coefficients f' and f is also insignificant ($f' \approx 1.03\, f$).

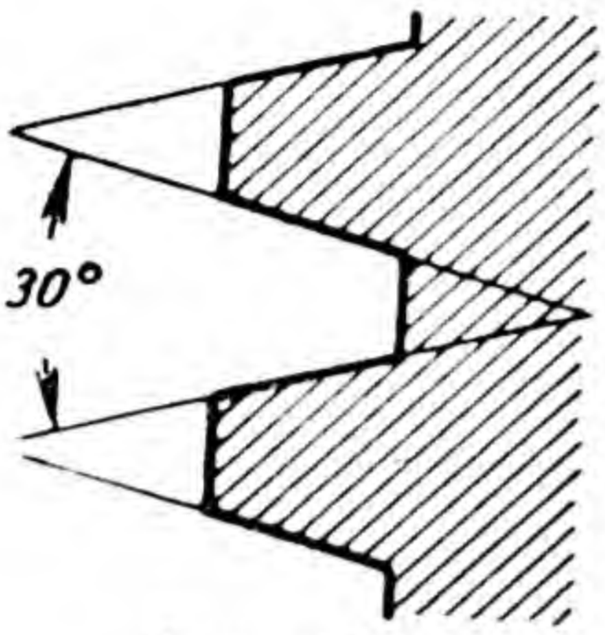

Fig. 144

In a metric thread, the name used for the standard thread for fasteners, the angle at the profile apex is 60°, hence

$$f' = \frac{f}{\cos 30^\circ} = 1.15\, f.$$

In screw fasteners the thread must certainly be self-breaking, as otherwise these elements could not serve their purpose.

Let us find, by using formulae (8), (9) and (10), how to solve the problem of the magnitudes of the forces that act on a bolt and nut when mounting the bolt.

In joining elements A and B with a bolt (Fig. 145, a) the bolt is inserted into the holes of these elements, and then a nut is screwed on the upper threaded portion of the bolt. Until the nut reaches element A the thread of the stationary bolt resembles an inclined plane, which is turned onto a cylinder, and the nut, a load on this plane displaced in the position of the bolt, as shown in Fig. 145, a, from the top downwards. Left in any position, for instance, as shown in Fig. 145, a the nut does not displace downwards under the action of its own weight because the triangular thread of the bolt is self-breaking, i. e. it satisfies the condition $\lambda < \varphi'$. In order to bring the lower surface ab of the nut into contact with the upper surface cd of element A it is necessary to turn the nut by torque Pr, where r is the mean radius of the thread, P is the force

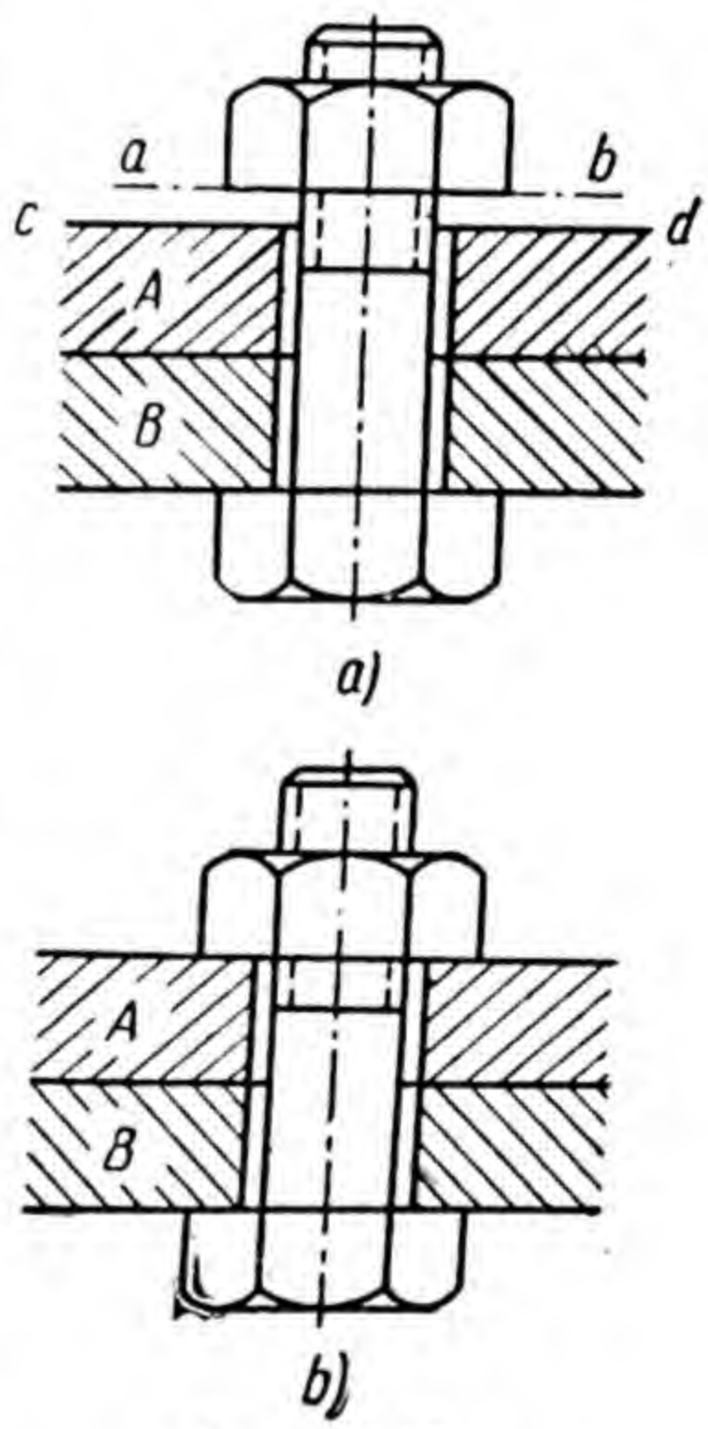

Fig. 145

which is reduced to the mean radius and determined by formula (10), in which the angle φ of friction is replaced by imaginary angle φ′ of friction, and force Q is the insignificant weight of the nut. The small torque, which is required for moving the nut to element A, is usually provided by the operator's fingers.

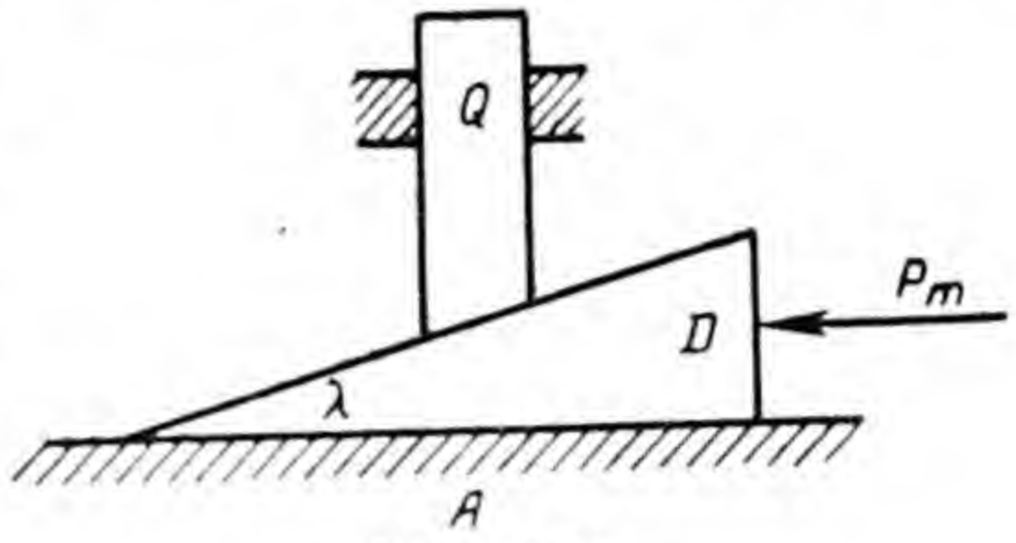

Fig. 146

When the nut lower surface has reached the upper surface of element A, a much greater torque is required in the subsequent turning of the nut to tighten the bolt. As it turns, the nut must displace along the bolt, as shown in Fig. 145, *b*, downwards, but this is prevented by element A into which the nut already presses. In turning and remaining in contact with element A the nut could move downwards relative to the bolt, if the bolt were able to move upwards, but element B into which the bolt thrusts with the head prevents that. Further rotation of the nut is still possible at a certain angle, which is certainly performed in the mounting of the bolt. During such rotation the nut, pressing with its lower surface against element A and acting with the fillets of its thread on the thread of the bolt, stretches the bolt increasing its length a little. At this stage the functions of the bolt and nut change: the nut becomes, as it were, an inclined plane, and the bolt becomes the load which is displaced upwards along the inclined plane.

When the bolt is stretched what happens is essentially the same as would happen in the device, shown in Fig. 146, if load Q (analogous to the bolt), which can displace only vertically, were to be displaced by element D (analogous to the nut).

Acting with certain force P_m, which is directed in Fig. 146 from right to left, we can lift load Q (in Fig. 145, *b* to stretch the bolt by force Q), shifting at the same time the load relative to element D from left to right (similar to the rotation relative to the bolt in Fig. 145, *b*).

In Fig. 146 force P_m must overcome the resistance of load Q and the friction forces on the inclined plane and, in addition, the force of friction on the horizontal plane of

contacting parts A and D. The required force for moving load Q relative to element D to the right should be determined by formula (8): the force of friction on the plane of contact of elements A and D equals Qf (the weight of element D is not taken into consideration). Therefore

$$P_m = Q \tan (\lambda + \varphi) + Qf,$$

where φ is the angle of friction on the inclined plane and f is the coefficient of friction on the horizontal plane.

Similar to this the torque, created by the operator, which acts during tightening of the bolt on the spanner end with force P_0 (see Fig. 138), must overcome the moment $P_r = Qr \tan (\lambda + \varphi')$, where P_r is the force on the mean radius of the thread, and Q is the force which stretches the bolt, and also the moment QfR of the force of friction on the contact plane of the nut and element A, where R is the radius of the circle, onto which it may be assumed the resultant of the elementary forces of friction is applied (determination of magnitude R see below in item "H").

The bolt which is fastened with a spanner remains in stretched position in a state of tension, since with the self-breaking thread under the action of axial force the bolt cannot turn in the nut and return to its initial position.

In dismounting the joint it is necessary to turn the nut by torque

$$M > Qr \tan (\varphi_0' - \lambda) + Qf_0R_1,$$

where φ is the imaginary angle of friction of rest in the thread and f_0 is the coefficient of friction of rest between the nut and element A.

G. Friction in Turning Pairs

A turning kinematic pair is formed by the journal (the supporting portion of the shaft) and the bearing enveloping it.

In order that the journal, which is under the action of a number of forces applied to it, may rotate it is necessary to have the resultant Q of these forces (Fig. 147) create a moment which is not less than the moment of the force of friction.

By resolving force Q into components, normal Q^n and tangential Q^τ and denoting by r the arm of force Q relative to the axis of rotation of the journal, by R the journal radius and by λ the angle between the line of action of force Q and the radius, which is drawn to the point of application of force Q, we find:

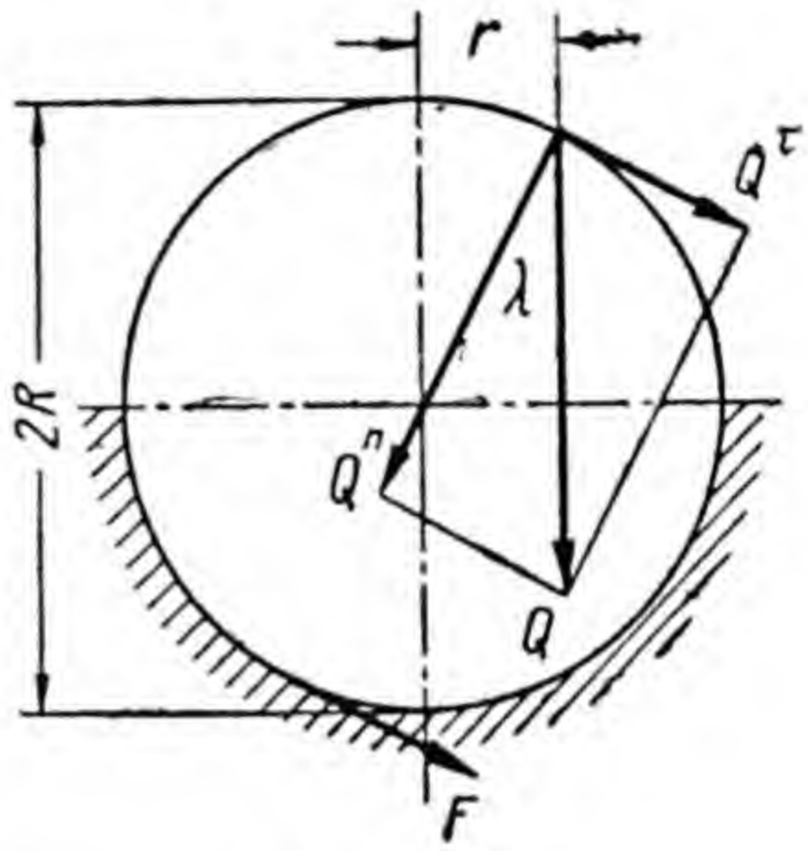

Fig. 147

the moment that rotates the journal to equal

$$Q^\tau R = QR \sin \lambda;$$

the moment of the force of friction F to equal

$$FR = fQ^n R = QRf \cos \lambda = QR \tan \varphi \cos \lambda.$$

For the possibility of rotation it is necessary to observe the condition

$$QR \sin \lambda \geqslant QR \tan \varphi \cos \lambda,$$

whence

$$\tan \lambda \geqslant \tan \varphi; \ \lambda \geqslant \varphi,$$

and therefore

$$r = R \sin \lambda \geqslant R \sin \varphi.$$

Hence, the moment of force Q cannot rotate the journal, if the line of action of force Q passes inside the circle of radius $R \sin \varphi$.

This circle is called the circle of friction.

H. Friction in Pivots

Friction in pivots takes place on the contact surface of two bodies that are pressed to each other, rotating relative to each other about the normal to the surface of contact (Fig. 148).

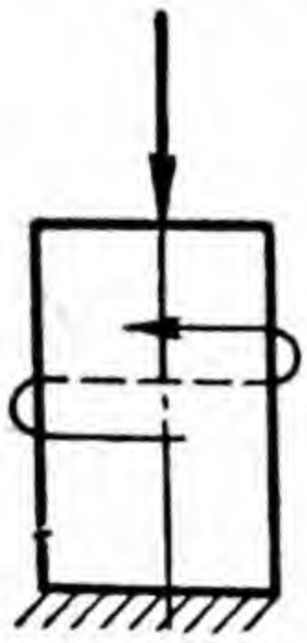
Fig. 148

In considering the resistance of the forces of friction to the moment which rotates one body relative to the other, we have to determine the resultant moment of frictional forces, replacing the elementary forces of friction on the entire surface of friction by a resultant force, which is applied on the circle of radius R. Let us determine the magnitude of radius R, assuming that

the friction surface is a circular area with external radius r_1 and internal radius r_2 and that rotation takes place about a common centre of circles with these radii (Fig. 149).

The total force of sliding friction equals

$$pf\pi(r_1^2-r_2^2),$$

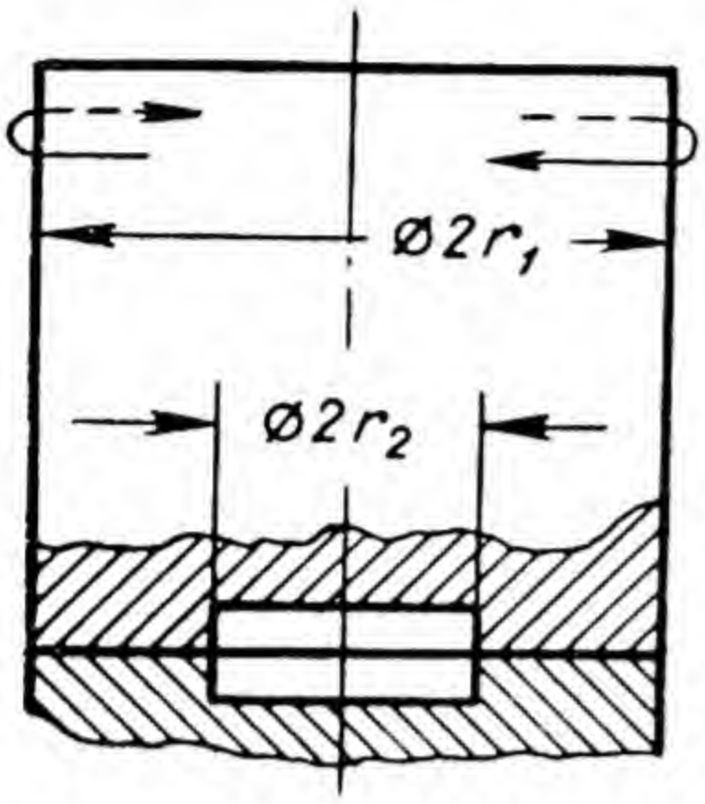

Fig. 149

where p is the pressure on the friction surface, i. e. the force per unit of the friction surface, and $\pi(r_1^2-r_2^2)$ is the magnitude of the friction surface.

The elementary force of friction, which is distributed along the circle with area $2\pi\, rdr$, equals

$$pf2\pi\, rdr.$$

The moment of the total frictional force

$$pf\pi(r_1^2-r_2^2)R,$$

where R is the radius of the circle onto which the resultant of the elementary forces of friction is applied.

The same moment can also be expressed in the following way:

$$\int_{r_2}^{r_1} pf2\pi\, r^2dr = 2pf\pi\int_{r_2}^{r_1} r^2\,dr.$$

By equating and reducing to $pf\pi$, we get equation:

$$(r_1^2-r_2^2)R = 2\int_{r_2}^{r_1} r^2\,dr,$$

$$(r_1^2-r_2^2)R = \frac{2}{3}(r_1^3-r_2^3),$$

whence

$$R=\frac{2}{3}\times\frac{r_1^3-r_2^3}{r_1^2-r_2^2}=\frac{2}{3}\times\frac{r_1^2+r_1r_2+r_2^2}{r_1+r_2}.$$

Where $r_2=0$ we obtain

$$R=\frac{2}{3}r_1.$$

32. SLIDING FRICTION OF LUBRICATED BODIES

If the surfaces of friction bodies are fully separated by a lubricant film, then friction, as was pointed out previously, is called liquid friction. Resistance to relative motion with liquid friction is dependent on factors different from those determining the frictional force with dry friction.

The resistance to relative motion occurs on unlubricated surfaces of frictional bodies primarily because of some minute unevenness on the surface of one of the frictional bodies, imperceptible to the naked eye, and shown in an extremely enlarged form in Fig. 150, is retained by similarly minute unevenness on the surface of the other body. This is substantiated by the fact that, other conditions being equal, the force of friction decreases when the friction surfaces are more carefully finished.

However, the decrease of the force of friction is not widely determined by the increase of the finishing accuracy of the surfaces; for if we leave all other conditions unchanged, and proceed to surfaces which have been more and more carefully processed we will find that after reaching a certain limit of processing accuracy the force of friction will begin to increase. This is explained by the fact that with very close contact of surfaces the forces of molecular adhesion begin to have a noticeable effect. For example, carefully polished surfaces of two bodies with the degree of unevenness not exceeding a two-thousandth of a millimetre (the surfaces of plates which are used for checking the limit gauges are processed this way) are attracted to one another with a force of about 125 g/cm².

In the presence of a liquid film between the surfaces of two bodies moving relative to each other the influence of the above-mentioned factors, roughness of surfaces and molecular adhesion are eliminated, and resistance to relative motion depends on friction only inside the liquid film.

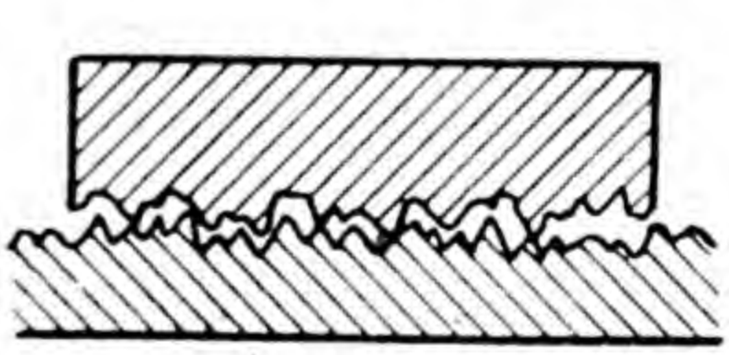

Fig. 150

In this case the finest films of liquid adhere to the surfaces of bodies which displace relative to each other and move relative to the adhering films of liquid, entraining and partly moving ahead of them.

Determination of the forces of friction in the case of liquid friction is based on Newton's law for viscous fluids, according to which

$$F = \frac{\eta \times Sv}{h},$$

where F is the force of friction in kg;
η is the viscosity factor of liquid in kg×sec/m²;
S is the surface of friction in m²;
v is the relative velocity of motion in m/sec;
h is the thickness of the liquid film in m.

If we determine the force of friction in a liquid film by Coulomb's formula (6), coefficient of friction f has to be determined by the formula

$$f = \frac{\eta_1 v}{hp},$$

which is obtained from Newton's equation after substitutions:

$$F = Qf \text{ and } \frac{Q}{S} = p.$$

In Coulomb's formula it is assumed that the coefficient of dry friction does not depend on the sliding speed; however as we said previously, it was subsequently ascertained by later researchers that at speeds which exceed those that were applied in Coulomb's experiments the coefficient of friction decreases considerably. The coefficient of liquid friction, on the contrary, increases in proportion to the sliding speed.

The complex phenomena, which take place in a lubricant film, were first studied by the founder of the hydraulic theory of friction N. P. Petrov, professor of the St. Petersburg Technological Institute, in his remarkable work *Friction in Machines and the Effect of Lubricating Liquid,* published in 1883.

In the majority of cases on the lubricated surfaces of bodies, which move relative to each other, a process takes place not of liquid friction, but of semifluid or semidry friction. For this process no theoretical substantiated formulae have so far been established, and therefore the determination of the forces of friction in such cases is performed by Coulomb's formula at greatly reduced coef-

ficients of friction by comparison with those which have to be accepted for the process of dry friction. Thus, for example, the coefficient of friction of steel on bronze at dry friction can be taken to equal about 0.18, and at the process of semidry friction depending on various circumstances its value varies from 0.02 to 0.08.

33. FRICTION OF FLEXIBLE BODIES

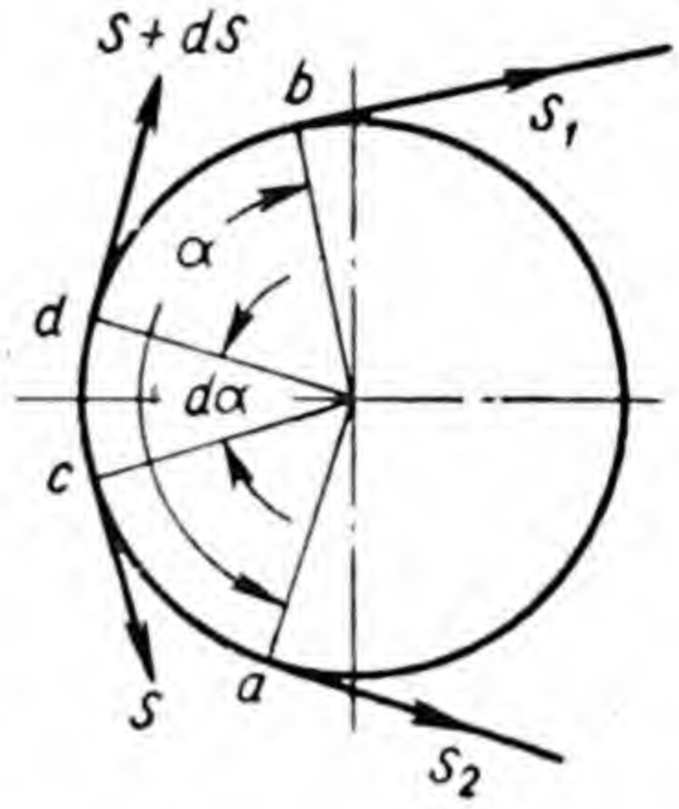

Fig. 151

If a perfectly flexible and non-stretchable body, i. e. a body which does not undergo any deformation under the action of the tensile force and does not show any resistance at its flexure, envelops a fixed cylinder, embracing it along arc ab with centre angle α (Fig. 151), and is under the action of forces S_1 and S_2 then for its motion along the cylinder with constant velocity it is necessary to observe the condition

$$S_1 = S_2 + F,$$

where F is the force of friction between the flexible body and the cylinder.

Since the force of friction is distributed on the arc ab of contact of the flexible body with the cylinder, tension of the flexible body from point a of its moving onto the cylinder to point b of running off from the cylinder increases by a known law from S_2 to S_1. At point c of infinitely small arc cd the tension reaches a certain magnitude S, at point d the tension increases to $S+dS$.

The infinitely small force on arc cd, which determines the increase of tension to value dS and is therefore equal to dS, can be expressed as follows:

$$dS = f dN,$$

where f is the coefficient of friction and dN is the infinitely small force, which is normal to the friction surface.

The magnitude of force dN is created by projections

of tensions S and $S+dS$ on the radius, which is drawn at the centre of arc cd:

$$dN=S\sin\frac{d\alpha}{2}+(S+dS)\sin\frac{d\alpha}{2}=$$

$$=2S\sin\frac{d\alpha}{2}+dS\sin\frac{d\alpha}{2}.$$

Since $\sin d\alpha=d\alpha$ and $dS\sin\frac{d\alpha}{2}=0$, as the member of the higher order of smallness, then

$$dN=Sd\alpha;$$
$$dS=fdN=fSd\alpha.$$

After dividing the variables, we obtain

$$\frac{dS}{S}=fd\alpha.$$

By integration and then involution, we obtain

$$\int_{S_2}^{S_1}\frac{dS}{S}=\int_0^{\alpha}fd\alpha.$$

$$\int_{S_2}^{S_1}d\ln S=f\int_0^{\alpha}d\alpha;$$

$$\ln\frac{S_1}{S_2}=f\alpha;$$

$$S_1=S_2e^{f\alpha}.$$

This relation between force S_1, which moves the perfectly flexible and nonstretchable body that envelops the cylinder, and force S_2, which is resistant to motion, has been established by the outstanding scientist L. Euler, a member of the Russian Academy of Sciences.

According to Euler's formula the force of friction on the contact surface of a flexible body and the cylinder enveloped by it is

$$F=S_1-S_2=S_2(e^{f\alpha}-1).$$

As can be seen from the formula, the magnitude of the force of friction depends largely also on the coefficient of friction and on the angle of contact; it can be easily seen, by making corresponding substitutions in Euler's formula, that at $f=0.35$, when the flexible body has been wound around the cylinder by four complete turns ($\alpha=8\pi$), we can balance the force of 6500 kg with the force of 1 kg.

In the calculation of a belt drive we deal approximately with the following magnitudes: $f\approx0.35$; $\alpha=\pi$. At these magnitudes the tension of the driving portion of the belt, which imparts rotation to the driven pulley, is approximately three times greater than the tension of the driven portion. However, in calculating a belt drive, Euler's formula cannot be used without important empirical corrections. The necessity for such corrections arises, firstly, from the fact that the belt is not a perfectly flexible and nonstretchable body, and, secondly, from the fact that during rotation of the pulley the belt is subjected to the action of centrifugal force, which reduces the belt pressure on the pulley and, consequently, reduces the force of friction.

34. ROLLING FRICTION

During the rolling of a cylinder or ball a continuous rotation of the rolling body takes place on the rolling surface. If we assume that the rolling body is in contact

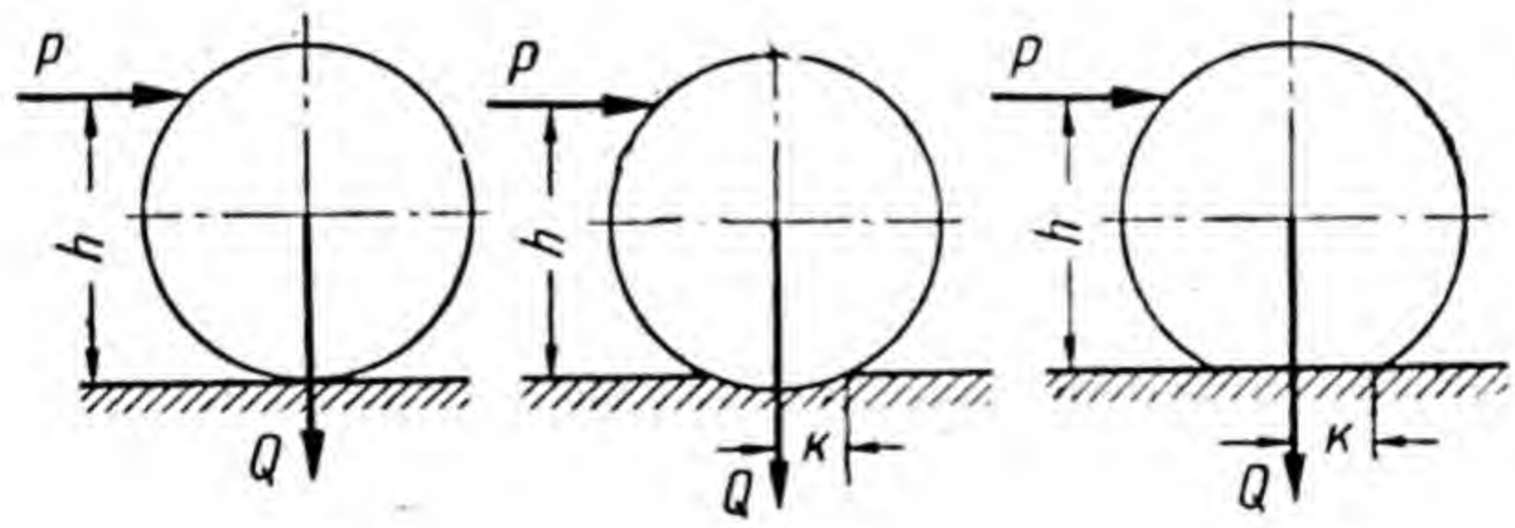

Fig. 152

with the rolling surface in line (in the case of a cylinder) or at point (in case of a ball) and assume thereby that the line of action of the force, which presses the rolling body to the rolling surface, passes through the line or point of contact, we arrive at the conclusion that in

such case no resistance to rolling takes place; the moment of force Q (Fig. 152, a), which presses the rolling body to the rolling surface, is zero, and, therefore, the moment of force P, which effects continuous rotation of the body, meets with no resistance. Nevertheless experience shows that there is resistance to rolling.

Resistance to rolling develops because the bodies, which are pressed to each other even by insignificant force, are becoming deformed and contact in deformed condition not in line or at point, but at a certain surface which is adjoining the line or point. During the deformation of the surface under the rolling body (Fig. 152, b), and during the deformation of the rolling body (Fig. 152, c), and, consequently, during the simultaneous deformation of both the body and surface the line or point, near to which rotation occurs, departs at certain distance k from the line of action of force Q. As a result of this develops arm k of force Q and moment Qk, which counteracts the rotating moment Ph.

During rolling with constant velocity this obvious relation takes place

$$Ph = Qk,$$

where k is the magnitude characterizing the conditions at which rolling takes place; it is called **the coefficient of rolling friction**. As distinct from the coefficient of sliding friction the coefficient of rolling friction is a magnitude with linear dimension.

The rolling phenomenon is observed because of the presence of sliding friction: rolling of one body on another can take place only when the resistance to sliding exceeds the resistance to rolling.

In order to make a body roll on the plane it is necessary to apply a force to the body, which equals

$$P_r = Q\,\frac{k}{h},$$

and for sliding it is necessary to apply a force, which equals

$$P_s = Qf.$$

If $\frac{k}{h} < f$ and, hence, $P_r < P_s$, the body will roll without sliding, otherwise the body will slide without rolling. When

$\frac{k}{h}=f$ there will be an identical possibility for rolling and sliding.

Since in replacing sliding friction by rolling friction the force of friction decreases and in the majority of cases considerably so, it is expedient during the shifting of loads on the plane to place rollers, such as cylindrical rods or sections of pipes, under the loads. This is frequently done.

In shifting a load of weight Q on rollers of radii R (Fig. 153) the forces of rolling friction between the load and rollers and between the rollers and the plane are being overcome. In this case force P acting on the load is applied to the rollers at their points of contact with the load and creates the moment $P2R$, which rotates the rollers. Resistance to rolling is effected by the moments $\frac{Q}{n}k_1$ and $\left(\frac{Q}{n}+G\right)k_2$,

where G is the roller weight;

n is the number of rollers;

k_2 and k_1 are the coefficients of rolling friction between the rollers and the plane and between the rollers and the load respectively.

During motion with constant velocity, we obtain

$$2PR=n\frac{Q}{n}k_1+n\left(\frac{Q}{n}+G\right)k_2=Qk_1+(Q+nG)k_2.$$

Where $k_1=k_2=k$, discounting the weight of rollers, we obtain

$$P=Q\frac{k}{R}.$$

Since the rollers relative to the load move to the side opposite to the direction of load motion, it becomes necessary repeatedly to replace the rollers, which are left behind as the load moves forward. This makes it inconvenient to transfer a load on rollers at a large distance or at a high speed.

During the transportation of a load on wheels (Fig. 154), the wheels are entrained by the loaded truck body, but since the wheels rotate on axles

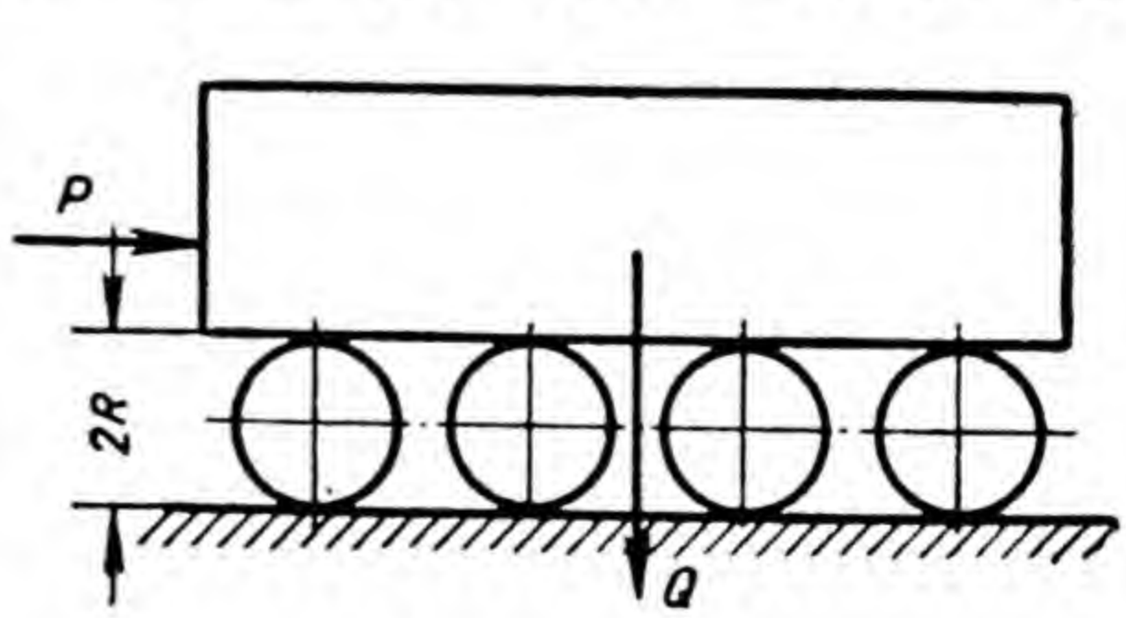

Fig. 153

which are connected to the load, then besides the forces of rolling friction between the wheels and plane during the motion of the load the force of sliding friction between the wheels and axles on which the wheels rotate is also overcome.

During the movement of a load with constant velocity the moment PR of force P, which should be considered as applied at distance R from the plane along the line of action which is parallel to the plane, is being counteracted by: 1) moment of the force of rolling friction $(Q+G)k$, where G is the total weight of the wheels, and 2) moment of the force of sliding friction frQ, where r is the radius of the wheel axles. We therefore obtain

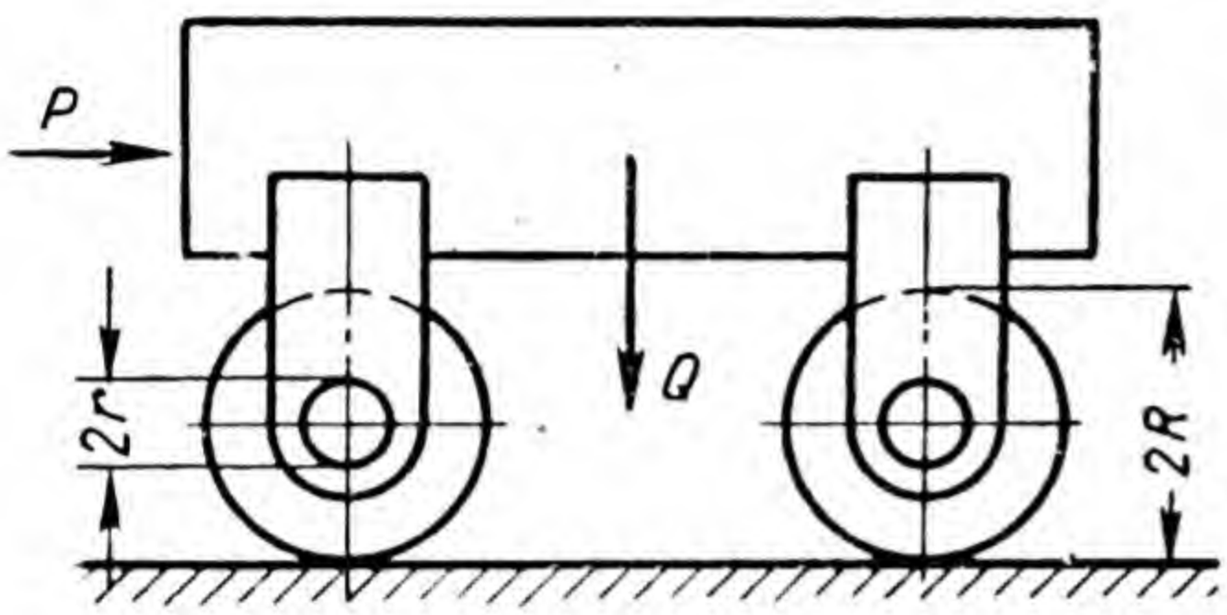

Fig. 154

$$PR=(Q+G)k+frQ,$$

whence

$$P=\frac{(Q+G)k+frQ}{R};$$

discounting the wheel weight, we obtain

$$P=Q\frac{k+fr}{R}=Qk_0,$$

where dimensionless magnitude k_0 is called the pull factor.

The desirability of replacing sliding friction by rolling friction in bearings of shafts and axles led to the creation of various designs of antifriction bearings, which are widely used in modern engineering.

We proceed to the sliding bearing from load J, which slides along plane P (Fig. 155); by giving the friction surfaces of the load and plane cylindrical forms (Fig. 156), instead of the load we obtain a bearing surface of a shaft or axle, i. e. journal J, and instead of the plane we obtain surface P of the sliding bearing. An antifriction bearing can be obtained in similar manner from load J which moves

on rollers R on plane P (Fig. 157), in this case also giving the bearing surfaces cylindrical shapes (Fig. 158). Since the coefficient of rolling friction is less the harder the materials of the rolling bodies (in bearings the balls or rollers) and elements, on the surface of which rolling takes place, for this and other reasons the antifriction bearings are manufactured from hard materials in the shape

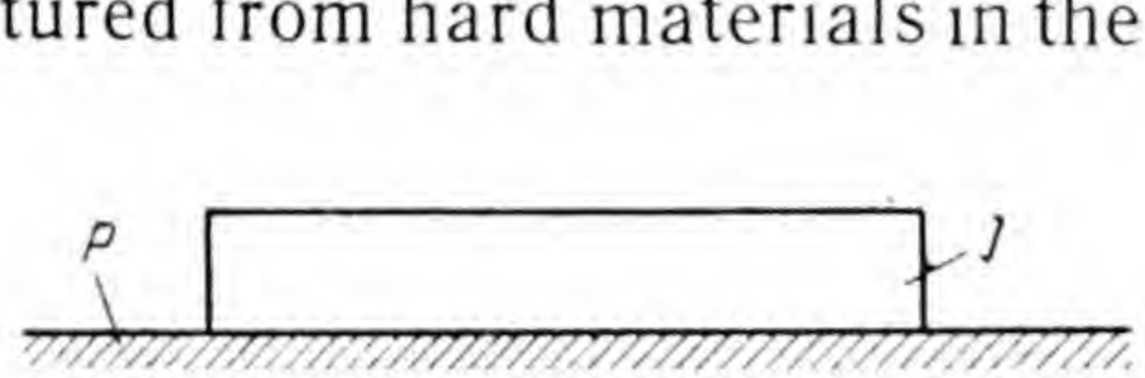

Fig. 155

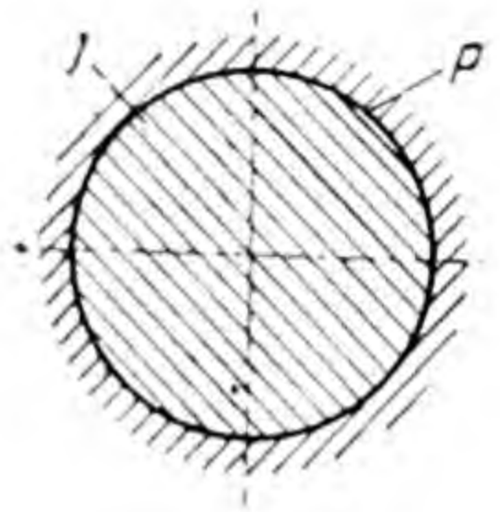

Fig. 156

of two rings with balls or rollers in between. In order to maintain the distances between the rolling bodies during their rolling on the ring surfaces invariable, in modern bearings the rolling bodies are separated from each other by means of special elements, known as cages.

In the USSR antifriction bearings are manufactured in large and mechanized plants and are produced on a mass scale. A great variety of types, designs and sizes of antifriction bearings is standardized.

Fig. 159 shows a standard design of a radial bearing, i. e. a bearing which is designed for absorbing loads in the radial direction; these bearings can absorb loads also in the axial direction, approximately 1.5 times less than

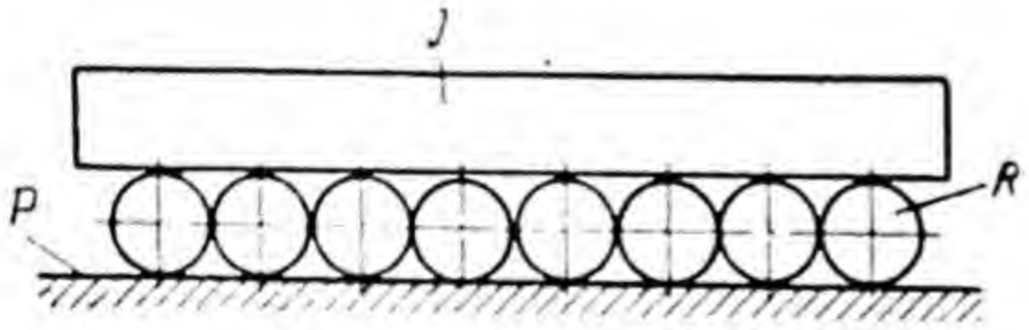

Fig. 157

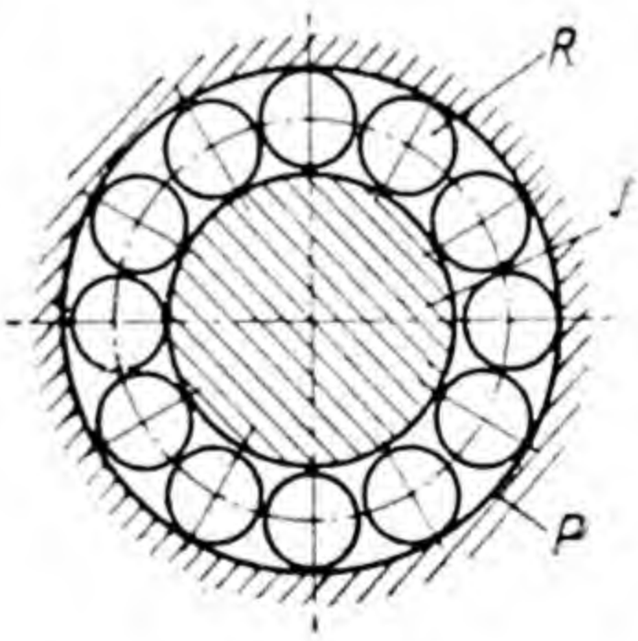

Fig. 158

the radial. Fig. 160 shows one of the standard designs of a thrust bearing, i. e. a bearing which is designed for absorbing loads in the axial direction; these bearings are completely unsuitable for absorbing radial loads. In Figs. 159 and 160 the cages are marked by letter C.

The coefficient of rolling friction in antifriction bearings amounts to about one micron.

Example 1. The bar, which slides in guides A and B (Fig. 161) located at distance l from each other, is under the action of force P applied at distance l from guide A at angle α to the bar axis. The coefficient of friction of rest between the bar and guides is $f_0=0.2$. Determine the maximum angle α at which motion of the bar in the guides can develop.

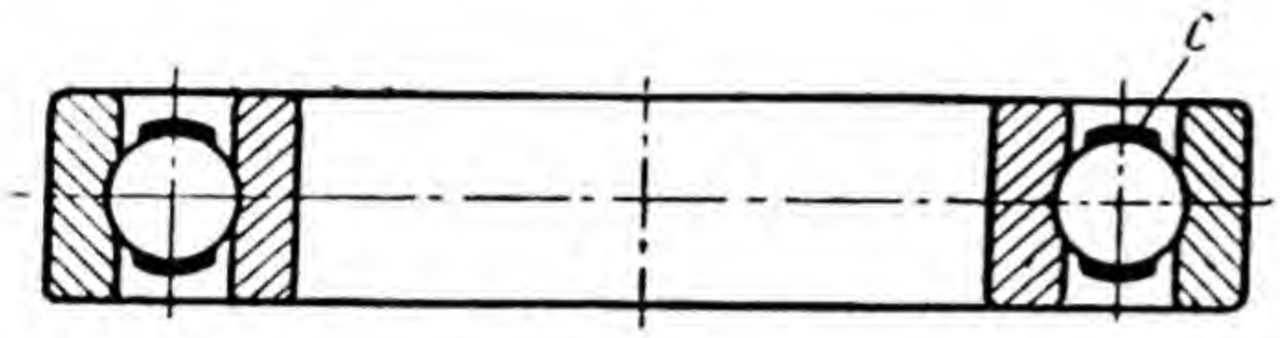

Fig. 159

Fig. 160

We resolve force P into forces $P\cos\alpha$ and $P\sin\alpha$. The first of these forces is a driving one, the other, braking, which creates in the guides pressures P_A and P_B in the direction perpendicular to the bar axis, generating the forces of friction which counteract the force $P\cos\alpha$.

From the equations of moments relative to B and then relative to A we find that guide A presses on the bar with force $P_A=2P\sin\alpha$, which in Fig. 161 is directed downwards, and guide B presses with force $P_B=P\sin\alpha$, which is directed upwards. Both forces P_A and P_B generate a total force of friction in the guides which is equal to $3fP\sin\alpha$ and the reacting force $P\cos\alpha$. For the possibility of motion it is necessary to observe the condition

$$P\cos\alpha>3f_0P\sin\alpha.$$

Whence

$$\tan\alpha<\frac{1}{3f_0}=\frac{1}{0.6}=1.67;$$

$$\alpha<59°.$$

Example 2. Load $Q_1=10$ kg (Fig. 162), which lies on an inclined plane with the angle of inclination $\alpha_1=30°$, is connected by a flexible cord that is flung over the pulley with load Q_2, which lies on the inclined plane with an angle of inclination $\alpha_2=45°$. Discounting the stiffness of

the cord and resistance by friction in the pulley bearing, determine the magnitude of load Q_2 at which both loads will be stationary. Coefficient of friction f_0 of rest between the loads and the inclined planes should be taken as 0.2.

We resolve the weight Q of each load into force $Q \sin \alpha$, which is directed parallel to the inclined plane downwards and into force $Q \cos \alpha$, which is directed perpendicular to the inclined plane.

So that load Q_1 is unable to move downwards and

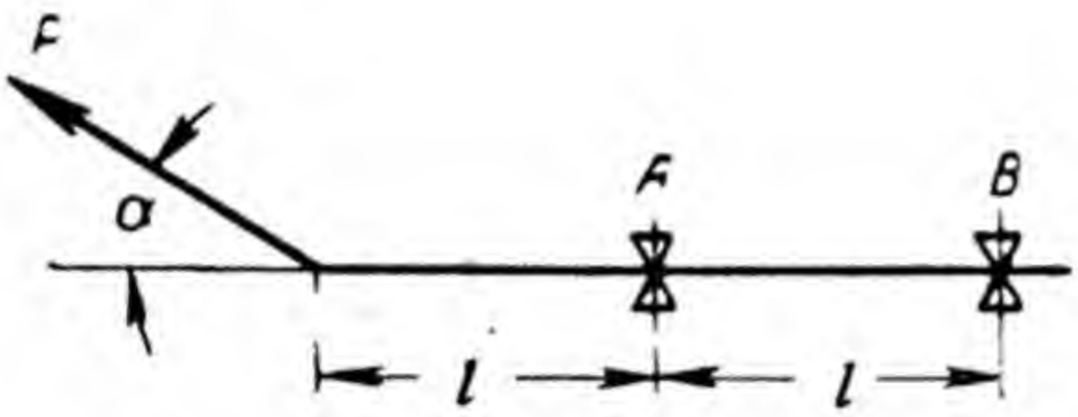

Fig. 161

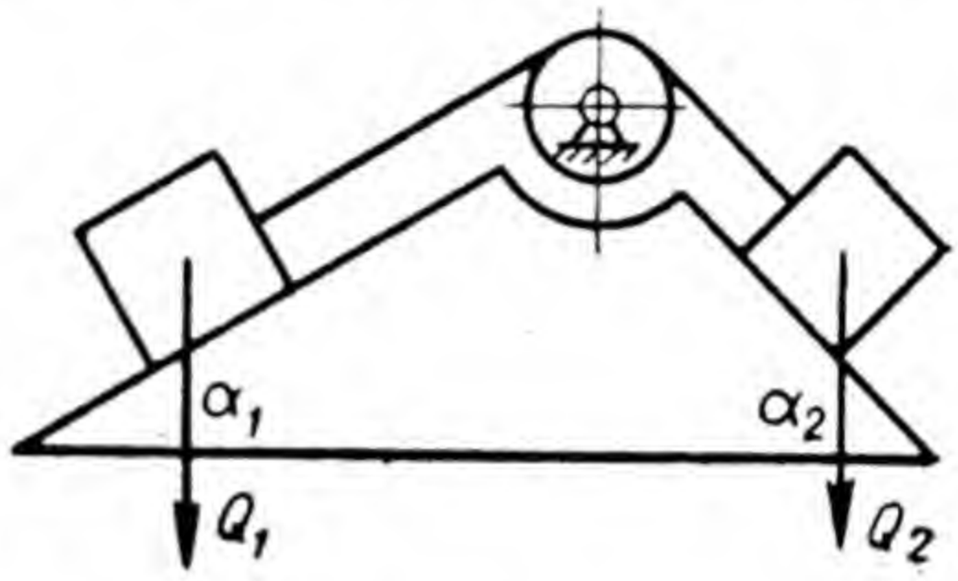

Fig. 162

entrain load Q_2 along the plane upwards, it is necessary to observe the condition

$$Q_1 \sin \alpha_1 - Q_1 f_0 \cos \alpha_1 \leqslant Q_2 \sin \alpha_2 + Q_2 f_0 \cos \alpha_2,$$

whence

$$Q_2 \geqslant Q_1 \frac{\sin \alpha_1 - f_0 \cos \alpha_1}{\sin \alpha_2 + f_0 \cos \alpha_2}.$$

So that load Q_2 is unable to move on the plane downwards and entrain load Q_1, it is necessary to observe the condition

$$Q_2 \sin \alpha_2 - Q_2 f_0 \cos \alpha_2 \leqslant Q_1 \sin \alpha_1 + Q_1 f_0 \cos \alpha_1,$$

whence

$$Q_2 \leqslant Q_1 \frac{\sin \alpha_1 + f_0 \cos \alpha_1}{\sin \alpha_2 - f_0 \cos \alpha_2}.$$

Therefore, the magnitude of load Q_2 must not exceed the limits

$$Q_1 \frac{\sin \alpha_1 + f_0 \cos \alpha_1}{\sin \alpha_2 - f_0 \cos \alpha_2} \geqslant Q_2 \geqslant Q_1 \frac{\sin \alpha_1 - f_0 \cos \alpha_1}{\sin \alpha_2 + f_0 \cos \alpha_2}.$$

After substituting the given magnitudes and making calculations, we obtain

$$11.89 \text{ kg} \geqslant Q_2 \geqslant 3.86 \text{ kg}.$$

Example 3. The V-shaped slider weighing 100 kg moves along horizontal guides (Fig. 163). The slider edge angle $2\gamma = 60°$. The coefficient of sliding friction between the slider and guides is $f = 0.2$. Determine the magnitude of the driving force P, which is directed parallel to the guides, at

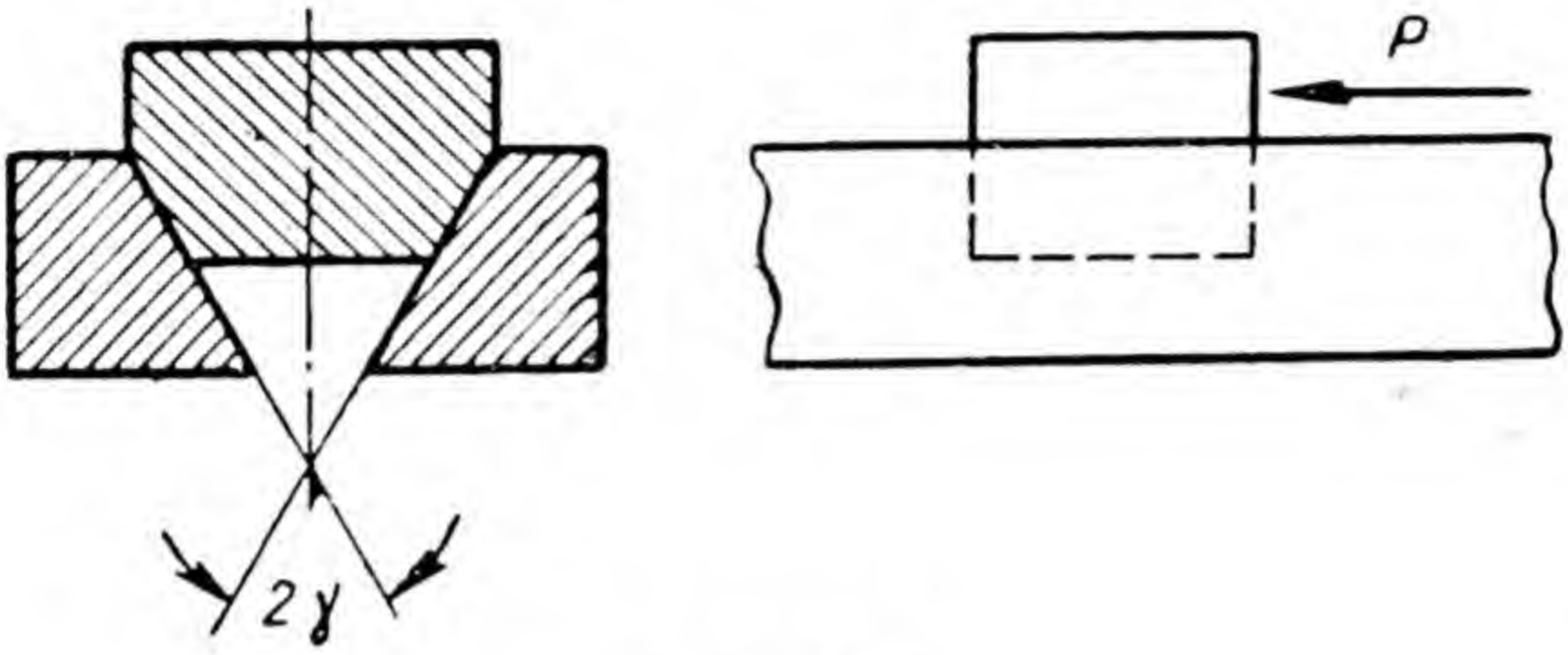

Fig. 163

slider motion with constant velocity and acceleration 4.9 m/sec.^{2}

The imaginary coefficient of friction

$$f' = \frac{f}{\sin \gamma} = \frac{f}{\sin 30°} = 2f = 0.4.$$

The force of friction

$$F = 100 \text{ kg} \times 0.4 = 40 \text{ kg}.$$

The force which is required to maintain constant velocity of motion

$$P = F = 40 \text{ kg}.$$

The slider mass

$$m = \frac{100}{9.8} \text{ kg} \times \text{sec}^2/\text{m}.$$

The force which is required for slider motion with acceleration 4.9 m/sec^2

$$P = F + 4.9\, m = 40 + 4.9 \frac{100}{9.8} = 90 \text{ kg}.$$

Example 4. The driving friction wheel of diameter $D_1=300$ mm (Fig. 164) and number of revolutions per minute $n_1=300$ transmits power $N=4$ HP to the driven wheel of diameter $D_2=450$ mm. The coefficient of friction at the place of contact of the wheel rims is $f=0.2$. The shafts, on which the wheels are set, rotate in bearings 40 mm in diameter. The coefficient of friction in the bearings of the shafts is $f_1=0.08$. Determine the loss of power due to friction in the shaft bearings for wheels with cylindrical rims and wheels with V-grooved rims.

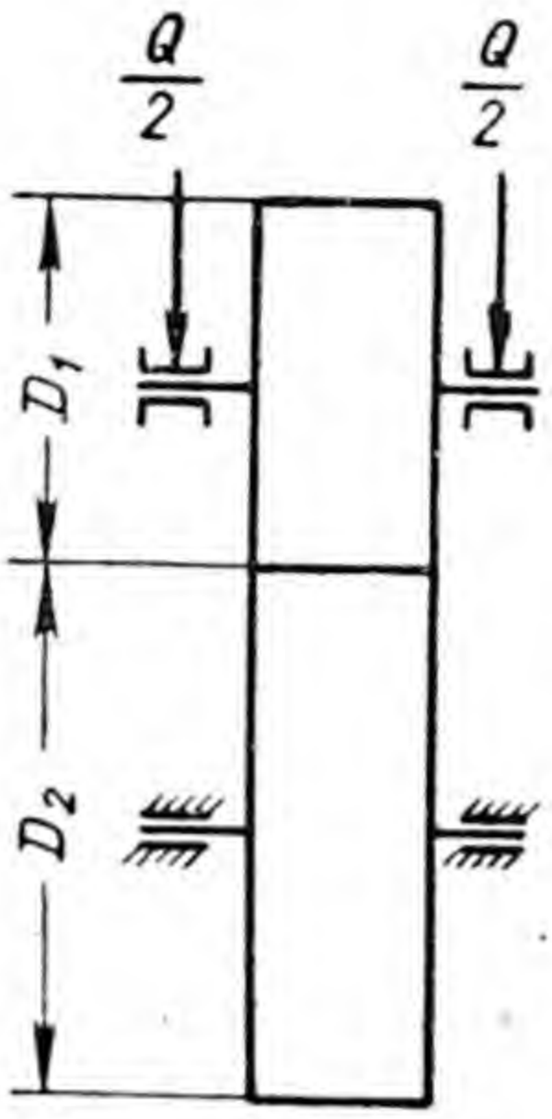

Fig. 164

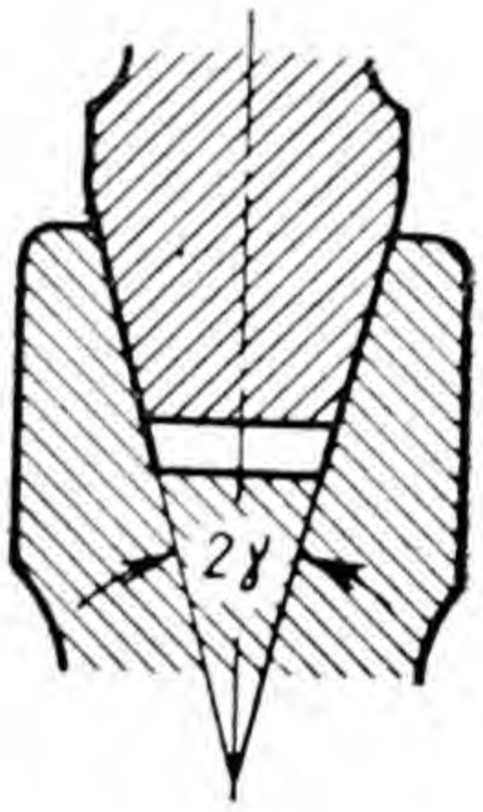

Fig. 165

The edge angle of the V-grooved rim is $2\gamma=30°$ (Fig. 165).

The angular velocity of rotation of the driving wheel

$$\omega_1=\frac{\pi n_1}{30}=\frac{\pi\times 300}{30}=31.4\ \text{sec}^{-1}.$$

At power $N=4$ HP $=4\times 75$ kgm/sec $=300$ kgm/sec the torque on the shaft of the driving wheel

$$M=300\ \text{kgm/sec}/31.4\ \text{sec}^{-1}=9.55\ \text{kgm}.$$

The turning force

$$P=9.55\ \text{kgm}/\frac{0.3\ \text{m}}{2}=63.7\approx 64\ \text{kg}.$$

The force with which the wheels must be pressed to each other in cylindrical rims

$$Q=\frac{P}{f}=\frac{64\ \text{kg}}{0.2}=320\ \text{kg}.$$

Force S, which is absorbed by the bearings of each of the shafts, is a geometric sum of two components: the turning force and force Q. Since the lines of action of these forces are perpendicular to each other, then

$$S=\sqrt{P^2+Q^2}=\sqrt{64^2+320^2}=326\ \text{kg}.$$

The force of friction in the bearings of each of the shafts equals

$$Sf = 326 \text{ kg} \times 0.08 = 26 \text{ kg}.$$

The moment of the frictional force in the bearings of each of the shafts

$$26 \text{ kg} \times \frac{40}{2} \text{ mm} = 520 \text{ kgmm} = 0.52 \text{ kgm}.$$

The angular velocity of rotation of the driven wheel

$$\omega_2 = \omega_1 \frac{D_1}{D_2} = 31.4 \times \frac{300}{450} = 20.9 \text{ sec}^{-1}.$$

Loss of power at friction in the bearings:

of the driving shaft

$$0.52 \text{ kgm} \times 31.4 \text{ sec}^{-1} = 16.3 \text{ kgm/sec};$$

of the driven shaft

$$0.52 \text{ kgm} \times 20.9 \text{ sec}^{-1} = 10.9 \text{ kgm/sec}.$$

With V-grooved rims of wheels the imaginary coefficient of friction

$$f' = \frac{f}{\sin \gamma} = \frac{f}{\sin 15^\circ} = 3.84f = 3.84 \times 0.2 \approx 0.77.$$

With this coefficient of friction the required force of compression is

$$Q = \frac{P}{f'} = \frac{64}{0.77} = 83.5 \approx 84 \text{ kg}.$$

The force which is absorbed by the shaft bearings

$$S = \sqrt{64^2 + 84^2} = 106 \text{ kg}.$$

Since the loss in power on friction in the shaft bearings is proportional to force S, the loss in power in shaft bearings will be less in the case of V-grooved rims than with cylindrical rims, by $326/106 \approx 3$ times.

Note. Despite the advantage, which follows from the given comparative calculation, of friction wheels with V-grooved rims over wheels with cylindrical rims, the friction drive with grooved wheels is widely used only in instruments which are designed to transmit low power,

and is seldom used in power plants. This is because the relative sliding of V-grooved rims with accompanying wear cannot be eliminated: only the contact points of the rim surfaces, which lie on the pitch circles, do not slide relative to each other.

Example 5. Elements A and B (Fig. 166) are joined by a bolt. The diameter of the hole for the bolt is slightly (by 1-2 mm) larger than the bolt diameter. The major thread diameter of the bolt is $d=20$ mm, the mean diameter of the thread is $d_{mean}=18.4$ mm, the pitch $s=2.5$ mm, and angle of the thread at the profile apex $2\beta=60°$. The bolt is tightened by a spanner with force $P_0=20$ kg, which has been applied to the spanner at distance $l=250$ mm from the bolt axis. The coefficient of sliding friction on all friction surfaces is $f=0.2$, the coefficient of friction of rest is $f_0=0.25$. The resultant of elementary forces of friction on the contact surface of the nut and element A is to be taken as applied on a circle with diameter $D=30$ mm.

Determine: 1) by what force T, which is directed perpendicular to the bolt axis, can elements A and B be moved relative to each other, and 2) what force has to be applied to the spanner at distance l from the bolt axis when dismounting the joint.

The displacement of elements A and B relative to each other is prevented by the force of friction on the surface of their contact. The force of friction, which prevents displacement, equals Qf_0, where Q is the force that presses the elements between the nut and bolt head. Exerting pressure on element A, the tightened nut with the same force, but directed to the opposite side, stretches the bolt.

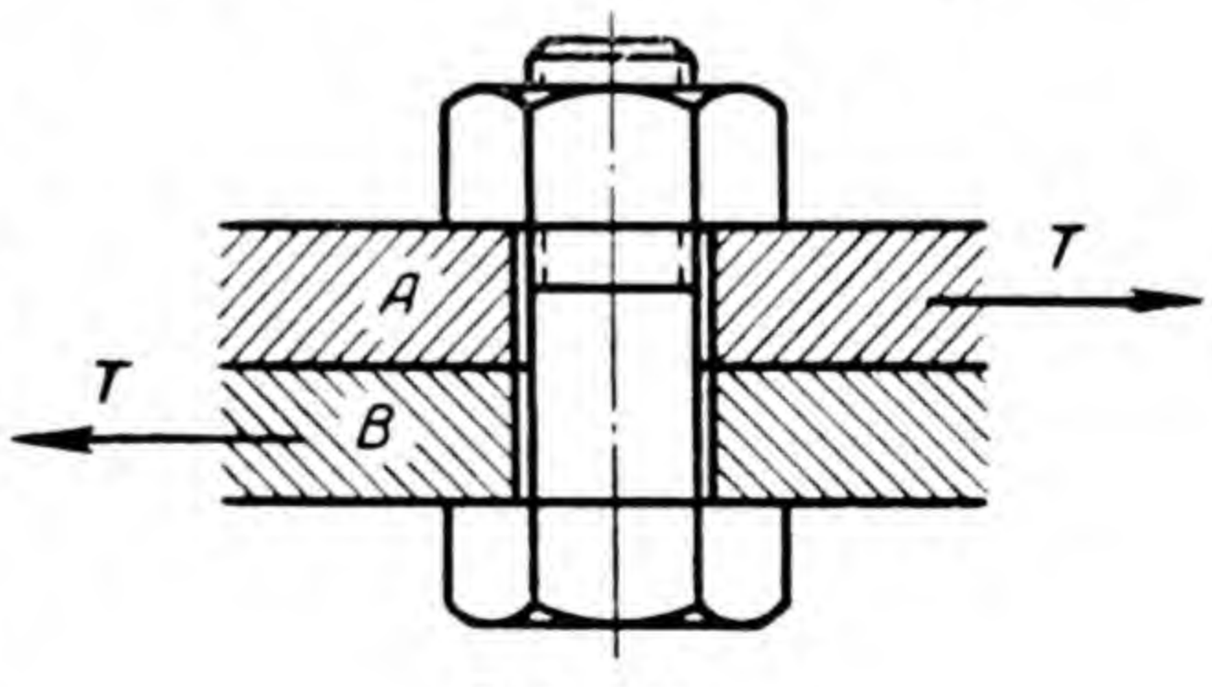

Fig. 166

The bolt is tightened by moment $M=20$ kg$\times$ $\times 250$ mm$=5000$ kgmm.

When tightening is ended this moment has been balanced: 1) by moment Pr, where P is the force on the mean radius of the thread, and r is the mean radius of the thread, and 2) by moment QfR of the forces of friction on the surface of contact of the nut and element A, where R

is the mean radius to which the resultant of the elementary forces of friction is applied.

Hence

$$5000 = Pr + QfR = P\frac{18.4}{2} + Q \times 0.2\frac{30}{2};$$

$$5000 = 9.2P + 3Q.$$

Since

$$P = Q \tan (\lambda + \varphi'),$$

then

$$5000 = Q[9.2 \tan (\lambda + \varphi') + 3].$$

With pitch $s = 2.5$ mm and mean diameter of the thread $d_{mean} = 18.4$ mm

$$\tan \lambda = \frac{2.5}{\pi \times 18.4} \approx 0.043,$$

whence

$$\lambda = 2°30'.$$

Where $f = 0.2$ and angle $2\beta = 60°$ at the profile apex of the thread, the imaginary coefficient of friction

$$f' = \frac{f}{\cos \beta} = \frac{0.2}{0.866} \approx 0.23,$$

and its corresponding imaginary angle of friction

$$\varphi' = \text{arc tan } 0.23 = 13°00'.$$

Hence

$$\tan (\lambda + \varphi') = \tan (2°30' + 13°) = 0.277;$$

$$5000 = Q(9.2 \times 0.277 + 3) = 5.55Q,$$

whence

$$Q = 5000/5.55 = 900 \text{ kg}.$$

Where $f_0 = 0.25$, we get the force T to equal

$$T = Qf_0 = 900 \times 0.25 = 225 \text{ kg}.$$

Where dismounting the joint the force P_0', which is applied to the spanner for unscrewing the nut at distance

$l=250$ mm from the bolt axis, creates the moment $P'_0 l$ which overcomes the resistance: 1) of moment P'_r, where P' is force on the mean radius r of the thread, and 2) of moment QfR on the surface of contact of the nut and element A.

In accordance with formula (10)

$$P' = Q \tan (\varphi'_0 - \lambda),$$

where φ'_0, the imaginary friction angle of rest, equals

$$\varphi'_0 = \text{arc tan } f'_0 = \text{arc tan } \frac{f_0}{\cos \beta} = \text{arc tan } \frac{0.25}{0.866} = 16°10'.$$

The magnitude of force P' will equal

$$P' = 900 \tan (16°10' - 2°30') = 218.7 \approx 219 \text{ kg}.$$

Hence

$$P'_0 l = P'r + Qf_0R, \text{ i. e.}$$

$$P'_0 \times 250 = 219 \times 9.2 + 900 \times 0.25 \times 15 = 5390 \text{ kgmm},$$

whence

$$P'_0 = 5390/250 \approx 21.6 \text{ kg}.$$

Example 6. Determine the force to be applied on a hoisting jack handle at a distance of 800 mm from its screw axis (Fig. 167) in order to lift a 2000-kg load with constant velocity, according to the following data:

1) the screw thread is trapezoidal with the angle at the profile apex $2\beta=30°$, major diameter $d=50$ mm, mean diameter $d_{mean}=46$ mm, pitch $s=8$ mm;

2) the coefficient of friction between nut and screw is $f=0.12$;

3) the coefficient of friction between the screw head and the non-turning head of the hoisting jack is $f_1=0.2$;

4) the diameters of the

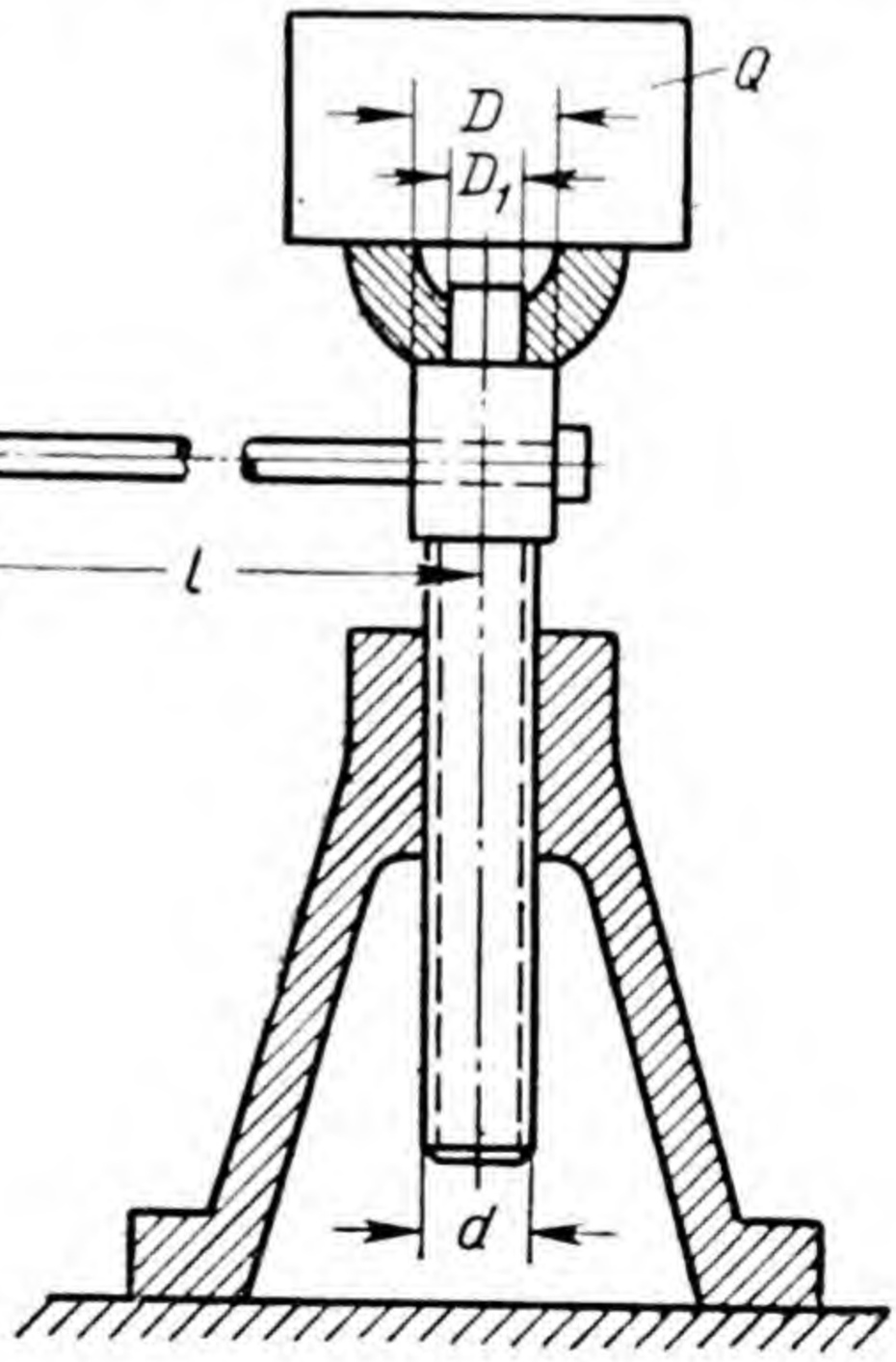

Fig. 167

annular area of contact of the screw and hoisting jack heads: major $D=80$ mm, minor $D_1=40$ mm.

The lead angle λ on the mean diameter

$$\tan\lambda=\frac{s}{\pi d_{mean}}=\frac{8}{\pi\times 46}\approx 0.055;$$

$$\lambda=3°10'.$$

The imaginary coefficient of friction between the screw and nut

$$f'=\frac{f}{\cos\beta}=\frac{0.12}{\cos 15°}=0.124.$$

The imaginary angle of friction

$$\varphi'=\text{arc}\tan f'=\text{arc}\tan 0.124=7°05'.$$

The force P', which has to be applied on the mean radius of the thread in order to overcome the weight Q of the load and the force of friction in the thread:

$$P'=Q\tan(\lambda+\varphi')=2000\tan(3°10'+7°05')=360\text{ kg}.$$

The moment M' of force P'

$$M'=P'\frac{d_{mean}}{2}=360\text{ kg}\times\frac{4.6}{2}\text{ cm}=828\text{ kgcm}.$$

The force F of friction between the heads of the screw and hoisting jack

$$F=f_1\times Q=0.2\times 2000=400\text{ kg}$$

(the insignificant weight of the head is neglected). The arm L of the resultant of elementary forces of friction

$$L=\frac{2}{3}\times\frac{D^2+DD_1+D_1^2}{2(D+D_1)}=\frac{2}{3}\times\frac{8^2+8\times 4+4^2}{2(8+4)}=3.1\text{ cm}.$$

The moment M'' of force F

$$M''=400\text{ kg}\times 3.1\text{ cm}=1240\text{ kgcm}.$$

The moment M which is required to lift the load with constant velocity:

$$M=M'+M''=828+1240=2068\text{ kgcm}.$$

The required force P_0 on the handle

$$P_0 = M/l = 2068/80 = 25.85 \approx 26 \text{ kg}.$$

Example 7. Vertical shaft S (Fig. 168), which is under the action of force $Q = 400$ kg, rests with the inserted ring pivot P on the fixed cushion G of the gudgeon bearing. The pivot is inserted in the shaft by the conical tail with an angle at the cone apex $2\gamma = 30°$. The number of shaft revolutions per minute is $n = 300$. The coefficient of friction of rest on the surface of contact of the pivot and shaft is $f_0 = 0.2$; the coefficient of sliding friction between the pivot and footstep pillow is $f = 0.08$. The dimensions of the contact surfaces are given in Fig. 168. Determine the loss in power on friction and find out if rotation of the pivot relative to the shaft is possible during shaft rotation.

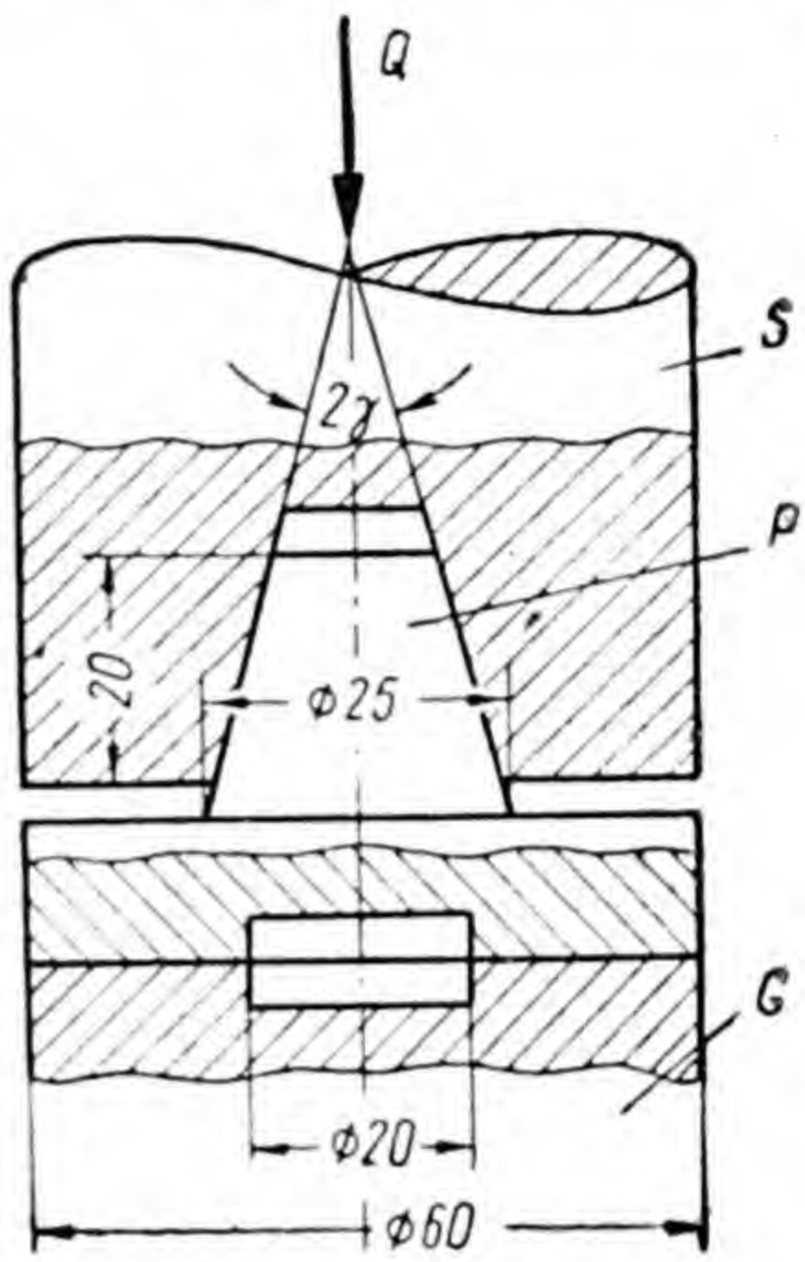

Fig. 168

The force of friction on the surface of contact of the pivot and footstep pillow

$$Qf = 400 \times 0.08 = 32 \text{ kg}.$$

The arm R of the force of friction

$$R = \frac{2}{3} \times \frac{30^2 + 30 \times 10 + 10^2}{30 + 10} = 21.7 \approx 22 \text{ mm}.$$

The moment of the force of friction

$$Mf = 32 \text{ kg} \times 22 \text{ mm} = 704 \text{ kgmm} \approx 0.7 \text{ kgm}.$$

The angular velocity of rotation of the shaft

$$\omega = \frac{\pi \times n}{30} = \frac{\pi \times 300}{30} = 31.4 \text{ sec}^{-1}.$$

The loss in power on friction

$$Mf \times \omega = 0.7 \text{ kgm} \times 31.4 \text{ sec}^{-1} = 21.98 \approx 22 \text{ kgm/sec.}$$

The imaginary coefficient of friction of rest on the surface of contact of the pivot and shaft

$$f_0' = f_0/\sin \gamma = 0.2/\sin 15° \approx 0.77.$$

The force of friction on the surface of contact of the pivot and shaft

$$Qf_0' = 400 \text{ kg} \times 0.77 = 308 \text{ g.}$$

With uniform distribution of the elementary forces of friction by the height of the contact surface of the pivot and shaft (which can be assumed when there has been sufficiently accurate processing of the surfaces of the solid and hollow frustums) the resultant of the elementary forces of friction can be considered as applied at an equal distance from the large and small bases of the conical contact surface, i. e. at a height of this surface, which equals 20 mm at a 10-mm distance from the lower base.

The radius of the circles of the lower base equals $25/2 = 12.5$ mm; at a 10-mm height from the lower base the radius of cross section equals

$$12.5 - 10 \tan 15° = 9.9 \text{ mm.}$$

The moment that is required for rotation of the pivot relative to the shaft equals

$$308 \text{ kg} \times 9.9 \text{ mm} = 2999 \text{ kgmm} \approx 3 \text{ kgm,}$$

exceeds the moment $M_f = 0.7$ kgm of the forces of friction on the contact surface of the pivot and footstep pillow by $3/0.7 = 4.3$ times. Hence, the possibility of pivot rotation relative to the shaft is excluded.

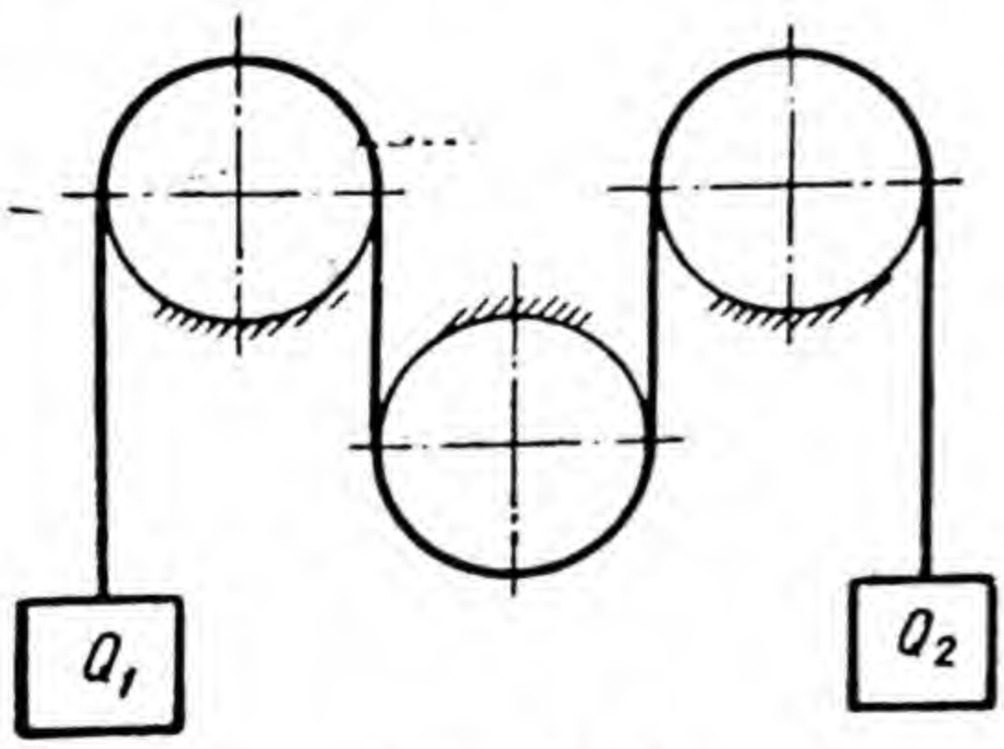

Fig. 169

Example 8. A flexible body envelops three stationary cylinders, as shown in Fig. 169. Load $Q_1 = 100$ kg is suspended at one end of the flexible body. Determine at what magnitude of load Q_2, suspended at the other end of the flexible body, both loads

will be stationary. The coefficient of friction between the flexible body and cylinders is $f=0.32$.

The total angle of contact of all cylinders by the flexible body equals 3π. By accepting the exponent in Euler's formula to equal $f\alpha=0.32\times3\pi\approx3$, we get the conditions for impossibility of motion downwards

$$\text{of load } Q_1\leqslant Q_1e^3;$$

$$\text{of load } Q_2\leqslant Q_1e^3.$$

Hence, the magnitude of load Q_2 should be within the limits

$$\frac{Q_1}{e^3}\leqslant Q_2\leqslant Q_1e^3.$$

Having accepted $e^3=2.72^3\approx20$, we obtain $5\,\text{kg}\leqslant Q_2\leqslant\leqslant2000\,\text{kg}$.

Chapter VIII

MOTION AND WORK OF MACHINES

35. EFFICIENCY

The energy consumed by a machine is used to overcome useful and parasitic resistances. Those resistances for the overcoming of which the machine is designed are called useful resistances, for example, the resistance to cutting of metal in metal-working machines the weight of hoisted loads in hoisting machines, etc. Those resistances for the overcoming of which energy is spent that produces no productive effect are called parasitic resistances, for instance, resistance of the medium in which the motion of machine elements takes place (if the machine is not intended for moving the medium), the forces of friction.

The greater the proportion of the energy consumed by a machine that is used for overcoming the useful resistances, the more efficient the machine. The degree of machine efficiency is characterized by the relation

$$\eta = \frac{A_{u.r}}{A_d},$$

where $A_{u.r}$ is the work done by a machine to overcome the useful resistances;

A_d is the work of driving forces or energy consumed by a machine;

η is the efficiency.

From its efficiency it is possible to assess the degree of perfection not only of a machine, i. e. of a more or less compound mechanical device, but also of any simple device, which is not a machine, but absorbs and delivers energy, for example, of furnaces of steam boilers, in which the chemical energy of fuel is transformed into heat energy, of a steam line which serves for transmitting energy at a distance, of an inclined plane, etc.

In examining a machine or any given compound installation, consisting of a number of machines and various units, in which a loss of energy is found to take place, it is always advisable to determine not only the efficiency of the machine or the installation as a whole, but also the efficiency of its individual elements. For example, in an installation, which is designed for illuminating premises and which consists of a power plant, cables and incandescent lamps, not only the efficiency of the entire installation may be of concern, but also the efficiency of the engine by itself, of the mechanism which transmits rotary motion from the engine to the generator, of the generator, of the network of electric cables which transmit energy from the power plant to the place of consumption, and, finally, of the incandescent lamps which transform electrical energy into energy of light.

In all cases where energy is supplied to one part of a machine or of any compound device, and is then transmitted in turn from one part to another and is delivered by the last part in the form required for practical utilization, the efficiency of the machine or of the device as a whole is equal to the product of efficiency of the individual parts. This can easily be seen from the following.

If the device consists of n units, which act in such a way that the energy is transmitted from each of these units to the next, and if $\eta_1, \eta_2, \eta_3, \ldots \eta_n$ are the efficiency of the separate units, the first unit of the device consumes work done A_d, which is consumed by the entire device, whereas the last one, for overcoming the useful resistances, uses up work done $A_{u.r}$, which is consumed by the entire device.

Denoting by $A_1, A_2, A_3, \ldots A_n$ the amount of work done, which is delivered by different parts of the device, we get

$$\eta_1 = \frac{A_1}{A_d}, \quad \eta_2 = \frac{A_2}{A_1}, \quad \eta_3 = \frac{A_3}{A_2} \quad \ldots \eta_n = \frac{A_{u.r}}{A_{n-1}}.$$

After multiplying the left side and the right side of these equations and reducing them, we get

$$\eta_1 \times \eta_2 \times \eta_3 \times \ldots \eta_n = \frac{A_{u.r}}{A_d} = \eta,$$

where η is the efficiency of the entire device.

Most losses of mechanical power are due to friction. Let us find out what influence the forces of friction have on the magnitude of efficiency in some simple cases.

A. Efficiency of the Inclined Plane

If a body with weight Q (Fig. 170) is displaced upwards along the inclined plane with the angle of inclination λ by force P, which is directed parallel to the inclined plane, the work done by the driving force will equal Ps, and the useful work done by force P is Qh, where s is the path of force P in the direction of its motion, and h is the lifting height of the body. Therefore

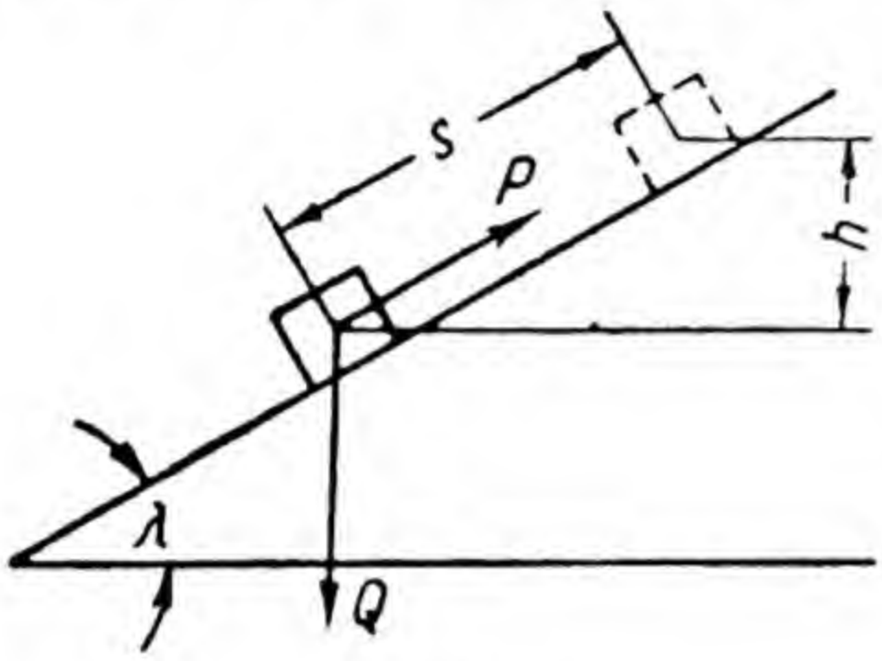

Fig. 170

$$\eta_L = \frac{Qh}{Ps}.$$

In moving the body force P overcomes the resistance of two forces: the component $Q \sin \lambda$ of force Q in the direction parallel to the inclined plane, and force $fQ \cos \lambda$ of friction, which is stimulated by the component $Q \cos \lambda$ of force Q in the direction perpendicular to the inclined plane. Therefore

$$P = Q \sin \lambda + fQ \cos \lambda,$$

and since $h = s \sin \lambda$, then

$$\eta_L = \frac{Qh}{Ps} = \frac{Qs \sin \lambda}{Qs (\sin \lambda + f \cos \lambda)} = \frac{\sin \lambda}{\sin \lambda + f \cos \lambda}.$$

By substituting the coefficient of friction with the tangent of the angle of friction, we get the efficiency at lifting to equal

$$\eta_L = \frac{\sin \lambda}{\sin \lambda + \tan \varphi \cos \lambda} = \frac{\sin \lambda \cos \varphi}{\sin (\lambda + \varphi)}.$$

During motion of the body downwards the driving force is force Q and the resisting force is force P. Therefore the efficiency at descent is

$$\eta_{desc} = \frac{Ps}{Qh}.$$

In this case $P=Q\sin\lambda-fQ\cos\lambda$. Following from this and substituting $s\sin\lambda$ for h and $\tan\varphi$ for f, we get

$$\eta_{desc}=\frac{\sin\lambda-f\cos\lambda}{\sin\lambda}=\frac{\sin(\lambda-\varphi)}{\sin\lambda\cos\varphi}$$

On a self-braking plane during downward motion within limit $\lambda=\varphi$, $\eta_{desc}=0$, which was to be expected.

On a self-braking plane during upward motion at $\lambda=\varphi$, in the best case

$$\eta_L=\frac{\sin\lambda\cos\lambda}{\sin 2\lambda}=0.5.$$

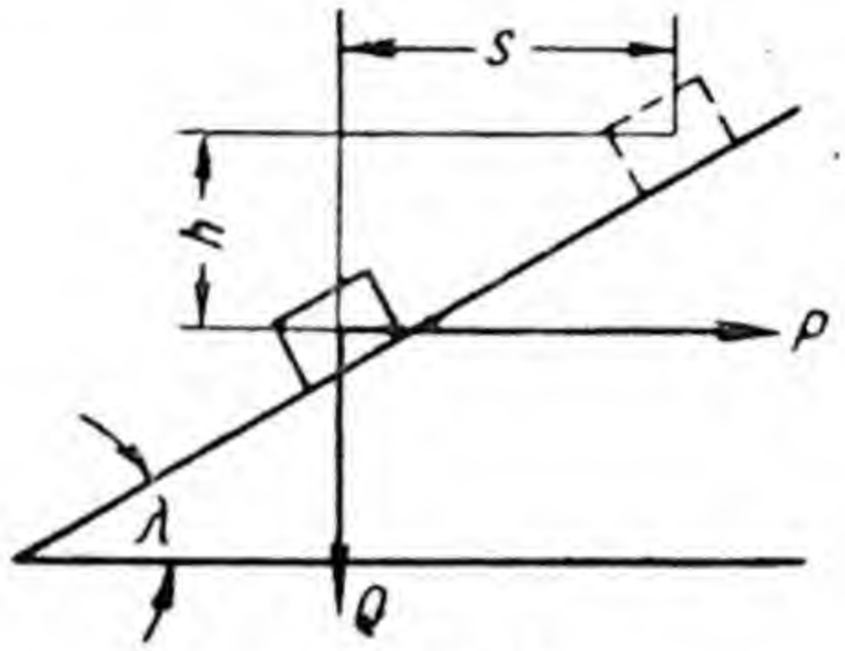

Fig. 171

The self-braking plane is very convenient for lifting a load on an inclined plane, because in the intervals between actions of the driving force there is no necessity for appliances to maintain the load on the inclined plane. The result we have just obtained shows, however, that this convenient feature of the self-braking plane is obtained at a very high price. This also applies to different hand hoisting devices with self-breaking drives (for example, worm gears).

In lifting a load on an inclined plane the most expedient direction for the driving force is parallel to the inclined plane. Considering the screw efficiency and assuming the inclined plane as a developed helical surface, we must direct force P parallel to the base of the plane (Fig. 171).

With upward motion in this case we get

$$\eta_L=\frac{Qh}{Ps};$$

$$P=Q\tan(\lambda+\varphi);\ h=s\tan\lambda;$$

$$\eta_L=\frac{\tan\lambda}{\tan(\lambda+\varphi)};$$

and with downward motion

$$\eta_{desc}=\frac{Ps}{Qh};$$

$$P=Q\tan(\lambda-\varphi);\ h=s\tan\lambda;$$

$$\eta_{desc}=\frac{\tan(\lambda-\varphi)}{\tan\lambda}.$$

Where $\lambda=\varphi$ (beginning of self-braking),

$$\eta_L=\frac{\tan\lambda}{\tan 2\lambda}=\frac{1}{2}-\frac{1}{2}\tan^2\lambda,$$

i. e. the efficiency of the self-braking helical surface is always less than 0.5.

Let us determine the maximum degree of efficiency at a given angle of friction.

By differentiating the equation

$$\eta=\frac{\tan\lambda}{\tan(\lambda+\varphi)},$$

we get

$$d\eta=\frac{\tan(\lambda+\varphi)d\tan\lambda-\tan\lambda d\tan(\lambda+\varphi)}{\tan^2(\lambda+\varphi)}=$$

$$=\frac{\tan(\lambda+\varphi)\ \frac{d\lambda}{\cos^2\lambda}-\tan\lambda\frac{d\lambda}{\cos^2(\lambda+\varphi)}}{\tan^2(\lambda+\varphi)};$$

$$\frac{d\eta}{d\lambda}=\frac{\frac{\tan(\lambda+\varphi)}{\cos^2\lambda}-\frac{\tan\lambda}{\cos^2(\lambda+\varphi)}}{\tan^2(\lambda+\varphi)}=\frac{\cot(\lambda+\varphi)}{\cos^2\lambda}-\frac{\tan\lambda}{\sin^2(\lambda+\varphi)};$$

by equating the derivative to zero, we get

$$\frac{\cot(\lambda+\varphi)}{\cos^2\lambda}=\frac{\tan\lambda}{\sin^2(\lambda+\varphi)}.$$

Solving this equation, we get

$$\sin 2(\lambda+\varphi)=\sin 2\lambda;$$

$$\sin 2(\lambda+\varphi)=\sin(180^\circ-2\lambda);$$

$$2(\lambda+\varphi)=180^\circ-2\lambda;$$

$$\lambda=45^\circ-\frac{\varphi}{2}.$$

Substituting value λ in the original equation, we get

$$\eta^{max}=\frac{\tan\left(45°-\frac{\varphi}{2}\right)}{\tan\left(45°+\frac{\varphi}{2}\right)}=\frac{\tan\left(45°-\frac{\varphi}{2}\right)}{\cot\left[90°-\left(45°+\frac{\varphi}{2}\right)\right]}=\tan^2\left(45°-\frac{\varphi}{2}\right).$$

The lead angle λ, at which we get the maximum efficiency, is inconvenient in screws that transmit motion for certain reasons, which are discussed in the course on machine elements, and therefore in worm gears the angle λ has to be much less. This, however, entails no appreciable reduction of efficiency below the maximum possible. Given proper lubrication of the worm and wheel gearing, which is always provided for in high-speed gears, the coefficient of friction in gearing is within the limits $0.02\div0.04$; if we take $f=0.03$ and therefore the angle of friction is $\varphi=1°34'$, then at different values of λ the degrees of efficiency, which are determined by equation

$$\eta=\frac{\tan\lambda}{\tan\lambda(\lambda+\varphi)},$$

are

$\lambda=20°$	25°	30°	35°	40°	45°
$\eta=0.914$	0.927	0.934	0.939	0.941	0.942.

It is clear from these data that even a considerable change in angle λ reduces the efficiency of gearing only insignificantly.

B. Efficiency of Linkages

Determining the efficiency of a linkage consists in calculating how much energy is used for overcoming the forces of friction in joints (turning pairs).

If reaction in the joint is Q, the force of friction is $F=fQ$, and the moment of the frictional force at diameter d of the journal equals

$$M_f=fQ\frac{d}{2}.$$

If the angular velocity of rotation of one of the links in a turning pair relative to the other is ω_{rel}, the power of the force of friction

$$N_f = M_f \omega_{rel}.$$

Therefore in order to determine how much energy is lost in the joint through friction, it is necessary to know the reaction in it, the coefficient of friction, the journal diameter and the relative angular velocity of rotation.

Reactions in joints are determined during the combined static and inertia-force analysis of the mechanism. The relative velocities can be determined by the velocity diagram.

Fig. 172, *a* shows a diagram of a four-bar mechanism, and Fig. 172, *b* the velocity diagram for this mechanism.

For joint *A*

$$\omega_1 = \frac{pb\mu_v}{l_1},$$

where ω_1 is the angular velocity of rotation of link *AB*;

l_1 is the length of link *AB*;

μ_v is the scale of the velocity diagram.

Proceeding to joint *B* and using the velocity diagram, we ascertain:

1) the direction of vector $\overline{ba}$ shows that point *A* and, consequently, the entire link *AB* relative to point *B* rotates (in the instant corresponding to the position of the links as shown in Fig. 172) clockwise;

2) point *C* of link *BC* and, consequently the entire link *BC* relative to point *B* rotates in the direction which is indicated by vector $\overline{bc}$, i. e. counter-clockwise.

Therefore the kinematic pair element *B*, which is rigidly connected with link *AB*, rotates relative to the other element of the same pair, which is rigidly connected with link *BC*,

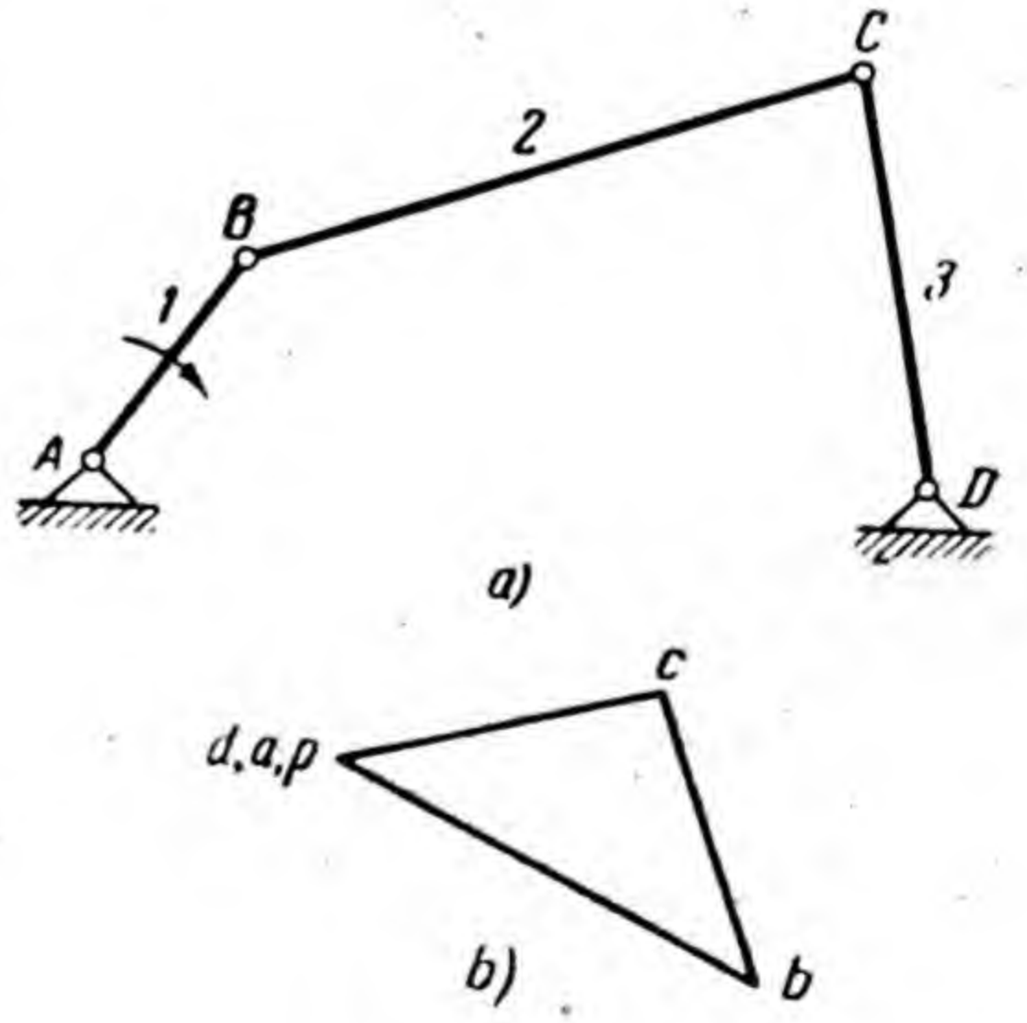

Fig. 172

with angular velocity ω_B, which is equal to the sum of the angular velocities of links AB and BC, i. e.

$$\omega_B = \omega_1 + \omega_2 = \left(\frac{ba}{l_1} + \frac{bd}{l_2}\right)\mu_v,$$

where ω_1 and ω_2 are the angular velocities of rotation of links AB and BC; l_2 is the length of link BC.

Point B relative to point C rotates in the direction of vector $\overline{cb}$, and therefore link BC relative to point C rotates counter-clockwise. Point D relative to point C rotates in the direction of vector $\overline{cd}$, and therefore link CD relative to point C rotates clockwise. It follows that the element of kinematic pair C, which is rigidly connected with link BC, relative to the other element, which is rigidly connected with link CD, rotates with angular velocity ω_C, which is equal to the sum of the angular velocities of links BC and CD, i. e.

$$\omega_C = \omega_2 + \omega_3 = \left(\frac{cb}{l_2} + \frac{cd}{l_3}\right)\mu_v,$$

where ω_3 is the angular velocity of rotation of link CD; l_3 is the length of link CD.

Since link AD is fixed, the kinematic pair element D, which is connected with link CD, relative to the element which is connected with link AD, rotates with angular velocity ω_D, which is equal to the angular velocity of link CD, i. e.

$$\omega_D = \omega_3 = \frac{cd}{l_3}\mu_v.$$

After determining in this way the amount of energy used for overcoming the forces of friction in links at various positions of the mechanism, we can plot by points the curve $N_f = f(\varphi)$, where φ is the angle of rotation of the crank.

On determination of the magnitude of the mean ordinate of this curve, which expresses in the course of one cycle the mean energy $(N_f)_{\text{mean}}$, used to overcome the forces of friction, the efficiency will be

$$\eta = \frac{N - (N_f)_{\text{mean}}}{N},$$

where N is the energy consumed by the mechanism.

The efficiency should, of course, be determined only for the period of steady motion.

The efficiency of mechanisms which include, besides turning pairs, also sliding pairs and higher pairs can be determined in a similar manner.

It sometimes happens that mechanical devices consume mechanical energy and perform their functions without overcoming any useful resistances, but use up all the energy consumed to overcome parasitic resistances. For example, the force applied to a conveying device in moving the load by a certain distance in a horizontal direction performs necessary and therefore useful work which, however, cannot be expressed by any other magnitude than zero, since during the entire period of load moving only parasitic resistances are being overcome; the motive force applied to a clock mechanism, heaviness of the weight or pressure of the wound spring, performs necessary and therefore useful work in moving the hands, but does not overcome any useful resistances in this process.

From what has been said it follows that the term "useful work" had a conditional meaning and that from their efficiency we can assess the degree of perfection only of those devices, which either transform one kind of energy into another, or transmit energy from one point to another. The following are examples of devices which transform one kind of energy into another: an internal-combustion engine, in which chemical energy of fuel is first transformed into heat energy and then into mechanical energy; an electric current generator, which transforms mechanical energy into electrical energy; an electric motor, which transforms electrical energy into mechanical energy.

Examples of devices which transmit energy from one point to another are the following: a steam line, an electric wire, a shaft with two pulleys, which rotates in bearings, etc.

Conveying devices, which move loads in a horizontal direction, and also certain other instruments, do not use energy to overcome useful resistances. The degree of perfection of such devices can be assessed by different indices, but not by efficiency, which for such devices is zero or very near zero.

36. EQUATION OF THE MOTION OF A MACHINE

When a machine operates all the points connected with its moving elements move along closed paths with different velocities and accelerations at different positions. When the machine is operating steadily, the velocities and accelerations of all points are repeated at fixed intervals of time with the same magnitude and direction. For example, during crank rotation with constant angular velocity the machine operation will be steady, since the velocities and accelerations of all points of the links will change according to definite laws in the course of every revolution of the crank. The duration of the cycle, during which the velocities and accelerations change according to definite laws, may be greater than the time taken by one revolution of the crank: the crank may also rotate with variable angular velocity, which changes according to definite law in the course of two or more revolutions.

The operation of a machine from the moment it is set in motion up to the moment of stopping can be divided into three periods: starting period, period of steady motion and stopping period (running out).

In the starting period work done A_d by the driving forces, which is consumed by the machine, is used to overcome the useful and parasitic resistances and to transmit kinetic energy to the moving parts. The equation of machine motion in relation to any given time interval (for instance, to one revolution of the crank) for this period takes the form

$$A_d = A_r + \left(\sum \frac{mv^2}{2} - \sum \frac{mv_0^2}{2} \right),$$

where A_r is the work done by useful and parasitic resistances;

m is the mass of the material point of the moving link;

v and v_0 are the velocities of the material point at the end and at the beginning of the interval under examination;

$\sum \frac{mv^2}{2}$ is the kinetic energy of all material points of the moving links at the end of the interval;

$\sum \frac{mv_0^2}{2}$ is the kinetic energy of all material points of the moving links at the beginning of the interval.

In the starting period the motion of the machine is irregular.

In the period of steady motion the velocity of every material point at the final moment of the cycle is equal to the velocity at the initial moment of the cycle, since the final moment of the preceding cycle coincides with the initial moment of the following one. Therefore the factor in brackets in the right-hand side of the above equation is zero, and the equation for the period of steady motion takes the form

$$A_d = A_r.$$

This means that in the period of steady motion the work of the driving forces is used for overcoming the useful and parasitic resistances.

The period of running out begins, when $A_d < A_r$, in particular, from the moment when the driving forces cease to work. When $A_d = 0$, motion continues for a certain time owing to the kinetic energy stored by the moving elements of the machine. Since in this case the velocities of all points decrease gradually, the factor in brackets in the above equation becomes negative. By transferring it to the left side of the equation, we obtain the equation of motion for this period in the form

$$\sum \frac{mv_0^2}{2} - \sum \frac{mv^2}{2} = A_r.$$

This means that in the period of running out the kinetic energy of the moving elements of the machine is absorbed by the work of the useful and parasitic resistances.

The application of the above equations for the solution of practical problems is frequently inconvenient, since the forces in action are applied to different links with different masses. In order to simplify the problems connected with the solution of these equations, methods are used whereby all forces and masses are reduced to one link. After such reduction the dynamic study of a machine consists in the examination of one link, called the link of reduction.

37. REDUCTION OF FORCES

The energy, which must be constantly supplied from external sources to the driving link in order for the mechanism to function in accordance with specified law is determined by the joint action of all the forces applied to different links of the mechanism. If the magnitudes, directions and points of application of the forces acting on different links are known, the problem of determining the energy which has to be supplied to the driving link can be solved, since the velocities of the points of application of forces, which are necessary for the determination of the energy, can be obtained from the velocity diagram. For the solution of this problem, all the forces acting on the mechanism are replaced by one force, applied to the driving link, the energy of which is equal to the sum of energy of all the forces acting on different links.

This force is called r e d u c e d.

The magnitude of the reduced force is calculated in accordance with its specified direction and the specified point of its application. The point of application of the reduced force is called t h e p o i n t o f r e d u c t i o n.

The problem of determining the reduced force is solved simply and precisely by using N. E. Zhukovsky's theorem of the lever.

Zhukovsky's theorem. The sum of the moments of all the forces acting on the links of the mechanism (including the force of inertia), transferred parallel to themselves at analogous points of the velocity diagram, which is turned through 90°, relative to its pole is zero.

This theorem can be proved on the basis of the principle of possible displacements, according to which the sum of elementary work done by all the forces acting on the system (including the force of inertia) on the possible displacements for the system is zero.

For a mechanism, the motions of whose links are determined by the motions of its driving link, the mathematical expression of this principle will take the form

$$P_1 ds_1 \cos \alpha_1 + P_2 ds_2 \cos \alpha_2 + \ldots + P_n ds_n \cos \alpha_n = 0,$$

or shorter

$$\sum_1^n P_i ds_i \cos \alpha_i = 0,$$

where P_i denotes the forces;
ds_i — the infinitely small displacements of the points of application of forces;
α_i — the angles between the directions of forces and the directions of displacements of the points of application of forces.

After dividing both parts of the equation by infinitely small time interval dt, in the course of which the displacements are accomplished, we get

$$\sum_1^n P_i \frac{ds_i}{dt} \cos \alpha_i = \sum_1^n P_i v_i \cos \alpha_i = \sum_1^n N_i = 0,$$

where v_i denotes the velocities of the points of application of forces P_i;
$v_i \cos \alpha_i$ — the projections of velocities of the same points on the line of action of forces P_i;
N_i — the powers of forces P_i.

Fig. 173, *a* and *b* shows the diagram of link BC with the vector of force P_i, which is applied at point J, and the velocity diagram of the link with the vector of force P_i turned through 90°, the force being transferred parallel to itself at point i of the diagram.

Using the velocity diagram, turned through 90°, the power of force P_i can be expressed as follows:

$$N_i = P_i v_i \cos \alpha_i = P_i (pi) \mu_v \cos \alpha_i = P_i h_i \mu_v,$$

where h_i is the perpendicular which is drawn from pole p to the line of action of force P_i;
μ_v is the scale of velocity diagram.

The angle between $\overline{pi}$ and h_i is α_i, since $\overline{pi} \perp v_j$ and $h_i \perp P_i$.

Since the equation above is true for all forces P_i, it follows that:

$$\sum_1^n N_i = \sum_1^n P_i h_i \mu_v = \mu_v \sum_1^n P_i h_i = 0,$$

and since $\mu_v \neq 0$, then

$$\sum_1^n P_i h_i = 0,$$

which is proof of the theorem.

By applying Zhukovsky's theorem it is easy to determine the force, which has to be applied to the driving link at the specified point and on the specified line of action in order to balance all the forces acting on different links of the mechanism. This problem comes down to the determining of the moment, which balances the moments of the forces applied to the lever, which in accordance with Zhukovsky's theorem can be considered as the velocity diagram turned.

We shall explain this by example.

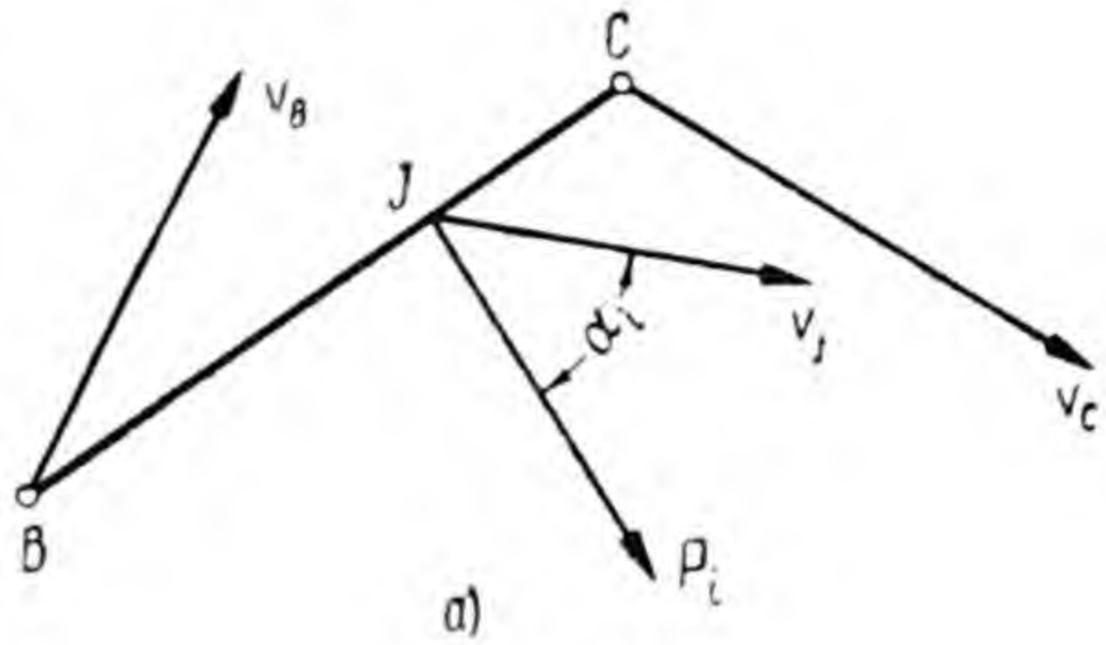

Fig. 173

Let forces P_2 and P_3, applied at points E and F, act on links BC and CD of the mechanism which is shown in Fig. 174, *a*. In determining these resultant forces the forces of inertia have been taken into consideration. Determine the force P, which in the position of the mechanism as shown in Fig. 174, *a* should be applied at point B perpendicular to driving link AB in order to balance forces P_2 and P_3. The link AB rotates clockwise with unknown angular velocity. The scale of the mechanism diagram is unknown.

We plot the velocity diagram to an arbitrary scale, which it is impossible to determine, since neither the angular velocity of rotation of link AB, nor its length are specified. On the velocity diagram (Fig. 174, *b*) we draw vectors $\overline{pe}$ and $\overline{pf}$ of velocities $\overline{v}_E$ and $\overline{v}_F$.

We turn the velocity diagram through 90° (Fig. 175) and at points e and f we transfer from the mechanism diagram the vectors of forces P_2 and P_3 parallel to themselves. We draw from pole p the perpendiculars h_2 and h_3 to the line of action of forces P_2 and P_3.

Considering in accordance with Zhukovsky's theorem the turned velocity diagram as the lever, which is rotated

by moments P_2h_2 and P_3h_3, and considering that the unknown force P must be applied at point B of the mechanism perpendicular to link AB and therefore at point b of the turned velocity diagram perpendicular to $\overline{pb}$, we shall get the equation of moments in the following form:

$$P(pb) = P_2h_2 + P_3h_3,$$

whence the magnitude of the balancing force is found to be

$$P = \frac{P_2h_2 + P_3h_3}{pb}.$$

In Fig. 175 the balancing force P must create a moment, which rotates the turned velocity diagram clockwise, but rotates the reduced force P_n, which is equal to it in magnitude, but opposite to it in direction, counter-clockwise.

From what has been said it follows that: 1) in order to determine the reduced force there is no necessity to take into consideration the dimensions of the links, but only to know their relative lengths and their relative position, and 2) the velocity diagram can be plotted to an arbitrary scale, since in the expression of force P are included not the lengths of perpendiculars h, which depend on the diagram scale, but their relations to the arm of force P, and these relations do not depend on the scales.

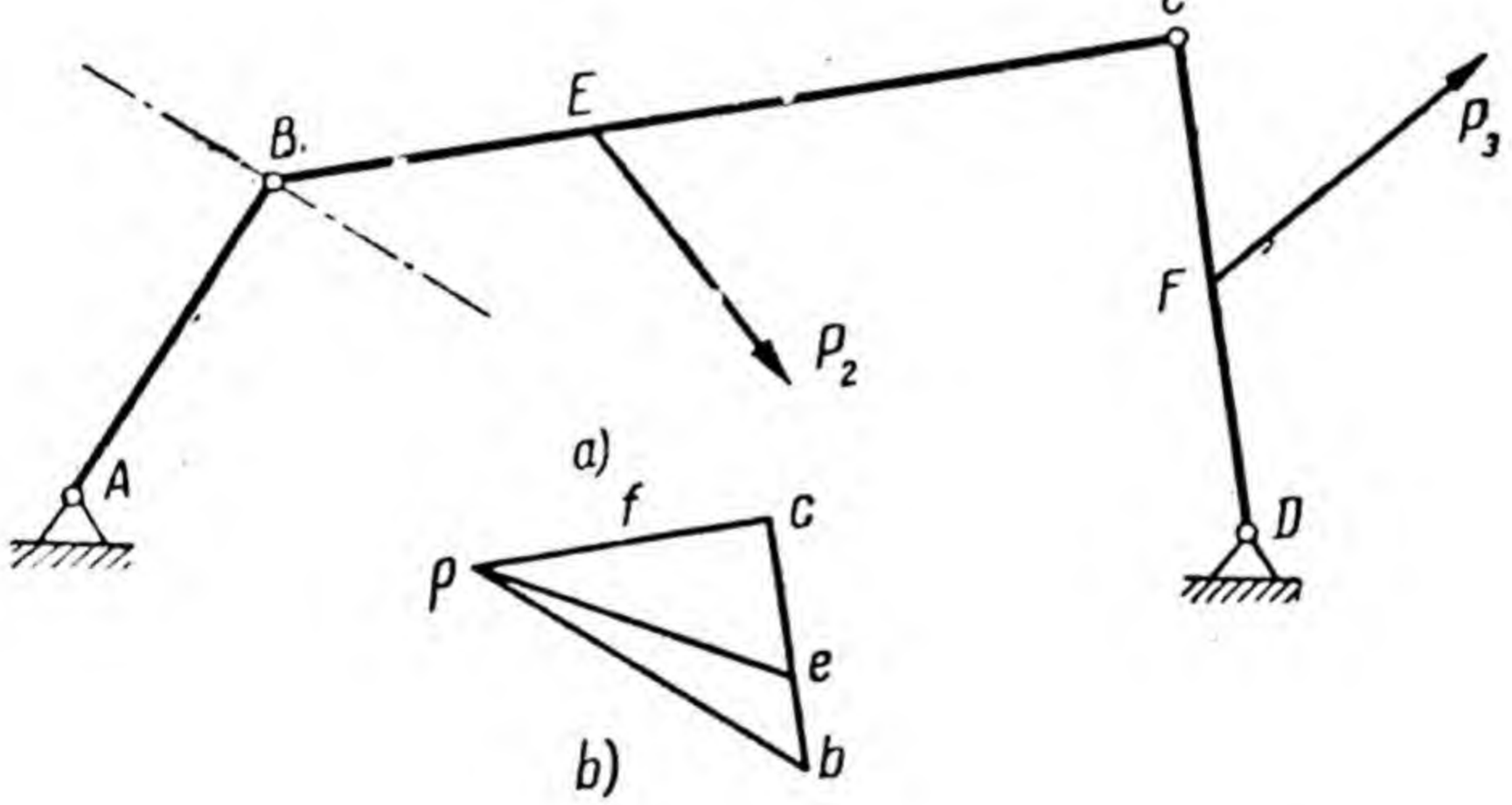

Fig. 174

In determining the magnitude of force P we have transferred on the turned velocity diagram only the active forces P_2 and P_3, while the reactions in the kinematic pairs

have not been transferred. This was done because the reactions in pairs *A* and *D* would have had to be transferred at the pole of the turned velocity diagram, so that each of the moments of these forces would have been obtained as zero. As for the reactions in pairs *B* and *C*, we would have had to transfer from each of these pairs two equal forces, opposite to each other in direction, to the same point of the turned velocity diagram, one force acting on one link of the pair, and the other acting on the other, so that the total moment of these forces would have been obtained as zero.

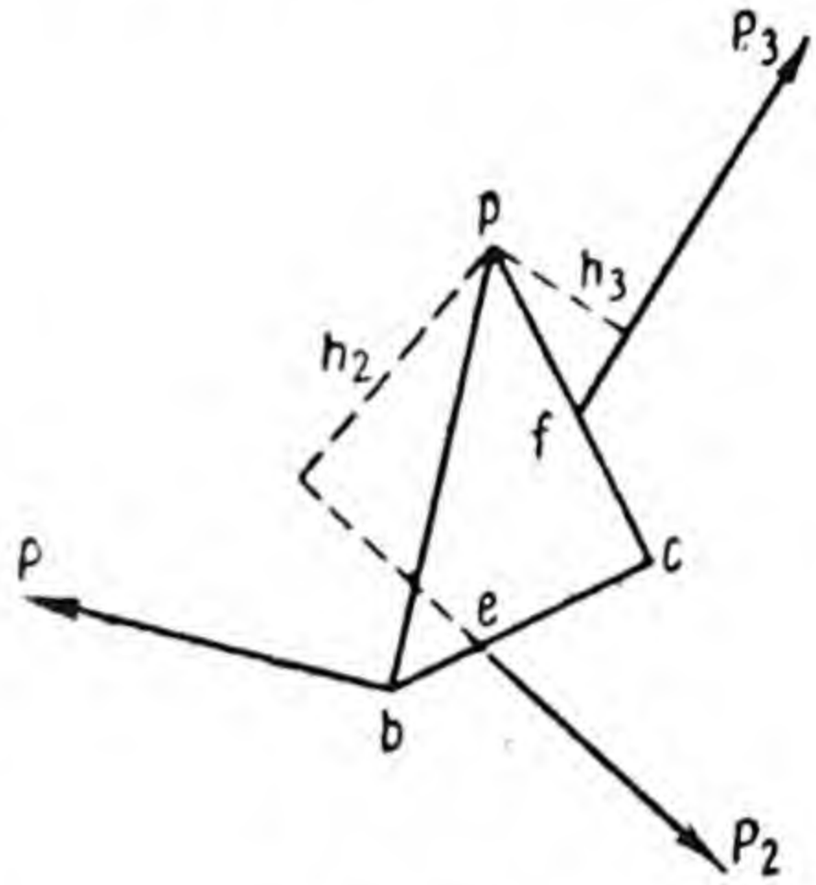

Fig. 175

If the dimensions of the mechanism links are known, then from the magnitude, direction and point of application of the reduced force it is possible to determine the balancing moment, which is created by the engine, and also the instantaneous power of the engine, if the angular velocity of the driving link is known. After the instantaneous powers of the engine for various positions of the driving link are determined and the diagram is plotted, we can determine the mean power of the engine during one revolution of the driving link, or during one cycle, if the cycle continues for more than one revolution. The thus determined mean power of the engine will be the power which is used for overcoming the useful resistances. In order to obtain the total power, it is necessary to add to the power used for overcoming the useful resistances, the power that is used for overcoming the forces of friction in kinematic pairs.

It should be remembered that the reduced force is a conditional force. Since the reduced force is a force under the action of which the mechanism power is equal to the power of all the forces applied to it, and since the magnitude of the reduced force is determined not only by the forces acting on the mechanism, but also by its point of application and the line of action, the magnitude of the reduced force can be used only in solving those problems of the dynamics of a mechanism which are connected with

the determination of the powers or amount of work done. It would be a mistake, for instance, to determine the reactions in kinematic pairs or to calculate the wear resistance of a link to which the reduced force is applied, proceeding from the magnitude, point of application and direction of the reduced force.

Example. For the mechanism shown in Fig. 124, *a* determine the magnitude and direction of the force reduced to point *B*, whose line of action is perpendicular to link *AB*.

In Fig. 124, *a* we extend the lines of action of forces P_2 and P_4 up to their point of intersection with links *BC* and *DE*, and mark the points at which these forces are applied to the links. Force P_5 is applied at the point coinciding with the centre of oscillation O_5, force P_3 is applied at point *C*. Fig. 176, *a* shows the mechanism, presented in Fig. 124, *a* with forces P_2, P_3, P_4, and P_5, which are applied at points N_2, *C*, N_4, and N_5. Force P_1 is directed along link *AB*.

Fig. 176, *b* shows an exact copy of the velocity diagram, shown in Fig. 124, *b*.

We determine the positions of points n_2, n_4 and n_5 on the velocity diagram, leaving the velocity diagram in the form in which it was obtained in Fig. 124, *b*. Then we transfer to these points the vectors of forces P_2, P_4 and P_5, and to point *c* the vector of force P_3, parallel to themselves, turned preliminarily through 90° counter-clockwise.

By drawing the arms h_2, h_4 and h_5 of the forces P_2, P_4 and P_5, we arrive at the equation relative to point *p* in the form

$$P_{bal}pb = P_2h_2 + P_3pc - P_4h_4 - P_5h_5,$$

where P_{bal} is the magnitude of the force, applied at point *b*, which balances the action of the other four forces.

The magnitudes of the forces (see p. 152) are: $P_2 = 18$ kg, $P_3 = 17.5$ kg, $P_4 = 15.6$ kg, $P_5 = 7$ kg.

The lengths of the arms are: $h_2 = 17$ mm, $pc = 39$ mm, $h_4 = 4.5$ mm, $h_5 = 17$ mm, $pb \approx 39$ mm.

Substituting the numerical values, we get $P_{bal} \times \times 39$ mm $= 18$ kg $\times 17$ mm $+ 17.5$ kg $\times 39$ mm $- 15.6$ kg $\times \times 4.5$ mm $- 7$ kg $\times 17$ mm, whence $P_{bal} = 20.4$ kg.

The total moment of forces P_2, P_3, P_4 and P_5 tends to rotate the velocity diagram about pole *p* counter-clockwise,

therefore force P_{bal} which is applied at point b and directed perpendicular to pb must create a moment which rotates the velocity diagram clockwise. Consequently, P_{bal} must be directed from point b downwards and to the right, and the unknown force P_R from point b upwards and to the left.

After turning all the forces through 90° clockwise and transferring them parallel to themselves at the points of

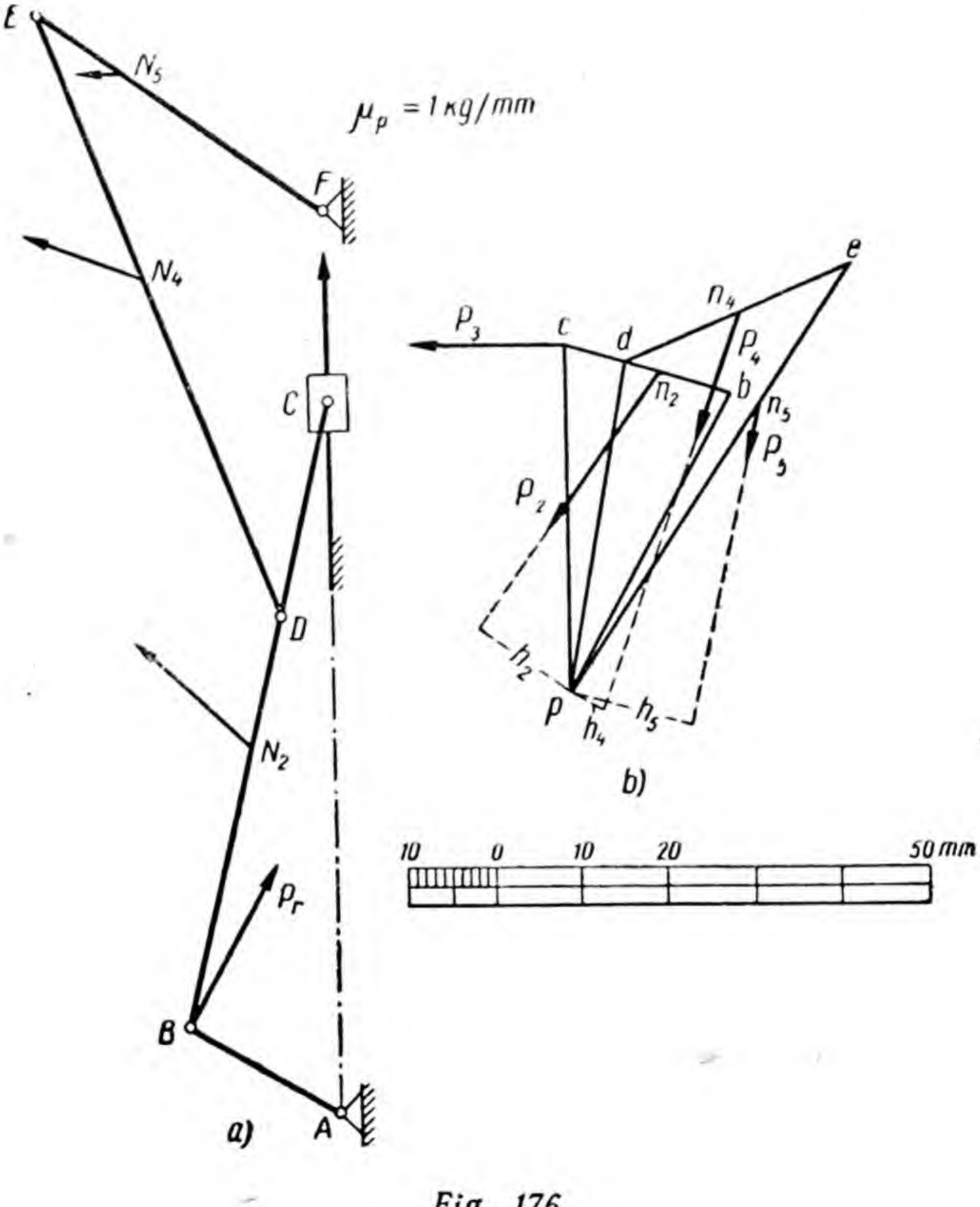

Fig. 176

their application on the mechanism links, we obtain them and the unknown force P_R in the form, shown in Fig. 176, *a*.

The forces P_1, P_{61} and P_{65} were not taken into consideration, since the latter two would have had to be applied at pole p, and the vector of force P_1, after being

turned through 90°, would have been directed along line *pb* and therefore would not create the moment relative to point *p* either.

38. REDUCTION OF MASSES

The masses of all links can be reduced to a specified point on a specified link in the same way as forces acting on the mechanism. It is most convenient to reduce both the forces and the masses to the same point of one link, and this is the usual practice.

A reduced mass is called a conditional mass concentrated at one point of the mechanism and its kinetic energy is equal to the sum of the kinetic energy of the masses of all links of the mechanism. The point at which the reduced mass is assumed to be concentrated is called the point of reduction. The link on which the point of reduction is located is called the link of reduction.

The method of determining the magnitude of the reduced mass follows from its definition: we have to add the kinetic energy of all links and divide the sum obtained by half the square of the velocity of the point of reduction. If $T_1, T_2, T_3, \ldots, T_k$ are the kinetic energies of the links, m_r is the reduced mass, v_r is the velocity of the point of reduction, then

$$m_r = \frac{T_1+T_2+T_3+\ldots+T_k}{0.5v_r^2}.$$

In order to calculate the magnitude of the reduced mass we have to know: 1) the lengths l of the links of the mechanism; 2) the masses m of the links; 3) the moments of inertia J of the links relative to the axes, which pass through the centres of gravity, and 4) the positions of the centres of gravity S. The magnitudes and directions of the angular velocities of the links do not come into consideration.

Let us determine the magnitude of the mass reduced to point B of the mechanism, shown in Fig. 177, *a*. We assume that we have at our disposal the data mentioned above. By lower indices we will indicate which magnitude relates to which link. The number of links is given in Fig. 177, *a*.

We plot the velocity diagram to an arbitrary scale, assuming that the angular velocity of rotation ω_1 is directed clockwise (Fig. 177, *b*). For the solution of the problem in hand the direction of angular velocity ω_1 is of no significance, since the lengths of the vectors on the velocity diagrams, plotted for different directions of angular velocity ω_1, are identical, and all the vectors on one diagram will be opposite in direction to the corresponding vectors on the other diagram. The directions of the linear and angular velocities do not come into consideration in determining

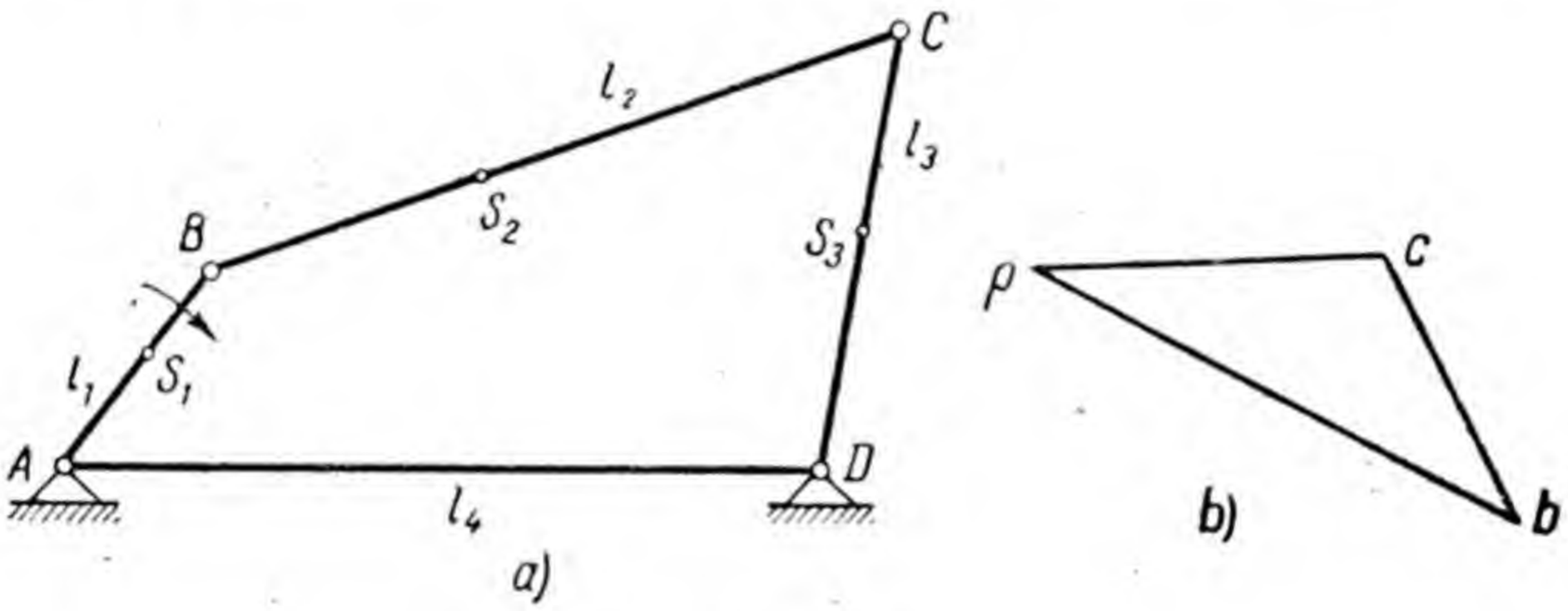

Fig. 177

the magnitudes of kinetic energy, since in the expressions $\frac{mv^2}{2}$ and $J\frac{\omega^2}{2}$ the squares of the velocities are included.

The kinetic energy of link *l* is

$$T_1 = J_A \frac{\omega_1^2}{2},$$

where J_A is the moment of inertia relative to axis of rotation *A*.

Since

$$J_A = J_1 + m_1 l^2_{AS_1},$$

then

$$T_1 = J_1 \frac{\omega_1^2}{2} + m_1 l^2_{AS_1} \frac{\omega_1^2}{2}.$$

Link *3*, like link *1*, performs rotary motion, so that we obtain similarly

$$T_3 = J_3 \frac{\omega_3^2}{2} + m_3 l^2_{DS_3} \frac{\omega_3^2}{2}.$$

The compound motion of link *2* can be considered as translation with centre of gravity S_2 and rotary motion about it. By resolving the motion of link *2* into these two motions, we get

$$T_2 = m_2 \frac{v_{S_2}^2}{2} + J_2 \frac{\omega_2^2}{2}.$$

The reduced mass to point B will be

$$m_r = \frac{T_1 + T_2 + T_3}{0.5 v_B^2} =$$

$$= \frac{(J_1 + m_1 l_{AS_1}^2)\frac{\omega_1^2}{2} + \frac{m_2 v_{S_2}^2}{2} + J_2 \frac{\omega_2^2}{2} + \left(J_3 + m_3 l_{DS_3}^2\right)\frac{\omega_3^2}{2}}{0.5 v_B^2}.$$

Substituting

$$v_B = (pb)\,\mu_v,\ v_{S_2} = (pS_2)\,\mu_v,\ \omega_1 = \frac{Pb}{l_1}\mu_v,$$

$$\omega_2 = \frac{bc}{l_2}\mu_v,\ \omega_3 = \frac{pc}{l_3}\mu_v,$$

where μ_v is the unknown scale of the velocity diagram, we reduce the above equation to the form:

$$m_r = \frac{J_1 + m_1 l_{AS_1}^2}{l_1^2} + m_2\left(\frac{pS_2}{pb}\right)^2 + \frac{J_2}{l_2^2}\left(\frac{bc}{pb}\right)^2 + \frac{J_3 + m_3 l_{DS_3}^2}{l_3^2}\left(\frac{pc}{pb}\right)^2.$$

The expression of the reduced mass does not include the magnitudes of angular accelerations of the links or the scale of the velocity diagram. As multipliers the last three factors on the right-hand side comprise the relations of the vector lengths of the velocity diagram, but not the absolute lengths of these vectors. The velocity diagram can therefore be plotted to any scale.

The magnitude of the reduced moment of inertia J_r equals

$$J_r = m_r l_1^2.$$

Example 1. For the mechanism, which is shown in Fig. 124, *a*, according to the data given on p. 147, deter-

mine the mass reduced to point B from the masses of links BC, DE, EF and the slider.

We determine the kinetic energies of the links.

The compound motion of link BC (link No. 2) we consider as translation with the centre of gravity S_2 and rotary motion about it. In accordance with this we get

$$T_2 = m_2 \times \frac{v_{S_2}^2}{2} + J_2 \frac{\omega_2^2}{2}.$$

The kinetic energy of the slider (link No. 3), which performs translatory motion, equals

$$T_3 = m_3 \frac{v_C^2}{2}.$$

The compound motion of link DE (link No. 4) we consider as translation with the centre of gravity S_4 and rotary motion about it. Therefore

$$T_4 = m_4 \frac{v_{S_4}^2}{2} + J_4 \frac{\omega_4^2}{2}.$$

The moment of inertia J_{EF} of link EF (link No. 5), which performs rotary motion, equals

$$J_{EF} = J_5 + m_5 l_{FS_5}^2.$$

The kinetic energy of link EF is

$$T_5 = (J_5 + m_5 l_{FS_5}) \frac{\omega_5^2}{2}.$$

The kinetic energy of all the four links equals

$$T = \frac{m_2 v_{S_2}^2 + J_2 \omega_2^2 + m_3 v_C^2 + m_4 v_{S_4}^2 + J_4 \omega_4^2 + (J_5 + m_5 l_{FS_5}) \omega_5^2}{2}.$$

The moments of inertia relative to the axes, which pass through the centres of gravity, are given on p. 147, the masses of the links on p. 152. In order to determine the velocities of the centres of gravity we use the velocity diagram plotted in Fig. 124, *b*, a copy of which is given in

Fig. 178. After we have determined the positions of points s_2, s_4 and s_5 on the diagram, drawn the vectors $\overline{ps_2}$, $\overline{ps_4}$ and $\overline{ps_5}$, and measured the lengths of these vectors, and also of the vectors $\overline{pc}$, we get

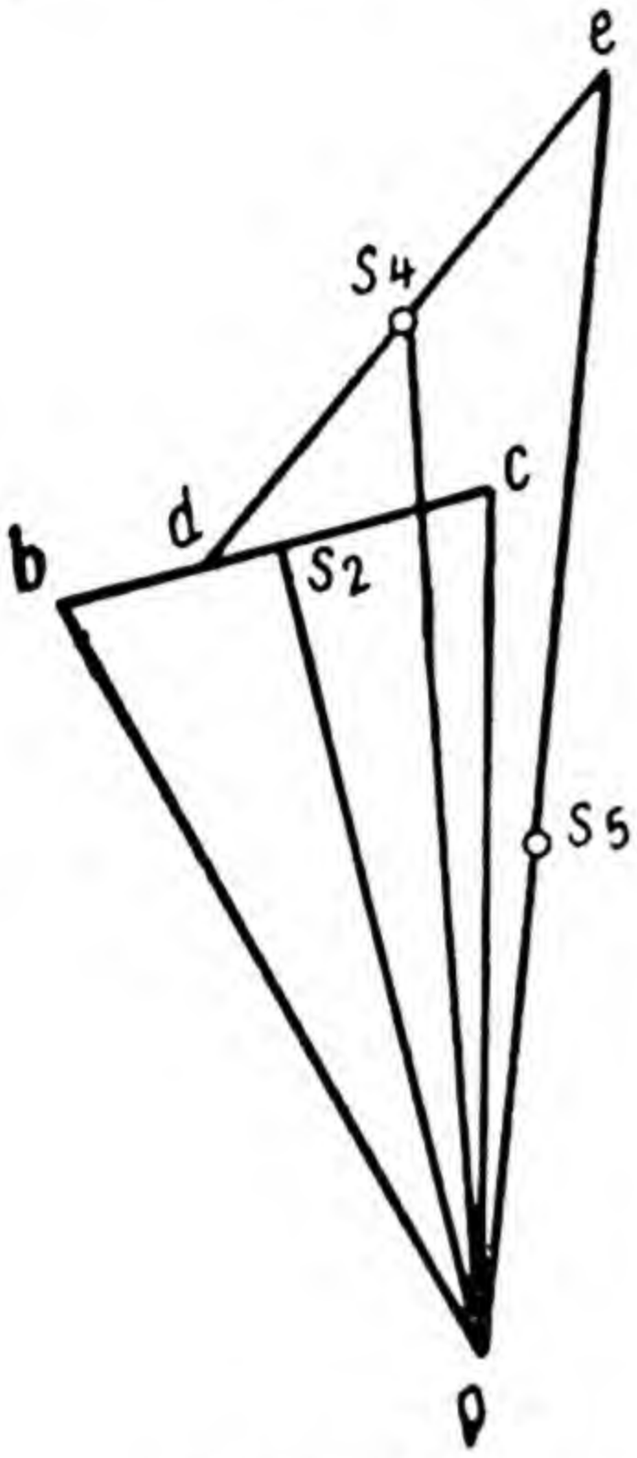

$$v_{s_2} = ps_2\mu_v = 38 \text{ mm} \times 0.04 \text{ m/sec} \times \times \text{mm} = 1.52 \text{ m/sec};$$

$$v_{s_4} = ps_4\mu_v = 47 \text{ mm} \times 0.04 \text{ m/sec} \times \times \text{mm} = 1.88 \text{ m/sec};$$

$$v_{s_5} = ps_5\mu_v = 23.2 \text{ mm} \times 0.04 \text{ m/sec} \times \times \text{mm} = 0.93 \text{ m/sec};$$

$$v_c = pc\mu_v = 39 \text{ mm} \times 0.04 \text{ m/sec} \times \times \text{mm} = 1.56 \text{ m/sec}.$$

The angular velocities of rotation of the links:

$$\omega_2 = \frac{bc\mu_v}{l_{BC}} = \frac{19.5 \text{ mm} \times 0.04 \text{ m/sec} \times \text{mm}}{0.18 \text{ m}} = 4.3 \text{ sec}^{-1};$$

$$\omega_4 = \frac{de\mu_v}{l_{ED}} = \frac{28 \text{ mm} \times 0.04 \text{ m/sec} \times \text{mm}}{0.18 \text{ m}} = 6.2 \text{ sec}^{-1};$$

$$\omega_5 = \frac{pe\mu_v}{l_{EF}} = \frac{58 \text{ mm} \times 0.04 \text{ m/sec} \times \text{mm}}{0.1 \text{ m}} = 23.2 \text{ sec}^{-1}.$$

Fig. 178

Substituting these values, we get $T = 2.85$ kgm.

At the same time $T = m_R \frac{v_B^2}{2}$.

Taking into consideration that the velocity of point B $v_B = 1.57$ m/sec (see p. 147), we get $2.85 = 0.5\ m_R\ 1.57^2$, whence $m_R = 2.32 \text{ kg} \times \text{sec}^2/\text{m}$.

The reduced moment of inertia $J_R = m_R l_{AB}^2 = 2.32 \times \times 0.05^2 = 0.0058 \text{ kg} \times \text{m} \times \text{sec}^2$.

Example 2. Fig. 179 shows the pitch circles of three engaged toothed wheels whose respective numbers of teeth

are: $z_1=20$, $z_2=30$, and $z_3=40$. The moments of inertia of the wheels in $\text{kg}\times\text{m}\times\text{sec}^2$ are: $J_1=0.01$, $J_2=0.0225$, $J_3=0.04$. Determine the moment of inertia J_R reduced to the shaft of wheel *1* from the masses of all toothed wheels.

The angular velocities of rotation of the wheels are inversely proportional to the numbers of their teeth. We shall express the angular velocities of rotation of wheels *2* and *3* through the angular velocity of wheel *1*:

$$\omega_2=\omega_1\frac{z_1}{z_2}=\omega_1\frac{20}{30}=\frac{\omega_1}{1.5};\quad \omega_3=\omega_1\frac{z_1}{z_3}=\omega_1\frac{20}{40}=\frac{\omega_1}{2}.$$

The kinetic energies of the wheels:

$$T_1=J_1\frac{\omega_1^2}{2}=0.5\times0.01\times\omega_1^2\ \text{kg}\times\text{m};$$

$$T_2=J_2\frac{\omega_2^2}{2}=0.5\times0.0225\times\left(\frac{\omega_1}{1.5}\right)^2=0.5\times0.01\times\omega_1^2\ \text{kg}\times\text{m};$$

$$T_3=J_3\frac{\omega_3^2}{2}=0.5\times0.04\times\left(\frac{\omega_1}{2}\right)^2=0.5\times0.01\times\omega_1^2\ \text{kg}\times\text{m}.$$

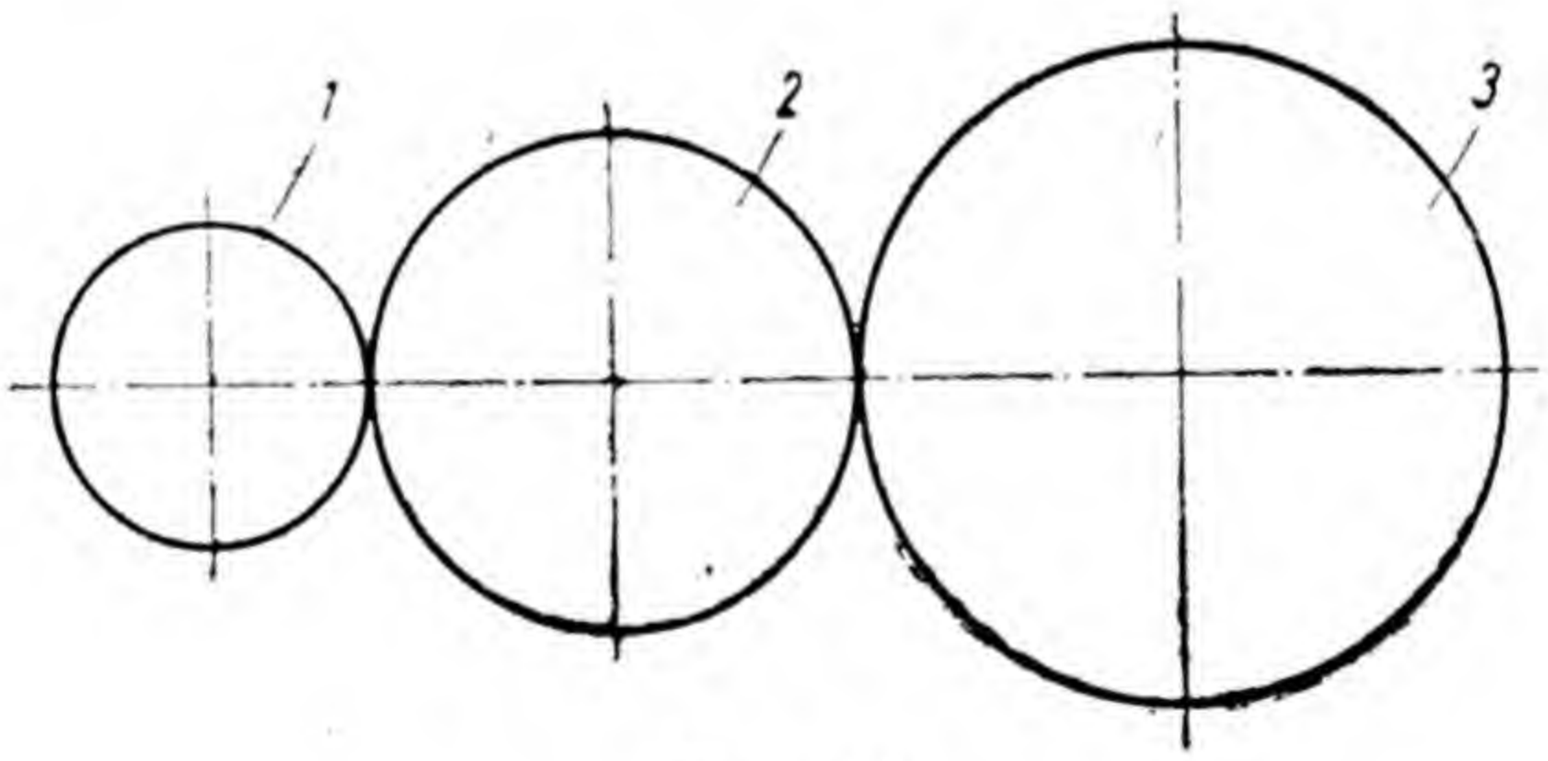

Fig. 179

The kinetic energy of all the wheels:

$$T=T_1+T_2+T_3=0.5\times0.03\times\omega_1^2\text{kg}\times\text{m}.$$

At the same time $T=J_R\frac{\omega_1^2}{2}$,

whence $J_R=0.03\ \text{kg}\times\text{m}\times\text{sec}^2$.

39. EQUATION OF THE MOTION OF THE POINT AND LINK OF REDUCTION

After reducing the forces and masses to one point the equation of motion

$$A_d = A_{res} + \sum \frac{mv^2}{2} - \sum \frac{mv_0^2}{2}$$

is reduced to a simpler form:

$$A_{r_d} = A_{r_{res}} + \frac{m_r v_r^2}{2} - \frac{mr_0 v_{r_o}^2}{2},$$

where A_{r_d} and $A_{r_{res}}$ are amount of work done by the driving forces and resistances during the time interval under consideration;

m_r and m_{r_o} are the magnitudes of the reduced masses at the end and beginning of the time interval under consideration;

v_r and v_{r_o} are the linear velocities of the point of reduction at the end and beginning of the time interval under consideration.

If the forces and masses are reduced to one point and the laws of changing the reduced force and mass are ascertained, the problem of the motion of the link of reduction can be solved by the following equation in differential form:

$$(P_d + P_{res})\, ds = \frac{1}{2} d(m_r v_r^2) = m_r v_r dv_r + \frac{1}{2} v_r^2 dm_r,$$

where the factors P_d and P_{res} in the algebraic sum $P_d + P_{res}$ must be taken with corresponding signs.

The equation of motion is suitable in this form if the link of reduction performs translatory motion. If the link of reduction performs rotary motion it is more convenient to use instead of the reduced forces P_d and P_{es} the reduced moments M_d and M_{res} and instead of the reduced mass m_r

the reduced moment of inertia J_r. In this case the equation of motion will assume the form:

$$(M_d+M_{res})\,d\varphi=\frac{1}{2}\,d(J_r\omega_r^2)=J_r\omega_r d\omega_r+\frac{1}{2}\omega_r^2\,dJ_r,$$

where φ is the angle of rotation of the link of reduction, and

ω_r is the angular velocity of rotation of the link of reduction.

In different cases the forces P_d and P_{res} may be either constants or functions of the velocity, or functions of the path of the point of reduction, while moments M_d and M_{res} are correspondingly either constants or functions of the angular velocity of rotation, or functions of the angle of rotation of the link of reduction. The magnitude of the reduced mass may be either a constant or a function of the path of the point of reduction; the magnitude of the reduced moment of inertia is correspondingly either a constant or a function of the angle of rotation of the link of reduction. The laws for changing all the magnitudes that have been indicated above can be specified either analytically or graphically. The particular form to which the equations of motion are reduced depends on the laws governing the forces (or moments) and reduced masses (or reduced moments of inertia).

40. REGULATION OF THE MOTION OF MACHINES

Depending on the purpose of a machine either the speed of its operating member has to be regulated, or its efficiency or the pressure created by it. For example, in a stationary engine it is necessary to maintain a constant speed of the operating member, in a transport engine (for instance, a car engine) it is necessary to be able to change the speed within wide limits. In compressors, used to transfer gases, or pumps used to transfer fluids, either the pressure which causes the substance being transferred to flow into the delivery pipeline or the efficiency, i. e. the quantity of substance transferred per unit of time may be regulated. In subsequent discussion we will consider only the speed regulation of operating members of engines.

From the equation of motion of a machine it follows that in order to change the velocities of material points of moving machine elements it is necessary to change the

difference ($A_d - A_{res}$) of work done by the driving forces and resistances. This difference can be changed by either changing the magnitude of work done by the driving forces or the magnitude of work done by resistances, or both simultaneously.

Regulation of the operating-member speed by decreasing work done by resistances is inexpedient: in order to be able to decrease the parasitic resistances the machine has to work under deliberately increased parasitic resistances (which consumes additional energy); in the case of the useful resistances, their decrease during the regulation of speed would mean depriving the machine of the possibility to accomplish its purpose.

Devices, which help to increase the parasitic resistances when it is necessary to decrease speed, take the form of brakes in various transport machines, where they are not only expedient, but absolutely essential. Such devices are used only in cases where complete termination of the work of the driving forces is insufficient for a rapid decrease of speed or when the action of the driving forces cannot be eliminated, for instance, in the downhill movement of a car.

Stationary engines, which are designed to actuate machine-tools, pumps, electrical current generators, etc., are not equipped with brakes. In cases where it is necessary to decrease rapidly the speed of the moving parts the braking devices are positioned not on the engines, but on the machine-tools; such a necessity arises from considerations of safety precautions or production requirements. In such cases devices are also installed to effect the rapid disconnection of the machine-tool from the engine.

It is apparent therefore that, apart from brakes which are basic equipment in transport machines and serve only to decrease the speed of the machine's operating members, the only means to regulate the difference between the work done by the driving forces and the forces of resistance is usually a change in the work of the driving forces. This can be accomplished by adopting the member of the machine by which energy is supplied to the member, which absorbs the work done by external forces, to the piston of a steam engine or an internal-combustion engine, to the blades of a water or steam turbine, etc. In the case of a transport engine it is the operator controlling the engine operation

who regulates its motion; in a stationary engine, whose operating member has to rotate with constant angular velocity, the regulation is automatic.

According to the method of speed regulation (number of revolutions per unit of time) of the operating member, stationary engines may be divided into three types: 1) electric motors; 2) engines, in which the members, that absorb the supplied energy to the engine, perform rotary motion (water and steam turbines), and 3) piston engines (steam engines, internal-combustion engines).

In stationary electric motors maintenance of a definite speed is automatically accomplished without any regulating devices, since the design of the electrical portion of these engines provides for a constant conformity between the developed power of the engine and the energy consumed by it. The unit, which is supplied with energy for consumption by the electric motor, is located in direct interaction with the energy source. This interaction is produced in such a way that the amount of consumed energy by the engine is in inverse (but not proportional) relation to the angular velocity of rotation of the operating member: with an increase in the work done by resistances the angular velocity of rotation of the operating member decreases slightly, which gives an increase in the energy influx into the engine; on the other hand, with a decrease in work done by the resistances the angular velocity increases and as a result the influx of energy decreases. The number of revolutions of the operating member per unit of time is therefore not maintained constant when a change in work done by the resistances occurs, although these remain within certain close limits to each other. Thus, for example, in the most widely applied industrial engines (three-phase asynchronous engines) the minimum number of revolutions per minute at full load is only 3-4 per cent less than the maximum at idle run. Such difference is of no practical importance in the majority of cases, as is shown by the wide application of engines of this type.

In engines of the second type (a water or steam turbine) the unit which absorbs the energy supplied to the engine, as is the case in the electric motor, is under the constant action of the energy source. For example, in a water turbine (Fig. 180) through the guiding passages *A* (which are

located around wheel *C* fixed on crankshaft *B*) water under pressure flows continuously through the wheel passages, formed by blades *D*, which absorb the mechanical energy that is supplied to the turbine by the water. However, as distinct from the action in electric motors, the unit which absorbs the work done by the external forces (the wheel with blades) is not in direct interaction with the energy source in engines of the second type. Interaction in these engines is achieved by means of special mechanical devices called governors.

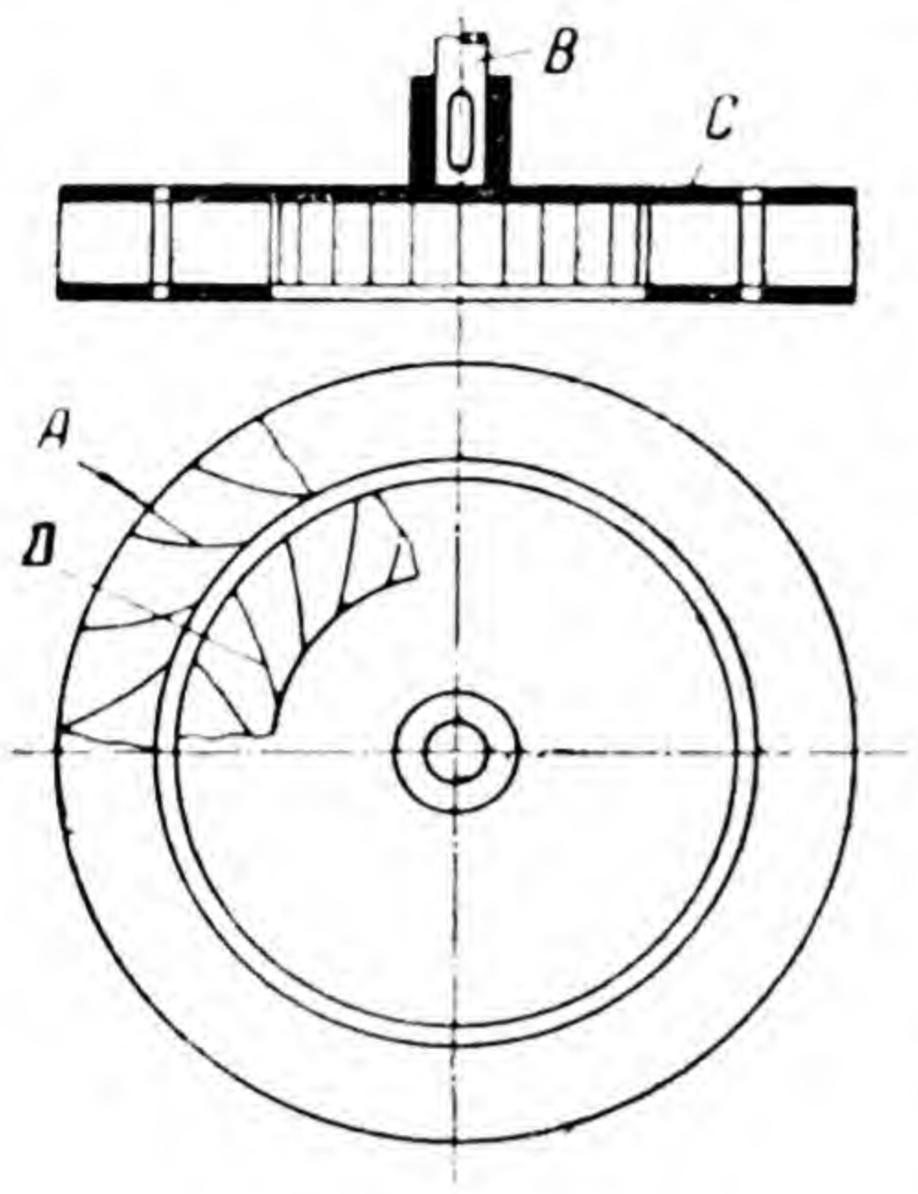

Fig. 180

Up to the present day many governor designs, based on different principles, have found practical application. One of the most widely applied governors is the centrifugal governor, shown diagrammatically in Fig. 181, where *M* are heavy balls secured to the ends of levers *AC* and *BD* connected with vertical shaft *S* to turning pairs *A* and *B*. Slider *K*, connected to turning pairs *E* and *F* by levers *CE* and *DF*, slides on shaft *S* driven by the engine crankshaft through a transmission system (not shown in Fig. 181); levers *CE* and *DF* are connected to turning pairs *C* and *D* by levers *AC* and *BD*. Slider *K* is connected to the engine member, which supplies the unit that absorbs work done by external forces with the working substance (steam or water under pressure, liquid fuel or fuel gas). The joint not shown in Fig. 181 is arranged so that during slider motion upwards the influx of energy to the engine decreases, and during motion downwards, increases.

With a definite angular velocity of rotation of the engine crankshaft and, consequently, also of shaft *S* of the governor, the levers *AC* and *BD* together with slider *K* assume definite positions also, since the elastic force of spring *R* is balanced by the centrifugal force of inertia of balls *M*.

With a decrease in work done by resistances the angular

velocity of rotation of the engine crankshaft and, consequently, also of shaft *S* of the governor increases; as a result the centrifugal forces from the balls increase, and slider *K* moving upwards decreases the influx of energy to the engine, thus restoring the equilibrium between work done by the driving forces and work done by resistances. With an increase in work done by resistances slider *K*, moving downwards, increases the influx of energy to the engine, and thus restores the equilibrium.

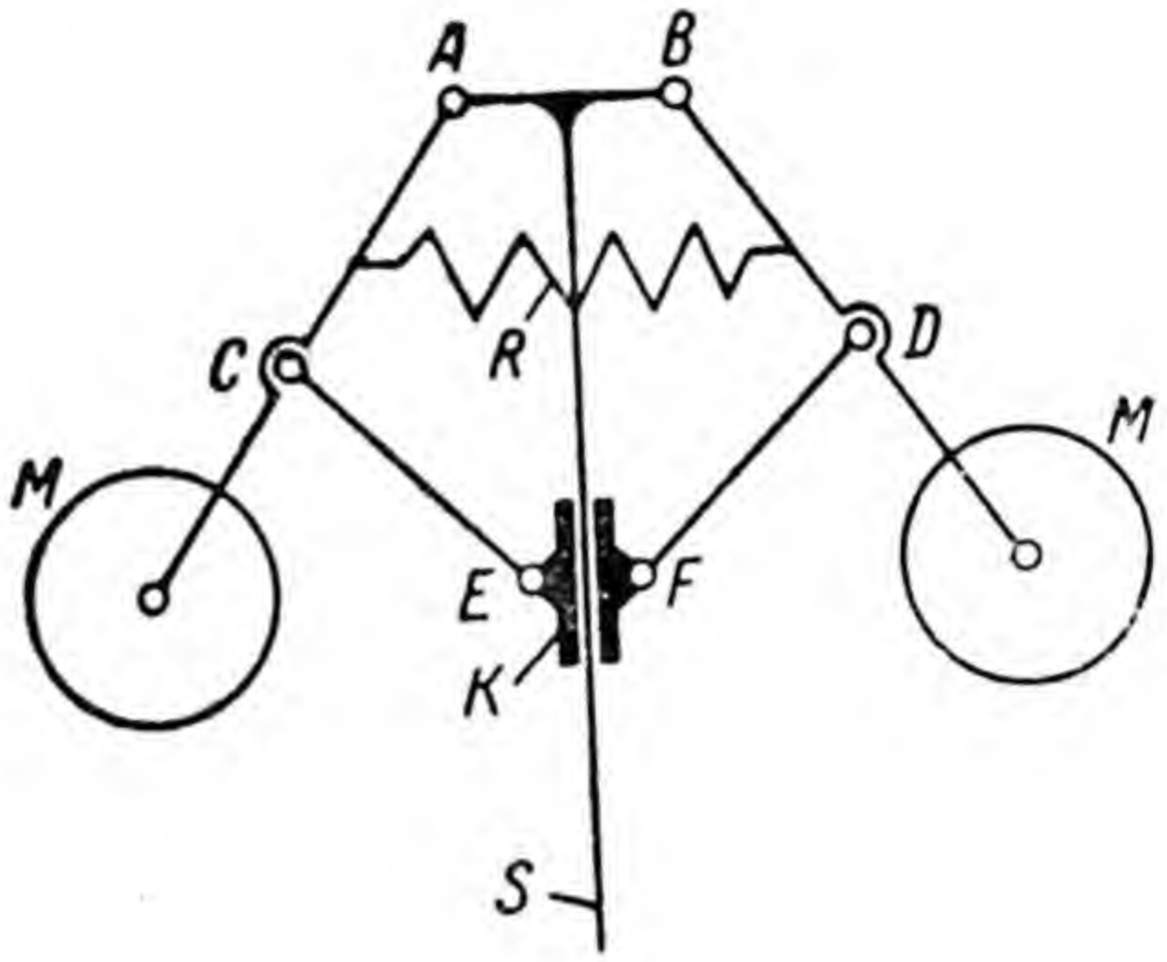

Fig. 181

From what has been said it follows that as long as the work done by resistances does not change, the governor maintains the angular velocity of rotation of the engine crankshaft very near to constant, but with different magnitudes of work done by resistances the slider must be in different positions on the governor shaft; this, however, is possible only with the different angular velocity of rotation of the engine crankshaft.

It is obvious that in designing governors, consideration is given to the fact that the angular velocity of rotation of the engine crankshaft during regulation will not exceed the practical limits. If it is necessary to maintain the angular velocity at an invariable level regardless of the power developed by the engine, more complex governing devices are used.

In piston engines the unit, which absorbs work done by the motive forces (the piston), performs reciprocating motion. This complicates considerably the regulation of the angular velocity of rotation of the engine crankshaft.

All piston engines are based on the slider crank mechanism. In Chapter I Fig. 13, *a* (see p. 14) shows a simplified design scheme of a single cylinder internal-combustion engine and Fig. 13, *b* shows the design scheme of the main mechanism of this engine, which transforms reciprocating motion of the motive link (piston) into

rotary motion of the crank and the engine crankshaft, rigidly coupled to the crank.

Fig. 182 shows an indicator diagram of a four-stroke diesel engine, a type of internal-combustion engine very widely applied, indicating to what action of force the piston is subjected during the operation of this engine. By the axis of abscissae of the diagram the volumes are laid off, and by the axis of ordinates, the pressures of gases over the piston. When the piston is in the extreme top position as shown in Fig. 13, *a* volume V_0 (Fig. 182) of the gases over the piston is minimum; volume V_0 is called "dead space". In the extreme bottom position of the piston, located from the extreme top at a distance equal to the double length of the crank, the volume V_{max} of the gases over the piston is maximum. The volume V of gases over the piston with distance s of the piston from the extreme top position and area F of the piston cross section is connected by the obvious relation:

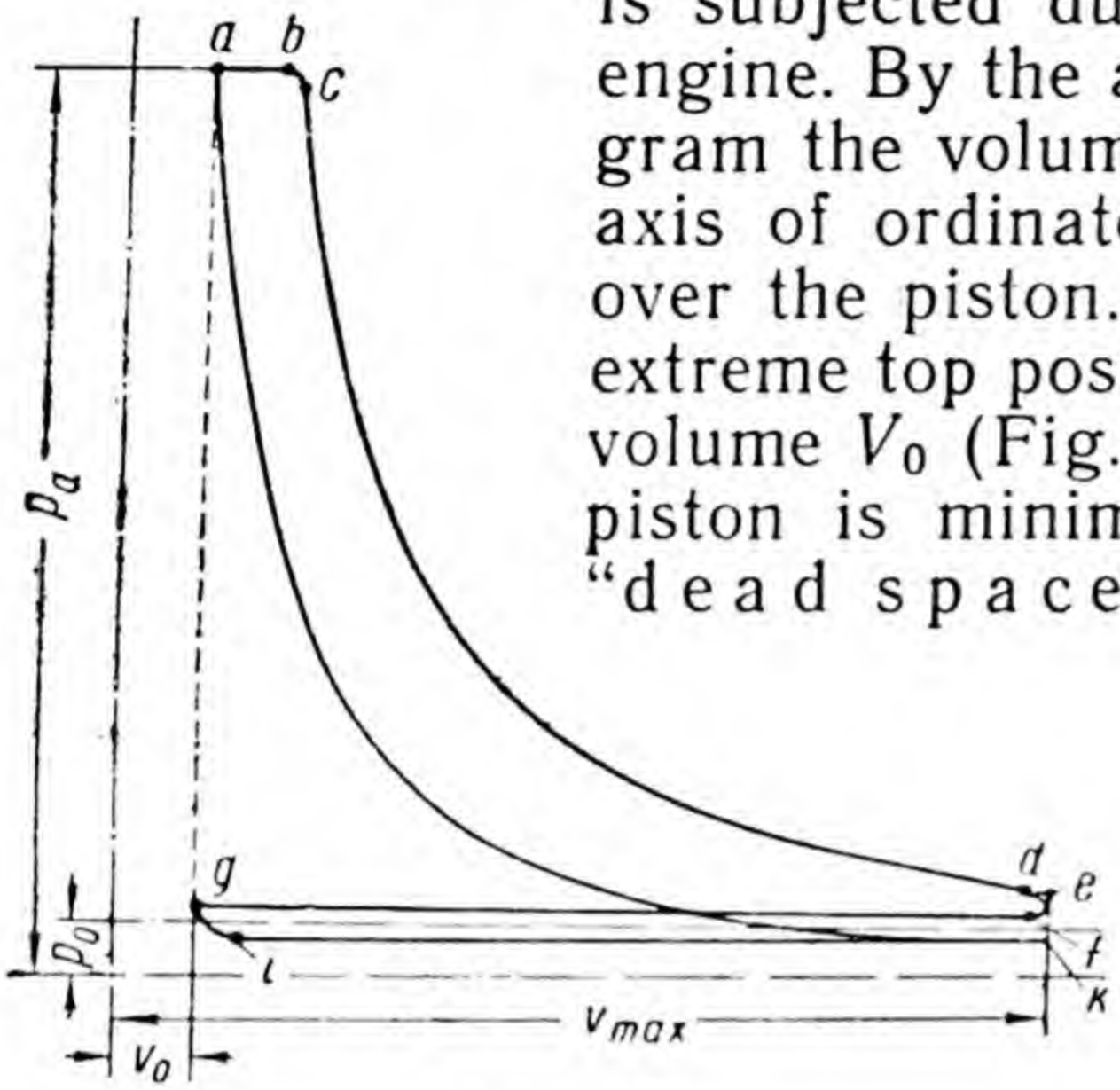

Fig. 182

$$V = V_0 + F \times s.$$

At point *a* of the diagram, which corresponds to the extreme top position of the piston, pressure p_a of the gases is maximum, since in the cylinder there is air at high temperature, caused by the rapid compression of the air up to several tens of atmospheres at the preceding piston stroke upwards.

The upper portion of the diagram from point *a* to the right shows the process in the cylinder during piston motion downwards from the extreme top position. The pressure of the gases does not change from point *a* to point *b*, even though the volume increases; this is because at this position of the piston stroke the cylinder receives finely pulverized liquid fuel (oil), which quickly burns out entering the compressed air with a temperature which exceeds the temperature of self-ignition of the liquid. Despite the

increasing volume of gases during piston motion, the pressure does not decrease, firstly, because the amount of gases increases as the liquid burns out and, secondly, because an increase in the temperature of the gases should have decreased when the volume increased without the influx of heat, liberated when the liquid burnt out.

In the piston position, which corresponds to point *b* of the diagram, the inlet of liquid to the cylinder is stopped and as a result the pressure begins to decrease. At first the pressure decreases rather slowly: from point *b* to point *c* that portion of the liquid, which did not burn out when the inlet of liquid to the cylinder was stopped, continues to burn. From point *c* the pressure decreases rapidly by curve *cd* during piston motion to the extreme bottom position. Point *e* of the diagram corresponds to the extreme bottom position of the piston.

From point *d* the pressure decreases not by curve *de*, but much quicker. This occurs because in the position of the piston, which corresponds to point *d* of the diagram, the exhaust valve (not shown in Fig. 13, *a*) opens, joining the cylinder volume over the piston with the atmosphere. Therefore, on the diagram portion from point *d* to the right the pressure decreases not only because of the increase in the volume of gases, but also because of the escape of some of the gases into the atmosphere.

At the return stroke of the piston upwards the products of combustion are pushed out into the atmosphere through the opened exhaust valve. The pressure of gases is then maintained near to the atmospheric (line *fg* of the diagram), but slightly greater than atmospheric pressure p_0, since only at the expense of a certain difference in pressures on both sides of the exhaust valve can the gases achieve the speed required to escape from the cylinder and the resistances to their motion be overcome.

Point *g* of the diagram corresponds to the extreme top position of the piston. At the following stroke of the piston downwards with the exhaust valve closed and the inlet valve open the air is sucked into the cylinder from the atmosphere. At the beginning of the stroke pressure decreases by curve *gi* and subsequently until the end of the piston stroke downwards (line *ik* of the diagram) is retained slightly below the atmospheric because of the reason just stated.

At the next piston stroke upwards with the inlet and exhaust valves closed the air is compressed (curve *ka*) to a pressure of several tens of atmospheres, as a result of which the air temperature towards the end of the piston stroke rises to several hundred degrees and exceeds the temperature of self-ignition of the liquid, which begins to flow into the cylinder in finely pulverized form at the beginning of the following piston stroke downwards.

We have described briefly, without going into details unimportant for the purpose that we are here concerned with, the four-stroke diesel, an internal-combustion engine. From what has been said previously it follows that out of the four piston strokes there is only one during which pressure $(p—p_0)$, where p is the pressure of gases over the piston and p_0 is the atmospheric pressure, is directed along the piston stroke, thereby creating a force which moves the piston; this piston stroke is called the working stroke. In the course of the next two strokes after the working one the piston overcomes insignificant resistances to its motion, and during the following stroke considerable and ever increasing resistances.

Under such action of the force, to which the piston is subjected by the gases, the engine would not only be unable to operate continuously, but the piston would be unable to accomplish one stroke upwards, even without any resistances to its motion, if rotation of the crankshaft did not continue by inertia during the next three piston strokes after the working stroke.

The work of an engine becomes possible only when there is on the crankshaft a wheel with a sufficiently great moment of inertia. This wheel is called a flywheel. The purpose of the flywheel is to absorb the energy during the working stroke of the piston and use it during the entire period of engine operation to overcome all the resistances, including also those which the piston has to overcome during the three strokes following the working stroke.

The kinetic energy $J\frac{\omega^2}{2}$ of the flywheel, where J is the moment of inertia, and ω is the angular velocity of flywheel rotation, can be compared with potential energy Qh of liquid in a vessel, where Q is the weight and h is the liquid height. If in the course of every fourth second the vessel takes in, for instance, $0.01Q$ of liquid with any constant or

variable velocity and during all four seconds the same quantity of liquid will flow out from the vessel also with any constant or variable velocity, the change in liquid height in the vessel will not exceed $0.01Q$. Therefore the potential energy of liquid in the vessel will not decrease by more than 1 per cent. Similarly, if in the course of the piston working stroke the flywheel receives energy in a quantity, which is much less than its kinetic energy $J\frac{\omega^2}{2}$, and the same quantity is used by the flywheel to rotate the crankshaft during all four piston strokes, the kinetic energy, and consequently, also the angular velocity of the flywheel will change insignificantly.

In designing a flywheel due consideration is given to permissible changes, that depend on the engine purpose, of the angular velocity of crankshaft rotation within the limits of one cycle. These changes are allowed for by the coefficient of irregularity, which equals

$$\delta = \frac{\omega_{max} - \omega_{min}}{\omega_{mean}},$$

where ω_{mean}, ω_{max}, ω_{min} are the mean, maximum and minimum angular velocities of rotation of the engine crankshaft in the course of one cycle.

Stricter requirements with regard to uniformity of motion have to be satisfied by engines, which impart motion to generators of alternating current; in these engines the coefficient of irregularity is not taken beyond 1/200—1/300 and in some cases much less (up to 1/1000).

From what has been said it follows that the angular velocity of crankshaft rotation is equalized by the flywheel in each cycle. But, if the power, which is used by the flywheel to overcome the resistances, begins to exceed the amount of energy, received by the flywheel in unit time, or becomes less than this amount the angular velocity of the flywheel will gradually change. In this case the mentioned governor or any other type will start working. In the example given above the action of the governor will take place on portion *ab* of the diagram (Fig. 182): depending on the direction of change of the magnitude of the angular velocity of crankshaft rotation, the portion *ab* will be respectively shortened or lengthened by the governor, i. e. a lesser or greater quantity of the liquid fuel will be

introduced into the cylinder at the beginning of the working stroke of the piston.

The flywheel is an absolutely essential appliance not only in piston engines; flywheels have to be installed also on machine-tools, the working units of which have to overcome strong and intermittently acting resistances by the processed materials. The flywheel in such machines is like a reservoir of energy, receiving energy from the engine continuously and uniformly and in turn from time to time using separate portions of it.

41. DETERMINING THE BASIC DIMENSIONS OF THE ENGINE FLYWHEEL

Variations of the angular velocity of rotation of the flywheel within the limits of one cycle occur mainly, as indicated previously, as a result of the non-coincidence of the laws of change of the reduced moment of the driving forces and the moment of the forces of resistance. Let us examine in detail the phenomena which take place during steady motion, and the considerations which ought to guide us when determining the basic dimensions of a flywheel (Fig. 183).

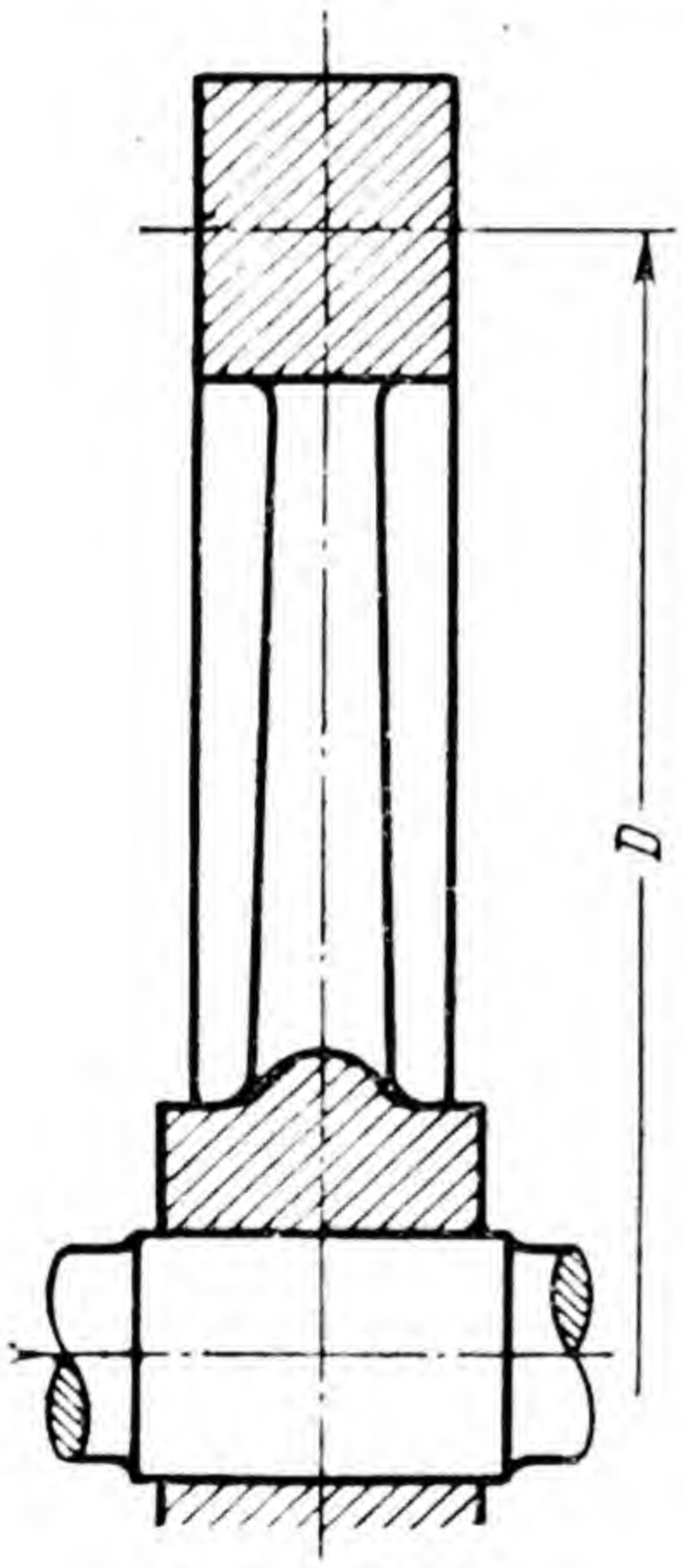

Fig. 183

Let us refer to the type of engine that we discussed previously, i. e. the single cylinder four-stroke diesel, one cycle of which consists of four piston strokes accomplished in the course of two crank revolutions. We shall proceed from the indicator diagram, shown in Fig. 182, and assume that this diagram was taken during steady motion and operation of the engine at total power.

The ordinates on the diagram express the pressures of the gases on the piston in its various positions. After multiplying the ordinates by the piston area, we obtain the forces by which the gases press on the piston. The volumes of gases over the piston are laid off by the axis of abscissae on the diagram. After dividing the

abscissae by the piston area, we obtain the paths which are passed by the piston from the initial upper position to the lower and back. In so doing we will not change the diagram, but will only obtain different scales of the abscissae and ordinates.

Referring to the kinematic diagram of the slider crank mechanism (Fig. 184), which is the basis of the engine under discussion, we assume that force P acting through the gases on the piston (the slider in the diagram) acts at point C in the direction parallel to the directrix x—x. Taking up this force at point C the connecting rod acts on the crank at point B with a certain force, whose component in the direction perpendicular to AB is the tangential force T, which creates the moment TR that rotates the crank, where R is the crank length.

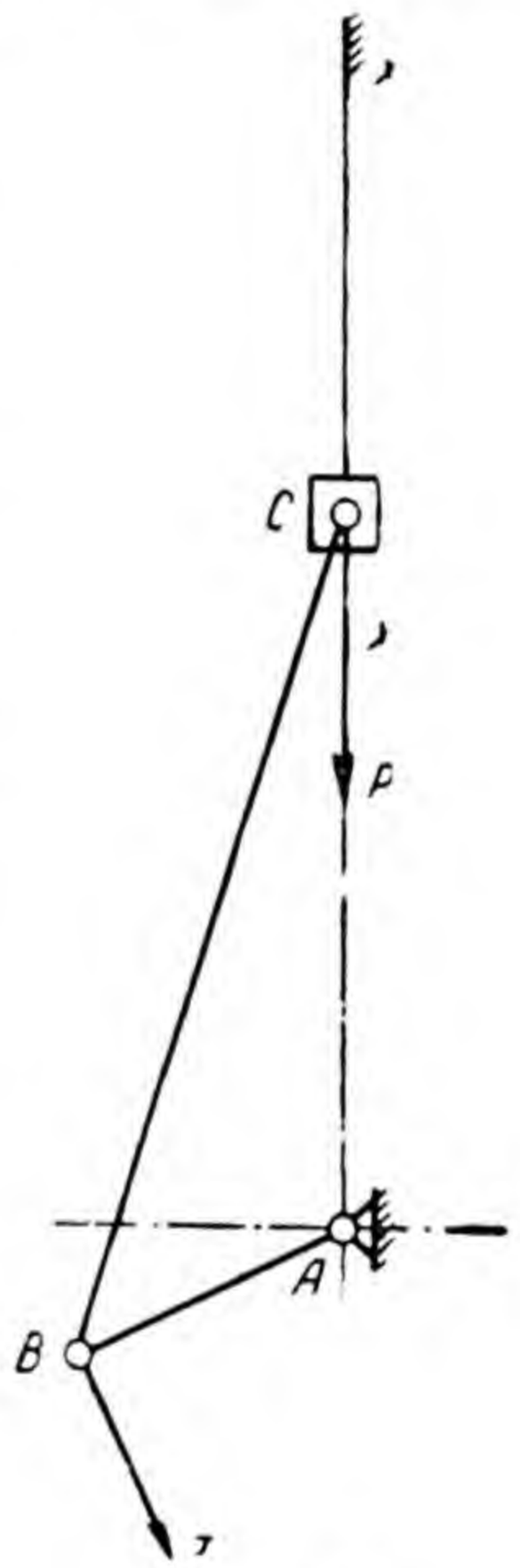

Fig. 184

Neglecting the losses in friction, the relation between force P and the tangential force T at point B of the crank can be obtained by expressing the instantaneous power of the engine as follows

$$Pv_C = Tv_B,$$

whence

$$T = P\frac{v_C}{v_B}.$$

Since the magnitude of velocity v_B changes only within very narrow limits, we shall consider it hereafter as constant. The magnitude of force P in various positions of point C on its path at different strokes of the piston can be determined by the diagram produced in the manner described above. The velocities v_C in various positions of point C on its path can be determined from the velocity diagrams. The kinematic diagram shown in Fig. 53, *b* (p. 53) gives a clear representation of the change in this magnitude. The insignificant resistances that the piston meets at the second and third strokes, i. e. when the products of combustion are pushed out from the cylinder and suction of air into the cylinder takes place, will not be considered.

Let us lay off by the axis of abscissae (Fig. 185) in one direction the path developed into a straight line, which is passed by point B in the course of one cycle, i. e. during four strokes of the piston or, what is exactly the same, two revolutions of the crank. By the axis of ordinates we shall lay off the magnitudes of tangential forces T, which are determined in the manner previously shown.

During the first stroke the magnitudes of the tangential forces change according to the law of curve *adf*. The area of this curve (and its equivalent area of rectangle *amnf*)

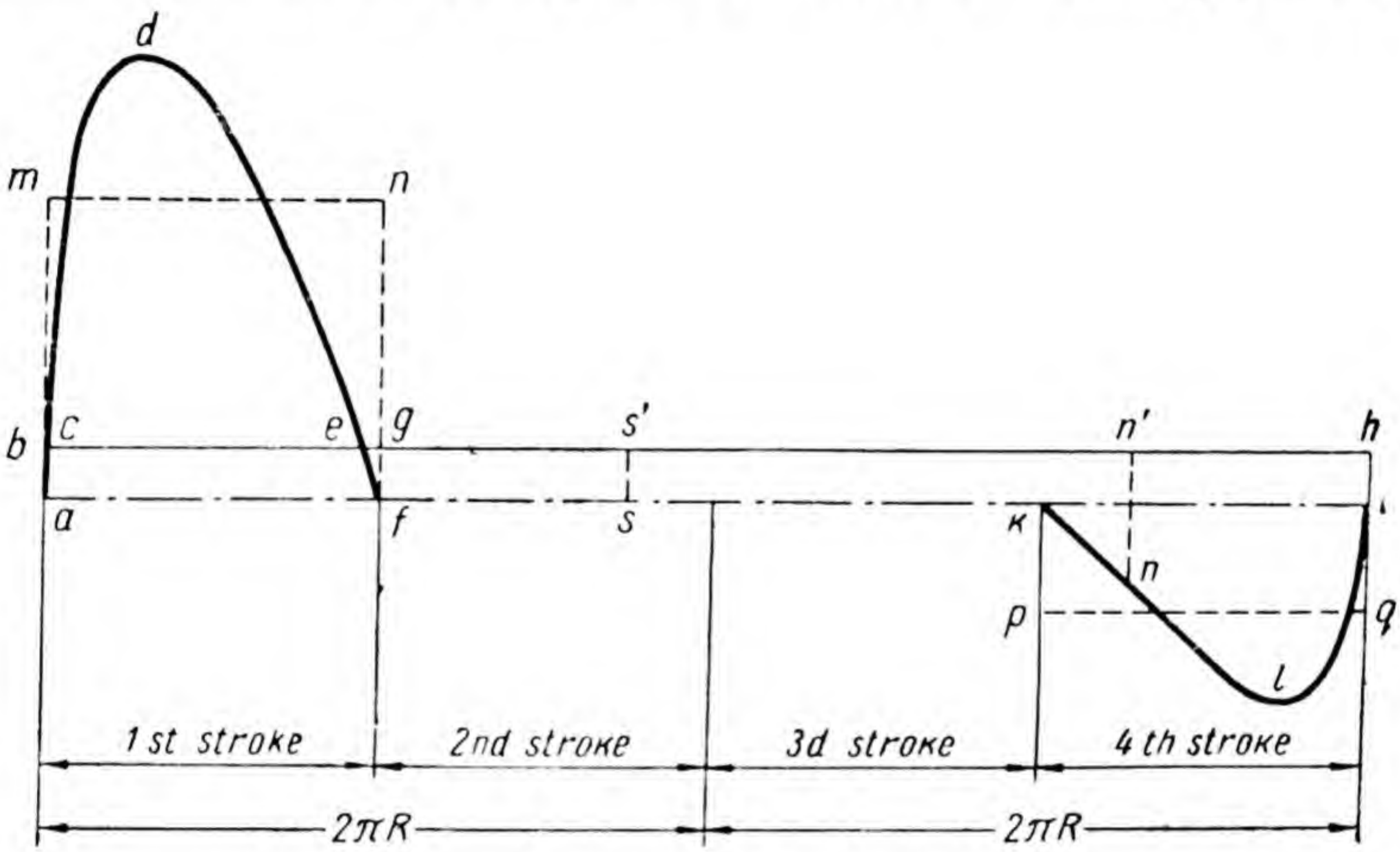

Fig. 185

expresses the quantity of energy which is supplied to the crank in the first stroke of engine operation.

The insignificant resistances by the gases in the second and third strokes will not be considered, and work done by the useful and parasitic resistances will be temporarily ignored. We therefore proceed to point *k*, the beginning of the fourth stroke. From the beginning of this stroke compression of the air, which entered into the cylinder during the third stroke, takes place. Since piston motion during the fourth stroke is accomplished at the expense of the energy produced by the flywheel, and since in this stroke it is not the connecting rod that rotates the crank, but, on the contrary, the crank that actuates the connecting rod, the tangential forces change signs; the tangential forces

change according to the law of curve *kli*. The area of this curve (and its equidimensional area of rectangle *kpqi*) expresses the quantity of energy, which is returned by the flywheel to the very same source from which it received the energy in the first stroke. This energy, returned by the flywheel and contained in the compressed air, is fully utilized by the engine in the first stroke of the following cycle.

From what has been said it follows that for work done by the useful and parasitic resistances can be used only the difference of energies, which are expressed by the areas of curves *adf* and *kli*. Since at steady motion the resistance, which is reduced to point *B* of the crank, in the course of one cycle should be considered constant, by dividing the difference of the areas of curves *adf* and *kli* by the path $4\pi R$, which is passed by point *B* during one cycle, we obtain the magnitude of ordinate $ab=hi$, which expresses the magnitude of this resistance. The area *abhia* expresses, consequently, work done by the resistances.

Let us now proceed to the angular velocity of rotation of the flywheel. In the first stroke the tangential forces from the connecting rod onto the crank at point *B* exceed considerably the resistance which is exerted by the crank; therefore the angular velocity of rotation of the crank and flywheel increases. The increase in the angular velocity ceases when the tangential force becomes equal to the resistance of the crank; this takes place at point *e* where curve *adf* and the straight line *bh* intersect. Therefore, at this point the angular velocity assumes the value ω_{max}. During the following strokes only resistances to its motion are acting on the piston, not only to the end of the fourth stroke, but also in the very beginning of the first stroke when point *B* passes a small portion of the path which equals *bc*. Hence, at point *c* the angular velocity equals ω_{min}.

An increase in the angular velocity of rotation of the flywheel from ω_{min} to ω_{max} occurs at the expense of the energy which is communicated to the flywheel, which is expressed by area *cdec*. Denoting the energy, which is expressed by this area through *A*, we obtain

$$A=\frac{1}{2}J(\omega^2_{max}-\omega^2_{min}),$$

where A is expressed in kgm, J is the moment of inertia of the flywheel in kgm $\times$ sec^2, and ω is expressed in sec^{-1}.

Denoting by δ the coefficient of irregularity, which equals

$$\delta = \frac{\omega_{max} - \omega_{min}}{\omega_{mean}},$$

and taking into consideration that

$$\omega_{mean} = \frac{\omega_{max} + \omega_{min}}{2},$$

we obtain

$$\omega_{max} = \omega_{mean} + \frac{\delta \times \omega_{mean}}{2}, \quad \omega_{min} = \omega_{mean} - \frac{\delta \times \omega_{mean}}{2}.$$

After substituting we get

$$A = J \times \omega^2_{mean} \delta = J\left(\frac{\pi n}{30}\right)^2 \delta = J\frac{n^2}{90}\delta,$$

where n is the number of revolutions of the flywheel per minute at mean angular velocity of rotation.

The moment of inertia of the flywheel will be

$$J = \frac{90 \times A}{n^2 \delta}.$$

Denoting the flywheel weight in kg by G and assuming the mass $\frac{G}{g}$ of the flywheel as uniformly distributed along the circle with diameter D, where $\frac{D}{2}$ is the distance from the axis of rotation of the flywheel to the centre of gravity of the rim cross section (see Fig. 183), we obtain

$$J = \frac{G}{g}\left(\frac{D}{2}\right)^2 = \frac{90A}{n_2 \delta},$$

whence

$$GD^2 = \frac{4g \times 90A}{n^2 \delta} \approx 3600 \frac{A}{n^2 \delta}.$$

The product GD^2 in kg $\times$ m^2 is called the moment of gyration or flywheel characteristic.

After we have determined the required magnitude of the moment of gyration we fix the diameter D of the flywheel, guided by design considerations, and then the weight corresponding to the diameter.

Taking into consideration the moment of inertia of the arms which join the rim with the bushing, the actual weight of the rim is taken approximately at 10 per cent less than the figure obtained by calculation. The total weight of the flywheel, including the weight of the arms and bushing, will equal (1.25-1.35) G.

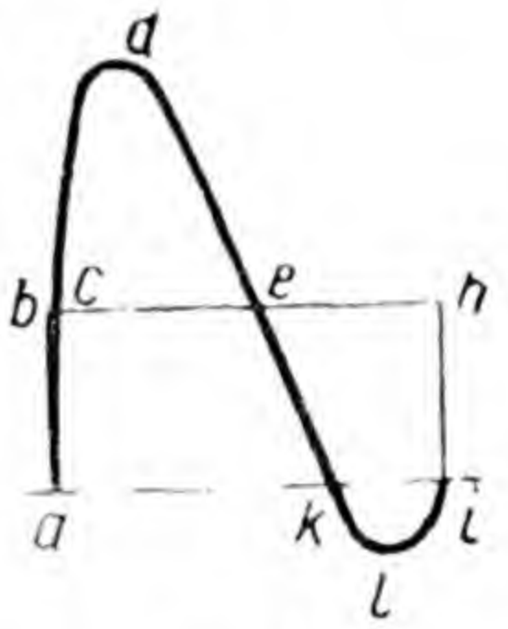

Fig. 186

By enlarging the diameter, the weight of the flywheel can be considerably decreased, with alteration to the magnitude of the moment of gyration. However, in addition to the general design considerations, we have to bear in mind that we must not exceed the limit of the peripheral velocity beyond which there is the danger of rim rupture under the action of centrifugal forces. There have been cases in practice when heavy pieces of the rim have come away from the flywheel at high speed, and caused casualties among the servicing personnel and damages to equipment and installations.

For a flywheel of ordinary cast iron the peripheral velocity is accepted as not exceeding 30 m/sec; for high-grade cast iron a somewhat greater velocity may be allowed.

In multicylinder engines the energy cycles in different cylinders displace relative to each other; for instance, in a four-cylinder four-stroke engine the working strokes in different cylinders take place in turn. With such an engine arrangement the required moment of gyration is considerably less: since the first stroke in one cylinder coincides in time with the fourth stroke in another cylinder, the action on the flywheel in the course of every half turn of the crankshaft is effected according to the law of curve *adkli*, as shown in Fig. 186, the ordinates of which are the differences in ordinates of curves *adf* and *kli* in Fig. 185. The energy, which is expressed by the difference in areas *adk* and *kli*, is used to overcome work done by resistances, and is expressed by area *abhia*. The angular velocity ω_{max} in this case, as well as in Fig. 185, is at point *e*, and ω_{min} is at point *c*. When determining the moment of gyration, the energy A expressed by area *cdec*, which is much less

than the area denoted in Fig. 185 by the same letters, should be substituted in the formula given above. We have also to take into consideration that a much lesser moment of gyration is obtained despite the fourfold greater power of the four-cylinder engine.

We have marked above those points of the path, passed by point B, in which the angular velocity of rotation of the link of reduction assumes the extreme values, but did not deal with the problem of the changes from one extreme value to another of the angular velocity. This can be easily understood by using the diagram of Fig. 185 and proceeding from the equation of motion of the link of reduction.

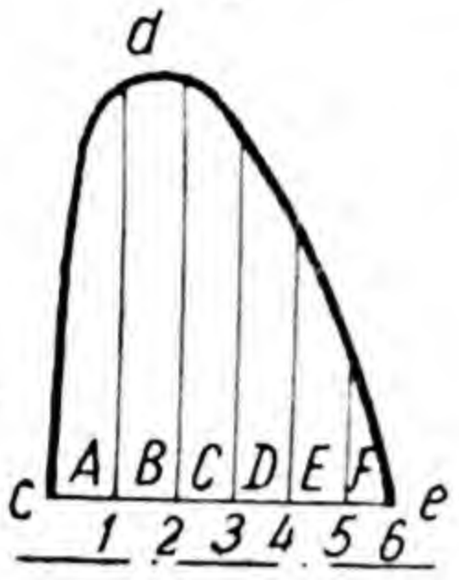

Fig. 187

In order to understand the law, by which the angular velocity increases from ω_{min} to ω_{max}, we divide the portion *ce* of the path of point *B* by points *1*, *2*, . . . , *5* into equal parts and by perpendicular lines to *ce*, drawn from these points, we divide the area *cde* into areas *A*, *B*, *C* . . . (Fig. 187).

The angular velocity ω_1 at point *1* exceeds ω_{min} at the expense of work done by driving forces and received by the flywheel; work done is expressed by area *A* in kg × m and therefore can be determined from equation

$$A = \frac{J}{2}(\omega_1^2 - \omega_{min}^2).$$

The angular velocity ω_2 at point *2* is determined from equation

$$A + B = \frac{J}{2}(\omega_2^2 - \omega_{min}^2), \text{ etc.}$$

From point *e* (Fig. 185) the angular velocity from ω_{max} begins to decrease because of the consumption by the flywheel of kinetic energy to overcome the external resistances. The angular velocity ω_s at any point *s* of the path prior to the beginning of the fourth stroke is determined from equation

$$\text{Area } fess'f = \frac{J}{2}(\omega_{max}^2 - \omega_s^2).$$

The angular velocity ω_n at any point n of the path in the course of the fourth stroke can be determined from equation

$$\text{Area } fen'nkf = \frac{J}{2}(\omega^2_{max} - \omega^2_n).$$

Having thus determined the angular velocities at a sufficient number of points of the path, passed by point B, we can plot a smooth curve which gives a clear representation of the change of the angular velocity of rotation of the link of reduction from ω_{min} to ω_{max} and back to ω_{min}.

Fig. 188 shows a curve plotted in this manner using the equation of motion of the link of reduction.

In all of the previously cited examples of the kinematic analysis and of the combined static and inertia force analysis of various mechanisms, based on the kinematic analysis, the angular velocity of rotation of the crank has been assumed as constant. We know now that by constant

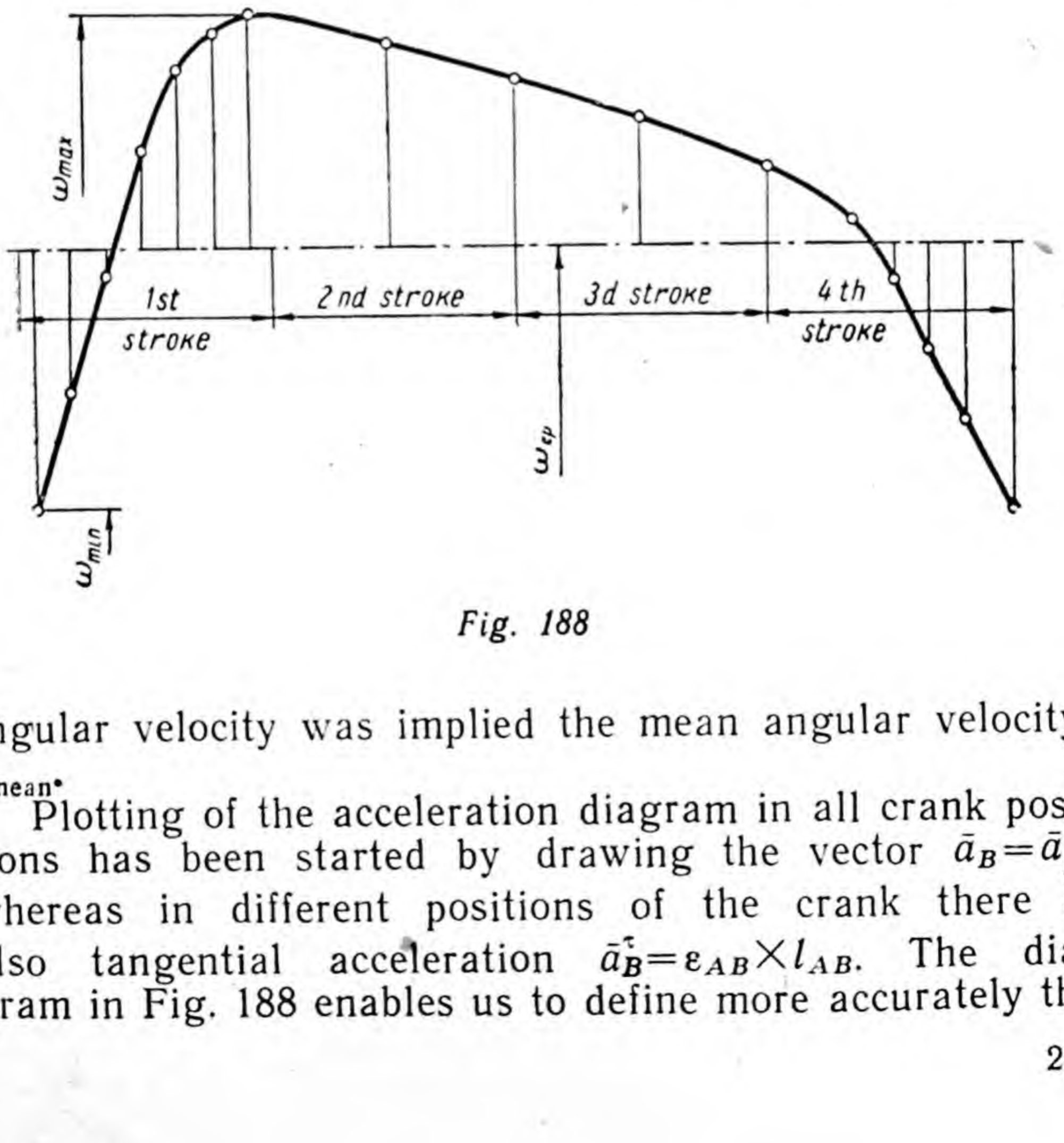

Fig. 188

angular velocity was implied the mean angular velocity, ω_{mean}.

Plotting of the acceleration diagram in all crank positions has been started by drawing the vector $\bar{a}_B = \bar{a}^n_B$, whereas in different positions of the crank there is also tangential acceleration $\bar{a}^\tau_B = \varepsilon_{AB} \times l_{AB}$. The diagram in Fig. 188 enables us to define more accurately the

acceleration diagrams and the magnitudes of the forces of inertia which are based on these diagrams.

For this purpose the scale of abscissae in Fig. 188 should be divided by radius R of rotation of point B, and as a result the abscissae will express the angles φ of rotation of the link of reduction, and the curve in Fig. 188 the function $\omega=f(\varphi)$ graphically. By differentiating graphically the curve $\omega=f(\varphi)$ we shall get the magnitudes $\frac{d\omega}{d\varphi}$, while the angular velocities will be as follows

$$\frac{d\omega}{dt}=\frac{d\omega}{dt}\times\frac{d\varphi}{d\varphi}=\frac{d\omega}{d\varphi}\times\frac{d\varphi}{dt}=\frac{d\omega}{d\varphi}\times\omega,$$

where ω is the angular velocity of rotation in the corresponding position.

If we take into consideration the angular velocities of the link of reduction, the acceleration diagrams which have been plotted at ω_{mean} in all positions have to be replotted, but the velocity diagrams may remain unchanged, since only their scales can be made more accurate.

The actual and not the mean angular velocity of rotation of the crank has to be taken into consideration in plotting the acceleration diagrams only at large coefficients δ of permissible variations of speed, for instance, for shock action machines (press, shearing machine, etc.), during the operation of which the angular velocity of the driving link drops swiftly to minimum in the course of the working strokes and rises rapidly to maximum during idle strokes.

Fig. 188 shows the curve $\omega=f(\varphi)$ for an internal-combustion engine (four-stroke diesel). For these engines the coefficient δ is taken as not exceeding 1/80, and much less if they are intended to actuate electric current generators. The most rapid change of angular velocity by the magnitude $\omega_{mean}-\omega_{min}=\frac{\delta\omega_{mean}}{2}$ takes place during the first half turn in the first stroke. Since the angular velocity on this portion changes according to the law of straight line (see Fig. 188), the angular acceleration on this portion can be assumed as

$$\varepsilon=\frac{\delta\omega_{mean}}{2}\Big/\frac{30}{n}=\frac{\delta n\omega_{mean}}{60}\ \text{sec}^{-2},$$

where n is the number of crank revolutions per minute, and $\frac{30}{n}$ is the time interval during which the angular velocity changes.

The relation of magnitudes of the normal and tangential accelerations of point B of the link of reduction on this portion will equal

$$a_B^n / a_B^\tau = \omega_{\text{mean}}^2 l_{AB} \Big/ \frac{\delta n \omega_{\text{mean}}}{60} = l_{AB} = \frac{60\,\omega_{\text{mean}}}{\delta n} = \frac{60\pi n}{30\delta n} = \frac{2\pi}{\delta}.$$

Where $\delta = 1/80$, the relation is $a_B^n / a_B^\tau \approx 500$. This means that when the length of vector $\bar{a}_B^n$ on the acceleration diagram is 100 mm, the length of vector $\bar{a}_B^\tau$ would be 0.2 mm; in the graphic analysis it would have to be zero.

Вл. А. Зиновьев

Теория механизмов и машин

(на английском языке)

Редактор *В. П. Кочин*
Издательский редактор *Л. А. Долгопятова*
Художественный редактор *Е. И. Ильенко*
Технический редактор *Л. Л. Ежова*
Корректор *И. А. Краснова*

Москва — 1963

Сдано в набор 30/III-63 г. Подписано к печати 30/IX-63 г. Бумага 84×108. 7,5 печ. л. 12,3 усл. печ. л. 12,48 уч.-изд. л. Тираж 12 000. Изд. № ИН/103. Цена 40 коп.

Издательство «Высшая школа».
Москва, К-62, Подсосенский пер., 20.

Отпечатано в типографии № 2 «Советская Латвия» г. Рига, ул. Дзирнаву, 57. Зак. № 1115.